

DTIC FILE COPY

AD-A227 193

EMPIRICAL NETWORK MODEL OF HUMAN HIGHER  
COGNITIVE BRAIN FUNCTIONS

FINAL TECHNICAL REPORT

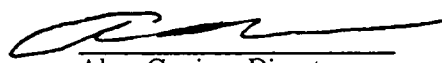
AFOSR Contract F49620-87-C-0047  
1 APR 87 to 31 MAR 90

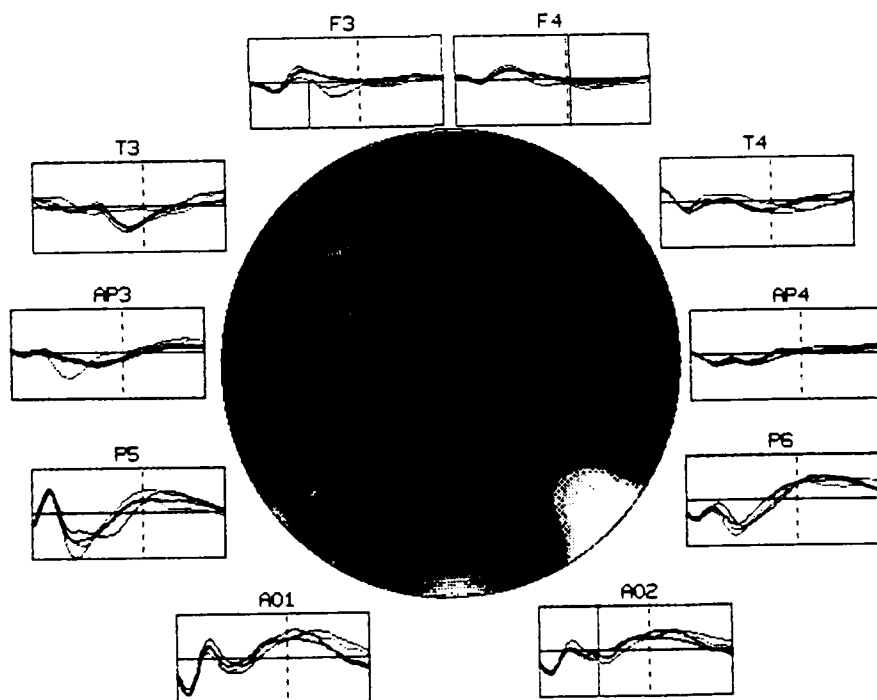
DTIC  
ELECTE  
OCT 01 1990  
S B D

PREPARED FOR

Dr. A.R. Fregly  
Directorate of Life Sciences  
Air Force Office of Scientific Research  
Bolling AFB, D.C. 20332-6448

APPROVED BY

  
Alan Gevins, Director



The views and conclusions in this document are those of the authors and should not be interpreted as necessarily representing the official policies or endorsements, either expressed or implied, of the Air Force Office of Scientific Research or the U.S. Government.

DISTRIBUTION STATEMENT A

Approved for public release;  
Distribution Unlimited

1 - EP 1898

UNCLASSIFIED

SECURITY CLASSIFICATION OF THIS PAGE

## REPORT DOCUMENTATION PAGE

Form Approved  
OMB No. 0704-0188

1a. REPORT SECURITY CLASSIFICATION UNCLASSIFIED			1b. RESTRICTIVE MARKINGS		
2a. SECURITY CLASSIFICATION AUTHORITY			3. DISTRIBUTION/AVAILABILITY OF REPORT AFOSR ONLY		
2b. DECLASSIFICATION/DOWNGRADING SCHEDULE			5. MONITORING ORGANIZATION REPORT NUMBER(S) AFOSR TR-510 1008		
4. PERFORMING ORGANIZATION REPORT NUMBER(S) EEG88001			7a. NAME OF MONITORING ORGANIZATION DIRECTORATE OF LIFE SCIENCES, AFOSR		
6a. NAME OF PERFORMING ORGANIZATION EEG SYSTEMS LABORATORY	6b. OFFICE SYMBOL (If applicable)	7b. ADDRESS (City, State, and ZIP Code) BUILDING 410 BOLLING AFB, DC 20332-6448			
6c. ADDRESS (City, State, and ZIP Code) 51 FEDERAL STREET, SUITE 401 SAN FRANCISCO, CA 94107	9. PROCUREMENT INSTRUMENT IDENTIFICATION NUMBER F49620-87-0047				
8a. NAME OF FUNDING/SPONSORING ORGANIZATION AFOSR	8b. OFFICE SYMBOL (If applicable)	10. SOURCE OF FUNDING NUMBERS			
8c. ADDRESS (City, State, and ZIP Code) USAF/AFSC, AIR FORCE OFFICE OF SCIENTIFIC RESEARCH; BLDG 410 BOLLING AFB, DC 20332-6448		PROGRAM ELEMENT NO. 61102F	PROJECT NO. 2313	TASK NO. A4	WORK UNIT ACCESSION NO.
11. TITLE (Include Security Classification) EMPIRICAL NETWORK MODEL OF HUMAN HIGHER COGNITIVE BRAIN FUNCTIONS					
12. PERSONAL AUTHOR(S) GEVINS, A.S., CUTILLO, B.A., ILLES, J., BRESSLER, S.L., BRICKETT, P.A.					
13a. TYPE OF REPORT FINAL TECHNICAL	13b. TIME COVERED FROM 1APR87 TO 31MAR90	14. DATE OF REPORT (Year, Month, Day) 31 MAR 90		15. PAGE COUNT 101	
16. SUPPLEMENTARY NOTATION					
17. COSATI CODES			18. SUBJECT TERMS (Continue on reverse if necessary and identify by block number)		
FIELD	GROUP	SUB-GROUP	Cognition, Brain, Sustained mental work, Language EEG, evoked potentials, MRI, Functional neural networks		
	87072				
19. ABSTRACT (Continue on reverse if necessary and identify by block number)  EEG Systems Laboratory (EEGSL) develops and applies advanced technologies for measuring neurocognitive signals in the human brain. Results during the period 1APR87 to 31MAR90 included: 1) measurement of "leading indicator" neuroelectric patterns preceding performance decrements in five Air Force fighter test pilots who performed difficult cognitive tasks for 10-14 hours; 2) measurement of split-second neurocognitive patterns of basic linguistic operations which distinguished letter from non-letter, word from non-word, and syntactic from non-syntactic processing; and 3) functional-anatomical localization based on 124-channel evoked potential recordings and three-dimensional finite-element brain models constructed from magnetic resonance images.					
20. DISTRIBUTION/AVAILABILITY OF ABSTRACT <input type="checkbox"/> UNCLASSIFIED/UNLIMITED <input checked="" type="checkbox"/> SAME AS RPT. <input type="checkbox"/> DTIC USERS			21. ABSTRACT SECURITY CLASSIFICATION UNCLASSIFIED		
22a. NAME OF RESPONSIBLE INDIVIDUAL DR. A.R. FREGLY			22b. TELEPHONE (Include Area Code) (202) 767-5021		22c. OFFICE SYMBOL AFOSR/NL

## TABLE OF CONTENTS

	Page
<b>I. OVERVIEW .....</b>	<b>4</b>
A. Summary .....	4
B. Scientific Personnel of EEG Systems Laboratory .....	5
C. Publications .....	6
<b>II. EFFECTS OF SUSTAINED MENTAL WORK ON FUNCTIONAL NETWORKS OF THE HUMAN BRAIN</b> (In Press, EEG clin. Neurophysiol.) .....	9
<b>III. FUNCTIONAL TOPOGRAPHY OF LANGUAGE .....</b>	<b>10</b>
A. Introduction .....	10
B. Hypotheses .....	11
C. Piloting .....	11
D. Methods .....	12
E. Results .....	14
F. Discussion .....	27
1. Letter and Non-Letter Processing .....	27
2. Word and Non-Word Processing .....	28
3. Syntactic Processing .....	29
4. Comparison of Potential and Laplacian Derivation Topographies .....	29
5. Conclusion .....	29
G. References .....	31
<b>IV. TECHNICAL DEVELOPMENTS .....</b>	<b>34</b>
A. Overview .....	34
B. Dipole Localization .....	34
C. Beyond Topographic Mapping: Towards Functional-Anatomical Imaging with 124-Channel EEG's and 3-D MRI's (In Press, Brain Topography) .....	39
<b>V. DISSEMINATION OF TECHNICAL INFORMATION .....</b>	<b>40</b>
A. Publications dealing with methodology .....	40
B. Presentations at meetings .....	40
C. Visitors to EEGSL .....	41

STATEMENT "A" per Debra Tyrell  
AFOSR/XOTD, Bldg. 410, Bolling AFB, DC  
20332-6448  
TELECON 9/25/90

VG

ession For	
GRA&I	<input checked="" type="checkbox"/>
TAB	<input type="checkbox"/>
nnounced	<input type="checkbox"/>
ification	
<i>per telecon</i>	
tribution/	
Availability Codes	
Dist	Avail and/or Special
A-1	

## I. OVERVIEW

### A. Summary

EEG Systems Laboratory develops and applies advanced technologies for measuring and imaging neurocognitive signals of the human brain. During the three-year funding period, 4/1/87 to 3/31/90, a number of objectives were accomplished. First, we completed an experiment which measured, for the first time, the effects of sustained mental work on functional networks of the human brain. In addition to the well-known global decrease in cortical activation with operational fatigue, we found signs of differential alteration of cortical networks during split-second pre- and post-stimulus intervals of a difficult visuomotor--working memory task. The pattern from the prestimulus interval, which required maintenance of previous stimuli in memory, changed most dramatically during hours 7-9, which was before performance had significantly declined. The pattern associated with inhibiting a response, when the current stimulus matched the remembered stimulus from two trials back, changed most in the final two hours of the session. The pattern associated with feature registration of the visual stimuli was least affected. It seems feasible to further develop this technology into an early-warning system to detect immanent transient cognitive lapses. The report of these findings has been accepted for publication by the journal *Electroencephalography and Clinical Neurophysiology*, and the preprint is included in this report.

Second, we conducted an experiment to measure functional cortical patterns during elementary graphic, phonemic, semantic, and grammatical tasks. Nine 59-channel EEG recordings were made, and an initial analysis has been completed. Spatial and temporal evoked potential features distinguished letter from non-letter, word from non-word, and syntactic from non-syntactic processing. Differences between linguistic and non-linguistic conditions were mainly left-sided. The three language conditions exhibited sharply localized effects over left temporal and frontal cortex, with differences between the processing of closed class (functional, syntactic) versus open class (content) words. Evidence for bilaterality of semantic (lexical) function was also found, as was evidence of priming of visual association cortex for processing unfamiliar graphic figures.

Third, several technological advances were made during the past three years. We expanded our EEG recording and analysis capabilities from 64 to 128 channels. Data inspection and analysis has been assisted by the "Scientists' Workbench", an interactive exploratory data analysis and display program. Other technical developments include development of methods and programs for analyzing magnetic resonance images (MRIs) in order to construct three-dimensional models of each subject's brain. These models are used to improve functional-anatomical localization, both for equivalent current dipole analysis and improved spatial deblurring procedures. Applying dipole analysis to octant visual steady state stimuli produced sources located near the occipital pole contralateral to side of stimulation and inverted about the horizontal. These results are comparable to intercerebral locations reported for early latency transient EPs, as well as for equivalent dipoles computed from the MEG. However, the EEG equipment for this type of dipole analysis costs about 100 times less than MEG equipment with a comparable number of channels. Although this method proved very efficient and effective in locating dipoles for simple steady-state sensory stimuli, single equivalent dipoles are not a suitable model for the complex, distributed processes of cognitive functions. Work is underway at EEGSL on the development of more realistic models. Our 3-D brain imaging and deblurring techniques are described in a preprint included in this report, titled "Beyond Topographic Mapping: Towards Functional-Anatomic Imaging with 124-Channel EEG's and 3-D MRI's".



**B. Scientific Personnel at EEG Systems Laboratory**

Steven Bressler, Neurophysiologist  
Paul Brickett, Psychophysiologicalist  
Brian Cutillo, Cognitive Scientist, Co-Principal Investigator  
Alan Gevins, Neuroscientist, Principal Investigator  
Judy Illes, Neuropsychologist  
Jian Le, Numerical Analyst  
Bryan Reutter, Computer Scientist  
Michael Ward, Biomedical Engineer

**C. Publications FY87-89**In Press:

1. Gevins, A.S. (In Press) Distributed neuroelectric patterns of human neocortex during simple cognitive tasks. In H. Uylings et al., (Eds.) *Progress in Brain Research*, Elsevier: Amsterdam.
2. Gevins, A.S. (In press) Dynamic patterns in multiple lead data. In: J. Rohrbaugh, R. Johnson, R. Parasuraman (Eds.), *Event-Related Potentials of the Brain*. Oxford University Press: New York.
3. Gevins, A.S. & Illes, J. (In Press) Neurocognitive networks of the human brain. In Zappulla, R.A. (Ed.) *Windows on the Brain: Neuropsychology's Technological Frontiers*. New York Academy of Sciences: New York.
4. Gevins, A.S., Bressler, S.L., Cuttillo, B.A., Illes, J., Miller, J., Stern, J., Jex, H. (In Press) Effects of prolonged mental work on functional brain topography. *EEG clin. Neurophysiol.*
5. Gevins, A.S., Brickett, P., Costales, B., Le, J., Reutter, B. (In press) Beyond topographic mapping: Towards functional-anatomical imaging with 124-channel EEGs and 3-D MRIs. *Brain Topography*.

1990:

6. Bressler, S. (1990) The gamma wave: A cortical information carrier? *Trends in Neurosciences*, 13(5):161-162.
7. Gevins, A.S. (1990) Dynamic functional topography of cognitive tasks. *Brain Topography*, 2(1/2), 37-56.

1989:

8. Gevins, A. (1989) Signs of Model Making by the Human Brain. *Springer Series in Brain Dynamics*, 2, E. Basar and T. Bullock (Eds.), Springer-Verlag, Berlin, pp. 408-419.
9. Gevins, S.A., Bressler, S.L., Morgan, N.H., Cuttillo, B.A., White, R.M., Greer, D., Illes, J. (1989a) Event-related covariances during a bimanual visuomotor task, Part I: Methods and analysis of stimulus- and response-locked data. *Electroencephalogr. clin. Neurophysiol.*, 74:58-75.
10. Gevins, A.S., Cuttillo, B.A., Bressler, S.L., Morgan, N.H., White, R.M., Illes, J., Greer, D. (1989b) Event-related covariances during a bimanual visuomotor task, Part II: Preparation and feedback. *Electroencephalogr. clin. Neurophysiol.*, 74:147-160.
11. Illes, J. (1989) Neurolinguistic features of spontaneous language production dissociate three forms of neurodegenerative disease: Alzheimer's, Huntington's, Parkinson's *Brain and Language*, 37, 628-642.
12. Illes, J., Metter, E.J., Dennings, R., Jackson, C., Kempler, D., Hanson, W.R. (1989) Spontaneous language production in mild aphasia: Relationship to left prefrontal glucose hypometabolism. *Aphasiology*, 3(6), pp. 527-537.

1988:

13. Gevins, A.S. and Aminoff, M.J. (1988) Electroencephalography: Brain electrical activity. In: J. Webster (Ed.), *Encyclopedia of Medical Devices and Instrumentation*. Wiley & Sons, New York, pp. 1084-1107.
14. Gevins, A.S. & Morgan, N.H. (1988) Applications of neural-network (NN) signal processing in brain research. *IEEE ASSP Trans.*, 36(7), pp. 1152-1161.

15. Gevins, A.S., Cutillo, B.A., Fowler-White, R.M., Illes, J. and Bressler, S.L. (1988) Neurophysiological patterns of operational fatigue: preliminary results. *NATO/AAGARD Conference Proceedings*, 432, pp. 22-1 to 22-7.
16. Gevins, A.S., Cutillo, B.A., Bressler, S.L., Morgan, N.H., Fowler-White, R.M., Greer, D.S., Illes, J., Doyle, J.C., Tannehill, R.S. and Zeitlin, G.M. (1988) Neurophysiological precursors of accurate visuomotor performance. *NATO/AAGARD Conference Proceedings*, 432, pp. 25-1 to 25-9.
17. Gevins, A.S., Morgan, N.H., Bressler, S.L., Greer, D.S., Costales, B., Smith, K. and Faucette, R. (1988) Fourth generation neurocognitive pattern analysis system. *NATO/AAGARD Conference Proceedings*, 432, pp. 2-1 to 2-11.
18. Gevins, A.S. and Bressler, S.L. (1988) Functional topography of the human brain. In: G. Pfurtscheller and F. Lopes da Silva (Eds.), *Functional Brain Imaging*. Hans Huber: Bern, pp. 99-116.
19. Gevins, A.S., Cutillo, B.A., Fowler-White, R.M., Illes, J., Bressler, S.L. (1988) Neurophysiological patterns of operational fatigue: preliminary results. *NATO/AGARD Conference Proceedings*, 432, pp. 22-1 to 22-7.
20. Gevins, A.S., Cutillo, B.A., Bressler, S.L., Morgan, N.H., Fowler-White, R.M., Greer, J., Illes, J., Doyle, J.C., Tannehill, R.S., Zeitlin, G.M. (1988) Neurophysiological precursors of accurate visuomotor performance. *NATO/AGARD Conference Proceedings*, 432, pp. 25-1 to 25-9.
21. Gevins, A.S., Stone, R.K., Ragsdale, S.D. (1988) Differentiating the effects of three benzodiazepines on non-REM sleep EEG spectra: A neural-network pattern classification analysis. *Neuropsychobiology*, 19:108-115.
22. Gevins, A.S. (1988) Recent advances in neurocognitive pattern analysis. In: E. Basar (Ed.), *Dynamics of Sensory and Cognitive Processing of the Brain*. Heidelberg, Springer-Verlag, pp. 88-102.
23. Illes, J., Metter, E.J., Hanson, W.R., Iritani, S. (1988) Language production in Parkinson's Disease: Acoustic and linguistic considerations. *Brain and Language* 33, pp. 146-160.

#### 1987:

24. Bressler, S.L. (1987) Relation of olfactory bulb and cortex. I. Spatial variation of bulbo-cortical interdependence. *Brain Research*, 409, pp. 285-293.
25. Bressler, S.L. (1987) Relation of olfactory bulb and cortex. II. Model for driving of cortex by bulb. *Brain Research*, 409, pp. 294-301.
26. Gevins, A.S. (1987) Analysis of multiple lead data. In: J. Rohrbaugh, R. Johnson, R. Parasuraman (Eds.), *Event-Related Potentials of the Brain*. New York, Oxford University Press.
27. Gevins, A.S. (1987) Correlation Analysis. In: A.S. Gevins & A. Remond (Eds.), *Handbook of Electroencephalography and Clinical Neurophysiology, Vol.1: Methods of Analysis of Brain Electrical and Magnetic Signals*. Amsterdam, Elsevier, pp. 171-193.
28. Gevins, A.S. (1987) How the human brain thinks and acts: Results of latest research using neural networks to analyze brain signals. *Proc. IEEE 1st Internat. Conf. Neural Networks, IV*, pp. 41-47.
29. Gevins, A.S. (1987) Obstacles to progress. In: A.S. Gevins & A. Remond (Eds.), *Handbook of Electroencephalography and Clinical Neurophysiology, Vol.1: Methods of Analysis of Brain Electrical and Magnetic Signals*. Amsterdam, Elsevier, pp. 665-673.
30. Gevins, A.S. (1987) Overview of computer analysis. In: A.S. Gevins & A. Remond (Eds.), *Handbook of Electroencephalography and Clinical Neurophysiology, Vol.1: Methods of Analysis of Brain Electrical and Magnetic Signals*. Amsterdam, Elsevier, pp. 31-83.

31. Gevins, A.S. (1987) Statistical pattern recognition. In: A.S. Gevins & A. Remond (Eds.), *Handbook of Electroencephalography and Clinical Neurophysiology, Vol.1: Methods of Analysis of Brain Electrical and Magnetic Signals*. Amsterdam, Elsevier, pp. 541-582.
32. Gevins, A.S., Morgan, N.H. (1987) "Ignorance-based" neural-network signal processing in brain research. *Proc. IEEE 1st Internat. Conf. Neural Networks, IV*, pp. 705-716.
33. Gevins, A.S., Remond, A. (Eds.) (1987) *Methods of Analysis of Brain Electrical and Magnetic Signals. Handbook of Electroencephalography and Clinical Neurophysiology, Vol.1*. Amsterdam, Elsevier.
34. Gevins, A.S., Cuttillo, B.A., Morgan, N.H., Bressler, S.L., Illes, J., White, R.M., Greer, D.S. (1987) Event-related covariances of a bimanual visuomotor task. In: R. Johnson (Ed.), *Current Research in Event-Related Brain Potentials*. Amsterdam, Elsevier.
35. Gevins, A.S., Morgan, N.H., Bressler, S.L., Cuttillo, B.A., White, R.M., Illes, J., Greer, D.S., Doyle, J.C., Zeitlin, G.M. (1987) Human neuroelectric patterns predict performance accuracy. *Science*, 235, pp. 580-585.

#### REPRINTS INCLUDED

- Gevins, A. (1989) Signs of Model Making by the Human Brain. *Springer Series in Brain Dynamics*, 2, E. Basar and T. Bullock (Eds.), Springer-Verlag, Berlin, pp. 408-419.
- Gevins, A.S. and Bressler, S.L. (1988) Functional topography of the human brain. In: G. Pfurtscheller and F. Lopes da Silva (Eds.), *Functional Brain Imaging*. Hans Huber, Bern, pp. 99-116.
- Gevins, S.A., Bressler, S.L., Morgan, N.H., Cuttillo, B.A., White, R.M., Greer, D. and Illes, J. (1989) Event-related covariances during a bimanual visuomotor task, Part I: Methods and analysis of stimulus- and response-locked data. *Electroenceph. clin. Neurophys.*, 74(1): 58-75.
- Gevins, A.S., Cuttillo, B.A., Bressler, S.L., Morgan, N.H., White, R.M., Illes, J. & Greer, D. (1989) Event-related covariances during a bimanual visuomotor task, Part II: Preparation and feedback. *Electroenceph. clin. Neurophys.*, 74(2): 147-160.
- Gevins, A.S. & Morgan, N.H. (1988) Applications of neural-network (NN) signal processing in brain research. *IEEE ASSP Trans.*, 36(7): 1152-1161.
- Gevins, A.S., Morgan, N.H., Bressler, S.L., Cuttillo, B.A., White, R.M., Illes, J., Greer, D.S., Doyle, J.C. & Zeitlin, G.M. (1987) Human neuroelectric patterns predict performance accuracy. *Science*, 235: 580-585.
- Gevins, A.S. and Cuttillo, B. (1986) Signals of Cognition. In F. Lopes da Silva, et al. (Eds.), *Handbook of Encephalography and Clinical Neurophysiology, Vol. 2*, Elsevier, Amsterdam, pp. 335-381.

**II. EFFECTS OF SUSTAINED MENTAL WORK ON  
FUNCTIONAL NETWORKS OF THE HUMAN BRAIN**

## Effects of prolonged mental work on functional brain topography

Alan S. Gevins<sup>a</sup>, Steven L. Bressler<sup>a</sup>, Brian A. Cuttillo<sup>a</sup>, Judy Illes<sup>a</sup>,  
James C. Miller<sup>b</sup>, John Stern<sup>c</sup> and Henry R. Jex<sup>d</sup>

<sup>a</sup> EEG Systems Laboratory, San Francisco, CA (U.S.A.), <sup>b</sup> United States Airforce School of Aerospace Medicine, San Antonio, TX (U.S.A.), <sup>c</sup> Washington University, Department of Psychology, St. Louis, MO (U.S.A.), and <sup>d</sup> Systems Technology, Inc., Hawthorne, CA (U.S.A.)

(Accepted for publication: 15 December 1989)

**Summary** Topographic patterns of event-related covariance between electrodes were measured from subjects performing a difficult memory and fine-motor control task for 10–14 h. Striking changes occurred in the patterns after subjects performed the task for an average of 7–9 h, but before performance deteriorated. Pattern strength was reduced in a fraction-of-a-second-long response preparation interval over midline precentral areas and over the entire left hemisphere. By contrast, pattern strength in a succeeding response inhibition interval was reduced over all areas. The pattern changed least in an intervening interval associated with visual-stimulus processing. This suggests that, in addition to the well-known global reduction in neuroelectric signal strength, functional neural networks are selectively affected by sustained mental work in specific fraction-of-a-second task intervals.

**Key words:** Prolonged mental work; Functional neural networks; Event-related covariances; Event-related potentials; Laplacian derivation; Spatio-temporal maps; Contingent negative variation; N1-P2; P300

The high incidence of serious accidents caused by fatigued workers provides compelling motivation for study of the deleterious effects of prolonged mental work. Although psychological theories have been advanced to explain how prolonged mental work affects sensory, motor and higher cognitive functions (Warm and Parasuraman 1987), spatially and temporally detailed measurements of the associated changes in brain activity needed to test these theories have been lacking.

Some electroencephalographic correlates of decreasing alertness have been described, for example, replacement of alpha band activity by variable fast frequency, low voltage rhythms (Roth 1962; Williams et al., 1962; Kellaway and Mulsby, 1967; Walter et al., 1967), increase in delta and theta band power (Lubin et al., 1969),

and an increase in the theta-to-alpha band power ratio (Matoušek 1967; Gevins et al., 1977; reviewed in Matejcek 1982). Hori (1985) reported increases in alpha wave amplitude over central and posterior sites and decreases over frontal sites in the transition from waking to sleep. A study by Naitoh et al. (1971) demonstrated that the contingent negative variation (CNV) disappears with sleep deprivation. Aguirre and Broughton (1987) reported that the P300 wave, but not the CNV, is reduced during daytime sleepiness. Mane et al. (1983) also showed that the P300 peak is particularly sensitive to prolonged performance of a task. None of these studies, however, attempted to obtain temporally and spatially detailed neuroelectric measurements from subjects performing difficult cognitive tasks over extended periods of time.

The goal of the present study was to measure the effect of sustained mental work on the functional topography of the human brain (Gevins and

Correspondence to: Dr. A.S. Gevins, EEG Systems Laboratory, 51 Federal Street, San Francisco, CA 94107 (U.S.A.).

Bressler 1988). We used event-related covariance (ERC) analysis (Gevins et al., 1987, 1989a, b) to measure neuroelectric patterns related to performance of a difficult memory and fine-motor control task during a 10–14 h period. The task required that subjects monitor a low event rate (11 events/min), single modality (visual) stimulus presented from a single source (video screen), and make successive cognitive discrimination judgments (Davies and Parasuraman 1982). It involved many processes known to be affected by prolonged mental work, such as expectation and preparation, stimulus processing, short-term memory and attention (Matejcek 1982). The effects of practice and variations in performance accuracy, which can degrade the quality of sustained attention in successive discrimination tasks (Parasuraman et al. 1987), were carefully controlled so as not to confound the interpretation of neurophysiological data.

## Methods

### Subjects and task

Each of 5 healthy, right-handed, male Air Force jet test pilots practiced a battery of 4 tasks for

about 6 h, until the learning curves for response error stabilized. Subjects began at about 1.30 p.m. the following day, and during the ensuing 10–14 h performed several types of tracking and cognitive tasks, including about 1400 visuomotor memory task trials. The session consisted of a 5–8 h work period, a brief dinner break, then another 5–7 h work period which ended when the subject was too exhausted to continue.

Visuomotor memory task trials were presented in blocks of 50. Except for the first 2 trials in the block, subjects produced a precise finger pressure proportional to a number seen 2 trials back (about 11.5 sec earlier). Each trial began with the disappearance of the letter X from the video screen. A single-digit stimulus number, which the subject was required to remember, appeared 750 msec later. Stimuli were presented for 325 msec on a Videographics-II amber CRT monitor 70 cm from the subject. Stimuli subtended a visual angle under  $1.5^\circ$ , with an illumination of  $11 \text{ cd/m}^2$  against a background of  $0.1 \text{ cd/m}^2$ . When the stimulus number disappeared, the subject was required to produce a pressure of 0.1–0.9 kg with his right index finger on an isometric pressure transducer. The appropriate response pressure corresponded to the stimulus number presented 2 trials earlier.

### VISUOMOTOR MEMORY TASK (VMMT)

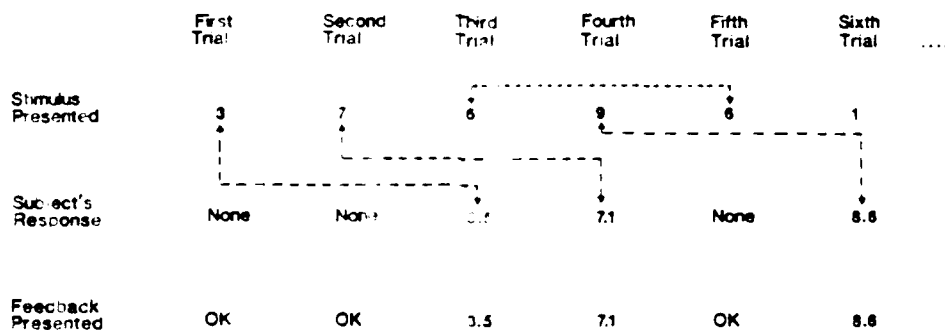


Fig. 1. The visuomotor memory task (VMMT) required that subjects remember, during each trial, a stimulus number from 2 trials back, and produce a precise right index finger pressure in response to that number. Each trial consisted of a warning (disappearance of the letter X from the video screen – not shown), followed 0.75 sec later by presentation of a single-digit visual stimulus to be remembered, followed by the subject's finger-pressure response to the stimulus number presented 2 trials back, followed 1 sec after the peak of the response by presentation of a 2-digit feedback number indicating the accuracy of the response. The feedback number was underlined when the subject's response was highly accurate. Subjects were required to withhold their response when the current stimulus number was identical to the stimulus 2 trials back. (No response was required on the first 2 trials of each block of 50 trials – signified by 'OK').

For example, if the stimulus numbers in 4 successive trials were 3, 7, 6, and 9, the correct responses would be 0.3 kg to the 6 and 0.7 kg to the 9 (Fig. 1). A two-digit feedback number was presented in each trial 1 sec after the peak of the response to indicate the actual pressure exerted. The feedback number was underlined if the response was close to the required response, based on an 'adaptive error tolerance', computed as the geometric mean of the response error (distance from the required pressure response) on the previous 5 trials.

To increase the difficulty, the subject was required to withhold his response in the approximately 20% of the trials when the stimulus number was the same as the number from 2 trials back. For example, if the numbers 6, 9, 6 were presented, the subject was not to respond to the second 6 (Fig. 1).

### Recording

Neuroelectric data were recorded from an array of electrodes built into a nylon mesh hat. Signals were recorded from 27 electrodes and were referenced to the right mastoid. All signals were amplified by a Bioelectric Systems Model AS-64P with 0.016–50 Hz passband and digitized to 11 bits at 128 Hz. Vertical and horizontal eye movements (VEO, HEO), activity of the right flexor digitorum muscle (EMG), cardiac rate (EKG), respiration, and EEG activity at left mastoid were recorded from all subjects. Two technicians, working independently, edited the time-series traces off-line and eliminated data with evidence of contamination by potentials generated by eye movements, muscle activity, or instrumental noise sources. An optimal, least-squares estimate of the laplacian operator was computed to reduce spatial low-pass distortion resulting from transmission through the skull and scalp. Electrodes at the edge of the array were eliminated from the analysis because it is not possible to reliably estimate their laplacian (Gevins et al. 1989a). Even though laplacian-transformed potentials are proportional to current density, we will refer to the wave forms as potentials, in keeping with common usage.

Recording sessions were divided into 3 epochs termed Early, Middle, and Late based on response error (Fig. 2). Each epoch was long enough to

allow us to form stable estimates of the functional brain patterns occurring during it. The Early epoch lasted approximately from 1.30 p.m. to 8.30 p.m., the Middle from 8.30 p.m. to 10.30 p.m., and the Late from 11.30 p.m. to 1.30 a.m.

### Signal analysis

ERCs, a statistical measure of functional inter-relatedness between the time series of 2 channels, were computed from pre- and poststimulus intervals of the task. Although the exact brain sources of scalp ERCs have not yet been determined, intracerebral recording from animals (John et al. 1973; Freeman 1975; Bressler 1987a, b) and scalp recordings from humans (Gevins 1987a; Gevins and Bressler 1988; Gevins et al. 1989a) suggest that ERC patterns reflect the coordinated, low-frequency, task-related dendritic activity pattern of distributed cortical neuronal networks.

ERCs were computed from bandpass-filtered event-related potentials (ERPs) time-locked to the presentation of the numeric stimulus, and averaged over the 5 subjects. Three well-known ERP waves were used as timing markers: the prestimulus CNV during the Finger-Pressure trials, the poststimulus N1-P2 peaks during stimulus processing on the Finger-Pressure trials, and the poststimulus P3 elicited during the infrequent No-Press trials. The prestimulus ERC interval was 500 msec wide and was centered 312 msec before the numeric stimulus (Fig. 3A). The 2 poststimulus ERC intervals were 187 msec wide. The first was centered at 125 msec after the stimulus for Finger-Pressure trials (Fig. 4A) and the second at 375 msec for No-Press trials (Fig. 5A).

Bandpass filters were chosen to enhance the ERP waves of interest. Thus the prestimulus interval was filtered with a 0.01–3 Hz passband to emphasize the CNV, whereas a 4–7 Hz passband was selected for the poststimulus intervals to accentuate the N1-P2 and P3 components. The cross-covariance function was computed to 16 lags ( $\pm 125$  msec) for the 0.01–3 Hz-filtered interval, and to 8 lags ( $\pm 62$  msec) for the 4–7 Hz-filtered intervals. The ERC was defined as the maximum absolute value of the lagged time series cross-covariance function. ERCs for the 3 intervals were computed between all 155 pairwise com-



4

binations of the 18 non-edge scalp electrodes common to all 5 subjects.

#### *Statistical evaluation*

To measure functional changes in the brain strictly related to sustained mental work and unconfounded by variations in performance accuracy, we controlled for the significant effect of response error across the Early, Middle and Late epochs. The most stringent method was to analyze only the most accurate trials from each of the 3 trial sets.

We first selected the most accurate half of each subject's Early trials, and then selected trials with comparable accuracy from corresponding Middle and Late sets. Accurate trials were those with response error less than the mean response error of the Early trial set. We then discarded the least accurate outlier trials of the accurate Middle and Late subsets (roughly 2% of the trials) so that the final accuracy distributions of the three epochs did not significantly differ ( $P > 0.2$  by the Student's  $t$  test). The numbers of total trials in the resulting accurate trial sets were 599 (Early), 520 (Middle), and 402 (Late) (Fig. 2). Measures of motor performance did not differ between these final accurate trial sets. We also selected, from all 3 epochs, No-press trials in which the subjects correctly inhibited their response.

We determined the significance of Early, Middle, and Late ERCs by referring to the standard deviation of the ERC 'noise' distributions obtained with a randomization procedure from the same trial sets. Significant ERCs were those with a probability of being less than 0.05 from the 'noise' distribution. ERC significances in each interval were displayed on computer graphic images of a model head; the thickness of a displayed ERC line is proportional to the negative log of significance. The relative involvement of each electrode site in an ERC pattern was determined by taking the sum of all significant ERCs in which it participated, and displaying at that site a disk whose size was proportional to the sum.

Analysis of variance (ANOVA) of the mean absolute ERC value (called ERC magnitude in Table I) provided an index of the change in mean level of between-site covariation over Early, Mid-

dle, and Late epochs. To compare any 2 epochs for differences in pattern configuration (called ERC pattern in Table I), the 2 patterns of significant ERCs were correlated. The ERCs in each set were pooled from the group of site pairs that had significant ERCs in either pattern. We used a distribution-independent 'Monte Carlo' procedure to estimate correlations between patterns (Efron 1982) since we could not confirm that the data were normally distributed after examining the small number of repeated measures. To compare the significance of ERC magnitude differences with ERP amplitude differences, we tested the change in root-mean-square amplitude over epochs for each ERP wave by ANOVA (ERP amplitude in Table I). Pairwise comparisons of ERC magnitude and ERP amplitude were performed by the Scheffé post-hoc procedure.

ERC patterns of individual subjects were compared by using artificial 'neural network' pattern classification procedures, based on the trial-by-trial discriminability of Early and Middle pre-stimulus intervals (Gevins 1980, 1987b; Gevins and Morgan 1986, 1988; Gevins et al., 1979, 1981, 1983, 1985, 1987, 1989a, b). Single-trial ERCs, computed for channel pairs of the average ERC patterns were considered as possible variables. The ratio of observations (trials) to variables (ERCs) exceeded 10:1 in each analysis. Significance of the average test set classification was assessed by reference to the binomial distribution.

## **Results**

### *Behavioral analysis*

By ANOVA, no significant differences were found between three 100-trial subsets at the beginning, middle and end of the Early epoch. This suggested that performance had asymptoted and that any subsequent performance degradation could be attributed to prolonged mental work. We observed that performance changed from Early to Middle to Late epochs (Fig. 2) with fewest errors occurring, as expected, in trials from the Early epoch. ANOVA revealed a significant increase in response error from Early to Late epochs ( $F(2, 12) = 12.5$ ,  $P < 0.005$ ) (Fig. 2); Scheffé post-hoc

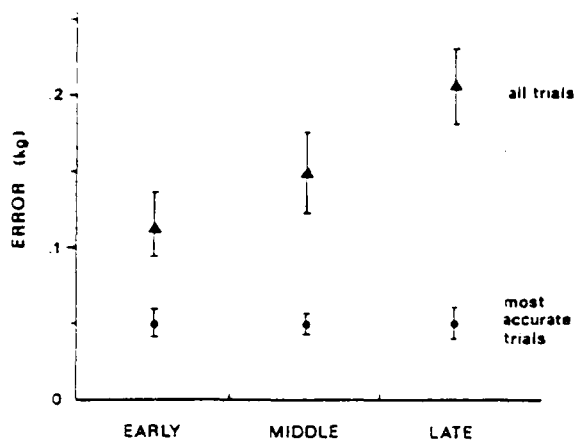


Fig. 2. Mean and standard deviation of response error for Early, Middle, and Late epochs. Upper set of points represents all Finger-Pressure trials, while lower set is from the most accurate Finger-Pressure trials.

comparison revealed that the differences were significant between Middle and Late epochs ( $F(2, 12) = 4.8, P < 0.05$ ) but not between Early and Middle epochs. Reaction time did not differ across

Early ( $543 \pm 169$  msec), Middle ( $584 \pm 155$  msec), and Late ( $593 \pm 97$  msec) epochs. The increase in the proportion of responses during No-Press trials across the 3 epochs (10%, 16%, and 32%) was significant ( $F(2, 12) = 7.4, P < 0.01$ ).

Subjective reports were consistent with the trends in the behavioral data (Table II). Using a 7-level subjective fatigue scale (1 indicates maximal alertness and 7 complete exhaustion), the 5 subjects reported mean ratings of  $3.42 \pm 0.75$  during the Early epoch,  $5.05 \pm 1.23$  during the Middle, and  $6.22 \pm 0.44$  during the Late ( $F(2, 12) = 13.2, P < 0.001$ ). There was little correlation between the subjective fatigue ratings and response error (bootstrap correlation =  $-0.17 \pm 0.25$ ).

#### ERC analysis: prestimulus preparatory interval

ERCs from the prestimulus interval declined in magnitude ( $F(2, 243) = 22.8, P < 10^{-9}$ ) and differed in pattern configuration across the 3 epochs (Fig. 3B and Table I). The greater change from Early to Middle epochs was revealed by the low

TABLE I

Significance of comparisons across Early, Middle, and Late epochs of the day for each of 3 neuroelectric measures in prestimulus, stimulus processing, and response inhibition intervals of the visuomotor memory task. For ERP amplitude and ERC magnitude, the Early vs. Middle vs. Late comparisons were performed by analysis of variance, whereas the pairwise comparisons were performed by the Scheffé post-hoc method. Values are probabilities ( $P <$ ) except in columns headed by 'ERC pattern' which are correlations between event-related covariance distributions. The standard deviation of correlation is shown in parentheses.

Interval (msec)	Early vs. Middle vs. Late epochs			Early vs. Middle epochs		
	ERP amp.	ERC magnitude		ERP amp.	ERC magnitude	ERC pattern
Prestimulus (-562 to -62 msec)	NS	$10^{-9}$		NS	$10^{-4}$	0.06 (0.09)
Stimulus processing (32-219 msec)	NS	0.01		NS	0.05	0.71 (0.09)
Response inhibition (282-469 msec)	0.05	$< 10^{-10}$		NS	$10^{-8}$	0.67 (0.09)
	Early vs. Late epochs			Middle vs. Late epochs		
	ERP amp.	ERC magnitude	ERC pattern	ERP amp.	ERC magnitude	ERC pattern
Prestimulus (-562 to -62 msec)	NS	$10^{-8}$	0.01 (0.09)	NS	NS	0.42 (0.11)
Stimulus processing (32-219 msec)	NS	NS	0.62 (0.07)	NS	0.05	0.44 (0.14)
Response inhibition (282-469 msec)	0.05	$< 10^{-10}$	0.66 (0.07)	NS	0.0005	0.51 (0.16)

headed

ERC

-562 to -62

TABLE II

Mean subjective fatigue ratings from each of the 3 epochs for the 5 subjects based on a 7-level subjective fatigue scale (1 indicates maximal alertness and 7 complete exhaustion).

Subject	Early	Middle	Late
1	3.51	5.00	6.12
2	4.12	6.00	6.00
3	3.20	5.25	6.00
4	4.00	6.00	7.00
5	2.25	3.00	6.00
Mean	3.42	5.05	6.22
(S.D.)	(0.75)	(1.23)	(0.44)

Early-to-Middle bootstrap correlation (0.06) when compared to the Middle-to-Late one (0.42), and by the significant decline in Early-to-Middle ERC magnitude ( $F(2, 243) = 11.2$ ,  $P < 0.0001$ ) when compared to the non-significant Middle-to-Late difference. Dominance by the midline central (Cz) site in the Early epoch was replaced by right-sided dominance (focused at the right antero-central (aC4) site) in the Middle epoch, which continued into the Late epoch (Table III). The ERP amplitude in this interval declined by 15% from Early to Middle epochs and then rose by 3% in the Late epoch; the change over the 3 epochs was not significant.

#### ERC analysis: visual stimulus processing interval

The amplitude of the poststimulus N1-P2 ERP component did not change with time-on-task (Fig. 4A and Table I, middle row). The mean absolute ERC magnitude declined from the Early (9.5

TABLE III

Sums of event-related covariances at top 3 sites in prestimulus, stimulus processing, and response inhibition intervals for Early, Middle and Late epochs of the day. Designation of sites is as follows: aC3 = left antero-central, aCz = midline antero-central, aC4 = right antero-central, C3 = left central, Cz = midline central, Pz = midline parietal, P4 = right parietal, pP1 = left postero-parietal, pP2 = right postero-parietal.

Interval		Early	Middle	Late
Prestimulus	1 Cz	624	aC4 282	aC4 235
	2 aCz	415	P4 277	P4 221
	3 pP1	330	aCz 240	C3 162
Stimulus processing	1 Pz	237	Pz 178	Cz 197
	2 Cz	200	Cz 140	pP2 196
	3 aCz	173	aC3 123	Pz 187
Response inhibition	1 aCz	574	aCz 284	aCz 103
	2 aC3	360	aC3 199	Cz 77
	3 aC4	344	aC4 186	aC4 30

+/- 5.8) to Middle (7.5 +/- 4.5) epochs, but then rose in the Late (9.9 +/- 4.8) epoch. Although this change across the 3 epochs was significant ( $F(2, 225) = 4.8$ ,  $P < 0.01$ ), the effect was considerably less robust than for either the prestimulus CNV or subsequent P3 intervals. The Early and Middle ERC patterns (Fig. 4B) were similar (bootstrap correlation = 0.71 +/- 0.09), and both had many features in common with the Late pattern. In particular, the midline parietal (Pz) and midline central (Cz) sites were among the top 3 focal sites in all 3 epochs (Table III). The Middle and Late patterns differed most (bootstrap correlation = 0.44 +/- 0.14), largely because involvement of the right postero-parietal (pP2) site increased in the Late pattern.

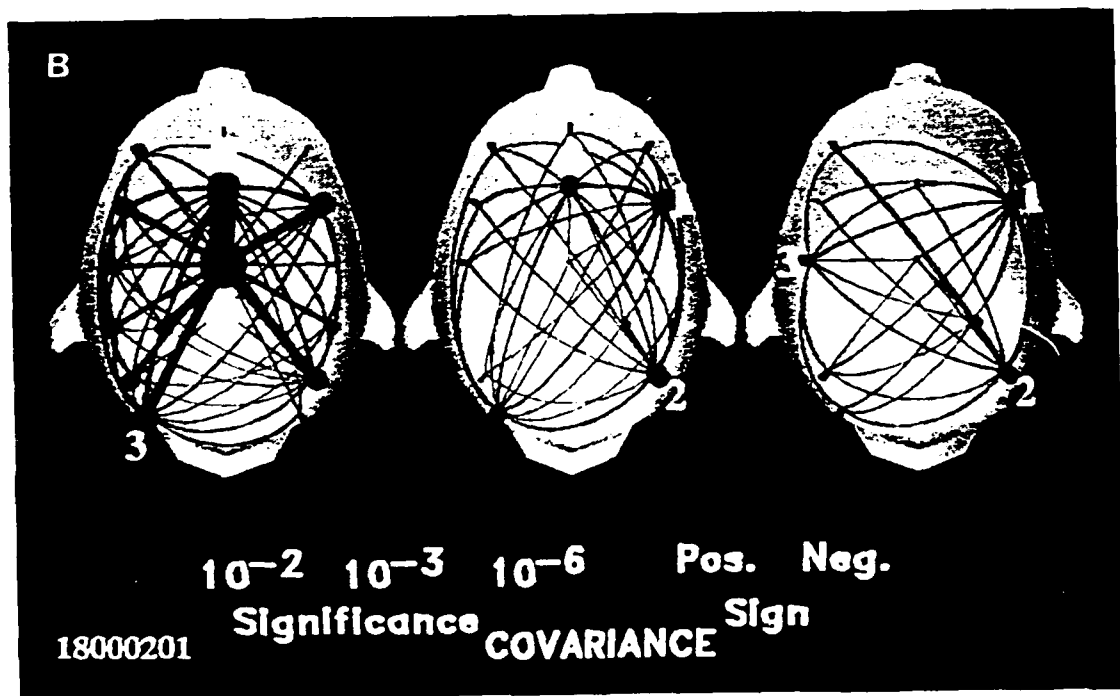
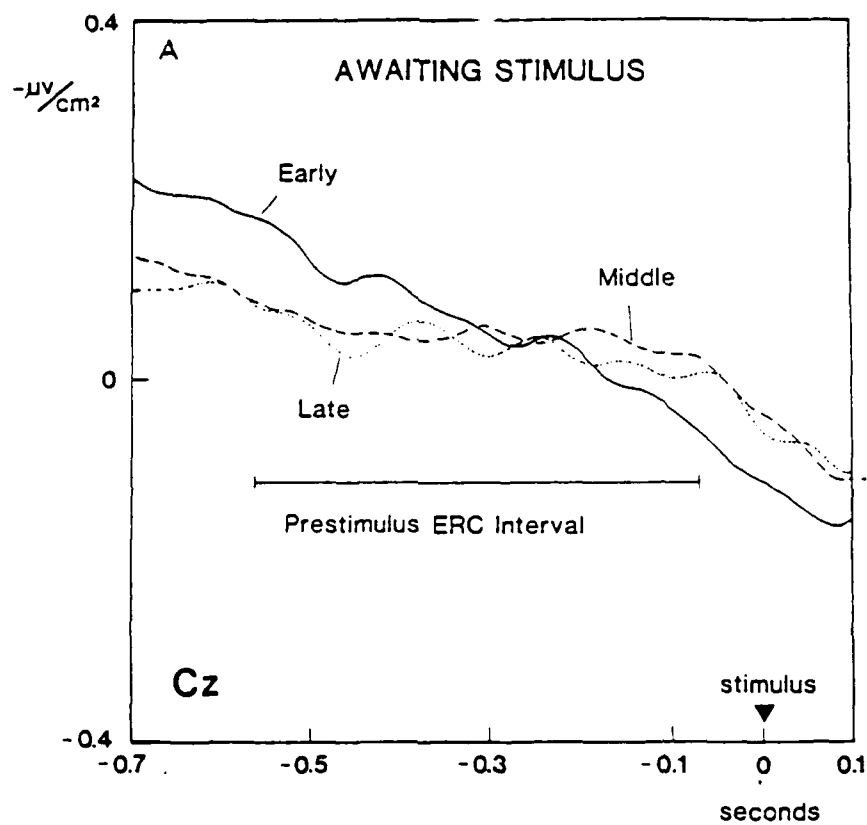
Fig. 3. A: Grand

average (over all 5 subjects), event-related potential (ERP) laplacian wave forms of the midline central (Cz) electrode during a 700 msec interval when subjects were expecting the next VMMT stimulus. Accurate Early (594 trials, solid line), Middle (517 trials, dashed line), and Late epoch (394 trials, dotted line) averages are shown. The indicated prestimulus ERC interval was used for computing the event-related covariance patterns shown in B. The root-mean-square ERP amplitude of this interval did not significantly differ across Early, Middle, and Late epochs. B: Event-related covariance (ERC) patterns characterizing the prestimulus Early (left), Middle (center), and Late (right) epochs. The view is from above the head with the nose at the top of the figure. ERCs were computed from ERPs across the -562 to -62 msec prestimulus interval shown in A. The thickness of a line is proportional to the negative logarithm of the significance (from 0.000005 to 0.05) of the covariance between 2 electrodes. A violet line indicates a positive covariance (waves of same polarity), while a blue line represents a negative covariance (waves of opposite polarity). The radius of the disk at each site is proportional to the sum of the absolute values of the significant ERCs in which that site participated. Not only did the ERC magnitude greatly decline from Early to Middle to Late epochs, but the ERC pattern also changed, with the emphasis shifting from the midline central and precentral and left parietal sites to the right antero-central and parietal and left central sites.

(2,225)

+/-

event



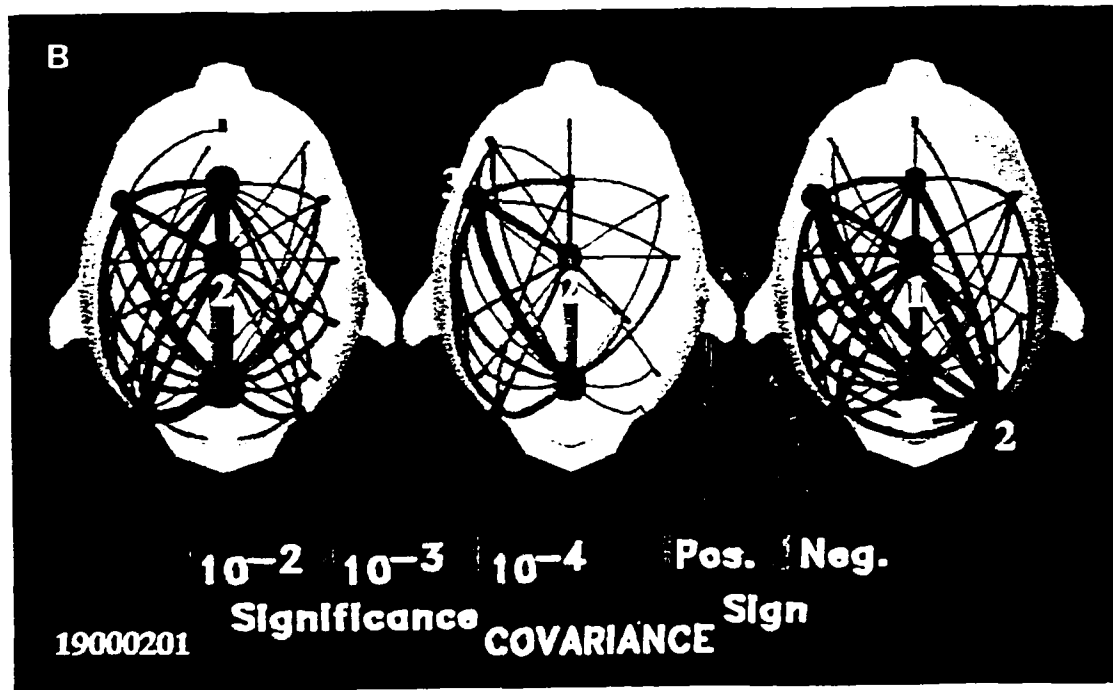
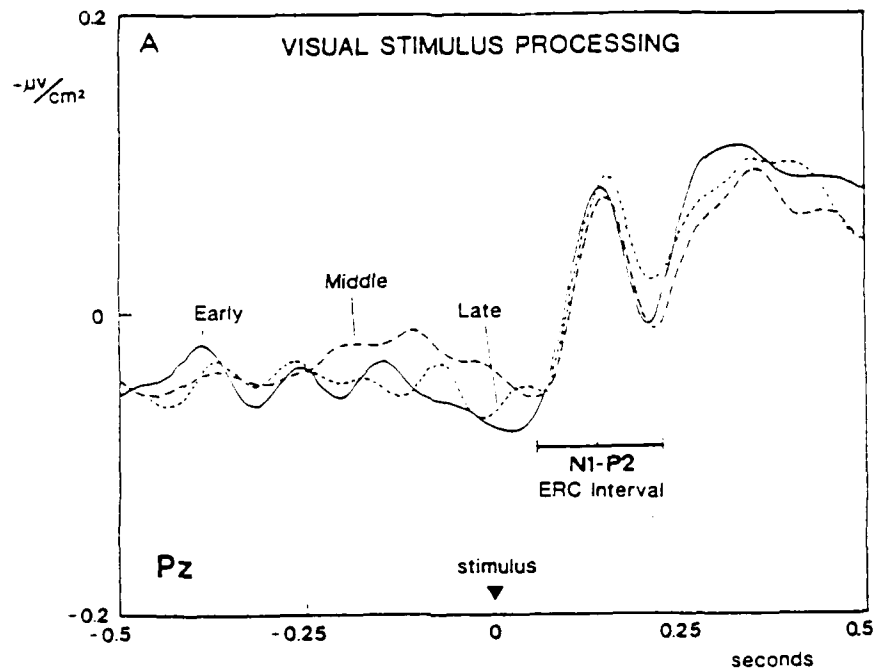


Fig. 4. <sup>A</sup> Accurate Early (562 trials, solid line), Middle (517 trials, dashed line), and Late (384 trials, dotted line) grand-average ERPs of the midline mid-parietal (Pz) electrode site, showing the N1-P2 interval following presentation of the visual stimulus. As in the prestimulus interval, the ERP amplitude did not differ significantly across the Early, Middle, and Late epochs. B: ERC patterns characterizing the poststimulus N1-P2 interval in Early (left), Middle (center), and Late (right) epochs. ERCs were computed from ERPs across the 187 msec long poststimulus interval shown in A. The mean ERC magnitude changed only moderately from Early to Middle to Late epochs: the top focal sites remained nearly the same.

A: Accurate

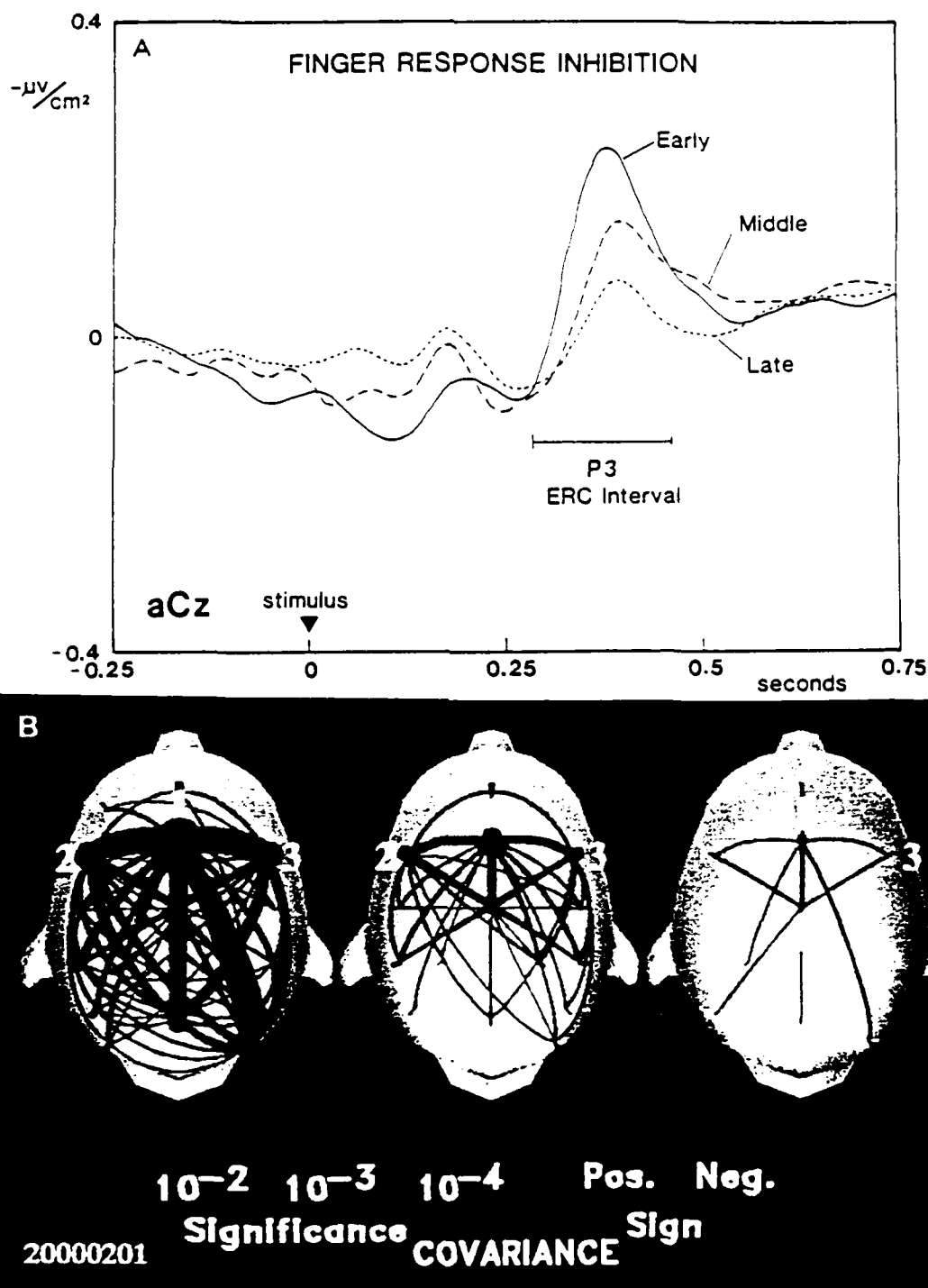


Fig. 5. A: accurate Early (243 trials, solid line), Middle (250 trials, dashed line), and Late (261 trials, dotted line) grand-average ERPs for the finger response inhibition ('No-Press') trials, showing the P3 peak at about 380 msec after the stimulus at the midline antero-central (aCz) electrode site. The P3 amplitude declined from Early to Middle to Late epochs. B: 'No-Press' ERC patterns characterizing Early (left), Middle (center), and Late (right) epochs. ERCs were computed from ERPs during the 231-468 msec poststimulus interval shown in A. As in the prestimulus interval, there was a marked global decline in ERC magnitude. However, unlike the case in the prestimulus interval (but like the N1-P2 interval), the 3 patterns were very similar.

Accurate

'No-Press'

### *ERC analysis: response-inhibition interval*

ERCs from the poststimulus interval of No-Press trials declined greatly in magnitude ( $F(2, 231) = 54.7$ ,  $P < 10^{-10}$ ), but did not differ greatly in pattern configuration (Table I and Fig. 5B). There was also a significant decline in P3 amplitude ( $F(2, 51) = 4.4$ ,  $P < 0.05$ ). The stability of the pattern configuration was seen in the similarity between the Early-to-Middle and the Middle-to-Late bootstrap correlations, and by the dominance of the patterns by the antero-central sites in all 3 epochs (Table III). There were highly significant ERCs between these sites and the midline parietal (Pz) and right posterior parietal (pP2) sites.

### *Individual subject analysis*

We next determined the extent to which individual subject patterns corresponded to the group patterns, and the extent to which it was possible to distinguish individual trials taken from different epochs of the session. Since the ERC patterns from the prestimulus intervals in the Early and Middle epochs were so strikingly different, we tested inter-subject variability on these data sets. Five equations were formed on four-fifths of the trials, and tested on the remaining one-fifth.

Discrimination was above 57% ( $P < 0.05$ ) for 3 subjects, but was 49% (chance) for the other two. Average test-set discrimination was 62% ( $P < 0.001$ ) for separate analyses of the first 3 subjects and 61% ( $P < 0.001$ ) for the latter two. Finally, a fourth analysis used only trials from the subject with the best classification in the 5- and 3-subject analyses. The average test-set discrimination was 81% ( $P < 0.001$ ). Thus, individual trials from the Early and Middle data sets could be distinguished with increased accuracy when the 5 subjects were divided into 2 groups, and for an individual subject.

### **Discussion**

A fundamental theme in contemporary cognitive neuroscience is that mental function is composed of multiple information-processing subsystems associated with neural networks in the brain.

The British neurologist Henry Head, an early 20th century proponent of this idea, considered that impaired 'vigilance' could cause 'high-grade functions (to) suffer in general or in part', and that neural systems could thus be affected either globally or selectively (Head 1926). We observed 2 major effects of sustained mental work that support Head's original ideas: (1) a global decrease in ERC magnitudes, consistent with the well-known spatially widespread reduction in neuroelectric signals with decreasing alertness (Gevins et al. 1977; Broughton 1982; Santamaria and Chiappa 1987); and (2) a previously unreported, temporally specific change in ERC pattern configuration.

The prestimulus ERCs underwent a considerable change in pattern, together with a large reduction in magnitude, from the Early to Middle epochs. The poststimulus response inhibition ERC pattern strength was also reduced, but without much pattern change from Early to Middle and from Middle to Late epochs. Except for the emergence of the right postero-parietal site in the Late epoch, the stimulus processing ERCs underwent relatively little change in ERC pattern or magnitude. These results suggest that specific cortical areas involved in response preparation were most affected by prolonged mental work and that those involved in response inhibition were also affected. Cortical areas involved in primary visual stimulus processing were considerably less affected.

Although the source of ERCs is still unknown, the present results conform to the hypothesis that ERC patterns reflect underlying cortical networks. The prominence of the midline central and antero-central sites in the prestimulus interval is consistent with a cortical network component responsible for motor preparation, since these sites overlie the supplementary motor area (Brodmann area 6). The declining prominence of these sites over the 3 epochs may reflect decreasing involvement of the motor planning component with sustained mental work, perhaps due to automatization. That these sites were also pronounced in the ERC pattern of the poststimulus N1-P2 interval suggests that this component remains in operation following the stimulus. Prominence of the midline parietal site may reflect a cortical network component concurrently involved in extracting the value

of the stimulus from the visual image. In the poststimulus P3 interval, when subjects were inhibiting their response, the three antero-central sites largely dominated the patterns in all three epochs. These sites overlaid supplementary and premotor areas, known to be necessary for higher order motor control such as response inhibition. The continued prominence of these sites in all 3 epochs suggests that these areas are critically involved in response inhibition, even as the strength of the pattern is reduced with sustained mental work.

Our findings also indicate that, since dramatic changes in brain activity patterns occurred before performance deteriorated significantly, measures of brain activity may be more sensitive indicators of the deleterious effects of sustained mental work than measures of overt behavior. This evidence could explain, in part, the increased vulnerability to life threatening accidents that exists during the early stages of prolonged mental activity, when performance has not yet become significantly degraded. Further refinement of the techniques used in this study, and their application to single-trial data, could lead to the development of on-line warning systems in which persons engaged in critical or hazardous work would be alerted to the possibility of impaired performance due to mental overwork.

The collaboration of Dr. William Storm, U.S. Air Force School of Aerospace Medicine, San Antonio, TX, and Dr. James Smith, Systems Technology Inc., Hawthorne, CA is gratefully acknowledged. Research support was provided by the USAF School of Aerospace Medicine, The USAF Office of Scientific Research, The National Institutes of Neurological Disorders and Strokes, and The National Science Foundation. Thanks to N. Morgan, D. Greer, R. Fauette and other EEG Systems Laboratory personnel for scientific and engineering support.

## References

- Aguirre, M. and Broughton, R.J. Complex event-related potentials (P300 and CNV) and MSLT in the assessment of excessive daytime sleepiness in narcolepsy-cataplexy. *Electroenceph. clin. Neurophysiol.*, 1987, 67: 298-316.
- Bressler, S.L. Relation of olfactory bulb and cortex. I. Spatial variation of bulbocortical interdependence. *Brain Res.*, 1987a, 409: 285-293.
- Bressler, S.L. Relation of olfactory bulb and cortex. II. Model for driving of cortex by bulb. *Brain Res.*, 1987b, 409: 294-301.
- Broughton, R. Performance and evoked potential measures of various states of daytime sleepiness. *Sleep*, 1982, 5: 135-146.
- Davies, D. and Parasuraman, R. *The Psychology of Vigilance*. Academic Press, New York, 1982.
- Efron, B. *The Jackknife, The Bootstrap, and Other Resampling Plans*. Society for Industrial and Applied Mathematics, Philadelphia, PA, 1982.
- Freeman, W. *Mass Action in the Nervous System*. Academic Press, New York, 1975.
- Gevins, A.S. Pattern recognition of human brain electrical potentials. *IEEE Trans. Patt. Anal. Mach. Intell.*, 1980, PAMI-2: 383-404.
- Gevins, A.S. Correlation analysis. In: A.S. Gevins and A. Rémond (Eds.), *Methods of Analysis of Brain Electrical and Magnetic Signals. Handbook of Electroencephalography and Clinical Neurophysiology, Revised Ser., Vol. 1*. Elsevier, Amsterdam, 1987a: 171-193.
- Gevins, A.S. Statistical pattern recognition. In: A.S. Gevins and A. Rémond (Eds.), *Methods of Analysis of Brain Electrical and Magnetic Signals. Handbook of Electroencephalography and Clinical Neurophysiology, Revised Ser., Vol. 1*. Elsevier, Amsterdam, 1987b: 541-582.
- Gevins, A.S. and Bressler, S.L. Functional topography of the human brain. In: G. Pfurtscheller and F.H. Lopes da Silva (Eds.), *Functional Brain Imaging*. Hans Huber, Bern, 1988: 99-116.
- Gevins, A.S. and Morgan, N.H. Classifier-directed signal processing in brain research. *IEEE Trans. Biomed. Eng.*, 1986, BME-33: 1054-1068.
- Gevins, A.S. and Morgan, N.H. Applications of neural-network (NN) signal processing in brain research. *IEEE ASSP Trans.*, 1988, 36: 1152-1161.
- Gevins, A.S., Zeitlin, G.M., Ancoli, S. and Yeager, C. Computer rejection of EEG artifact. II. Contamination by drowsiness. *Electroenceph. clin. Neurophysiol.*, 1977, 42: 31-42.
- Gevins, A.S., Zeitlin, G.M., Doyle, J.C., Schaffer, R.E., Yingling, C.D., Yeager, C.L. and Callaway, E. EEG correlates of higher cortical functions. *Science*, 1979, 203: 665-668.
- Gevins, A.S., Doyle, J., Cuttito, B., Schaffer, R., Tannehill, R., Ghannam, J., Gilcrease, V. and Yeager, C. Electrical potentials in human brain during cognition: new method reveals dynamic patterns of correlation. *Science*, 1981, 213: 918-922.
- Gevins, A.S., Schaffer, R.E., Doyle, J.C., Cuttito, B.A., Tannehill, R.S. and Bressler, S.L. Shadows of thought: shifting lateralization of human brain electrical patterns during brief visuomotor task. *Science*, 1983, 220: 97-99.
- Gevins, A.S., Doyle, J.C., Cuttito, B.A., Schaffer, R.E., Tannehill, R.S. and Bressler, S.L. Neurocognitive pattern analysis of a visuospatial task: rapidly-shifting foci of evoked correlations between electrodes. *Psychophysiology*, 1985, 22: 32-43.
- Gevins, A.S., Morgan, N.H., Bressler, S.L., Cuttito, B.A., White,

on-line

A. White



- R.M., Illes, J., Greer, D.S., Doyle, J.C. and Zeitlin, G.M. Human neuroelectric patterns predict performance accuracy. *Science*, 1987, 235: 580-585.
- Gevins, A.S., Bressler, S.L., Morgan, N.H., Cuttito, B.A., White, R.M., Greer, D.S. and Illes, J. Event-related covariances during a bimanual visuomotor task. I. Methods and analysis of stimulus- and response-locked data. *Electroenceph. clin. Neurophysiol.*, 1989a, 74: 58-75.
- Gevins, A.S., Cuttito, B.A., Bressler, S.L., Morgan, N.H., White, R.M., Illes, J. and Greer, D.S. Event-related covariances during a bimanual visuomotor task. II. Preparation and feedback. *Electroenceph. clin. Neurophysiol.*, 1989b, 74: 147-160.
- Head, H. *Aphasia and Kindred Disorders of Speech*. Cambridge University, Cambridge, 1926.
- Hori, T. Spatiotemporal changes of EEG activity during waking-sleep transition period. *Int. J. Neurosci.*, 1985, 27: 101-114.
- John, E.R., Bartlett, F., Schumokaochi, M. and Kleinman, D. Neural readout from memory. *J. Neurophysiol.*, 1973, 36: 893-924.
- Kellaway, P. and Maulsby, R. The normative electroencephalographic data reference library. Final report, NASA contractor report NAS9-1200, National Aeronautics and Space Administration, Washington, DC, 1967.
- Lubin, A., Johnson, L.C. and Austin, M.T. Discriminating among states of consciousness using EEG spectra. *Agressologie*, 1969, 10: 593-600.
- Mane, A., Sirevaag, E., Coles, M.G.H. and Donchin, E. ERPs and performance under stress conditions. *Proc. Soc. Psychophysiol. Res.*, 1983, 20: 458.
- Matejcek, M. Vigilance and the EEG: psychological, physiological and pharmacological aspects. In: W. Hermann (Ed.), *EEG in Drug Research*. Gustav Fischer, New York, 1982: 405-508.
- Matoušek, M. Automatic analysis in clinical electroencephalography. Research Report-9, Psychiatric Research Institute, Prague, 1967.
- Naitoh, P., Johnson, L.C. and Lubin, A. Modification of surface negative slow potential (CNV) in the human brain after total sleep loss. *Electroenceph. clin. Neurophysiol.*, 1971, 30: 17-22.
- Parasuraman, R., Warm, J.S. and Dember, W.N. Vigilance: taxonomy and utility. In: L.S. Mark, J.S. Warm and R.L. Huston (Eds.), *Ergonomics and Human Factors: Recent Research*. Springer, New York, 1987: 11-32.
- Roth, B. The theoretical and clinical importance of EEG rhythms corresponding to states of lowered vigilance. *Electroenceph. clin. Neurophysiol.*, 1962, 31: 231-237.
- Santamaria, J. and Chiappa, K.H. *The EEG of Drowsiness*. Demos Publications, New York, 1987.
- Walter, D.O., Rhodes, J.M. and Adey, W.R. Discriminating among states of consciousness by EEG measurements. *Electroenceph. clin. Neurophysiol.*, 1967, 22: 22-29.
- Warm, J.S. and Parasuraman, R. (Eds.), ~~*J. Hum. Factors Soc.*~~ 1987, 29: 623-740.
- Williams, H.L., Morris, G.O. and Lubin, A. Illusions, hallucinations and sleep loss. In: J.L. West (Ed.), *Hallucinations*. Grune and Stratton, New York, 1962: 158-165.

Title of  
article or  
book?

Vigilance: Basic and Applied Research. Human Factors,

### III. FUNCTIONAL TOPOGRAPHY OF LANGUAGE

#### A. Introduction

This study was designed to measure spatiotemporal evoked potential patterns during several types of linguistic operations. The well-substantiated role of the 'language' areas of posterior frontal and temporal cortices of the dominant hemisphere makes language a good choice for studying the localization of neurocognitive processes. Numerous studies have attempted to measure language-associated lateralization and/or localization in the EEG and EP, but to date the findings have been highly inconsistent (reviewed in Beaumont, 1983; Gevins, 1983; Molfese, 1983; Rugg, 1983; Butler and Glass, 1986; Gevins & Cutillo, 1986; Kutas and Van Petten, 1988). Processes studied include acoustic and phonemic processing (Wood, 1975; Molfese, 1979; Lovrich et al., 1986), semantic context (Brown et al., 1979; Kutas, et al., 1984), semantic priming (Rugg, 1985), lexical and semantic functions (Buchsbaum and Fedio, 1970; Chapman et al., 1978; Fishler et al., 1987), and syntax (Kutas and Hillyard, 1980a, 1983). The series of studies by Kutas and colleagues include, in addition to the N400 studies, studies of natural sentence processing, grammar, and differences between open-class (content) and closed-class (function) words (Kutas and Hillyard, 1980abc; Kutas et al., 1984; Kutas and Van Petten, 1988). Whereas the many studies concentrated on the EP correlates of fairly complex linguistic issues (e.g. "semantic appropriateness"), we directed this study toward the measurement of the spatial and temporal characteristics of very basic linguistic functions.

A number of studies have reported language-associated hemispheric lateralization of EP peaks, sometimes with larger amplitudes over the left (dominant) hemisphere. Unfortunately, many of these studies were methodologically flawed and had too few recording channels (review in Gevins and Cutilo, 1986). Regional cerebral blood-flow studies of language have shown patterns of activation in the non-dominant hemisphere which are almost mirror-images of those in the dominant hemisphere (Lassen et al., 1978), while more recent PET studies have reported more left-sided activity (Petersen et al., 1988). Further, brain stimulation mapping (Ojemann, 1983) indicates that at the cortical level, language functions are organized into a complex "mosaic" of local perisylvian areas on the order of a couple centimeters in size, which are involved in particular aspects of language processing. Brain potentials associated with bilateral activation might not exhibit gross lateralizations of amplitude, and the measurement of highly localized activity would require more detailed spatial sampling than is usually used. The present study demonstrates that there is both a great amount of commonality between elementary linguistic processes, as well as highly localized differences which are observable through the use of sufficiently dense spatial sampling and techniques of spatial enhancement such as Laplacian Transform.

Classical neurological and neurolinguistic thinking has emphasized a localizationist-serial model for language processing (see for example Geschwind, 1970), but more modern models consider networks of sub-processes and codes (visual or auditory encoding, phonological, semantic, syntactic processing) that operate in a parallel, distributed fashion during language processing (Petersen et al., 1988; Posner, 1978). In a recent study, Petersen et al. (1988) used Oxygen-15 Positron Emission Tomography (PET) to study healthy subjects performing a series of language tasks. The activation patterns they found were generally consistent with neurological theory. For example, activations were found in supplementary motor and inferior frontal areas for word generation, and in cingulate areas for attention. Their results also suggest that phonological decoding for familiar, visually presented words can be bypassed by good readers, consistent with current cognitive-reading theory. A somewhat unexpected finding, however, was the activation of frontal areas during the lexical processing of single words, which would be expected to involve Wernicke's language area in the posterior perisylvian region. Although their results were interpreted in terms of currently popular parallel-processing models, this interpretation must be considered speculative because of the 40 to 60-second measurement aperture of the O-15 PET technique. Without more precise timing information, it is difficult to say whether areas were active during the entire task processing, whether they were sequentially activated, or whether there was some complex combination of sequential and parallel processes. The present study was

designed to obtain temporal detail of cortical processing during receptive language processing: form (or letter) perception, phonemic encoding, semantic retrieval, and simple syntactic judgements.

In our experimental design, EEGs were measured while subjects processed sequential pairs of visual stimuli in four-second trials. First, a cue indicated the type of judgment to be made, and then the first and second stimuli (S1 and S2) were presented at successive 1 sec intervals. The subject had to determine whether the S2 formed a "match" to the S1. To form a "match," S1 and S2 had to be physically identical in the graphic condition, be homophones in the phonemic condition, be related as antonyms in the semantic condition, or form a correct subject-verb combination in the grammatical condition. Subjects responded to mismatches with a left-hand finger press, and received visual feedback about their performance.

There are conceptual similarities between our experiment and Petersen et al.'s (1988) paradigm, including the fact that neural measurements are made while subjects perform increasingly complex types of tasks. Petersen, et al., assume that each level can be "subtracted" from the next "higher" level in order to isolate distinct higher-order processes. This was necessitated in part by the 40 to 60 second sampling interval required by the O-15 PET technique. Our experiment differs in that we were also able to obtain information about sequential, split-second changes in the patterns of activity of cortical networks involved in graphic, phonemic, semantic and syntactic processing. (Our technique does not however, allow full three-dimensional imaging of neural activity.)

## B. Hypotheses

The four conditions were designed to differ along the following dimensions: letter/non-letter (graphic condition versus phonemic, semantic and grammatic conditions), word/non-word (graphic and phonemic versus semantic and grammatic conditions), and syntactic/non-syntactic (grammatic versus semantic conditions). Presumably, sites of the dominant hemisphere overlying Broca's and possibly Wernicke's areas would be important in these distinctions. This hypothesis follows from the findings of Zurif and others (Kolk, 1978; Bradley et al., 1980; Zurif, 1980), based on lesion studies, that Broca's area is involved in the receptive deficits of a phonemic nature. Similarly, semantic processing should be distinguishable from phonemic processing at sites involving Wernicke's area for the processing of meaning. Grammatical processing should be distinguishable from semantic processing in the relative involvement of sites over and anterior to Broca's area, and perhaps Wernicke's language area. On the basis of our studies of task-specific preparation (Gevins et al., 1987, 1989b), we expected that effects of task-specific preparatory processes might be seen in the cue-to stimulus epoch.

## C. Piloting

There were two phases in piloting the experiment. In the first phase, 50% of the trials were matches, 50% were mismatches, and subjects were required to make a motor response to both. Since we are particularly interested in the processing associated with match trials, we changed the probability of a match to 85%, and had subjects respond only to the mismatch trials (15%). This eliminated signals related to response preparation and execution from the match trials, while the 15% mismatch trials served primarily to ensure that the subjects were performing the task. To help ensure subjects' attention to the task, the rewards were changed so that subjects lost 25 cents for failing to respond to a mismatch.

## D. Methods

### 1. Subjects

Nine healthy, right-handed (modified Edinburgh Scale), male volunteers between the ages of 21 and 35 participated in the experiment. None had any history of neurologic or psychiatric disease, and all were native English speakers, with no knowledge of Japanese.

### 2. Stimuli

EEGs were recorded while subjects determined if pairs of visual stimuli were identical in appearance (graphic condition), were the same in pronunciation (phonemic condition), had opposite meaning (semantic condition), or formed a grammatically correct subject-verb combination (grammatical condition) (See Figure 1). Asterisks were positioned in front of and after each stimulus to adjust differences in stimulus length. The horizontal visual angle was under two degrees and the vertical visual angle under 0.5 degrees. The average luminance, based on a random sampling of the luminance of 240 stimuli (60 from each condition), was 1.43 lux.

#### *Graphic condition:*

Stimuli in the Graphic condition were strings of Katakana characters, which are a set of characters from Kana, the syllabic script of written Japanese. The strings were either three (50%) or four characters (50%) long. Characters that were highly similar to each other or that had disjointed elements were not used. In graphic match trials the two stimuli were identical. In mismatch trials, 1 or 2 characters of S2 were changed, but never the first character. The number of characters in a pair was always the same.

#### *Phonemic condition:*

Stimuli in the phonemic condition were pronounceable non-words which conformed to the rules of English orthography. They were three to six characters in length, and began and ended with one to three consonants. Each letter of the string contributed to its pronunciation; (e.g., the consonant combination "ck," or words ending in a consonant followed by "e" as in 'dove' were not used). All stimuli were monosyllabic, and words that were homophones to real English words or acronyms were not used.

The guidelines discussed by Vitz and Spiegel-Winkler (1973) were used to generate the non-words and their homophones for the match trials. In 19% of the pairs the first consonant or consonantal cluster was changed; in 40% of the pairs, the final consonant or consonantal cluster was changed; in 32% of the pairs, the vowel or vowel cluster was changed, and in 5% of the pairs both the vowel and consonant were changed.

Heterophonic pairs were generated by changing one or more of the phonemes of S2 non-words. In order to minimize motor cueing, at least the manner or place of articulation of the original phoneme and the phoneme changed in the S2 were preserved. For example, the stop consonants /b/ or /d/ were foiled by other stop consonants such as /p/ or /t/, but never by the nasal or fricative consonants such as /m/ or /f/. Vowel forms that have more than one pronunciation (eg: the present and past-tense forms of *read*) were not used. In 3% of the mismatch pairs the first consonant or consonantal cluster was changed; in 72% of the pairs the final consonant or consonantal cluster was changed; in 6% of the pairs the vowel or vowel cluster was changed, in 11% of the pairs both the vowel or consonant or vowel/consonantal cluster was changed, and in 5% of the pairs both the first and final consonants were changed. For example, *terp* and *tirb*, *trolph* and *trorf*.

*Semantic condition:*

The stimuli of the semantic task were formed from open-class, relatively high-frequency monosyllabic English words. Match trials were formed from two words that are antonyms, defined as two words representing a concept in oppositional relation to each other (Gardner et al., 1976). The antonyms were selected from a variety of sources including Bolander et al. (1985) and Urdang (1984), and were always of the same functional category (verbs with verbs, adjectives with adjectives). 75% were noun or verb pairs, 25% adjective or adverb pairs. Words with irregular pronunciation, or more than one pronunciation were not used. The mismatch pairs were composed of words meeting the criteria described above, except that they were not related semantically, phonetically or formally (e.g., *hot*, *real*).

*Grammatical condition:*

Grammatical stimulus pairs were composed of a pronoun followed by a verb which formed a short meaningful sentence (e.g., He swims). The verbs were all open class, high frequency, monosyllabic, and intransitive (Webster's New Universal Unabridged Dictionary, 1983). Verbs were used as many as three times, but always with a different agent. As in the semantic condition, words with irregular pronunciation or multiple pronunciations were not used. Mismatched pairs were composed of pronoun verb combinations which did not form a complete, grammatical sentence. The S2 was a noun or adjective that could not be used as a verb (such as: he *oat*), but the S2 was never neologistic (such as forming *bolds* from the adjective *bold*). Moreover, the S2 verb was conjugated incorrectly with respect to the agent, so that the third-person conjugation was given to the first-person forms, and first-person conjugation to third-person forms.

### 3. Types of Trials

Each trial of the task began with a visual cue that signaled the condition of that trial (L: "looks alike"; S: "sounds alike"; O: "opposites"; G: "grammatical"). Conditions were presented in random order. S1 was presented 1 sec later, and S2 1 sec after S1. Subjects were instructed to press a button with the left index finger for mismatched pairs (15% of the trials). The maximum allowable RT on mismatch trials was 1500 msec. Subjects were instructed to press when uncertain whether the trial was a match or mismatch. There were 5 possible types of feedback:

- (1) Correct match trial (no-press): Fixation dot appears 1500 msec after S2. The subject earned two cents for not responding.
- (2) Correct mismatch trial (press): feedback symbol "+" was presented one sec after response onset. The subject earned 2 cents for responding.
- (3) False positive (incorrect match trial): feedback "0" was presented 750 msec after response. The subject earned no money.
- (4) Incorrect mismatch trial (no-press): feedback symbol "-" was presented 1200 msec after S2. The subject lost 25 cents.
- (5) A downward triangle "▽" was presented immediately after a response that was produced too soon (less than 300 msec) after S2. The subject neither earned nor lost money.

The intertrial interval was automatically delayed until there were no detectable eye-movements, and was at least 2 sec long. Subjects were given 80 training trials before recording began. Duration of cue, S1, S2 and feedback was 150 msec.

#### 4. Recordings

Each subject performed 1200 task trials presented in blocks of 20, randomized as to condition and response requirement. Subjects were given four blocks of training before EEG data were recorded. This was sufficient in most cases for performance to reach a stable level. If not, a second set of 80 trials was given. Subjects earned \$7.00/hour, in addition to the bonuses for correct performance.

EEGs were recorded from 59 scalp electrodes referenced to the midline anterior-parietal (aPz) electrode. The montage was an extended 10-20 system (Gevins, 1988), and included the frontal sites aF1 and aF2, Fz, F3 to F8, and Fpz; the anterior central aCz, aC1 to aC6; Central Cz, C3 & C4; anterior temporal aT5 & aT6; temporal T3 to T8; lower temporal lT1, lT2, lT5, lT6; ventral temporal vT5 and vT6; anterior parietal aP1 to aP6; parietal Pz, P3 to P6; anterior occipital aO1 & aO2; occipital Oz, O1 & O2; ventral occipital vO1 & vO2; and the inion (I) and both mastoids (M1 & M2). Vertical eye movements were recorded bipolarly from an electrode pair placed supra- and suborbitally; horizontal eye movements were recorded bipolarly between electrodes at the outer canthus of each eye. Other bipolar pairs were placed over flexor digitorum muscles of left and right arms to record EMG, and at the submentalis to record subvocal movements of the larynx and mouth. The EEG was amplified 8333 times, band-pass filtered from 0.5-50 Hz and recorded at 128 samples per sec. Electrode positions were digitized in 3 dimensions with a Balhemus Navigation Sciences 3-SPACE ISOTRACK in order to accurately determine interelectrode distances for computation of a 2-dimensional nearest-neighbor local Laplacian transform.

#### 5. Analysis

Trials with eye movement, left-hand EMG in match trials, any right-hand EMG, or instrumental artifacts were eliminated by visual editing prior to averaging. An optimal, least-squares estimate of the Laplacian operator was applied to the single-trial potential timeseries to compute the Laplacian Derivation (LD - see section IV.C). This reduces the high degree of spatial overlap of potentials at the scalp, and removes the effect of the location of the reference electrode. Peripheral sites for which the Laplacian amplitude cannot be accurately calculated, and several bad amplifier channels (C3 and T7), along with their homologues (C4 and T8), were eliminated from the list of channels for which the Laplacian Derivation (LD) was calculated. There were 39 channels remaining: aF1, aF2, Fz, F3 to F8, Fpz; aCz, aC1 to aC6; Cz; aPz, aP1 to aP6; Pz, P3 to P6; T3 to T6; aO1, aO2; and O1, O2 and Oz (Figure 2).

Averages were formed from correctly performed match and mismatch trials for each condition, and lowpass filtered at 7 Hz. The four final data sets contained 1762 graphic, 1688 phonemic, 1592 semantic, and 1741 grammatic match trials. A digitally linked ears reference was computed to examine EPs. Since a large amount of common activity was evident in the linked-ears EPs, we will mostly discuss the Laplacian Derivation results, except where comparison with the potentials is helpful in interpreting the LD waveforms.

### E. Results

#### 1. Behavioral

For the infrequent (15%) mismatch trials, the mean reaction times were, for the edited/sorted (and unedited) data: graphic condition - 607 (605) msec; phonemic - 720 (713) msec; semantic - 847 (839) msec; grammatic - 737 (728) msec. Except for the phonemic-grammatic pair, all reaction time differences were significant. In the final edited data sets, however, the standard deviations were small and similar across subjects: graphic - 101 msec; phonemic - 117 msec; semantic - 131 msec; grammatic - 126 msec. Percentage of false positives (move to match) and missed targets (no-move to mismatch) in the unedited data were: graphic, 5.6%/12.9%; phonemic, 5.9%/14.0%; semantic, 12.8%/15.8%; grammatic, 3.8%/4.7%.

## 2. Neurophysiological

**Laplacian Derivation (LD) averages:** Differences between conditions in peak latency and topography were very complex in the linked-ears EPs, due to extensive overlap of potential fields at the scalp. The between-condition differences were highly simplified in the LD waveforms, where a peak is frequently seen at only a few locations.

The conditions were divided on the basis of task requirements into letter/non-letter conditions (phonemic, semantic and grammatic vs. graphic), word/non-word conditions (semantic and grammatic vs. phonemic and graphic, or simply semantic vs. phonemic), and syntactic/non-syntactic conditions (grammatic vs. semantic). Hypotheses were tested for each electrode separately. Figures 3, 4, and 5 show the 9-person, averaged LD waveforms for match trials for the cue, first stimulus, and second stimulus, respectively.

[NOTE: In labeling peaks in the LD waveforms a "P" is used to denote emerging current at the scalp, and an "N" for entering current. This polarity does not necessarily correspond with the positive and negative voltage polarity of the linked-ears EP peaks.

### *Letter/Non-letter Comparisons:*

A large number of between-condition differences were found between the letter and nonletter conditions. The cue for the graphic condition elicited an amplitude increase in the N323 peak, mainly at lateral anterior occipital channels. The three letter conditions all had smaller peaks. N323 was maximal at the aO1 electrode, where the negative (entering current) peak in the graphic condition was about twice as large as the language conditions ( $t(1,8)=2.63$ ,  $p<.05$ ). Figure 3 shows this effect on the N323 peak in posterior channels in the nine-person LD averages. The effect was slightly left-lateralized. The Contingent Negative Variation (CNV) preceding S1 was also larger for the graphic condition at left hemisphere channels, including aJ1 ( $t(1,8)=2.28$ ,  $p<.05$ ). For both the N323 and the CNV, an ANOVA on the three language conditions indicated that their amplitudes did not differ significantly at most of the electrodes where the graphic condition had significantly larger amplitudes. Figure 6 [TOP row] shows the electrodes whose amplitude significantly differed between the graphic and the language conditions presented on a cartoon of a lateral view of the head.

Post-S1 condition differences related to the letter/non-letter dimension were apparent in the averaged LD waveforms in the N250 peak (Figure 4), which was larger in the graphic condition. The effect was largest at P5 (P5:  $t(1,8)=6.15$ ,  $p<.0005$ ; T5:  $t(1,8)=4.12$ ,  $p<.005$ ; and aO1:  $t(1,8)=2.49$ ,  $p<.05$ ). At 326 msec after S1 there was a positive peak in the graphic condition, visible only at right frontal sites (F8:  $t(1,8)=5.16$ ,  $p<.001$ ; F6:  $t(1,8)=2.74$ ,  $p<.05$ ). At 568 msec there was a negative peak maximal at F4 ( $t(1,8)=4.18$ ,  $p<.01$ ). Figure 6 [MIDDLE row] shows the electrodes whose N250 and N568 amplitude significantly differed between the graphic and the language conditions.

S2 elicited a negative wave at 258 msec at posterior sites, which is similar in morphology to the N250 elicited by S1 (see Figure 5). It was likewise larger in amplitude in the graphic condition, the effect again being most significant at P5 ( $t(1,8)=5.32$ ,  $p<.001$ ). (An inspection of the waveforms of Figure 5 might suggest that the graphic condition should also be significantly larger at the P6 electrode. This is not the case, however, because the standard deviation of N258 at P6 is twice as large as the mean difference between conditions. By contrast, the standard deviation of N258 at P5 is only about half the mean difference. There are numerous other instances in these data where an apparently large amplitude difference in the waveforms does not reach significance due to variability across subjects.) An ANOVA on the three language conditions indicated that, except for the P5 and P3 electrodes, the language conditions did not differ significantly among themselves. At 460 msec after S2, there was a peak in the graphic condition that reverses polarity between anterior central and frontal midline sites (aCz and Fz), where it was positive, and right anterior central and frontal sites, where it was negative.

Its amplitude difference from language conditions was greatest at right frontal sites (F4:  $t(1,8)=4.82$ ,  $p<.005$ ; F6:  $t(1,8)=4.40$ ,  $p<.005$ ), and at the left occipital site O1 ( $t(1,8)=4.95$ ,  $p<.005$ ). These effects are illustrated in Figure 6 [BOTTOM row].

In the above instances the graphic condition had larger peaks than the language conditions. There were also instances in which the language conditions had larger peaks; in some cases, the waves were entirely absent in the graphic condition. A positive peak at 313 msec after S1 distinguished the language conditions most clearly at the left frontal site F5 ( $t(1,8)=2.63$ ,  $p<.05$ ). (Although the F3 site looks like it should differ between language and graphic conditions, the effect was not significant due to a large standard deviation.) A large negative peak occurred at 448 msec in the language conditions, most prominent at T3, aC5 and aO1 (T3:  $t(1,8)=5.45$ ,  $p<.001$ ; aC5:  $t(1,8)=5.90$ ,  $p<.001$ ; aO1:  $t(1,8)=5.45$ ,  $p<.001$ ). An ANOVA on the 3 language conditions indicated that the three language conditions did not differ in amplitude at the sites where they differed from the graphic condition (except for aO1 and aC1). After S2, the P279 peak exhibited both language and graphic effects: it was larger at left frontal sites for the three language conditions ( $t(1,8)=3.58$ ,  $p<.01$  at F3), and larger at the midline frontal site (Fz:  $t(1,8)=3.08$ ,  $p<.05$ ) for the graphic condition. The significantly larger amplitudes for the graphic condition at left posterior sites and at right anterior and posterior sites are due mainly to the descending limb of the N460 peak, which is significantly larger even at this early latency. Figure 7 shows the sites where language processing produced larger amplitudes than graphic processing (except the above mentioned complex of activity for P279, which was larger in the graphic condition at Fz, at right posterior, and at left hemisphere sites).

#### *Word the/Nonword Comparisons:*

Word/non-word differences were tested by comparing the graphic and phonemic conditions combined versus the semantic and grammatic conditions combined, and also by simply testing the phonemic versus semantic conditions. Differences between word-stimulus conditions and non-word-stimulus conditions occurred late in the epochs following S1 and S2.

Significant differences between word (semantic and grammatic) and non-word conditions (graphic and phonemic) were maximal at about 684 msec after S1. Electrodes where the phonemic condition had larger amplitudes were aC5, F5, F8, Fz, aP5, T3 and T4. The strongest effects were at T3 ( $t(1,8)=3.74$ ,  $p<.01$ ) and aC5 ( $t(1,8)=4.12$ ,  $p<.005$ ). In the case of the P719 peak following S1, the semantic condition had larger amplitudes than the phonemic at Fz ( $t(1,8)=4.33$ ,  $p<.005$ ), aP5 ( $t(1,8)=2.88$ ,  $p<.05$ ), aO1 ( $t(1,8)=2.32$ ,  $p<.05$ ), and O1 ( $t(1,8)=2.43$ ,  $p<.05$ ) and non-word processing following S1.

Although the strongest language effects in this study tended to occur over the left hemisphere, word/non-word differences after S2 occur earlier over the right hemisphere than the left. The mean difference was 204 msec, S.D.=87 msec ( $p<.005$ ). This distinction of word and non-word conditions, or simply between phonemic and semantic conditions, was significant at right hemisphere sites at about 365 msec, in a rather diffuse group of electrodes including T4, P4, aP2, aP4, aP6, F4 and aF2. Differences occur over the left hemisphere at a later latency (about 563 msec). The broad N563 wave, strongest at T3, aC5 and F5, and another wave of opposite polarity at aO1 and aO2, distinguished the phonemic from semantic and grammatic conditions, the phonemic condition having larger amplitudes in both cases. The word/non-word differences at 365 and 563 msec after S2 are illustrated in Figure 8 [BOTTOM row].

#### *Syntactic/Non-syntactic Comparisons:*

Syntactic effects, demonstrated by differences between the grammatic and semantic conditions, occur after both S1 and S2. After S1, there was a large negative peak at 442 msec at left frontal (F3 and F5) and anterior central (aC1) sites, which was larger in the grammatic than semantic condition (F3:  $t(1,8)=2.40$ ,  $p<.05$ ; F5:  $t(1,8)=2.52$ ,  $p<.05$ ; aC1:  $t(1,8)=3.07$ ,  $p<.05$ ). It appears to be an anterior



extension of the N448 peak which occurs at T3 in all language conditions (see Figure 4). However, examination of the linked-ears EP waveforms indicates that the picture was more complicated. In the aCz channel, where the EP peaks were largest, the semantic and phonemic peaks were negative in potential, but the grammatic peak was positive. There were even stronger differences at several posterior right-hemisphere sites including P4, P6, and T6 ( $p < .001$ ), an effect due to a positive wave peaking at about 450-500 msec. It is not clear how this posterior right-sided positive activity is related to the N448 and N442 waves at left frontal sites. The effects at aC6 ( $t(1,8)=4.96$ ,  $p < .005$ ) and F6 ( $t(1,8)=2.38$ ,  $p < .05$ ) differ from the other grammatic/semantic comparisons in that the semantic condition has larger amplitudes at these sites, with a polarity reversal, being negative at aC6 and positive at F6.

After S2, the grammatic condition was distinguished from the semantic condition by a larger amplitude of the P279 peak at midline and left frontal electrodes Fz ( $t(1,8)=3.58$ ,  $p < .01$ ), F5 ( $t=4.49$ ,  $p < .005$ ), and F3 ( $t=3.18$ ,  $p < .05$ ), and also at the left anterior parietal electrode aP3 ( $t(1,8)=3.63$ ,  $p < .01$ ), and the right anterior central site aC2 ( $t(1,8)=3.55$ ,  $p < .01$ ). A number of other electrodes reached significance at  $p < .05$ . The locations of the syntactic effects for N442 and P279 are shown in Figure 9. Finally, the N460 peak after S2 distinguished the grammatic condition at midline frontal sites Fz ( $t(1,8)=3.45$ ,  $p < .01$ ) and Fpz ( $t=3.46$ ;  $p < .01$ ), and at F3, P3, and T5 (all  $p < .05$ ). (N460 not included in illustrations.)

## LANGUAGE MONTAGE

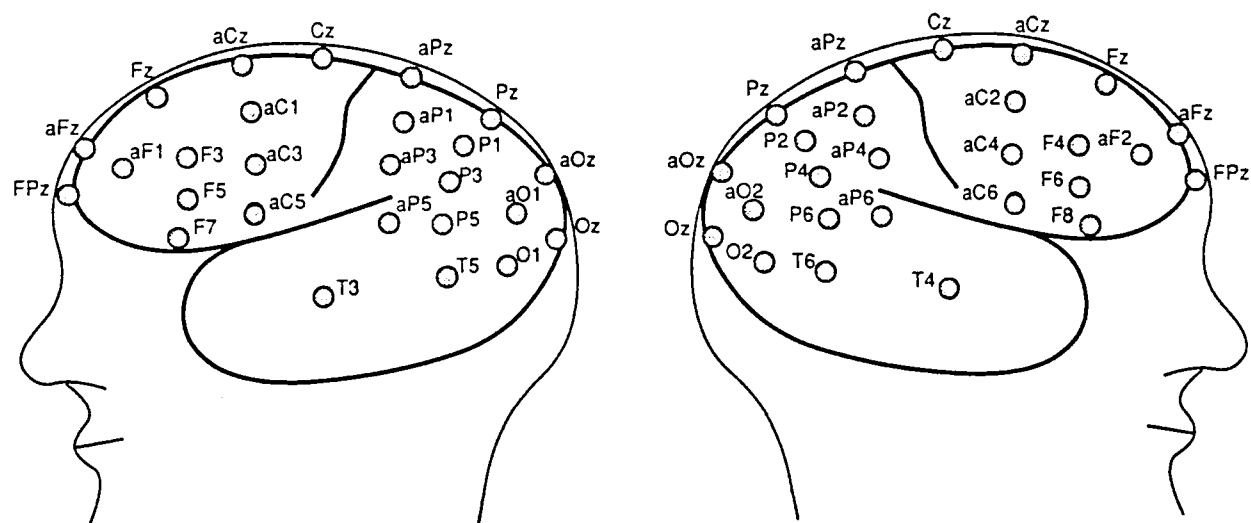


**Figure 1.** Examples of cues and stimuli, and their timing, for the graphic, phonemic, semantic and grammatic conditions. For each condition, the subject had to judge whether the second stimulus (S2) matched the first stimulus (S1).

LANGUAGE TASKS

GRAPHIC (Look alike?)	L	夕々キ	夕々キ
PHONEMIC (Sound alike?)	S	TIRP	TERP
SEMANTIC (Opposite?)	O	COLD	HOT
GRAMMATIC (Grammatical?)	G	HE	SWIMS

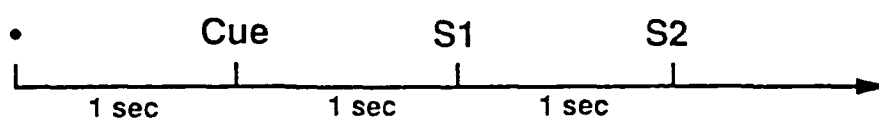
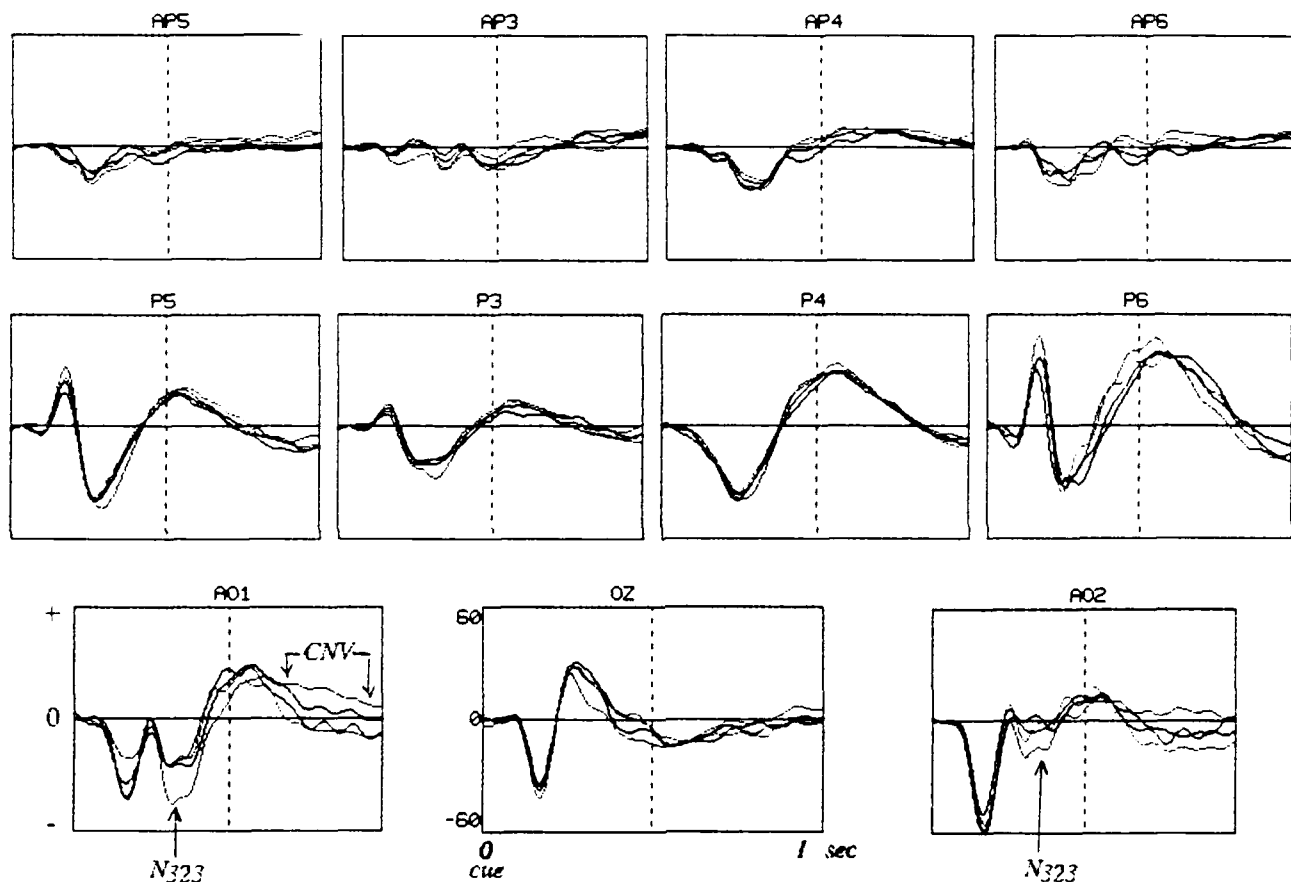


Figure 2. Cartoon showing the locations of the 39 non-peripheral Laplacian Derivation sites.



**Figure 3.** Cue-evoked Laplacian Derivation (LD) waveforms for eleven posterior channels averaged over all 9 subjects. The N323 peak and subsequent CNV were larger in the graphic condition over visual association cortex when subjects were cued to prepare for processing unfamiliar Japanese katakana characters. Waveforms were lowpass filtered at 7 Hz. The x-axis shows one second from Cue to the first stimulus. The y-axis corresponds to  $\pm 0.18$  microvolts per square centimeter. The waveforms for the 4 conditions are shown in the same colors in all illustrations: graphic [black], phonemic [blue], semantic [green], grammatic [red].

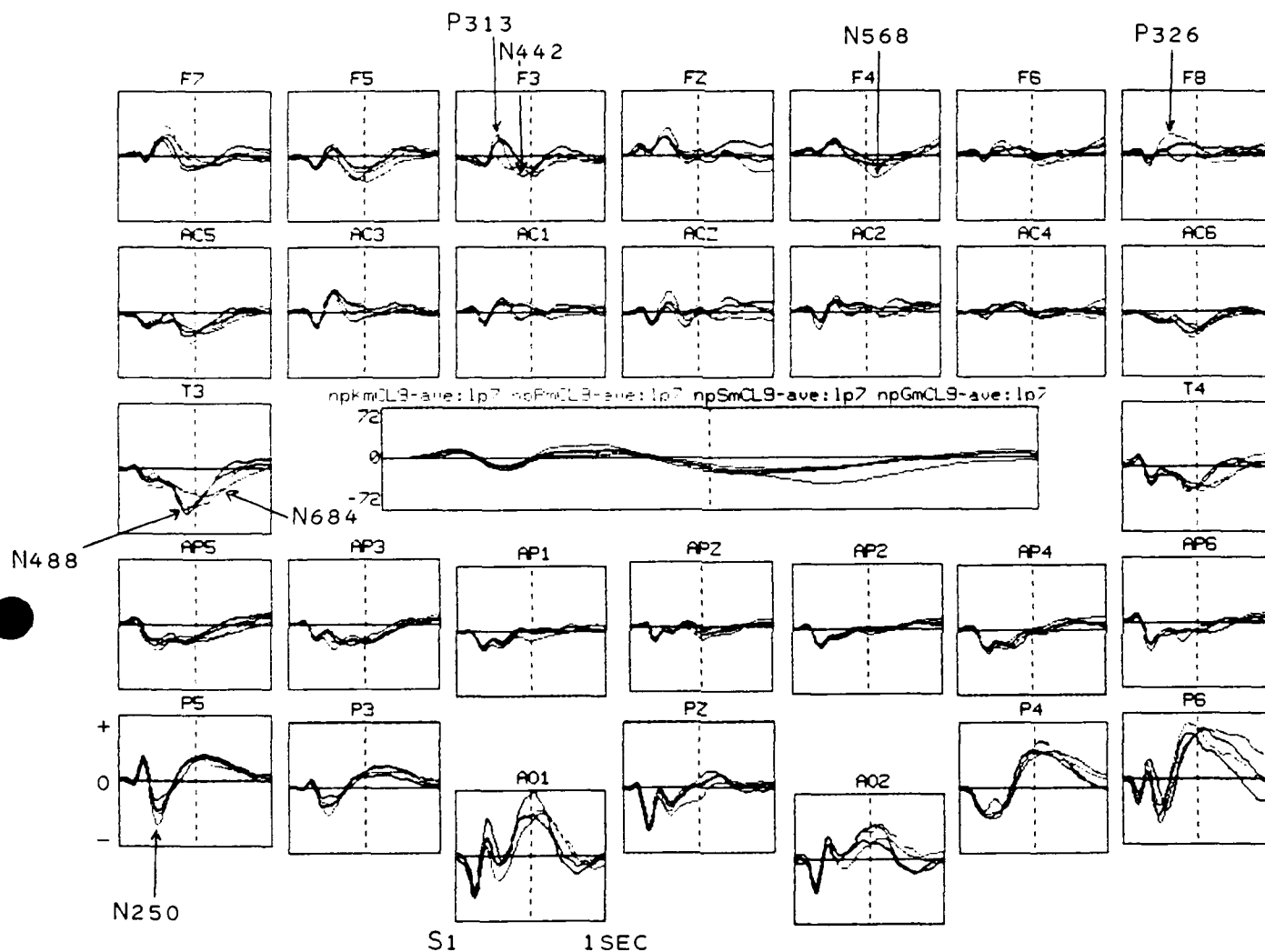
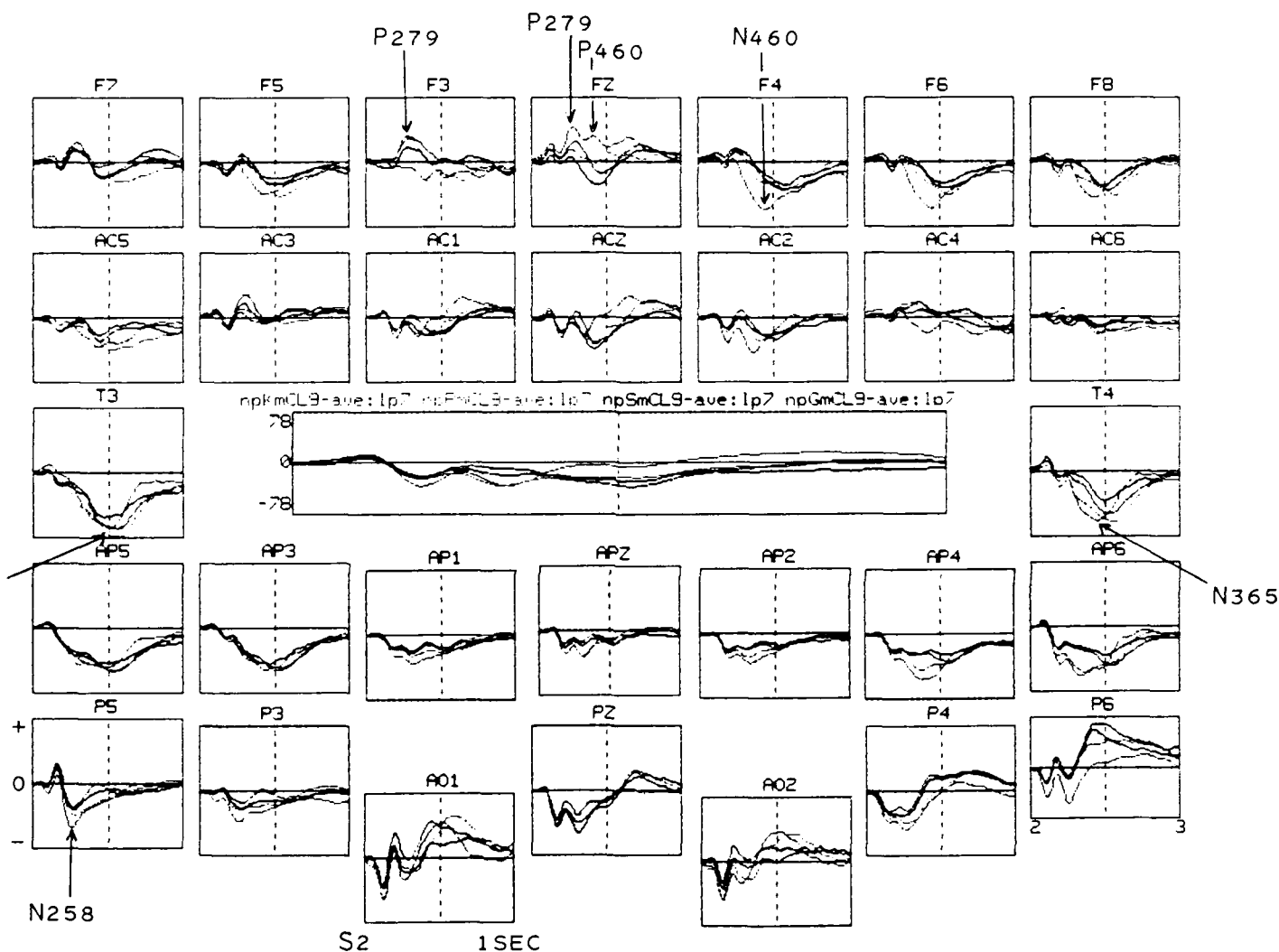
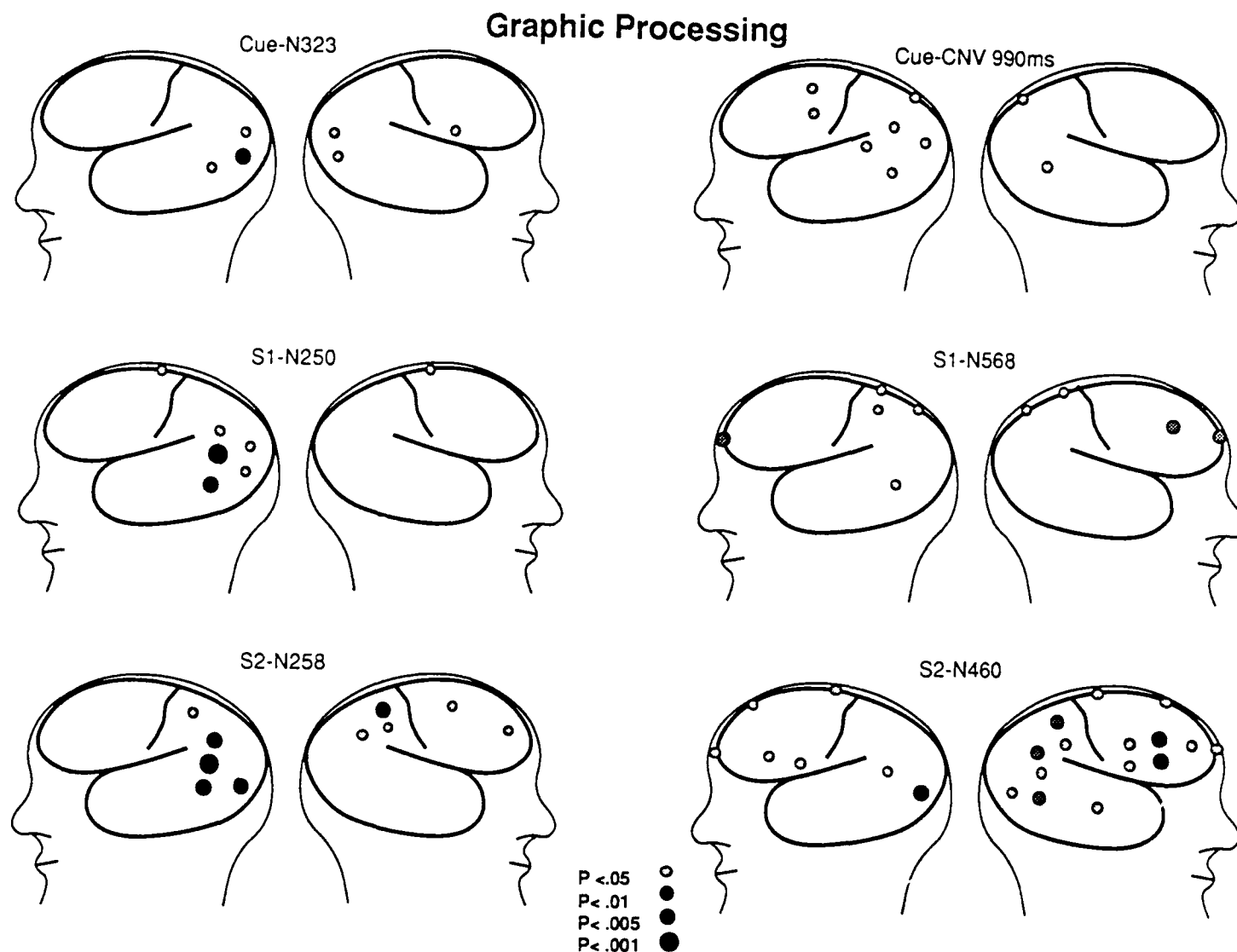


Figure 4. LD waveforms evoked by the first stimulus, averaged over 9 subjects and lowpass filtered at 7 Hz. The y-axis corresponds to  $\pm 0.216$  microvolts per square centimeter. Graphic [black], phonemic [blue], semantic [green], grammatic [red].



**Figure 5.** LD waveforms evoked by the second stimulus, averaged over 9 subjects and lowpass filtered at 7 Hz. The x-axis shows one second beginning with S2. The y-axis corresponds to  $\pm 0.234$  microvolts per square centimeter. Graphic [black], phonemic [blue], semantic [green], grammatic [red].



K&gt;PSG.V2

**Figure 6.** [TOP row] Left and right hemisphere electrode sites at which preparation for the graphic stimulus had a larger post-cue N323 peak and CNV than the for the three language conditions. [MIDDLE row] Sites where the first stimulus of the graphic condition evoked greater N250 and N568 peak amplitudes than language conditions. [BOTTOM row] Sites where the second stimulus and subsequent matching processes elicited larger N258 and N460 peaks in the graphic condition. [Significance level indicated by size and shading of dots; see Figure 2 for electrode names.]

## Letter/Phoneme Processing

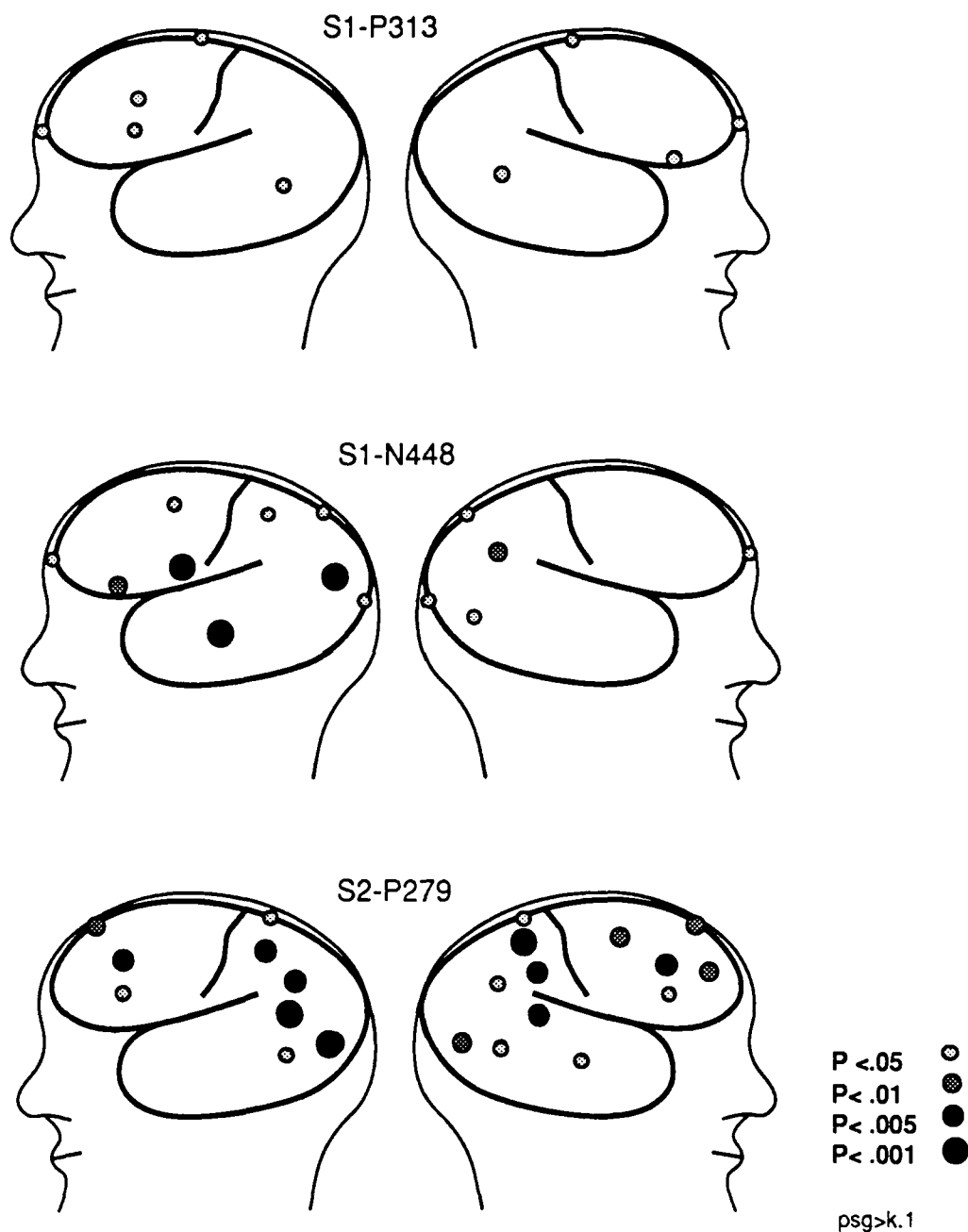


**Figure 7.** [TOP two rows] Sites where, after the first stimulus, the language conditions produced greater P313 and N448 peak amplitudes than the graphic condition. [BOTTOM row]. Sites where the S2-evoked P279 peak had differences between language and non-language conditions. [Significance level indicated by size and shading of dots; see Figure 2 for electrode names.]



## Phonemic/Lexical Process

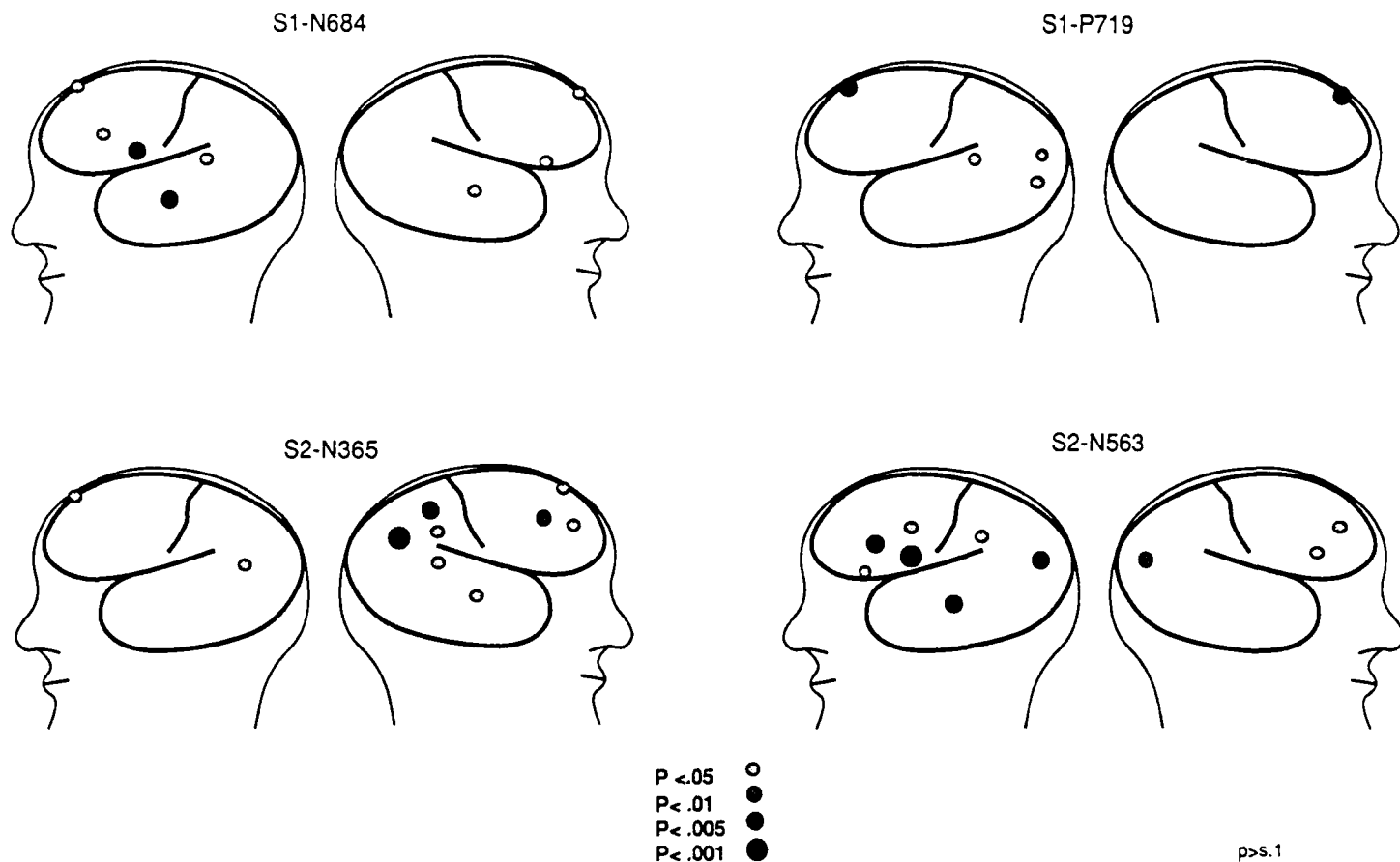


**Figure 8.** [TOP row] Word/non-word differences following the first stimulus: sites where the N684 peak was larger for phonemic stimuli (pronouncable non-words) compared to semantic stimuli (words), and where the semantic stimuli produced larger amplitudes than the phonemic for the P719 peak. [BOTTOM row] Following the second stimulus, the semantic and phonemic conditions differ over the right hemisphere by 365 msec, and considerably later, at 563 msec, over the left hemisphere. [Significance level indicated by size and shading of dots; see Figure 2 for electrode names.]

## Syntactic Processes

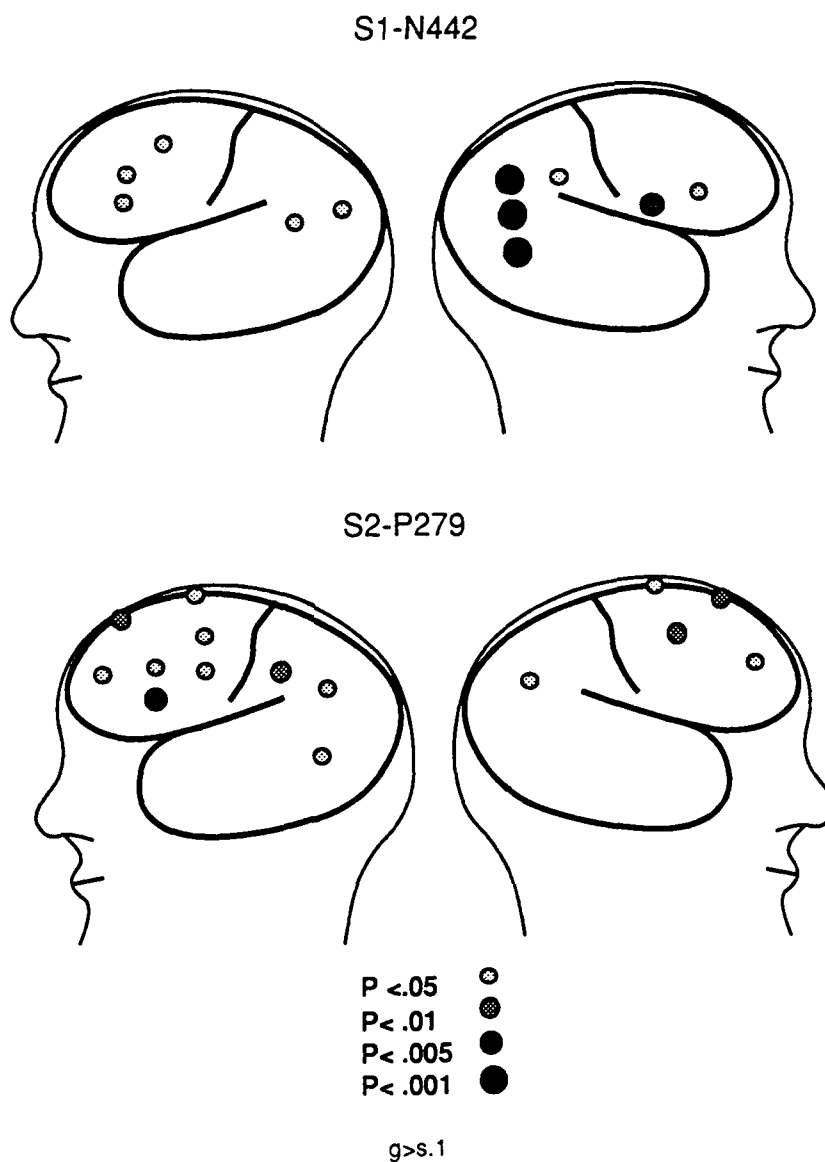


**Figure 9.** Sites of amplitude increases in the grammatic condition compared to the semantic condition for the N442 peak following S1 [TOP], and the P279 peak following S2 [BOTTOM]. [Significance level indicated by size and shading of dots; see Figure 2 for electrode names.]

## F. Discussion

### 1. Letter (phonemic, semantic and grammatic conditions) versus Non-letter (graphic condition) Comparison

Differences corresponding to the letter/non-letter distinction were the most numerous, the first difference being elicited by the task cue preceding the first stimulus. The augmentation of the N323 peak at occipital and posterior temporal electrodes in the graphic condition occurred in response to the task-specific cue letter "L", and not for cue-letters signaling one of the language conditions ("S", "O" or "G"). Since all four cues were alike in gross physical characteristics, such as size, location, luminance and duration, and since conditions were randomized, the increase in N323 may reflect a preparatory process involving the preparation of visual association (and inferotemporal) cortex for the processing of the unfamiliar katakana characters. Although the percentage of cues for the graphic condition was 25%, and thus rarer than cues for the language conditions, the distribution of P323 in the linked-ears EPs was not that of the "classic" oddball P300: it was left-lateralized, with positive maximum at aO1, and negative minima at central and frontal sites (Figure 10, LEFT). Further, the distribution of the P300 to the S2 of mismatch trials (not reported here) did have the "typical" P300 distribution for these subjects. Thus we may conclude that the P323 (and its Laplacian Derivation equivalent N323) was not simply a P300 produced by the relatively lower probability of graphic condition cues, and that its amplitude increase may be evidence for a greater priming of visual association (and inferotemporal) cortex in anticipation of the non-familiar visual stimuli, as compared to that needed for the highly familiar letters. Although such priming has been suggested by psychological studies, the result reported here presents direct neural evidence of this phenomena.

If the N323 effect does reflect some aspect of prestimulus priming of cortical areas involved in visual encoding, it would be reasonable to expect an increase in the Contingent Negative Variation (CNV) at electrodes overlying these cortical areas. This was indeed the case. The late cue epoch contained a negative shift (positive in the LD waveforms - Figure 3), mainly over left posterior and antero-central sites; of these sites, aO1 and T5 also had an amplitude increase in the N323. Finally, at most of the significant sites, the ANOVA indicated that the three language conditions did not differ among themselves. This was also true for the N250 and N258 peaks elicited by the first and second stimuli. This suggests that processes reflected in these peaks are affected purely by the letter/non-letter difference. In the case of the Cue-evoked N323, this process may be priming of visual association cortex, while for the S1-evoked N250 and S2-evoked N258 it may be the actual encoding or analysis of higher-order physical features.

The next difference between graphic and letter stimuli occurred in the N250 peak elicited by the first stimulus. Although all four conditions elicited an N250, it was significantly larger for graphic stimuli at the left lateral parietal (P5) and other nearby sites. This effect may reflect the greater amount of processing required to encode the unfamiliar graphic figures. It is not surprising that the stimuli used in the graphic condition produce more activity over the left, rather than right posterior hemisphere. Studies in primates (Ungerleider and Mishkin, 1982) and humans (Kosslyn, 1988) suggest that the encoding (and imaging) of complex visual figures occurs primarily in areas of left posterior cortex. The electrode sites at which the graphic condition produced significantly greater activity (aO1 for N323, P5 and neighboring electrodes for N250 following S1 and P258 following S2) are quite consistent with the above authors' proposed ventral system for visual encoding. This system extends via cortico-cortical connections from the visual cortex, through the left temporo-parieto-occipital region, to the inferior temporal cortex. After the second stimulus, the graphic condition again elicited larger negative peaks (N258) mainly at left posterior parietal and anterior occipital sites. N258 probably reflects the same processes as the N250 elicited by S1, perhaps the encoding of higher-order, detailed physical features of the graphic figures.

In the S1 epoch, there is a N568 peak, largest at the right frontal electrode F4 ( $t(1,8)=4.18$ ,  $p<.05$ ). S2 also elicits a right-lateralized N460 wave largest at frontal sites F4 and F6. Thus for each of the two stimuli there is a pattern of greater left posterior activity early in each epoch, possibly reflecting the encoding of complex, higher-order physical characteristics of the graphic figures, followed by greater right anterior activity later in the epoch, possibly related to the maintenance and comparison of the graphic codes, and to response selection.

Activity which produced larger peaks in the language conditions occurred first in the P313 peak, most distinct at left frontal sites (F3 and F5), followed by the N448 peaks at left temporal (T3), anterior central (aC5) anterior occipital (aO1) and frontal (F7) electrodes (Figure 7). The language conditions did not differ from each other at T3, aC5 and F7, but they did differ among themselves at aO1. Thus the significant amplitude difference at the left anterior occipital electrode (aO1) may be due to a different process, peaking slightly later than the N448. Since the language conditions do not differ from each other at T3, aC5 and F7, we might speculate that the N448 peaks reflect a process common to all language conditions, such as generation of phonemic codes. The complex of activity at the latency of the P279 peak elicited by S2 contained amplitude increases to the language stimuli at left frontal sites, and to graphic stimuli at midline frontal, right anterior sites, and posterior electrodes of both right and left hemispheres (where it was negative). Since this peak also exhibited significant differences between grammatic and semantic conditions, it appears that the P279 (and its negative counterpart over posterior regions) is sensitive to almost every condition difference in this experimental paradigm. Each condition causes a relative amplitude increase at one or more electrodes over some region of cortex. It is a point of theoretical interest whether this is the result of several different processes occurring co-incidentally at the same latency, or whether it results from one distributed process whose widely separated cortical processing nodes respond differently to the various task requirements of the four conditions. This is more than a moot point, and in fact bears on the whole concept of distributed processing networks versus notions of "parallel/sequential" models.

## 2. Word and Non-word Processing

The word/non-word distinction (semantic and grammatic versus graphic and phonemic conditions) produced differences in both the S1 and S2 epochs (Figure 8). Significant differences occurred at about 684 msec after S1 at right and left temporal and frontal sites. After S2, at the right parietal, temporal and frontal electrodes (P4, aP2, F4, T4, aP6, and aF2) at about 365 msec, and at left lateral antero-central (aC5), left temporal (T3), left frontal (F5), and anterior occipital (aO1) electrodes at about 563. The tendency in these cases was for the graphic/phonemic waveforms to have larger amplitudes than the semantic and grammatic. It is possible that the nonsense phonemic processing than familiar words of the semantic and grammatic conditions. In order to determine whether this effect was due to semantic processing or increased phonemic processing to nonsense words, the graphic and phonemic conditions combined were compared to the semantic and grammatic conditions combined, and the graphic and phonemic conditions were tested for differences. It was found that the graphic and phonemic conditions tended to behave similarly at most (but not all) sites where there were differences between the word and 'nonsense word' (phonemic) conditions. Separation of the phonemic non-word condition from the word conditions is consistent with models for lexical processing which posit activation of independent phonological and semantic pathways for visually presented words (Coltheart, 1985; Petersen et al., 1988). Evidence for this model is provided by dissociations of letter versus word reading in dyslexia (Marshall, 1984), and by access to phonological features of lexical targets, but not the lexical targets, in anomia and aphasia (Farmer, 1978; Illes et al., 1986; Joannette et al., 1980). The presence of bilateral word/non-word effects is not surprising, in view of the abundant evidence for basic lexical comprehension in the non-dominant hemisphere (Gazzaniga and Sperry, 1967; Ardila and Ostrosky-Solis, 1984). Somewhat unexpected, however, was that the effect occurred 200 msec earlier over the non-dominant hemisphere!

### 3. Syntactic Processing

Grammatical and semantic conditions were differentiated after the first stimulus by the N442 peak. Considering that both types of stimuli were words with similar physical characteristics, the main difference was that the semantic condition used open class words (content words such as nouns and adjectives) and the grammatical condition used closed class words (syntactic, or function words) in this case pronouns. It is thus reasonable to suppose that the N442 is related to processing closed-class words, to the initiation of a "syntactic parser" (Garrett, 1982), or to both. The "syntactic" effect at left frontal sites (F3, F5 and aC3) is consistent with neurophysiological observations of syntactic deficits and difficulties in handling closed class words in aphasia patients whose lesions involve and extend deep to Broca's area (e.g., Gordon, 1985; Metter et al., 1983). On the one hand, it is unlikely that these were independent processes since, based on cognitive studies with healthy and aphasic subjects, it is well known that processing of closed class words is closely linked to the processing of grammatical form (reviewed e.g. in Lecours et al., 1983). On the other hand, the existence of a specialized access system responsible for retrieving closed class items during language processing is still being investigated (e.g., Bradley et al., 1980; Gordon and Caramazza, 1983; Petocz and Oliphant, 1988; Matthei and Kean, 1989). The highly significant effects at right parietal sites is puzzling, and appears to be part of a different process peaking at a later latency.

The P279 which distinguishes the grammatical from semantic condition after the second stimulus is elicited by an open class word, specifically a verb which correctly completes the meaningful and grammatically correct sentences of the match trials. One possibility is that P279 reflects differences in processing of verbs versus stimulus words belonging to other lexical categories (e.g., nouns, adjectives, adverbs). This is unlikely, however, since 65% of the semantic stimuli were verb pairs themselves, or pairs in which the S2 could be either a verb or a noun. Thus, the alternative and most likely explanation is that the P279 may reflect syntactic closure of processes initiated by the first stimulus.

### 4. Comparison of Linked-Ears EPs and Laplacian Derivation Topographies

The major benefit of the LD is that it acts as a spatial high-pass filter, reducing common activity and enhancing local cortical activity. Thus the LD averages show considerably more localized effects than the linked-ears EP waveforms. The sharply defined effects in the LD waveforms elicited by the four conditions in this study stand in contrast to the conflicting reports of lateralizations and localizations in previous evoked-potential language studies (reviews in Kutas and Hillyard, 1980b; Regan, 1988). Although, the LD distributions should not always be literally interpreted as reflecting the activity of directly underlying cortical areas, their correspondence to language and other cortical association areas in this study is striking.

### 5. Conclusion

By designing four carefully controlled tasks, recording from 59 scalp locations, and spatially enhancing the task-related signals using the Laplacian Derivation, an unusually detailed picture of the complex spatial and temporal course of several types of linguistic processes was obtained. The language conditions exhibited sharply localized activity over left temporal and frontal cortices. All three language conditions were alike in that they elicited similar N448 peaks at the left temporal electrode (T3) in response to the first stimulus. However, they differed among themselves in the amplitudes of other waves which were maximal at left-frontal (F3 and F5) and anterior central (aC5), and temporal (T3 and T4) sites. Although the linguistic and graphic conditions differed greatly, many of the graphic effects occurred at left-sided posterior sites, supporting the view that the posterior left-hemisphere mediates the processing of complex visual figures. In addition, evidence for the priming of visual association cortex in anticipation of the greater processing requirements of unfamiliar graphic figures was found.

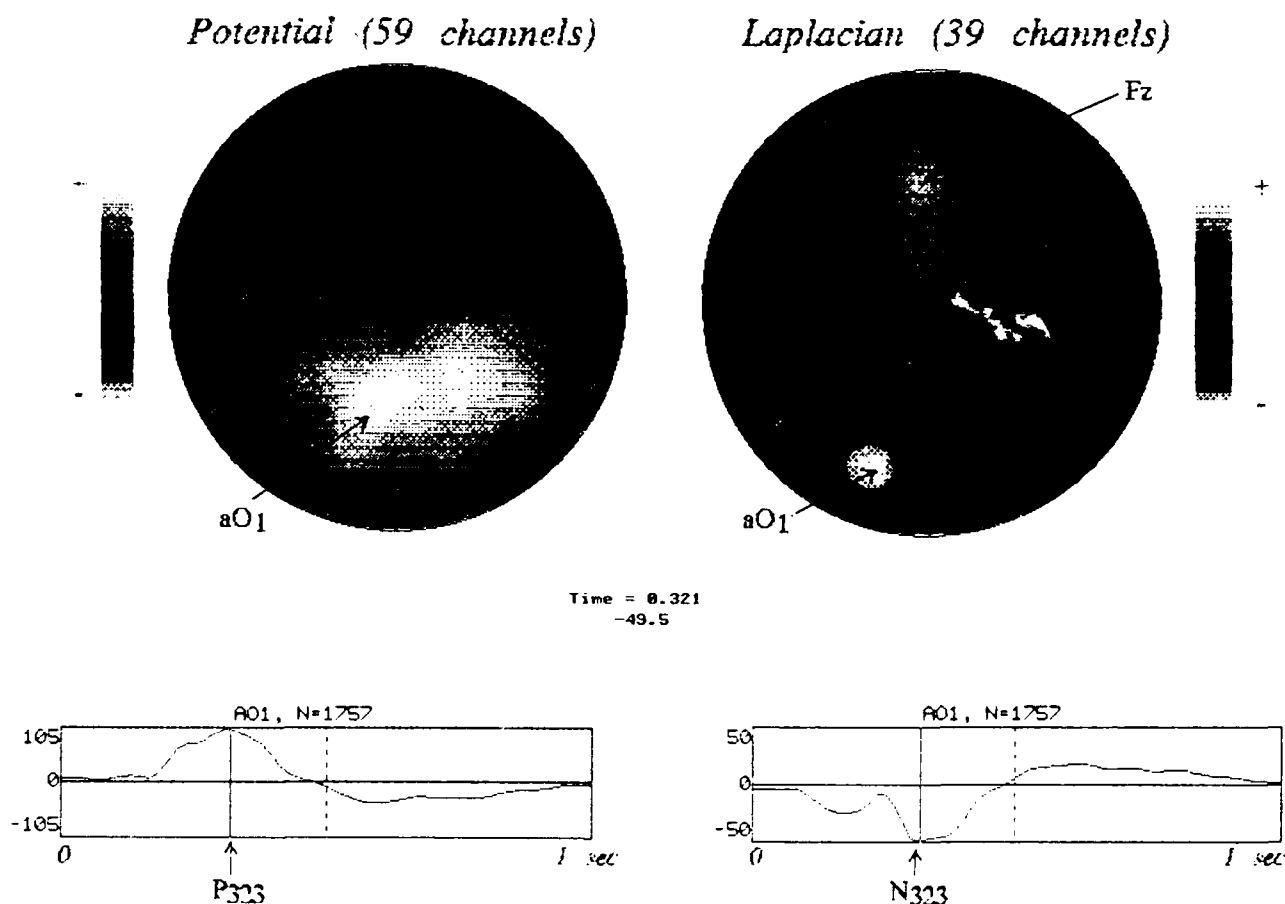


Figure 10. Topography of the Cue-evoked P323 evoked potential peak at all 59 scalp channels [LEFT], and corresponding Laplacian Derivation N323 peak at the 39 non-peripheral channels [RIGHT]. The P323 EP topography differs from that of the typical oddball "P300" peak in its anterior negativity and left-sided lateralization of the posterior positivity. The site of maximum amplitude in both the potential and LD distributions is at the left anterior occipital electrode (indicated by arrows). The LD distribution also contains a current source at the midline frontal electrode (Fz). [Scale: EP,  $\pm 3.15$  microvolts; LD,  $\pm 0.146$  microvolts per square centimeter.]

## G. References

- Ardila, A and Ostrosky-Solis, F. (1984) Right hemisphere participation in language. In A. Ardila and F. Ostrosky-Solis (Eds.): *The Right Hemisphere: Neurology and Neuropsychology*, New York, Gordon and Breach.
- Beaumont, J. (1983) The EEG and task performance: A tutorial review. In: A. Gaillard and W. Ritter (Eds.), *Tutorials in ERP Research: Endogenous Components*, Elsevier, Amsterdam, pp. 385-406.
- Bolander, D.O., Varner, D.D. and Pine, E. (1985) *Instant Synonyms and Antonyms*. Illinois, Career Pub.
- Bradley, D., Garrett, M. and Zurif, E. (1980) Syntactic deficits in Broca's aphasia. In: D. Caplan (Ed.) *Biological Studies of Mental Processes*. Cambridge, MIT Press.
- Brown, W., Marsh, J. and Smith, J. (1979) Principal components analysis of ERP differences related to the meaning of an ambiguous word. *Electroenceph. clin. Neurophysiol.*, 4: 7099-7140.
- Buschsbaum, M. and Fedio, P. (1970) Hemispheric differences in evoked potentials to verbal and non-verbal stimuli in left and right visual fields, *Physiol. Behav.*, 1970, 5: 207-210.
- Butler, S. and Glass, A. (1986) EEG alpha asymmetries. In D. Papakostopoulos, I. Mortin and S. Butler (Eds.), *Clinical and Experimental Neuropsychophysiology*, Croom-Helm, Beckenham.
- Chapman, R., McCreary, J., Chapman, J. and Bragdon, H. (1978) Brain responses to semantic meaning. *Brain and Lang.*, 5: 195-205.
- Coltheart, M. (1985) Attention and Performance XI. *Erlbaum, Hillsdale, N.J.*
- Donchin, E., Kutas, M. and McCarthy, G. (1977) Electrocortical indices of hemispheric utilization. In: S. Hernard et al. (Eds), *Lateralization in the Nervous System*, Academic, New York, pp. 339-384.
- Farmer, A., O'Connell, F. and O'Connell, E.J. Sound error self-correction in the conversational speech of non-fluent and fluent aphasics (1978) *Folia Phoniatrica*, 30: 293-302.
- Fischler, I., Jin, Y.S., Boaz, T.L., Perry, N.W. and Childers, D.G. (1987) Brain potentials related to seeing one's own name. *Brain and Language* 30: 245-262.
- Gardner, H., Silverman, J., Wapner, W. and Zurif, E. (1987) The appreciation of antonymic contrasts in aphasia. *Brain and Language* 6: 301-317.
- Garrett, M.F. (1982) Production of speech: Observations from normal and pathological use. In A.W. Ellis (Ed.) *Normality and pathology in cognitive functions*, 9, New York, Academic Press.
- Gazzaniga, M. and Sperry, R. (1967) Language after section of the cerebral commissures. *Brain*, 90: 131-148.
- Geschwind, N. (1970) The organization of language and the brain. *Science* 170: 940-944.
- Gevins, A.S. (1983) Brain potential evidence for lateralization of cognitive functions. In J.B. Hellige (Ed.): *Cerebral Hemisphere Asymmetry: Method, Theory and Application*, Praeger, N.Y., pp.335-382.
- Gevins, A.S. (1988) Recent advances in neurocognitive pattern analysis. In: E. Basar (Ed.), *Dynamics of Sensory and Cognitive Processing of the Brain*. Springer-Verlag: Heidelberg, pp. 88-102.
- Gevins, A.S and Cuttillo, B. (1986) Signals of Cognition. In F. Lopes da Silva, et al. (Eds.), *Handbook of Encephalography and Clinical Neurophysiology*, Vol. 2, Elsevier, Amsterdam, pp. 335-381.
- Gevins, A.S., Morgan, N.H., Bressler, S.L., Cuttillo, B.A., White, R.M., Illes, J., Greer, D.S., Doyle, J.C., and Zeitlin, G.M. (1987) Human neuroelectric patterns predict performance accuracy. *Science* 235: 580-585.

- Gevins, A.S., Bressler, S.L., Morgan, N.H., Cutillo, B.A., White, R.M., Greer, D.S. and Illes, J. (1989a) Event-related covariances during a bimanual visuomotor task, Part I: Methods and analysis of stimulus- and response-locked data. *Electroencephalogr. clin. Neurophys.*, 74(1): 58-75.
- Gevins, A.S., Cutillo, B.A., Bressler, S.L., Morgan, N.H., White, R.M., Illes, J. and Greer, D.S. (1989b) Event-related covariances during a bimanual visuomotor task, Part II: Preparation and feedback. *Electroencephalogr. clin. Neurophys.*, 74(2): 147-160.
- Gordon, W.P. (1985) Neuropsychological assessment of aphasia. In: J. Darby (Ed.) *Speech Evaluation in Neurology*. New York, Grune and Stratton.
- Gordon, B. and Caramazza, A. (1985) Closed- and open-class words: Failure to replicate differential frequency sensitivity. *Brain and Language*, 15: 143-160.
- Illes, J., Nespoulous, J.L. and Lecours, A.R. (1986) Hesitation patterns in neologistic jargonaphasia: A diachronic study. *La Linguistique*, 22(2): 75-93.
- Joanette, Y., Keller, E., Lecours, A.R. (1980) Sequences of phonemic approximations in aphasia. *Brain and Language*, 11: 30-44.
- Kolk, H.J.J. (1978) Judgment of sentence structure in Broca's aphasia. *Neuropsychologia* 16: 617-625.
- Kosslyn, S. (1988) Aspects of a cognitive science of mental imagery. *Science*, 240: 1621-1626.
- Kutas, M. and Hillyard, S. (1980a) Reading senseless sentences: Brain potentials reflect semantic incongruity. *Science*, 207: 203-205.
- Kutas, M. and Hillyard, S. (1980b) Reading between the lines: Event-related brain potentials during natural sentence processing. *Brain and Language*, 11: 354-373.
- Kutas, M. and Hillyard, S. (1983) Event-related brain potentials to grammatical errors and semantic anomalies. *Memory and Cognition* 11: 539-550.
- Kutas, M., Lindamood, T. and Hillyard, S. (1984) Word expectancy and event-related brain potentials during sentence processing. In S. Kornblum and J. Requin (Eds.): *Preparatory States and Processes*, Lawrence-Erlbaum, New Jersey. pp. 217-238.
- Kutas, M. and Van Petten, C. (1988) Event-related brain potential studies of language. *Advances in Psychophysiology*, 8: 139-187.
- Lassen, N., Ingvar, D. and Skinhoj, E. (1978) Brain function and blood flow. *Scientific American*, 239: 62-71.
- Lecours, A.R., Lhermitte, F. and Bryans, B. (1983) *Aphasiology*, Sussex, Balliere Tindall.
- Lovrich, D., Simson, R., Vaughan, Jr., H.G. and Ritter, W. (1986) Topography of visual event-related potentials during geometric and phonetic discriminations. *Electroencephalogr. clin. Neurophys.* 65: 1-12.
- Marshall, J.C. (1984) Toward a rational taxonomy of the developmental dyslexias. In R.N. Maltesha and H.A. Whitaker (Eds.) *Dyslexia: A Global Issue*. The Hague: Martinus Nijhoff.
- .IP
- Matthei, E.H. and Kean, M.L. (1989) Postaccess processes in the open vs. closed class distinction. *Brain and Language*, 36: 163-180.
- Metter, E.J., Riege, W.H., Hanson, W.R., Kuhl, D.E., Phelps, M.E., Squire, L.R., Wasterlain, C.G. and Benson, D.F. (1983) Comparison of metabolic rates, language and memory in subcortical aphasias. *Brain and Language*, 19: 33-47.
- Molfese, D. (1979) Cortical involvement in the semantic processing of co-articulated speech cues. *Brain and Lang.*, 7: 86-100.
- Molfese, D. (1983) Event-related potentials and language processes. In A. Gaillard and W. Ritter (Eds.): *Tutorials in Event-related Potential Research: Endogenous Components*. *Advances in Psychology*, Vol. 10, Elsevier, Amsterdam, pp. 345-368.



- Ojemann, G. (1983) Brain organization for language from the perspective of electrical stimulation mapping. *Behavioral and Brain Sciences*, 2: 189-230.
- Petersen, S.E., Fox, P.T., Posner, M.I. and Raichle, M.E. (1988) Studies of the processing of single words using averaged positron emission tomographic measurements of cerebral blood flow change. *Nature*, 331: 585-589.
- Petocz, A. and Oliphant, G. (1988) Closed-class words as first syllables do interfere with lexical decisions for non-words: implications for theories of agrammatism. *Brain and Language*, 34: 127-146.
- Posner, M.I. (1978) *Chronometric Explorations of Mind*. New Jersey, Lawrence Erlbaum.
- Regan, D. (1988) *Human Brain Electrophysiology*, Elsevier, New York, pg. 247.
- Rugg, M. (1983) The relationship between evoked-potentials and lateral asymmetries of processing. In A. Gaillard and W. Ritter (Eds.): *Advances in Event-Related Potential Research: Endogenous Components*. *Advances on Psychology*, Vol. 10, Elsevier, Amsterdam, pp. 369-383.
- Rugg, M. (1985) The effects of semantic priming and word repetition on event-related potentials. *Psychophysiology*, 22(6): 642-647.
- Ungerleider, L. and Mishkin, M. (1982) In: D. Ingle, M. Goodale, and R. Mansfield (Eds.), *Analysis of Visual Behavior*, MIT Press, Cambridge, pg. 549.
- Urdang, L. (1978) *Basic Book of Synonyms and Antonyms*. New York, NAL Pub.
- Vitz, P.C. and Spiegel-Winkler, B. (1973) Predicting the judged "similarity of sound" of English words. *J. Verbal Learning and Verbal Behav.*, 12: 373-388.
- Webster's New Universal Unabridged Dictionary, Vol. 2. (1983) New York, Simon and Schuster.
- Zurif, E. (1980) Language mechanisms: A neurological perspective. *American Scientist* 68: 305-311.

## IV. TECHNICAL DEVELOPMENTS

### A. Overview

All brain signals undergo considerable spatial smearing as they pass through the tissues between the brain and scalp, and in particular, the highly resistive skull. The popular technique of equivalent dipole localization, which exists in various degrees of sophistication, is adequate only for simple sources such as early exogenous transient responses or steady-state potentials. It cannot deal with multiple dipole-like sources or complex distributed sources without a great deal of prior knowledge about their location and orientation. In addition, concentric sphere or ellipsoid models of the skull, CSF and scalp do not resemble the actual geometries of the head and, moreover, the actual thickness of these tissues is variable. To accurately derive a picture of the electrical currents of the brain at the cortical surface, it is necessary to first construct a more accurate 3-D model of each subject's head from high quality 2-D MRI slices. A computationally intensive method of solving the Maxwell equations within a large number of 3-D polygons ("finite elements") comprising this reconstruction of brain, skull, etc., must then be applied. This method of "Finite Element Modeling" requires a high degree of spatial sampling, at least on the order of 120 or more electrodes. This laboratory is in the process of developing such a method and applying it to simple sensory stimulation as the first step toward application to complex signals generated during cognitive functions. Below we report first the results of simple visual dipole localization, and then our progress toward a more advanced deblurring technology in a preprint titled "Beyond Topographic Mapping".

### B. Dipole Localization

It is well known from anatomical and physiological investigations that the visual field (retina) projects in an orderly manner onto the striate area of the occipital cortex. In essence, the visual field is projected contralaterally and inverted about the horizontal midline, with foveal projections located at the occipital pole and the more peripheral retina projecting to cortex located deeper within the calcarine and longitudinal fissures. Evoked potential research has shown that the early-latency components of the visual evoked potential (VEP) for pattern stimuli presented to restricted retinal areas can be accounted for by equivalent dipole sources located in corresponding retinotopic projection areas. Evoked magnetic field data have indicated similar localization, primarily based on steady-state stimulation and analysis methods. This study evaluated dipole localization for the steady-state evoked potential to pattern reversal stimulation of all visual quadrants and octants in 4 subjects.

Quadrant and octant patterns (Figure 11, TOP) consisted of pie-shaped sections of a circular black-and-white checkerboard having 8 concentric tracks each extending 2-degrees from a central fixation point. Patterns reversed in phase 15 times per second on a computer monitor 1 meter in front of the subject. Duration of stimulation was either 50 or 100 seconds, and three stimulation runs were obtained for each pattern. Data recorded from the 4 normal male subjects consisted of horizontal and vertical eye-movements (EOG) as well as 24 channels of EEG (referenced to Fz) selected from an extended 10/20 system, including 17 electrodes on the posterior scalp. Artifact-free epochs of 0.533 sec, digitized at 128/s, were averaged and Fourier-transformed. Real and imaginary components of the 15-Hz response were drawn onto maps of the head for the 3 averages from each subject and stimulus, and for the grand average of the three stimulation runs. Data for each pair of adjacent octants and the corresponding quadrant were then combined for calculation of the "canonical" phase (i.e., the phase angle onto which the projections of all the phasors yielded the greatest squared amplitude). For dipole-fitting, the theoretical position of each electrode on a sphere centered halfway between Fpz and Oz was calculated. Least-squares analysis was used to find the location of the best-fitting current dipole within the sphere at a resolution of 2.5 mm.

The steady-state amplitude measures from the phasor analysis were used to construct topographical isopotential maps and for least-squares fitting of equivalent current dipoles. Figure 11 [BOTTOM] shows the electrode locations in a rear view of the head. Figure 12 [TOP] presents maps in this view for each of the stimuli for one subject. Also shown (Figure 12, BOTTOM) is the location in the coronal plane of the computed dipoles, and also its direction for that subject. The length of the 3-D extent of each dipole was set constant; the variation in length is due to the direction angle out of the coronal plane. Figure 13 summarizes of these dipole fittings by averaging the computed dipole parameters for the four subjects.

These results show potential topographies consistent with occipital generators, and very close linear summation of adjacent octant responses compared to those for corresponding quadrants. Each equivalent dipole fit for each subject (with the exception of just one octant combination) accounted for 81% of the variance in the response. These dipole locations were near the occipital pole contralateral to the side of stimulation and also showed inversion with respect to the horizontal meridian. These results are comparable to those found for early-latency transient EPs and for evoked magnetic sources. However, the EEG equipment for this type of dipole analysis costs about 100 times less than MEG equipment with a comparable number of channels. There were savings also in terms of time, since only about 5 minutes of data was required.

Although this method proved very efficient and effective in locating dipoles for simple steady-state sensory stimuli, single equivalent dipoles are not a suitable model for the complex, distributed processes of cognitive functions. Work is already underway in this laboratory on the development of more realistic models, as described below.

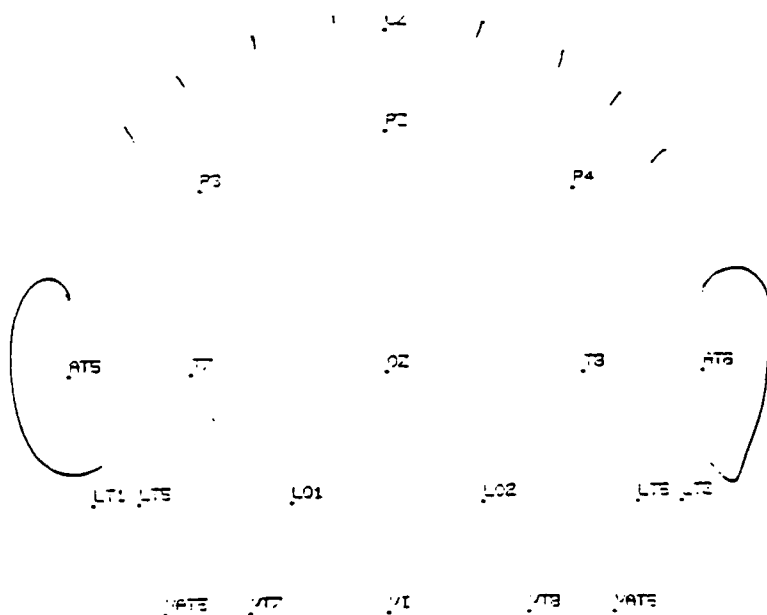
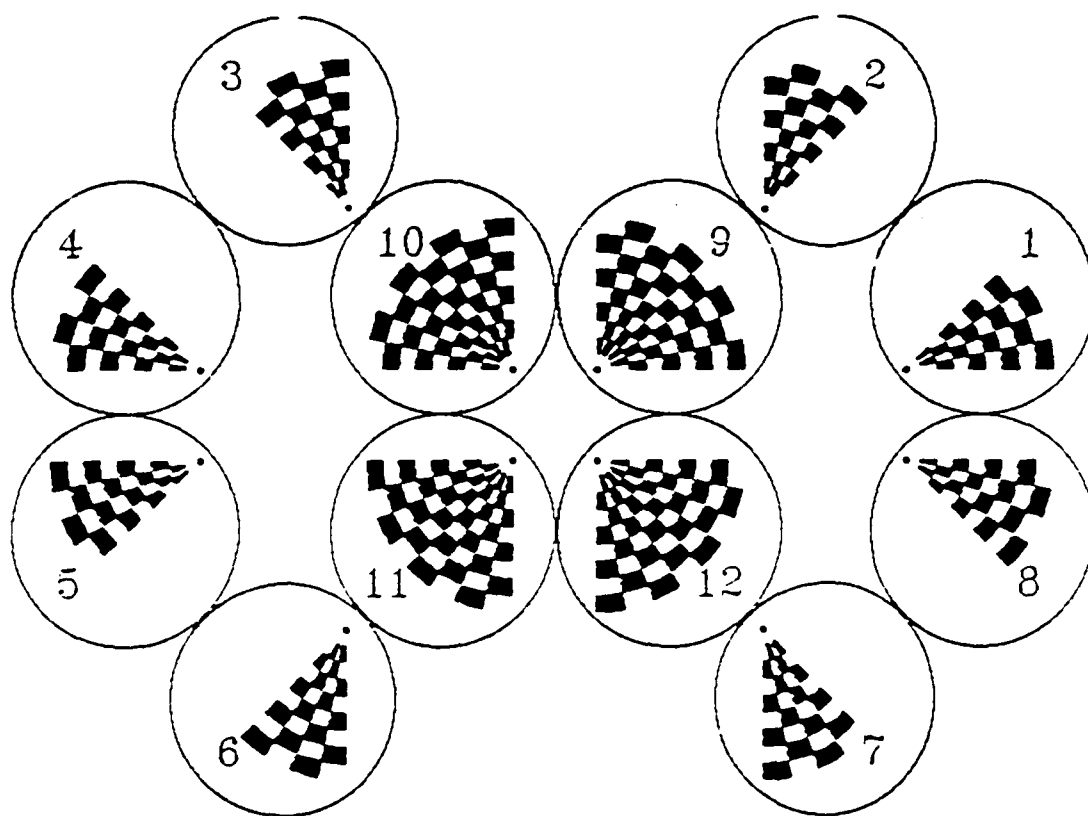
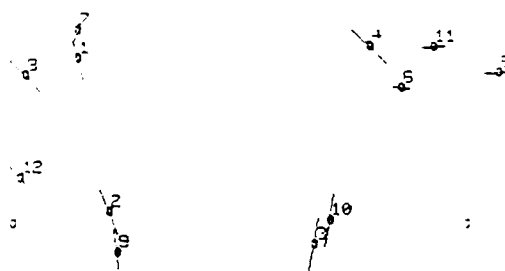
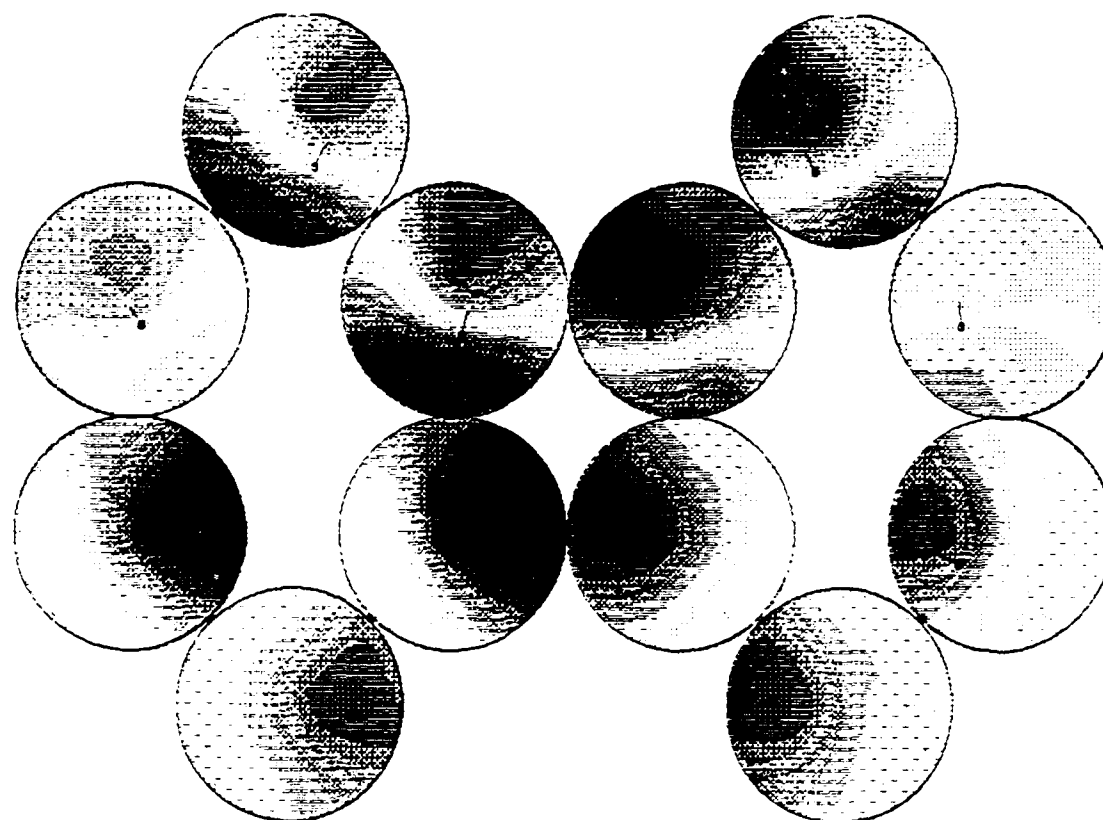
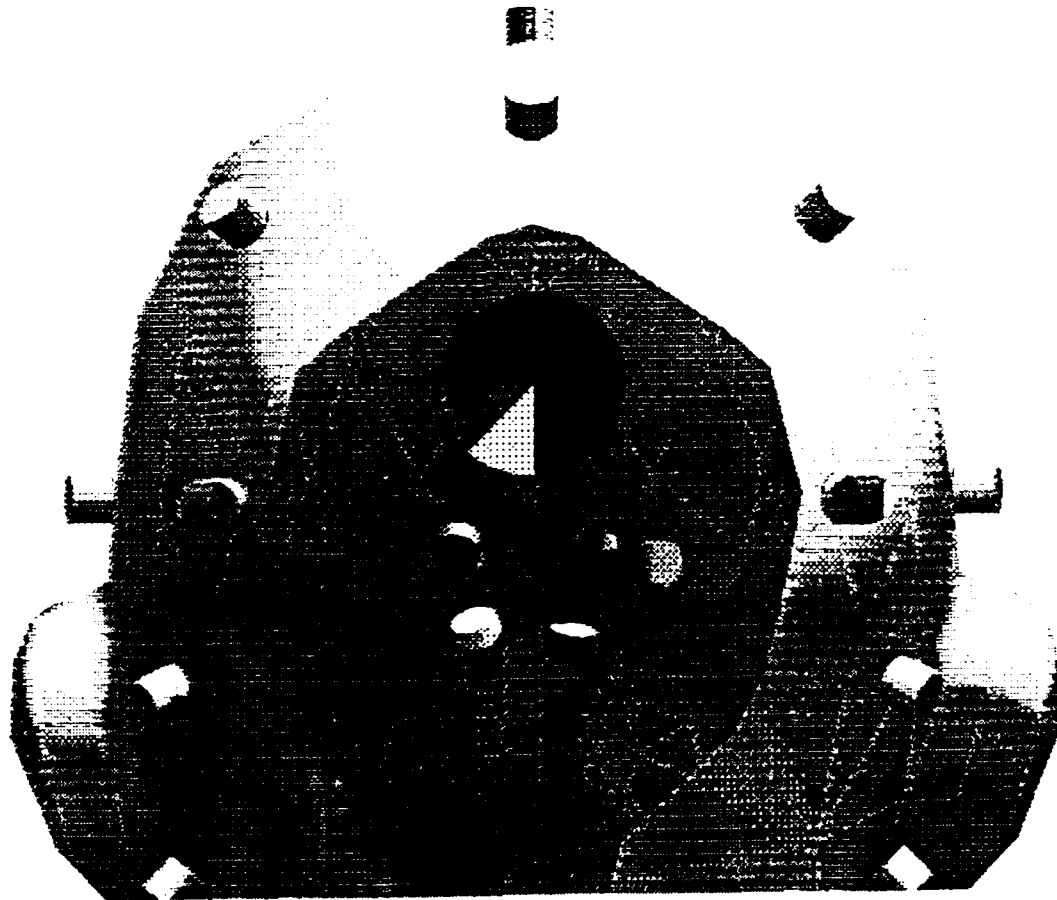


Figure 11. [TOP] - Visual stimulus patterns; [BOTTOM] - Electrode montage viewed from the back of the head.



**Figure 12.** Potential field topographies corresponding to the stimuli in Figure 12, from one subject [TOP], and the locations in the coronal plane and directions of the corresponding computed dipoles for that subject [BOTTOM].



**Figure 13.** Dipole locations for the 8 octant stimuli averaged across the four subjects are shown as colored cylinders. The rear surface of the head has been removed to view the dipole positions and orientations within. Direction of each dipole is indicated by the central axis of each flat cylinder. The large multicolor circle is a color legend indicating the visual stimulus octant corresponding to each dipole. In order to make the retinotopic projection easier to visualize, the color legend depicts which sectors in each retina were stimulated (e.g., blue colors indicate upper-right retinal stimulation resulting from a checkerboard in the lower-left visual field.)

**C. Beyond Topographic Mapping: Towards Functional-Anatomical Imaging  
with 124-Channel EEG's and 3-D MRI's**

**BEYOND TOPOGRAPHIC MAPPING: TOWARDS FUNCTIONAL-ANATOMICAL  
IMAGING WITH 124-CHANNEL EEGs and 3-D MRIs**

Alan Gevins, Paul Brickett, Bryan Costales,  
Jian Le, Bryan Reutter

EEG Systems Laboratory  
and  
SAM Technology  
51 Federal St.  
San Francisco, CA 94107  
415-957-1600  
FAX: 415-546-7122  
USENET Mail: alan@eeg.com

**BRAIN TOPOGRAPHY**, In Press

**Running Title: Beyond Topographic Mapping**



**ABSTRACT**

A functional-anatomical brain scanner that has a temporal resolution of less than a hundred milliseconds is needed to measure the neural substrate of higher cognitive functions in healthy people and neurological and psychiatric patients. Electrophysiological techniques have the requisite temporal resolution but their potential spatial resolution has not been realized. Here we briefly review progress in increasing the spatial detail of scalp-recorded EEGs and in registering this functional information with anatomical models of a person's brain. We describe methods and systems for 124-channel EEGs and magnetic resonance image (MRI) modeling, and present first results of the integration of equivalent-dipole EEG models of somatosensory stimulation with 3-D MRI brain models.

## INTRODUCTION

There are a number of techniques for monitoring brain function that are more or less noninvasive, including Positron Emission Tomography (PET), Single Photon Emission Computed Tomography (SPECT), Magnetic Resonance Spectroscopy (MRS), Electroencephalography (EEG) and Magnetoencephalography (MEG). Although the 3-Dimensional (3-D) anatomical imaging capabilities of EEG or MEG are not comparable to PET, SPECT or MRs, EEGs and MEGs uniquely offer temporal resolution in the millisecond range. This particular capability is invaluable for studying seizure disorders and neurocognitive processes. With improving recording and analysis technologies, other valuable information that generations of clinicians and researchers over the past 60 years have believed was hidden in the EEG is becoming more accessible (see reviews in Lopes da Silva et al., 1986; Gevins and Remond 1987). Indeed, as technical capabilities have increased, so has the specificity of information extracted from EEGs, and the value of further developing methods to mine this hidden information is clearly mandated by the noninvasiveness and low cost of scalp EEG measurements for obtaining split-second information about brain function.

While spatial EEG features have often been difficult to discern in polygraph tracings, the recent availability of EEG color topographic maps has made appreciating them easy, even for the non-EEG specialist. The utility of the maps would be even greater if more spatial detail were available, and if the scalp EEG patterns could be registered with underlying brain anatomy. During the past 8 years, we have made some modest progress towards this end. We have improved and expanded our recording and analysis capabilities to accommodate 124 EEG channels, and have developed methods for reducing blur distortion of EEGs by the skull. We have implemented programs for processing magnetic resonance images, and we are developing a means of automatically constructing three-dimensional (3-D) models of a subject's brain. In tests of our method for registering EEGs and MRIs using somatosensory stimulation data, we obtained good results. Previous reports of prior stages of progress in this regard have been published in Gevins (1987, 1988, 1989a,b).

## EEG RECORDING METHOD

### A. Extended 10-20 System

Several nomenclatures for defining electrode placements added to the original nineteen placements of the International 10-20 System (Jasper, 1958) have been published (see Gevins, 1988). Regardless of which nomenclature is used, the basic idea is that extra equidistant coronal rows are added between the original rows, and extra equidistant electrodes are added to fill in the spaces in each row. Our current 124-channel montage is shown in Figure 1. In the system we use, the letter "a" is prefixed to an existing 10-20 row name to indicate a position anterior to the existing one. For example, aO is anterior occipital, aP is anterior parietal, aC is anterior central and aF is anterior frontal. Two additional numbers appear after the location number (1-8) of the 10-20 positions. These two numbers (0-9) indicate the proportional distance to the next anterior and medial 10% electrode position, respectively. For example, an electrode halfway between P3 and aP1 would be named P355, while an electrode halfway between P3 and P1 would be named P305. With the original nineteen electrodes of the 10-20 System, the typical distance between electrodes on an average adult male head is about 6 cm; with 124 electrodes, the typical distance is 2.25 cm.

### B. Electrode Hat

In most routine clinical EEGs, electrodes are prepared and positioned on the head individually, while in some labs commercially available electrode caps with nineteen built-in electrodes are used. Extending the cap idea, we constructed one from a stretchable fabric, and populated it with 124 commercial tin-disk electrodes encased in plastic holders (Figure 2). The cap is positioned on the head by reference to the nasion,inion and preauricular notches. Individual recording sites are cleansed in

the usual manner, and conducting gel is injected with a blunt needle through the top of each electrode. It takes a team of four research assistants about an hour to prepare a subject. While this is acceptable for infrequent research recordings, it is far too long and costly for routine use. We are developing a more efficient system for recording EEGs which we expect to greatly reduce application time.

### C. Measuring Electrode Positions

Traditionally, individual electrodes are placed according to measurements taken with a tape measure. While this is sufficient when recording from 19 electrodes, greater precision is needed when many more electrodes are used and when one wishes to relate a recording position on the scalp to the underlying cortical anatomy. In our lab, the position of each electrode on a subject's head is measured with a probe that has coils for sensing the three-dimensional position of the probe tip with respect to a magnetic field source in the head support (Figure 3). Adjustable guides built into the head support hold the subject's head comfortably in place while the measurements are made. A menu-driven program is used to select electrodes to be measured and display the digitized position of each electrode on a two-dimensional projection display. Position measurement is accurate to better than 3mm [RMS]. Figure 4 shows the screen image of this program after all electrodes and some additional surface landmarks have been digitized.

### D. Software System for Data Collection and Analysis

Commercial EEG computer systems have vastly improved during the past few years, yet some important limitations still restrict their utility for researchers such as ourselves. This is a consequence of the fact that most systems have been designed for the clinical market where the central concern is to provide a series of fixed tests and measures. The most severe limitations are that: (1) a way to implement new experimental protocols flexibly is rarely provided; (2) artifact detection and editing capabilities are too limited; (3) the system capacity for recording large numbers of channels and collecting and storing large databases is inadequate; (4) there are limited means of subdividing data to explore relationships between subsets of data and variations in a subject's responses or state; and (5) spatial analyses are underdeveloped, with too few channels, a lack of spatial filters to reduce volume conduction distortion, a lack of cross-channel analyses (e.g., crosscovariance and crosspower, correlation and coherence), and the lack of means to investigate the relationship between neuroelectric data and cortical anatomy and physiology revealed by MRI and PET imaging technologies.

The system we have been developing, now in its fifth generation, is aimed at overcoming these limitations (Gevins & Yeager, 1972; Gevins et al., 1975, 1989; Gevins, 1980, 1984, 1987; 1988) (Figure 5). This generation is distinguished from its predecessors architecturally by its self-decoding Data Description Language, network extensibility, and multi-window graphical user interface. As of May 1990, all the functions described in the following two paragraphs are fully operational.

*1. Data Collection:* In the fifth generation EEGSL system, two computers are used for data collection: a Concurrent 5700 and an IBM PC-compatible 386. The PC is used to present stimuli and gather behavioral response data from the subject, while the Concurrent collects physiological data and controls the PC. The Concurrent runs a real-time version of the UNIX operating system, while the PC runs the DOS operating system. We have written an experiment control software system which runs the two computers, presents a variety of visual, auditory and somatosensory stimuli according to flexible task protocols, and digitizes up to 256 channels of physiological data. Up to 128 EEG traces can be monitored in real time as data are collected. Most parameters of an experiment can be altered via a menu-driven interactive display. A calibration module numerically adjusts the gain of all channels according to the magnitude of a calibration signal. Another module detects gross artifacts and color-codes contaminated data such as eye movements, gross head and body movements and bad electrode contacts on the operator's screen. Stimulus, behavioral and physiological data are stored on

hard disk according to a self-decoding Data Description Language, and archived to magnetic tape. The data are immediately available to researchers at their desks using either remote terminals, or SUN workstations via Ethernet and Network File System.

2. *Data Analysis:* For subsequent data analysis the current system also has a number of other functional improvements over its predecessors including: (1) least-squares Laplacian derivation estimation to reduce volume conduction distortion (Gevins, 1989b); (2) digital filters with user-specified characteristics; (3) time series analysis including spectral analysis, Wigner Distributions (Morgan and Gevins, 1986), and event-related covariance analysis (Gevins et al., 1987, 1989a; Gevins and Bressler, 1988); (4) neural-network-driven pattern recognition to extract optimal or near-optimal subsets of features for recognizing different experimental or clinical categories (Gevins, 1980, 1987; Gevins and Morgan, 1988); and (5) anatomical modeling to construct 3-D finite element models of the brain and head from MRI scans (Le et al., In Prep.; Brickett et al., In Prep.; Reutter et al., In Prep.). Four on-line, interactive subsystems are used to examine and edit data for residual artifacts (on an individual channel basis if desired), sort data according to stimulus, response or other categories, perform exploratory data analysis, and produce three-dimensional color graphics representations of the brain and head.

## MRI ANALYSIS AND MODELING METHODS

Since commercial MRI analysis packages are not designed for research on functional-anatomical integration and thus lack features essential to our undertaking, we have had to develop our own algorithms and software to produce 3-D brain models suitable for functional localization studies. Visualization software permits construction of 3-D composites of multiple 2-D image planes, as well as 3-D surface rendering based on surface contours. Since generating surface contours manually is laborious and subject to error, we have worked on automating the procedure. We have also automated the alignment of the digitized EEG electrode positions with the scalp surface contours, which is a critical first step in a functional-anatomical analysis. The MRI contour information is used to produce a mathematical finite element model (FEM) of the brain and head suitable for equivalent dipole source localization and scalp EEG deblurring development. Since complex FEM normally run on supercomputers, we made a significant effort to develop FEM algorithms and programs that could run efficiently on a desktop workstation.

### A. EEG-MRI alignment procedure

In order to visualize the brain areas underlying EEG electrodes, a procedure is needed for aligning scalp electrode positions with the MR Images. In the procedure we now use, x, y, z translation and x, y, z axis rotations are computed iteratively to align the digitized positions of the EEG electrodes with the MRI data. This is done for each electrode by finding the distance to the closest point on the scalp surface MRI contours and minimizing the mean distance for all electrodes. With MR images that have a 3 mm inter-slice spacing, we usually achieve a mean error distance better than 2 mm. This is more accurate and less subjective than alignment procedures that use skull landmarks such as the nasion and pre-auricular points located visually in the MR images. Figure 6 shows the electrodes displayed schematically on a scalp surface reconstructed from horizontal MR scalp contours as described below.

### B. 3-D Composite MRI displays

Figure 7 shows examples of 3-D composite images taken from a routine clinical MR exam of a patient with partial seizures. A combination of horizontal, coronal, and sagittal plane images are shown in five different views. Figure 8 shows another composite from the same data and also a partial surface reconstruction done as described below.

### C. Contour extraction and surface rendering

Both the scalp and cortical surface contours in Figures 7 and 8 were traced using an intensity thresholding technique, one of the two image analysis methods we developed to extract scalp and cortical surface contours from MRIs. The first technique uses intensity thresholding, which involves extracting contours along which the image intensity is equal to a defined threshold. This technique is useful for extracting the scalp surface contour which can be discerned easily from the black (approximately zero intensity) background of the image.

The current method of surface rendering has six steps: 1) for each pair of adjacent contours, find the point on the second contour closest to the first; 2) calculate the two distances from each of these points to the next point on the adjacent contour; 3) make a triangle using the point with the shortest distance, advancing on that contour; 4) repeat steps two and three until all points are exhausted; 5) repeat steps two to four in the reverse direction along the contours; and 6) piece together the "best" result. This was the surface reconstruction method used for Figure 8 showing a surface reconstruction of the cerebral cortex (in yellow), from the same patient as in Figure 7, using the available coronal slices.

The second contour extraction method we have used involves differential intensity analysis. Using this technique, contours that separate image regions with different local average intensities are extracted. Resulting contours pass through the points in the image at which the local average image intensity is changing most rapidly. This technique requires no a priori intensity threshold value, and is useful for extracting the cortical surface contour which has a less well-defined image intensity value throughout an image than the scalp surface contour. The first-order and second-order partial derivatives of the image are estimated using 2-D filters, and these derivatives are used to locate the local maxima in the gradient of the image intensity. Highly computationally efficient filtering techniques have been developed for the estimation of the partial derivatives of the image (Algazi et al., 1989). Figure 9 shows an example of contours corresponding to locations of local maxima in the gradient of the image intensity, which trace sulci.

### D. 3-D Cortical surface image model

3-D surface models of the external convexity of the cerebral cortex, such as those of Figure 8, are not sufficient to visualize and computationally model the cortical surface within fissures and sulci. As a result, we developed an algorithm to model cubic volume elements (voxels). The faces of the voxels lie in the horizontal, coronal, and sagittal planes for which MRI data have been obtained. The MRI data are mapped onto the faces of the voxels to obtain a 3-dimensional display of the image data. The image planes used are averaged horizontal planes that lie halfway between the horizontal planes in which MRI data have been acquired, and coronal and sagittal image planes that are synthesized from the acquired horizontal images using linear interpolation. The spacing between image planes is 3 mm, which yields voxels with dimensions of 3 mm by 3 mm by 3 mm. The images have pixel dimensions of approximately 1 mm by 1 mm.

The initial set of voxels is the set bounded by those voxels that lie just inside the cortical surface. To view the MRI data at a slightly deeper level, a mathematical morphology erosion operation is used to remove the boundary layer of voxels, thereby exposing the faces of the voxels that lie one layer deeper. By eroding the model iteratively, anatomical structures can be tracked and 3-dimensional models of the structures can be made (see Figure 12).

## E. Finite Element Modeling

Maxwell's Equation, (Landau et al., 1984, Nunez, 1981)

$$\nabla \bullet (\sigma \nabla u) + \nabla \bullet J = 0 \quad \text{in } \Omega \quad (1)$$

is frequently used to study the electromagnetic field generated by populations of neurons. Here  $\sigma$  ( $> 0$ ) is the conductivity tensor at a point  $R = (x, y, z)$  in  $\Omega$  (e.g., a human head),  $u$  is the electric potential at  $R$ , and  $J$  is the electric current density at  $R$ . When  $\Omega$  represents a human head, the following boundary condition for equation (1) is obtained

$$\sigma \nabla u \bullet \mathbf{n} = 0 \quad \text{on } S \quad (2)$$

since electric current does not flow out of the head in the direction normal to the surface. The limited scalp potential measurement specifies another boundary condition.

$$u = U(x, y, z) \quad \text{on } S_1. \quad (3)$$

Where  $S_1$  is a subsurface of  $S$  corresponding to area covered by electrodes.

The Finite Element Method (FEM) we developed finds the numerical solution of equation (1) with the boundary condition as specified in equation (2) when the electromagnetic field activities of a head are modeled. Advantages of this approach are: 1) it handles the Dirac Delta Function  $\nabla \bullet J$  smoothly by transforming equation (1) into a variational form when  $J$  represents a dipole-like kind of source; 2) it allows us to model the complicated geometries of different tissues within the head by generating finite elements using contours on pairs of adjacent MR images; and 3) it produces a sparse matrix in which many entries are zeroes. We developed efficient sparse matrix techniques (Le et al., in prep.) that can solve Maxwell's equation at 10,087 FEM nodes in about 100 min on a SUN Sparc-1 workstation (12 MIPS) with 8MB of memory (Figure 10).

We can use this analysis to localize single equivalent dipole sources of recorded scalp potentials, or obtain the potential distribution within the whole head given the localized source. To do this, we choose a specific function  $J$  and solve the corresponding potential distribution  $u$  using FEM such that the difference between  $u$  on  $S_1$  and  $U(x, y, z)$  defined on  $S_1$  is minimized using an iterative process. Another use of FEM, in which the current distribution on the surface of the brain is estimated from scalp recordings, is described in the next section.

## TOWARDS FUNCTIONAL-ANATOMICAL INTEGRATION

### A. Spatial filters to reduce blur distortion

Electrical currents generated by sources in the brain are volume conducted through brain, cerebrospinal fluid, skull and scalp to the recording electrodes. Because of this, potentials due to a localized source are spread over a considerable area of scalp and the potential measured at a scalp site represents the summation of signals from many sources over much of the brain. Using a 4-shell spherical head model, we have estimated the "point spread" for a radial dipole in the cortex to be about 2.5 cm (Doyle and Gevins, Submitted). The "simplest" way to reduce this distortion is to take the Laplacian in two dimensions about each electrode. Details of this method, however, are less straightforward than they might seem, as discussed below. Another improvement in distortion is possible, in principle, by using a Finite Element Method and estimates of the conductivity properties of the tissue between brain and scalp surface to estimate the potentials which would actually be recorded on the surface of the brain.

1. *Laplacian operator*: Neuroelectric signals recorded at the scalp are principally distorted by transmission through the low-conductance skull. This distortion manifests as a spatial low-pass filtering which causes the potential distribution at the scalp to appear blurred or out of focus. There are a number of methods for reducing this distortion, among which the spatial Laplacian operator is perhaps the simplest and most effective (Nunez, 1981). This method, which is often referred to as the *Laplacian Derivation*, is derived by computing the second derivative in space of the potential field at each electrode. This converts the potential into a quantity proportional to the current entering and exiting the scalp at each electrode site, and eliminates the effect of the reference electrode used during recording. An approximation to the Laplacian Derivation, introduced by Hjorth (1975, 1980) assumes that electrodes are equidistant and at right angles to each other. Although this approximation is fairly good for some electrode positions such as midline central (Cz), it is less accurate for others such as midtemporal (T5). We have been using a more accurate estimate of the Laplacian that is based on projecting the measured electrode positions onto a two-dimensional surface. Although this produces a dramatic improvement in topographic detail, some problems remain because of the assumptions that surrounding electrodes used to estimate the Laplacian of an electrode are near that electrode and that the current gradient is uniform over the region encompassed by the surrounding electrodes. Furthermore, it is not possible to estimate the Laplacian at peripheral electrodes since there are no surrounding electrodes on one side.

The objective of the LD calculation is an accurate estimate of

$$\left( \frac{\partial^2}{\partial x^2} + \frac{\partial^2}{\partial y^2} \right) V \quad (1)$$

When the electrodes are arranged in a uniform square grid, the method described by Hjorth will suffice. However, both variations in distance and variations in angle are always present to some degree, and can cause serious errors in calculation. Variations in distance can be corrected by dividing by the interelectrode distance (Thickbroom, 1984). Non-uniform angles between electrodes are more difficult to correct. Spline extrapolation methods have been used to account for both types of variation (Perrin, 1987), but require such large amounts of computation that they are practical only for small amounts of data. The method presented below also accounts for both types of variation, but requires only an initial large computation of coefficients based on the actual geometry of the electrodes.

Assume we wish to compute the LD at position  $q_0$  using  $N$  surrounding electrodes in an arbitrary configuration as shown:

Let the voltage at position  $q_i$  be designated by  $V_i$ . Put the origin of a cartesian coordinate system at  $q_0$  with the  $z$  axis pointing perpendicular to the plane nearest the electrodes. Let  $(q_{ix}, q_{iy})$  represent the  $x$  and  $y$  components of the electrode position within this plane.

Then  $\vec{E}(x,y) = -\nabla V(x,y)$  is the electric field in the plane or equivalently:

$$V_0 - V_i = \int_C \vec{E} \cdot d\vec{s} \quad (2)$$

Where  $C$  is any curve in the plane connecting  $q_0$  to  $q_i$ . If we let  $E_x$  and  $E_y$  designate the  $x$  and  $y$  components of  $\vec{E}$  then the two-dimensional laplacian of the voltage is given by:

$$\nabla^2 V = - \left( \frac{\partial E_x}{\partial x} + \frac{\partial E_y}{\partial y} \right) \quad (3)$$

The field  $\vec{E}$  can be expanded in a two-dimensional Taylor series (Rudin, 1976; Apostol, 1969) as:

$$\vec{E}(\vec{q}) = \vec{E}(0) + D\vec{E}(0)\vec{q} + \|\vec{q}\|^2 \vec{r}(\vec{q}) \quad (4)$$

where  $q^T = (q_x, q_y)$ ,  $\vec{r}$  is a remainder term which is bounded as  $q \rightarrow 0$  and  $D\vec{E}$  is the Jacobian matrix of  $E$  given by:

$$D\vec{E} = \begin{bmatrix} \frac{\partial E_x}{\partial x} & \frac{\partial E_x}{\partial y} \\ \frac{\partial E_y}{\partial x} & \frac{\partial E_y}{\partial y} \end{bmatrix} \quad (5)$$

If we let  $\vec{\alpha}(t)$  be a parameterization of the line segment connecting  $q_i$  with  $q_0$  then taking the first two terms in equation:

$$\begin{aligned} V_0 - V_i &= \int_{\alpha} \vec{E} \cdot d\vec{s} \\ &= \int_0^{t_0} \vec{E}(0) + \left( \frac{\partial E_x}{\partial x} x + \frac{\partial E_x}{\partial y} y, \frac{\partial E_y}{\partial x} x + \frac{\partial E_y}{\partial y} y \right) \vec{\alpha}'(t) dt \\ &= \left[ E_x(0) q_{iz} + E_y(0) q_{iy} + \frac{\partial E_x}{\partial x} q_{iz}^2 + \frac{\partial E_x}{\partial y} q_{iz} q_{iy} + \frac{\partial E_y}{\partial y} q_{iy}^2 \right] \end{aligned} \quad (6)$$

Here we have made use of the fact that the curl of an electric field is zero which implies

$$\frac{\partial E_x}{\partial y} = \frac{\partial E_y}{\partial x} \quad (7)$$

We can combine the above equation for each of the surrounding electrodes in a single matrix equation:

$$\begin{bmatrix} q_{1x} & q_{1y} & q_{1x}^2/2 & q_{1x}q_{1y} & q_{1y}^2/2 \\ q_{2x} & q_{2y} & q_{2x}^2/2 & q_{2x}q_{2y} & q_{2y}^2/2 \\ & & \cdot & & \\ & & \cdot & & \\ & & \cdot & & \\ q_{nx} & q_{ny} & q_{nx}^2/2 & q_{nx}q_{ny} & q_{ny}^2/2 \end{bmatrix} \begin{bmatrix} E_x(0) \\ E_y(0) \\ \frac{\partial E_x}{\partial x} \\ \frac{\partial E_x}{\partial y} \\ \frac{\partial E_y}{\partial y} \end{bmatrix} = \begin{bmatrix} V_0 - V_1 \\ V_0 - V_2 \\ \cdot \\ \cdot \\ V_0 - V_n \end{bmatrix} \quad (8)$$

or

$$QF = V \quad (9)$$



In this equation the  $Q$  matrix is composed of the  $x$  and  $y$  coordinates electrode positions and remains fixed during the entire recording. The voltage vector  $V$  is measured at each time point and vector  $F$  composed of the electric field components and their derivatives is unknown.

Multiplying the above by the transpose of  $Q$  gives

$$Q^T Q F = Q^T V \quad (10)$$

If  $Q$  premultiplied by its transpose  $Q^T$  is nonsingular then we can form the least squares estimate of  $F$  as

$$F = \left( Q^T Q \right)^{-1} Q^T V \quad (11)$$

If we let  $C$  be the sum of the third and fifth rows of  $\left( Q^T Q \right)^{-1} Q^T$  then from the above equation we can estimate the laplacian LD as:

$$\nabla^2 V = - \left[ \frac{\partial E_x}{\partial x} + \frac{\partial E_y}{\partial y} \right] \approx -CV \quad (12)$$

*2. Finite Element Method deblurring in a realistic head model:* Since an "image" of the potential distribution over local cortical areas is highly desirable, spatial deblurring methods can be used to reduce volume conduction and increase spatial resolution. One method of doing this without introducing an arbitrary model of the actual number and location of sources is to use finite element methods to represent the true geometry of cortex, cerebrospinal fluid, skull and scalp, and to model the potential activity described by Maxwell's equations in the scalp and skull layers. This operation could be performed without imposing an arbitrary source model because, regardless of where they are generated in the brain, potentials recorded at the scalp must arise from volume conduction from the cortical surface through the skull and scalp. While we expect this method to produce an estimate of the current distribution at the cortical surface, it does not identify the number, position, or orientations of sources. (For instance, the skull currents resulting from a tangential dipole source in the cortex might still be difficult to distinguish from that caused by two radial dipole sources.)

For this application, the region of interest is limited to the scalp volume and skull volume. The difference between the inner surface of the skull and the outer convexity of the cortical surface is assumed to be small enough to be neglected. We also assume that the potential activity in the region of interest is described by Maxwell's equation, that the boundary condition on the air-scalp surface is stated by equation (2), i.e., current cannot flow out of the scalp, and that the boundary condition on the cortical surface is stated by the following equation (4) which describes the cortical surface potentials.

$$u = G(x, y, z) \quad \text{on } S_2. \quad (4)$$

We also assume that there is no generating source within the scalp or skull which means the function  $J$  in equation (1) is zero. Although of course there is no general solution to the "inverse problem," because of the assumed boundary conditions there is a unique solution of equation (1), which may be obtained as follows. Applying the Finite Element Method to equation (1) with boundary conditions in (2) and (4), the following matrix vector relation is obtained (Le et al., in prep.)

$$A\mathbf{u} = \mathbf{f}. \quad (5)$$

Here  $\mathbf{u}$  is a vector of dimension  $n$ , which is a numerical approximation to the analytical potential distribution function  $u$  in equation (1). The value of  $n$  corresponds to the total number of vertices on all

the finite elements in the region of interest. Since we are assuming that no generating sources are present in the skull and scalp,  $J \equiv 0$  and therefore  $\mathbf{f} = 0$ . We then decompose  $\mathbf{u}$  into three sets, the potentials which correspond to the electrodes on the scalp, the potentials which correspond to the cortical surface, and the potentials in the rest of the region, and denote them by  $\mathbf{u}_1$ ,  $\mathbf{u}_3$  and  $\mathbf{u}_2$  respectively. If we decompose the matrix  $\mathbf{A}$  correspondingly, then equation (5) becomes:

$$\begin{pmatrix} \mathbf{A}_{11} & \mathbf{A}_{12} & \mathbf{A}_{13} \\ \mathbf{A}_{21} & \mathbf{A}_{22} & \mathbf{A}_{23} \\ \mathbf{A}_{31} & \mathbf{A}_{32} & \mathbf{A}_{33} \end{pmatrix} \begin{pmatrix} \mathbf{u}_1 \\ \mathbf{u}_2 \\ \mathbf{u}_3 \end{pmatrix} = 0.$$

Solving  $\mathbf{u}_1$  with respect to  $\mathbf{u}_3$ , we get

$$(\mathbf{A}_{11} - \mathbf{A}_{12}\mathbf{A}_{22}^{-1}\mathbf{A}_{21})\mathbf{u}_1 = (\mathbf{A}_{12}\mathbf{A}_{22}^{-1}\mathbf{A}_{23} - \mathbf{A}_{13})\mathbf{u}_3 \quad (6)$$

and solving  $\mathbf{u}_3$  with respect to  $\mathbf{u}_1$ , we get

$$\mathbf{A}_{22}^{-1}\mathbf{A}_{23})\mathbf{u}_3 = (\mathbf{A}_{32}\mathbf{A}_{22}^{-1}\mathbf{A}_{21} - \mathbf{A}_{31})\mathbf{u}_1. \quad (7)$$

For a given  $G_k$ ,  $\mathbf{u}_3^k$  is known. Then  $\mathbf{u}_1^k$  can be computed via equation (6) and the residual is calculated from  $\mathbf{u}_1^k$  and  $U(x, y, z)$  which correspond to the predicted and measured potentials, respectively.

*3. Estimating conductivities and evaluating deblurring method:* Up to now, estimates of conductivity for the scalp, skull, CSF and brain have been published (Geddes & Baker, 1967; Hosek, 1970). We have attempted to estimate skull conductivity by injecting small currents at one electrode and recording at the others for many combinations of stimulating and recording electrodes (Gevens and Doyle, Unpublished data). This has failed, however, because of the obvious shunting effect of the scalp. We are currently working on a more direct approach that does not involve applying external stimuli but rather uses known natural sources of activity. We are evaluating the method by comparing deblurred scalp data with subdural grid data recorded from the same patient.

## B. Equivalent Dipole Modeling of Somatosensory Stimulation

We are just beginning to apply the methods described above to functional-anatomical localization. The first application was to perform equivalent dipole modeling of somatosensory stimulation. For this purpose, the middle fingers of the left and right hands, and the right index finger were each electrically stimulated at 15 Hz for three 100-second intervals. Artifact-free epochs of 0.533 seconds were averaged, and Fourier-transformed real and imaginary components of the 15-Hz response were averaged over each 100-second run. Data for each of the three runs were then combined for each finger for calculation of the "canonical" phase, i.e., that phase angle onto which the projections of all the phasors yielded the greatest squared amplitude. These steady-state amplitude measures were used to construct topographical maps and for least-squares fitting of equivalent current dipoles. Preliminary results for the first subject (Figure 11) show topographical maps of the Laplacian of the evoked responses to stimulation of the left and right middle fingers. (Each map is scaled separately. Amplitude of the right finger response is approximately one half that of the left.) Figure 12 presents the result of fitting single equivalent dipoles to these data and also the result for the right middle finger. Dipoles are shown with respect to the scalp surface and eroded brain model described above. Each dipole is represented as a disk with its center on the dipole location, and axis in the dipole direction. Each dipole appears in the contralateral hemisphere, and the dipole for the forefinger is located slightly more lateral than that for the middle finger, consistent with the known locations of the sensory projection areas and other physiological source localization results (Luders et al., 1986; Wood et al., 1985).

## CONCLUSION

There is no doubt that much useful information lies hidden in the EEG. We are optimistic about advancing our technology to mine this hidden information, and to further our investigations of the neural substrate of human higher cognitive brain functions.

## ACKNOWLEDGMENTS

This work was supported by grants from agencies of the Federal government of the United States of America, including The National Institute of Neurological Diseases and Strokes, The National Institute of Mental Health, The Air Force Office of Scientific Research and The National Science Foundation. We gratefully acknowledge this support, as well as the efforts of our colleagues at the EEG Systems Laboratory, Drs. S. Bressler, B. Cutillo, and J. Illes, for their contributions to the research presented here.

## LITERATURE CITED

- Algazi, V.R., Reutter, B.W., van Warmerdam, W.L.G & Liu, C.C. Three-dimensional image analysis and display by space-scale matching of cross sections. *J. Opt. Soc. Am.*, 1989: 6, 890-899.
- Brickett, P. and Gevins, A. Retinotopic source localization of 15-Hz pattern-reversal evoked potentials, in preapration.
- Doyle, J.C. & Gevins, A.S. Technical Note: Spatial filters for event-related brain potentials. *EEG clin. Neurophysiol.*, submitted.
- Geddes, L.A. & Baker, L.E. The specific resistance of biological material - a compendium of data for the biomedical engineer and physiologist. *Med. Biol. Engr.*, 1967: 5, 271-293.
- Gevins, A.S. Application of pattern recognition to brain electrical potentials. *IEEE Trans. Pattern Ana. Mach. Intell.*, 1980: PAM-12, 383-404.
- Gevins, A.S. Analysis of the electromagnetic signals of the human brain: Milestones, obstacles and goals. *IEEE Trans. Biomed. Enginr.*, 1984: BME12(31), 833-850.
- Gevins, A.S. Statistical pattern recognition. In A. Gevins & A. Remond (Eds.), *Methods of Analysis of Brain Electrical and Magnetic Signals: Handbook of Electroencephalography and Clinical Neurophysiology (Vol. 1)*, Amsterdam, Elsevier, 1987.
- Gevins, A.S. Recent advances in neurocognitive pattern analysis. In: E. Basar (Ed.), *Dynamics of Sensory and Cognitive Processing of the Brain*. Heidelberg, Springer-Verlag, 1988: 88-102.
- Gevins, A.S. Signs of model making by the human brain. In: E. Basar & T. Bullock (Eds.), *Dynamics of Sensory and Cognitive Processing by the Brain*. Springer-Verlag, 1989a: 408-419.
- Gevins, A.S. Dynamic Functional Topography, *Brain Topography*, 1989b: 2(1), 37-56.
- Gevins, A.S. and Bressler, S.L. Functional topography of the human brain. In: G. Pfurtscheller (Ed.), *Functional Brain Imaging*. Hans Huber Publishers, Bern, 1988: 99-116.
- Gevins, A.S. and Morgan, N.H. Applications of neural-network (NN) signal processing in brain research. *IEEE ASSP Trans.*, 1988: 7, 1152-1161.
- Gevins, A.S. and Remond, A. (Eds.) *Methods of Analysis of Brain Electrical and Magnetic Signals. Handbook of Electroencephalography and Clinical Neurophysiology, Vol.1*. Amsterdam, Elsevier, 1987.
- Gevins, A.S. and Yeager, C.L. EEG spectral analysis in real time. *DECUS Proc. Computers in Medicine*, 3 1972: 4, 71-74.
- Gevins, A.S., Yeager, C.L., Diamond, S.L., Spire, J.P., Zeitlin, G.M. and Gevins, A.H. Automated analysis of the electrical activity of the human brain (EEG): A progress report. *IEEE Proc.*, 1975: 63(10), 1382-1399.
- Gevins, A.S., Doyle, J.C., Cutillo, B.A., Schaffer, R.F., Tannehill, R.L., Ghannam, J.H., Gilcrease, V.A. & Yeager, C.L. Electrical potentials in human brain during cognition: New method reveals dynamic patterns of correlation. *Science*, 213, 1981: 918-922.
- Gevins, A., A.S., Cutillo, B.A., Bressler, S.L., Morgan, N.H., White, R.M., Greer, D.S., Illes, J. Event-related covariances during a bimanual visuomotor task, Part I: Methods & analysis of stimulus-and

response-locked data. *EEG clin. Neurophysiol.*, 1989: 74(1), 58-75.

Hjorth, B. An on-line transformation of EEG scalp potentials into orthogonal source derivations *Electroenceph. clin. Neurophysiol.*, 1975: 39, 526-530.

Hjorth, B. Source derivation simplifies topographical EEG interpretation. *Amer. J. EEG Technol.*, 1980: 20, 121-132.

Hosek, A.R. *An experimental and theoretical analysis of effects of volume conduction in a nonhomogeneous medium on scalp and cortical potentials generated in the brain.* Doctoral dissertation, Marquette Univ. Biomed. Engr., 1970.

Jasper, H. H. The ten-twenty electrode system of the international federation. *Electroenceph. clin. Neurophysiol.*, 1958: 10, 371-375.

Landau, L.D., Lifshitz, E.M. & Pitaevskii, *Electrodynamics of Continuous Media.* New York: Pergamon, 1984.

Le, J., Brickett, P., Surkis, A. and Gevins, A.S. Finite element modeling of Maxwell's equations in a realistic human head, in preparation.

Lopes da Silva, F., Storm van Leeuwen W., Remond, A. (Eds.), *Handbook of Electroencephalography and Clinical Neurophysiology, Vol. 2: Clinical Applications of Computer Analysis of EEG and other Neurophysiological Signals.* Amsterdam, Elsevier, 1986.

Luders, H., Dinner, D.S., Lesser, R.P. & Morris, H.H. Evoked potentials in cortical localization. *J. Clin. Neurophysiol.*, 1986: 3, 75-84.

Nunez, P. *Electric Fields of the Brain.* New York: Oxford, 1981.

Reutter, B.W., Brickett, P., Gevins, A.S. Algorithms for analysis of Magnetic Resonance Images, in preparation.

Thickbroom, G., Mastaglia, F., Carroll, W. and Davies, H. Source derivation: application to topographic mapping of visual evoked potentials. *J. Electroenceph. clin. Neurophysiol.*, 1984: 59, 279-285.

Wood, C., Cohen, D., Cuffin, B.N., Yarita, M. & Allison, T. Electrical sources in human somatosensory cortex: Identification by combined magnetic and potential recordings. *Science*, 1985: 227, 1051-1053.

## FIGURE LEGENDS

**Figure 1:** Diagram of 124-channel scalp montage. Electrode names are based on 10-20 system with additional letter prefixes and numerical suffixes (see text).

**Figure 2:** Subject wearing 124-channel EEG hat.

**Figure 3:** Measurement of electrode coordinates. The research assistant touches each electrode with a magnetic position sensor while the subject is resting his head on a chin rest built into a head support which gently restricts head movement during the measurements. The 3-D coordinates of each electrode position are transmitted to the data collection computer.

**Figure 4:** Graphic display of measured electrode positions. The menu at the left lists each of the electrode names. An initial three positions are used to determine the coordinate system, usually T3, T4 and Fpz. A circle, representing the head circumference, is then drawn around these three positions. Subsequent electrodes are shown in equidistant projection, with electrodes outside the circle representing locations lower than the circumference through T3, T4 and Fpz.

**Figure 5:** Manscan\* functional-anatomical neuroimaging system.

**Figure 6:** Electrodes schematically displayed as small cylinders, at the actual measured positions, on a 3-D model of the subject's head constructed from his MRIs.

**Figure 7:** Five views of composite MR images. Horizontal slices are shown in yellow, sagittal in magenta and coronal in blue. For each slice, a closed contour which outlines the scalp is first automatically obtained with a thresholding algorithm. The composites are then drawn for each viewing position by displaying the MR intensity values contained within each contour.

**Figure 8:** Composite MR images showing a reconstructed cortical surface (in yellow) produced from the automatically traced cortical surface contours. Surface is relatively smooth because it was reconstructed from a standard clinical MRI scan with 5 mm interslice intervals. Also shown are images contained within the scalp contour for one sagittal section (magenta) and one posterior coronal section (blue). The anterior blue image is the coronal data contained within the cortical surface contour.

**Figure 9:** (Left) Midline sagittal MRI obtained with TR=600 and TE=20 ms. (Right) Output of automatic edge-detection software. The lines shown correspond to locations of local maxima in the gradient of the image intensity. These contours pass through the points in the image at which the local average intensity is changing most rapidly.

**Figure 10:** Automated construction of finite elements within brain, skull and scalp volumes, with alternating elements shown in red, green and blue, for the respective tissue type. (a) Tetrahedral elements generated in an outer ring in brain. (b) An entire horizontal slice at the level of the orbits. (c) All slices superimposed except for the topmost horizontal slices.

**Figure 11:** Laplacian of 124-channel evoked potentials evoked by 15-Hz stimulation of the middle finger on left (top) and right (middle) hands of this subject mapped onto his own MRI-derived scalp surface. The map for the right index finger is shown in the bottom panel. Color scale shows zero as white and the maximum as magenta.

**Figure 12:** Integration of EEG and MRI data as a step towards anatomical-functional localization. The data shown in Figure 11 were used to compute best-fitting single equivalent dipoles using a three-sphere head model. The figure shows top, left and right views of the scalp surface reconstructed from horizontal MR images. The voxel brain model shown in light blue corresponds to four stages of erosion of 3 mm layers, hence its shrunken appearance. The dipole for right index finger stimulation (dark

blue) is located most left-laterally. The middle finger dipoles (purple) are located appropriately in contralateral hemispheres.

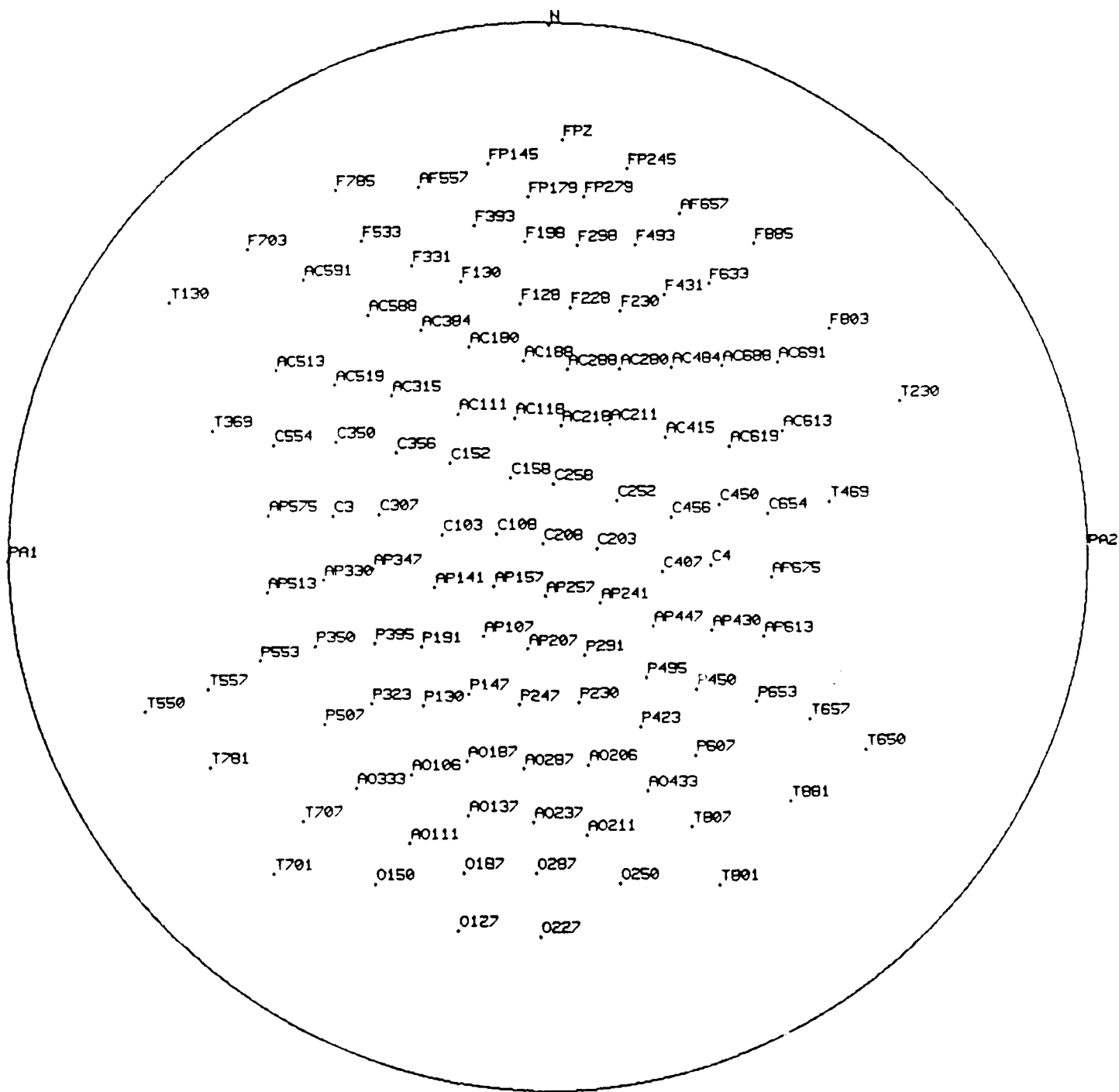


Figure 1





Figure 2

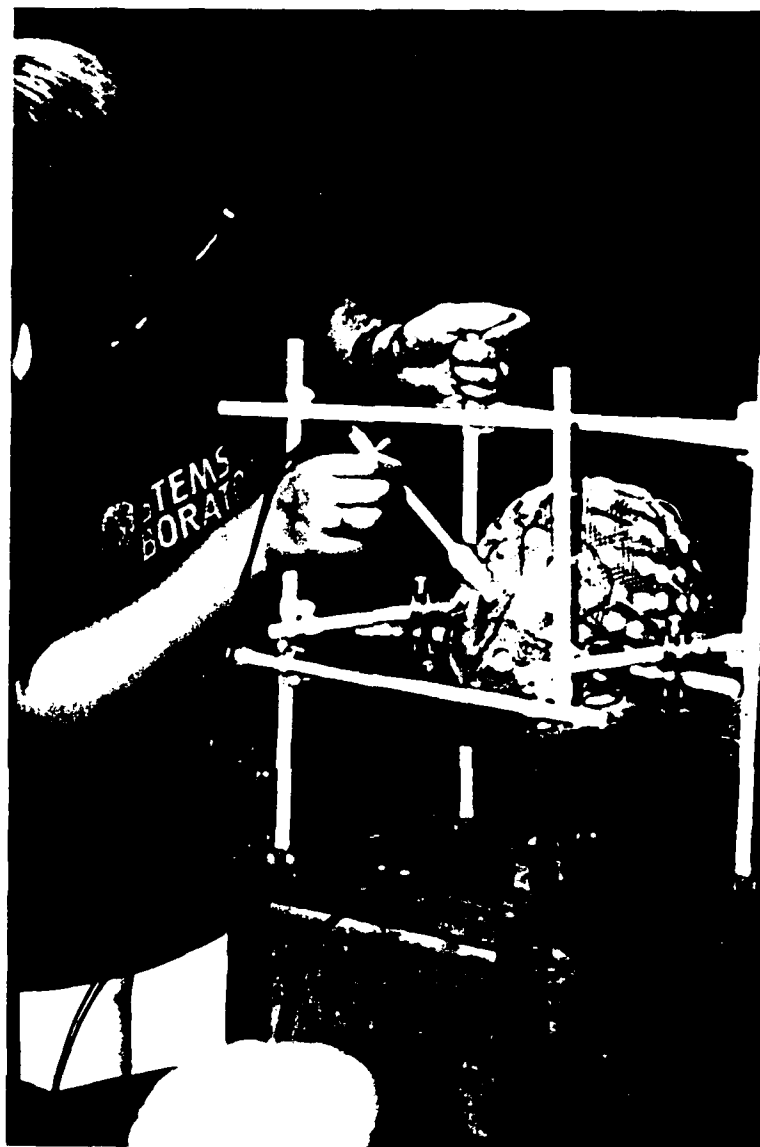


Figure 3

[illegible]

Figure 4

# MANSCAN<sup>®</sup> NEUROIMAGING SYSTEM

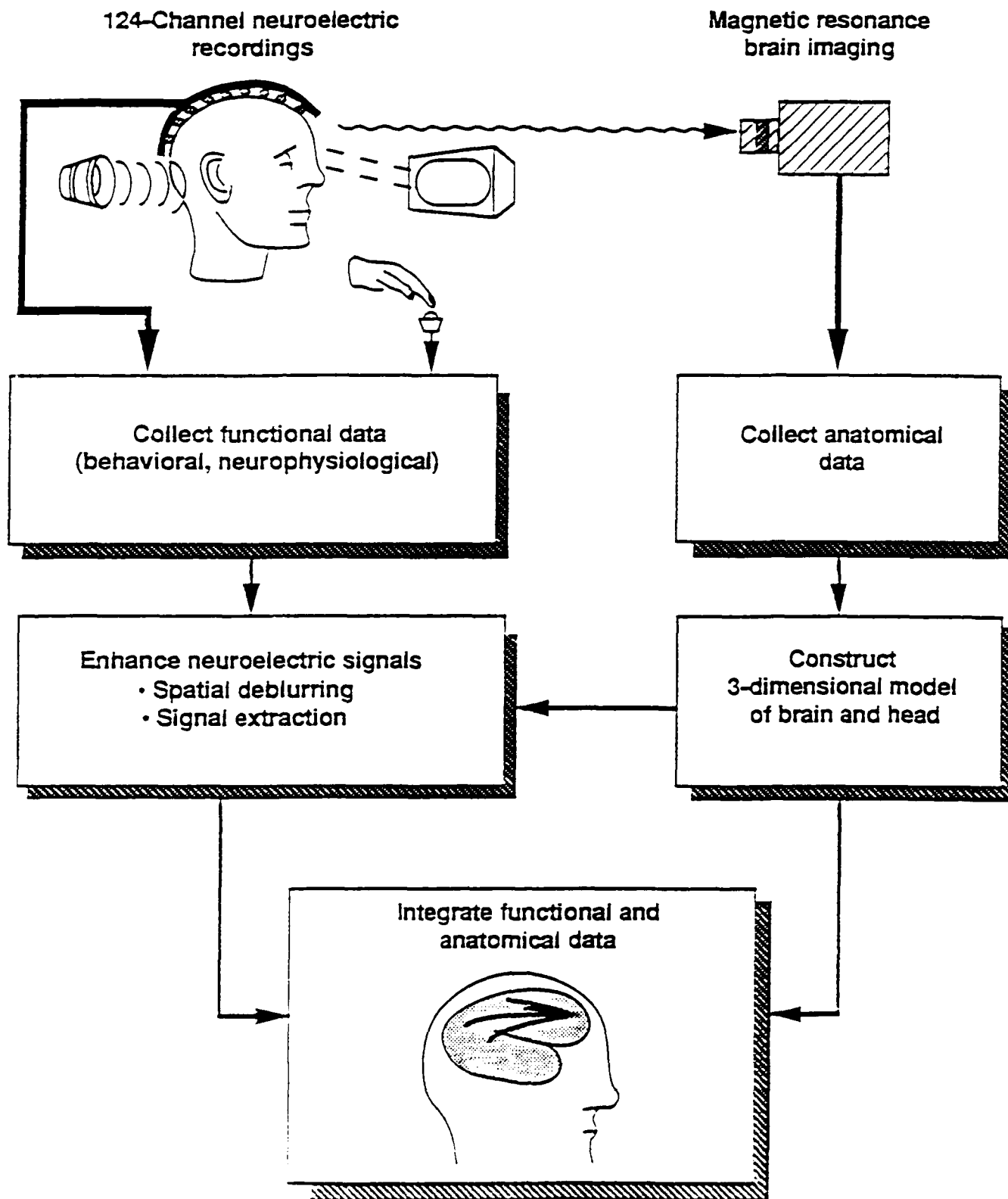


Figure 5

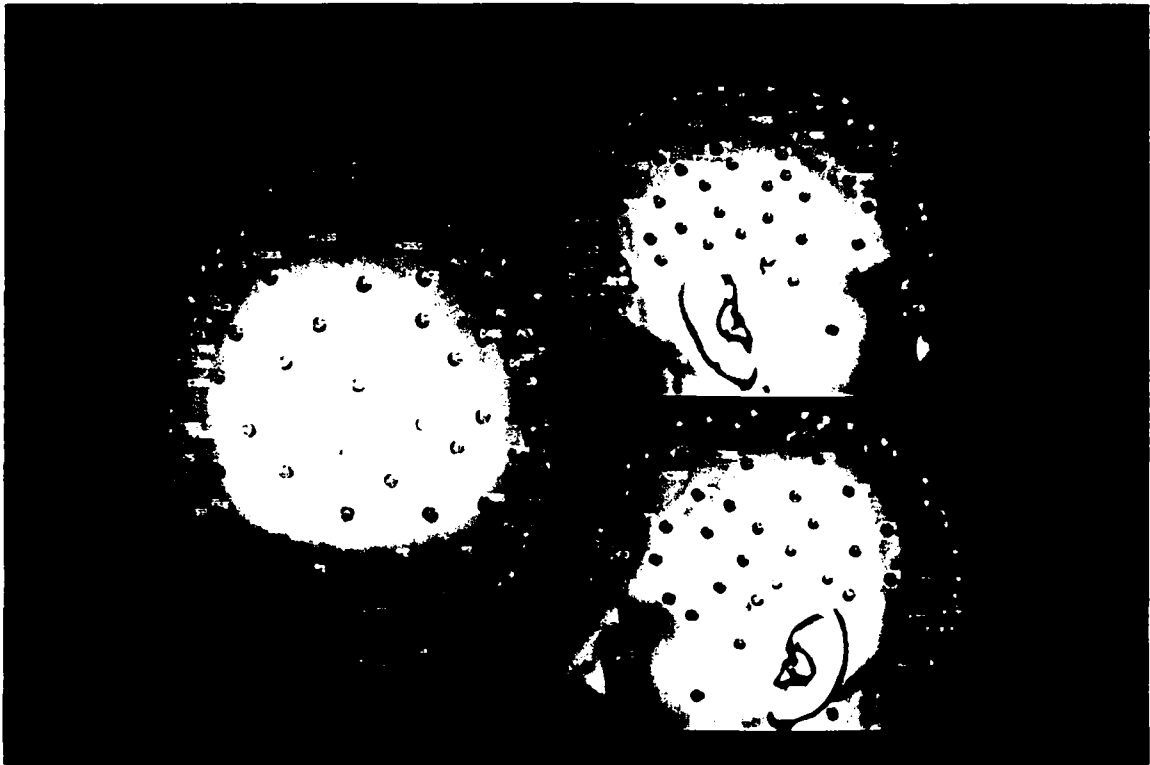


Figure 6

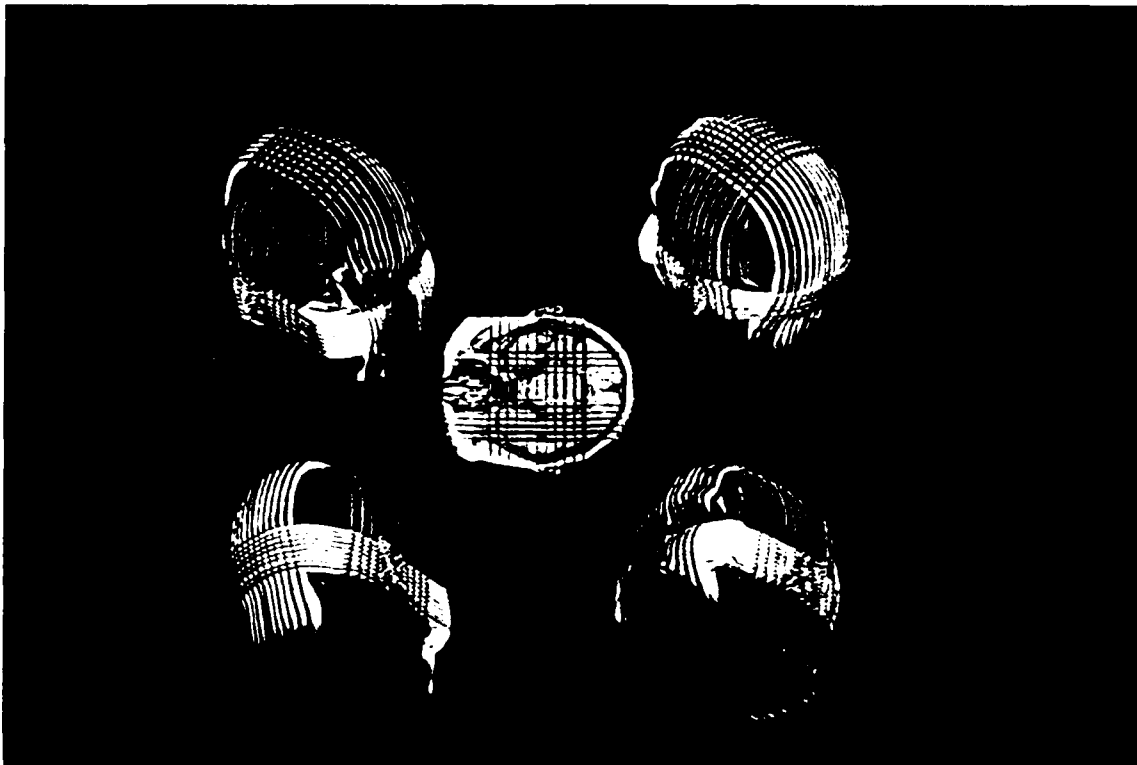


Figure 7



Figure 8

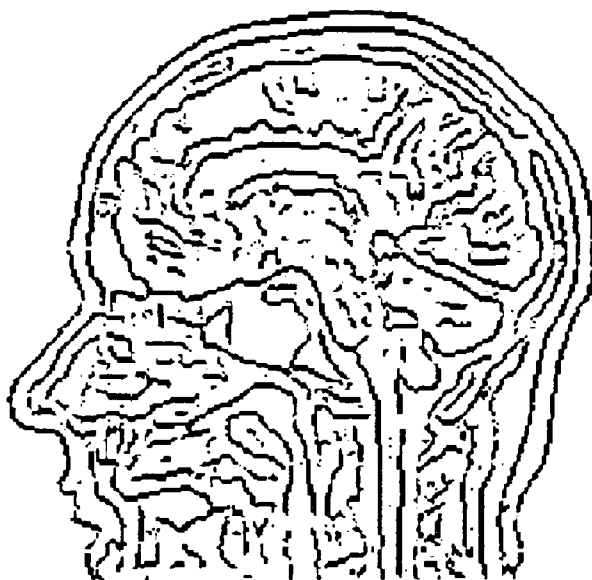
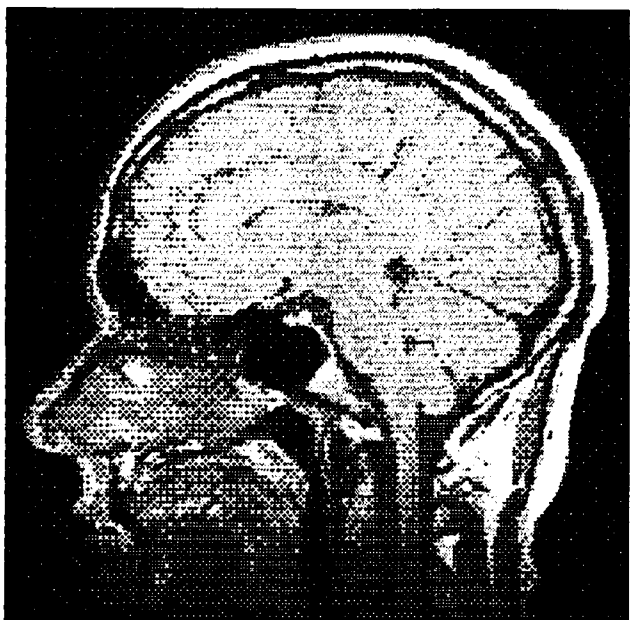


Figure 9





Figure 10

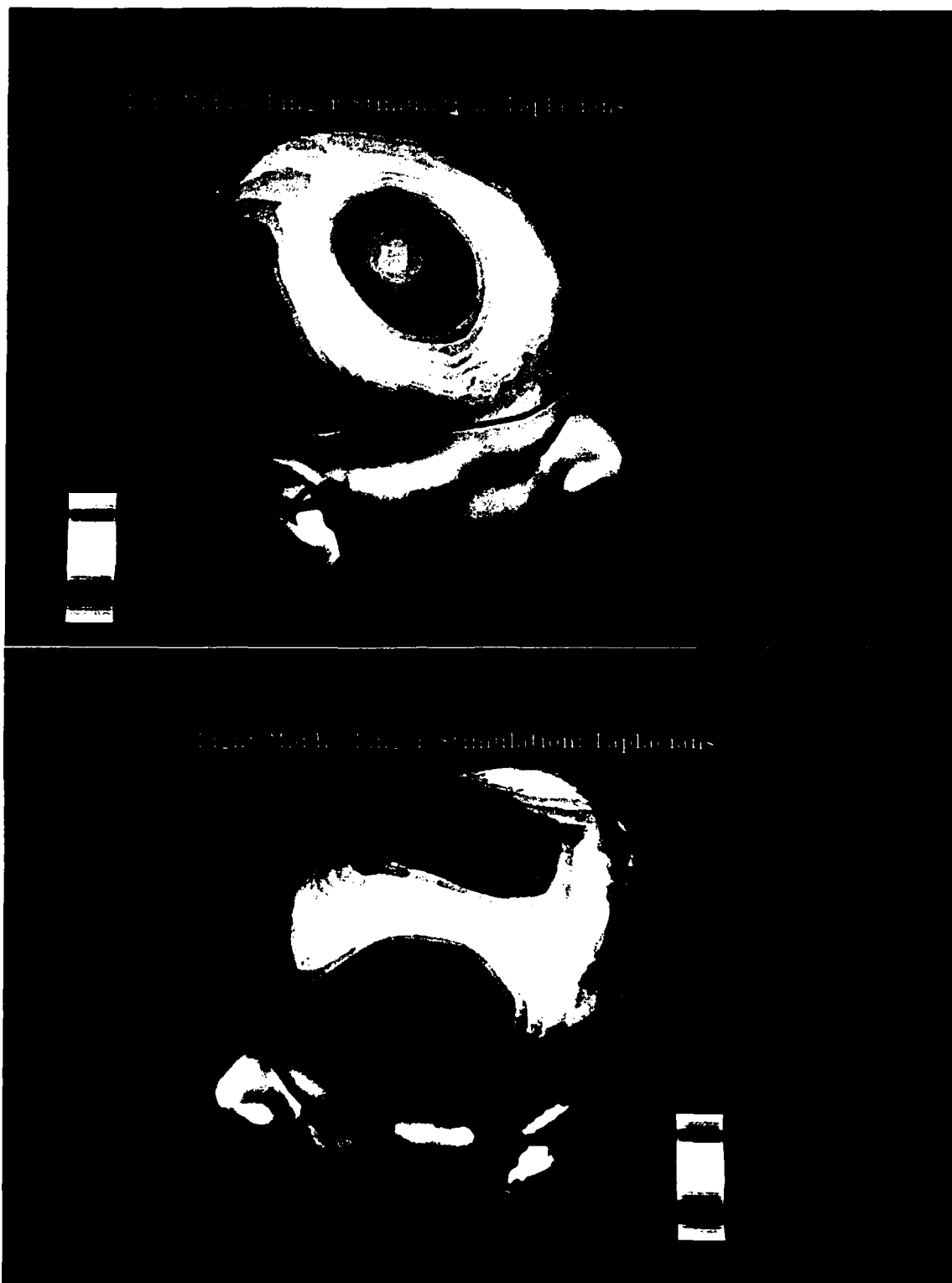


Figure 11

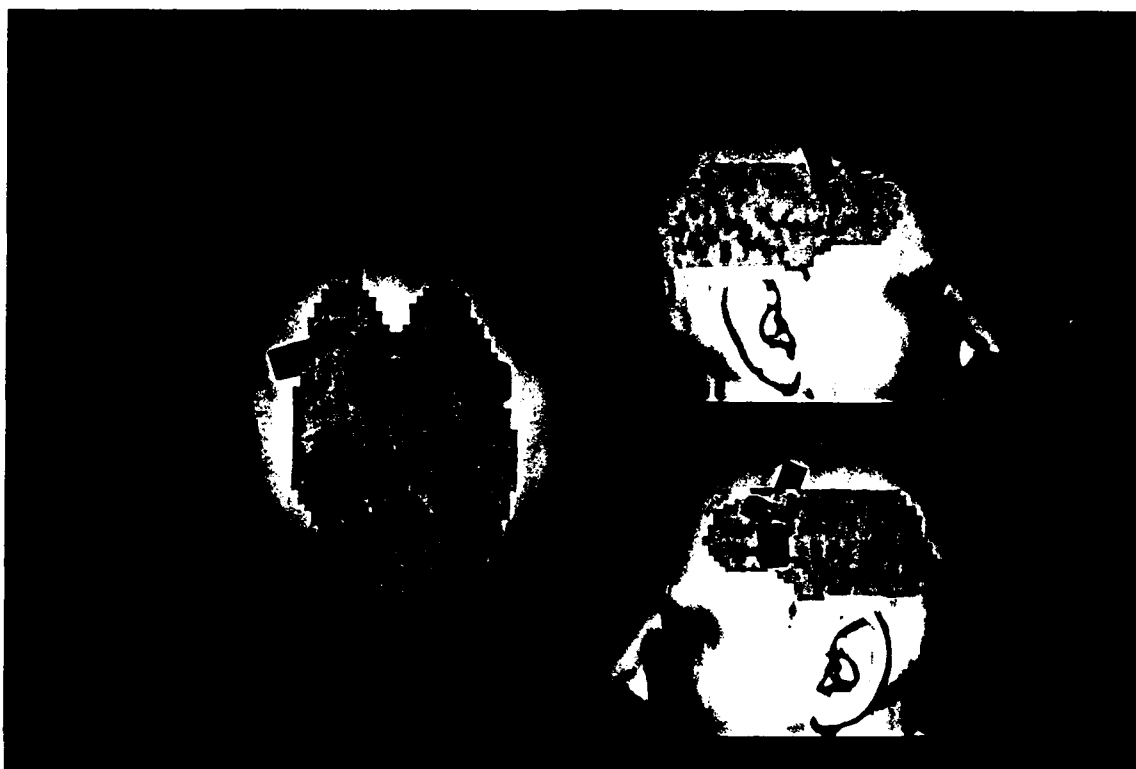


Figure 12

## V. DISSEMINATION OF TECHNICAL INFORMATION

### A. Publications dealing with methodology

Gevins, A.S., Brickett, P., Costales, B., Le, J., Reutter, B. (In press) Beyond topographic mapping: Towards functional-anatomical imaging with 124-channel EEGs and 3-D MRIs. *Brain topography* (see Section IV.D). Application of the method of Event-Related Covariance has been detailed in *EEG clin. Neurophys.*, 74(1), pp. 58-75, and in *Functional Topography of the Human Brain*, (G. Pfurtscheller, Editor) pp. 99-116. A historical discussion of between-channel correlation measures is presented in Chapter 6 of the *Handbook of Electroencephalography and Clinical Neurophysiology*, Vol. 1, (A.S. Gevins and A. Remond, Editors). The 128 channel recording system, and latest methods of measuring scalp positions and registration with MRI scans has been presented in *Brain Topography*, Dynamic functional topography of cognitive tasks (1989). More detailed descriptions are planned. The 64-channel system and earlier methods of registration were presented in *Dynamics of Sensory and Cognitive Processing of the Brain* (E. Basar, Editor) pp. 88-102. Our current Laplacian derivation procedure is described in *Brain Topography*, Dynamic functional topography of cognitive tasks (1989). Mathematical methods used in brain modeling are described in Beyond topographic mapping (In Press). Pattern recognition methods have been described in *IEEE ASSP Trans.*, 36(7), pp. 1152-1161. Tutorials on this topic were previously published in *IEEE Trans. Patt. Analy.* and in Chapter 17 of the *Handbook of Electroencephalography and Clinical Neurophysiology*, Vol. 1. We are also trying to increase awareness about the need for technological and methodological advances in mainstream psychophysiology by writing detailed analyses of the findings and limitations of contemporary ERP research, and the technical obstacles which must be overcome to bridge those limitations (Gevins and Cutillo, Chapter 11 in the *Handbook of Electroencephalography and Clinical Neurophysiology*, Vol. 2 (F. Lopes da Silva, W. Storm van Leeuwen and A. Remond, Editors).

### B. Presentations at meetings 1988-1989

We have increased the number and types of meetings at which we present our results, in order to disseminate our work and reach researchers with different specializations, e.g., psychologists, neurophysiologists, neurologists, psychiatrists and biomedical engineers. A partial list of meetings during 1988 and 1989 to which the PI was invited to speak is provided here. In addition to these, the PI, Co-PI and other EEGSL scientists have made invited and contributed presentations at a variety of national and international meetings.

#### *Invited lectures and symposia by A. Gevins, 1988 to March, 1990*

Int. Conf. Pharmaco-EEG, Japan, 1988 (Psychopharmacologists)  
 Soc. Psychophys. Res., San Francisco, 1988 (Psychophysicologists)  
 Amer. EEG Soc., San Diego, 1988 (Clinical Neurophysiologists)  
 Neurology Grand Rounds, NINDS, 1988 (Neurologists and Psychophysicologists)  
 IEEE Conf. Biomedical Engineering, New Orleans, 1988 (Biomedical Engineers)  
 AFOSR Cognitive Science Program Review, Colorado Springs, 1988 (Cognitive Psychologists)  
 IEEE Conf. Biomedical Engineering, Seattle, 1989 (Biomedical Engineers)  
 Int. Conf. Topographic EEG Analysis, Italy, 1989 (Clinical Neurophysiologists)  
 Int. Summer School of Brain Research, Netherlands, 1989 (Neuroscientists)  
 Int. Cong. EEG and Clin. Neurophysiol., Brazil, 1990 (Neurophysiologists)

**C. Visitors to EEGSL during 1988-1989**

G. Fuller, Psychophys., S.F.  
A. Amochaev, Psychophys., U. Colorado  
B. Davis, Psychol., U.S. Govt.  
B. Lynch, Neuropsych., Palo Alto VAMC  
R. Mueller and V. Calinshini, Neurol., Pres. Med. Cntr., S.F.  
B. Hudspeth, Psychophys., Colorado  
R. Thatcher, Psychophys., U. Maryland  
G. Pfurtscheller, Biomed. Eng., Tech. U. Graz  
D. Nelson, Physics, Tulane University  
W. Gersch, Statistics, U. Hawaii  
P. Stark, Statistics, U.C. Berkeley  
J. Moser, Biomed. Eng. SRI  
M. Melich, Physics, U.S. Navy  
L. Temoshok, Psychol., Walter Reed Hospital  
B. Englestad, Nuc. Med., UCSF  
A. Chen, Psychia., U. Wash. Seattle  
J. Baribeau, Psychophys., Concordia U., Montreal  
H. Hebenstreit, Psychia., Munich.  
C. Roy, Neurol., UCSF  
M. Toussaint, Biomed. Eng., U. Paris  
S. Klein, Physiol., U.C. Berkeley  
V. Pollack, Psychophys., U. So. California  
G. Meshegan, Physiol., U. Texas Dallas  
V. Reuss, Psychia., UCSF  
E. Sutter, Biomed. Eng., Smith Ketterwell Inst., S.F.  
R. Weiner, Psychia., U. No. Carolina  
J. Desmedt, Neurol., Brussels  
M. Scherg, Biomed. Eng., Munich  
R. Cracco, Neurol., SUNY Brooklyn  
D. Jewett, Physiol., UCSF

# Signs of Model Making by the Human Brain

A. S. GEVINS

## 1 Introduction

The brain is a type of Rorschach test for scientists. Each scientist describes the brain's structure or function with the language and imagery of his or her own particular trade, be it mathematics, physics, computer science, neurophysiology, or psychology. But these descriptions inevitably fall short because the brain itself is its own metaphor. With this in mind, I am going to speculate that recent neuroelectric measurements we made from people performing simple cognitive tasks may be interpreted as signs of the internal models that our brains use to interpret stimuli and take action. But first, I should review the methods and results.

## 2 Signal Processing Methods

### 2.1 New Methods for Measuring Neurocognitive Neuroelectric Patterns

During the last 15 years, my colleagues and I have devoted a full-time effort to developing mathematical procedures and computer systems for extracting more specific information from EEGs (reviews in Gevins and Yeager 1972; Gevins et al. 1975; Gevins 1980, 1984, 1987a, b, c, d; Gevins and Morgan 1986, 1988; Gevins and Bressler 1988). So far, we have applied these methods to six experiments which attempted to measure human higher cognitive functions with increasing specificity (Gevins et al. 1979a, b, c, 1981, 1985, 1987, 1988, 1989a, b). For each set of two experiments, we developed a novel set of experimental stimuli, analytic procedures, and software systems to overcome the shortcomings of the last set.

The increasing capability of laboratory computers has been the engine of our progress. Fifteen years ago, I naively thought that if I could only apply a trillion arithmetic operations to a billion bytes of neuroelectric data, I could find out something basic about how human brains worked. Now that this capability is routine, I am eagerly awaiting the 100-trillion operation, 10-billion-byte experiment.

The need for this much computation results from the increasing number of scalp EEG channels, as well as the increasingly complicated analyses required to measure subtle spatiotemporal neurocognitive signals from large sets of single-trial data. Currently, we are routinely recording 64 EEG channels, and analyzing

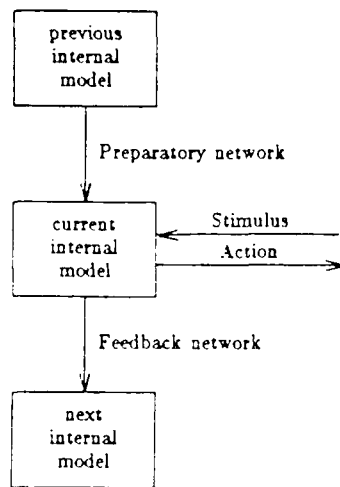


Fig. 5. Schematic diagram of how the previous moment's internal model influences the current moment's perception, decision, and action, and how the feedback from the present moment influences the next moment's internal model. Spatiotemporal neuroelectric signs of preparatory and feedback networks have recently been measured

the current moment. Based on these models, we use our body's effector and sensory systems to actively probe the environment for stimuli relevant to our needs (Fig. 5). When the model for a particular task is incorrect, as with incomplete or inappropriate preparation, subsequent performance is usually incorrect. When feedback follows action, the brain model updates.

I interpret the preparatory and feedback "networks," aspects of which we have measured, as signs of these situation-specific internal models. With further development, we can expect to have increasingly detailed direct measurements of how our experience of reality is synthesized in the brain.

## 5 Summary

Using state-of-the-art recording and signal processing procedures, we measured spatiotemporal neuroelectric patterns as subjects prepared to produce a precise finger pressure to a visual stimulus, as they made the response, and as they received feedback information about the accuracy of their response. For each of these three situations, we calculated ERC patterns between pairs of electrodes.

ERCs that preceded accurate left- or right-hand performances overlay the left frontal cortex, and the motor and parietal cortices contralateral to the performing hand. In addition, strong ERCs overlying midline motor and premotor cortices preceded left-hand performance. This "preparatory network" comprised distinct cognitive, somesthetic-motor, and integrative motor cortical areas. We used its presence or absence to predict the accuracy of responses that began 0.5–1 s later.

Similarly, we measured a "feedback network" in an interval spanning an early P300 peak. Signals from bilateral and midline frontal sites were involved in patterns related to inaccurate feedback, whereas the left and midline frontal sites

### 3.3 The Fourth Experiment (Gevins et al. 1988)

After learning and practicing a difficult visuomotor-memory task (VMMT) until their performance was stable, each of five healthy, right-handed, male subjects returned to the laboratory the next morning and performed several hundred trials of the task. This task required subjects to remember two continuously changing numbers, in the presence of numeric distractors, and produce precise finger pressures. Each trial consisted of a warning symbol, followed by a single-digit visual stimulus to be remembered, followed by the subject's finger-pressure response to the stimulus number presented two trials ago, followed by a two-digit feedback number indicating the accuracy of the response. For example, if the stimulus numbers in five successive trials were 8, 6, 1, 9, 4, the correct response would be a pressure of 0.8 kg when seeing the 1, 0.6 kg for the 9, and 0.1 kg for the 4. To increase the task difficulty, subjects were required to withhold their response on a random 20% of the trials. These "no-response catch trials" were trials in which the current stimulus number was identical to the stimulus two trials ago. After the experiment, we divided each subject's responses into "relatively accurate" and "relatively inaccurate" trials, depending on whether the error of an individual trial was less than or greater than that subject's mean accuracy over the session. Accurate and inaccurate trial sets were randomly distributed across the session.

EEGs were recorded with either 33 or 51 channels set in a nylon mesh cap. Vertical and horizontal eye movements were also recorded, as were the respond-

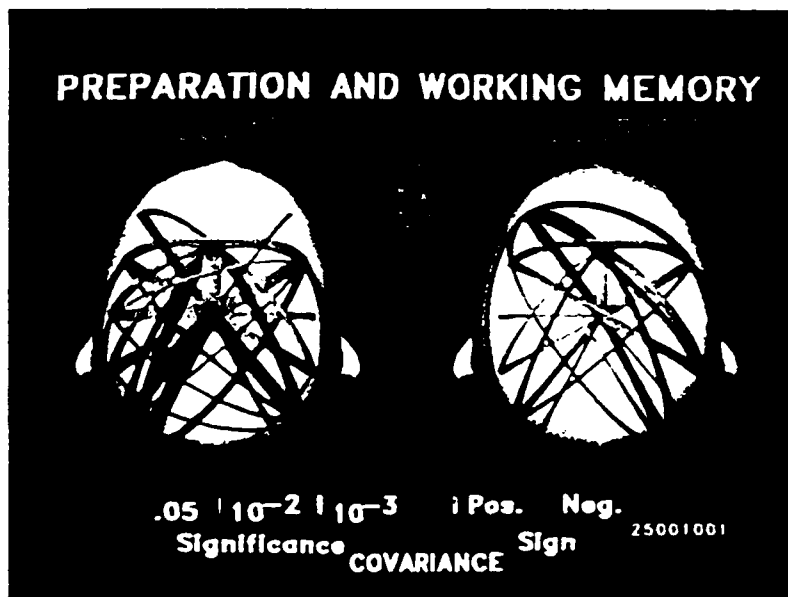


Fig. 4. ERCs preceding accurate and inaccurate performance of a task that required subjects to produce precise finger pressures proportional to numbers held in memory. Significant ( $P < 0.05$ ) ERC patterns during a 500-ms interval when five subjects were remembering two numbers and awaiting a new number to be remembered. The ERC pattern preceding accurate performance is stronger, and differs from the inaccurate pattern principally in the posterior channels



7. Using the magnitude of the maximum cross-covariance function and its lag time to characterize the ERC
8. Estimating significance of ERCs by the standard deviation of the "noise" ERC estimated from randomized data
9. Graphing the most significant ERCs in each interval
10. Statistically comparing ERC distributions between experimental conditions.

### 2.3 Validating ERC Measurements

The current ERC analysis has been applied to data recorded from several experiments. The validity of the method is demonstrated in analysis of visual stimulus processing and response execution intervals of a visuomotor task (Gevins et al. 1987). During the period of visual processing, ERC patterns involved posterior sites followed by anterior parietal and premotor sites. This finding was consistent with neuroanatomical considerations and clinical neuropsychological studies. Likewise, ERC patterns for movement-related intervals corresponded to prior functional neuroanatomical studies of primates and patients with intracerebral

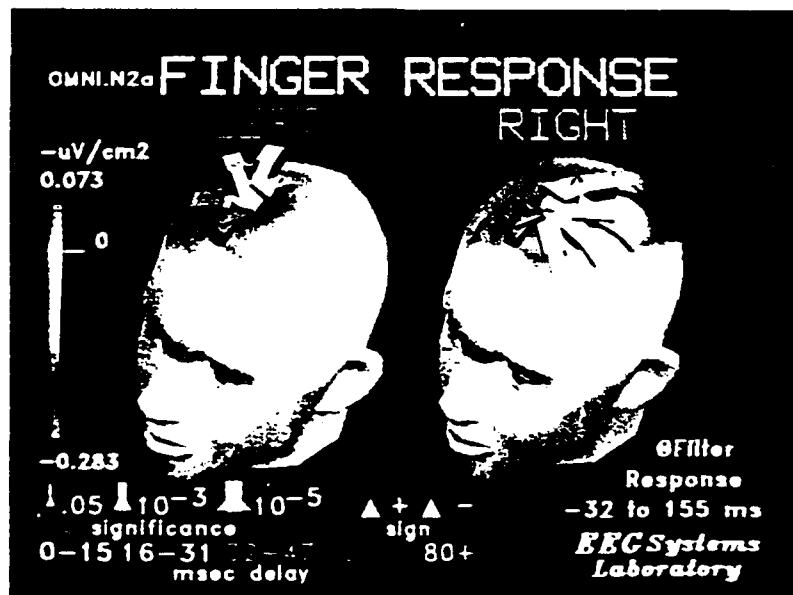


Fig. 1. Most significant (top one standard deviation) ERC patterns at the peak of the finger pressure for right- and left-hand trials from seven right-handed subjects, superimposed on maps of Laplacian response potential amplitude. The thickness of an ERC line is proportional to the negative log of its significance (from 0.05 to 0.00005). The color of a line shows the lag time (ms delay) between sites. Note that the anterior midline precentral (aCz) electrode is the focus of all ERCs. The patterns are distinctly lateralized according to responding hand. The sign of the aCz ERCs is positive (yellow) for lateral frontal, and negative (tan) for lateral central and anterior parietal electrodes



a



b

Fig. 2a, b. Significant ( $P < 0.05$ ) prestimulus ERC patterns superimposed on maps of Laplacian CNV amplitude. Same subjects and task as Fig. 1. Measurements are from an interval of 500-875 ms after the cue for subsequently accurate and inaccurate right- (a) and left-hand (b) visuomotor task performance by seven right-handed men. The thickness of a covariance line is proportional to its significance (from 0.05 to 0.005). A violet line indicates the covariance is positive, while a blue line is negative. ERCs involving left frontal and appropriately contralateral central and parietal electrode sites are prominent in patterns for subsequently accurate performance of both hands. The magnitude and number of ERCs are greater preceding subsequently inaccurate left-hand performance by these right-handed subjects, and are more widely distributed compared with the left-hand accurate pattern. For the right-hand, fewer and weaker ERCs characterize subsequently inaccurate performance. The amplitude maps are very similar for the four conditions, and do not indicate any of the specific differences evident in the covariance patterns

was followed by a visual numeric stimulus (number 1–9) indicating that a pressure of 0.1 to 0.9 kg should be made with the index finger of the previously indicated hand. A two-digit number, presented 1 s after the peak of the response pressure, provided feedback that indicated the subject's exact pressure. On a random 20% of the trials, the stimulus number was slanted in the opposite direction to the cue: subjects were to withhold their responses on these "catch trials." The next trial followed 1 s after disappearance of the feedback. Each subject performed several hundred trials, with rest breaks as needed.

Twenty-six channels of EEG data, as well as vertical and horizontal eye movements and flexor digitorum muscle activity from both arms, were recorded. All single-trial EEG data were screened for eye movement, muscle potential, and other artifacts. Contaminated data were discarded.

Intervals used for ERC analysis centered on major event-related potential peaks. ERCs were computed between each of the 120 pairwise combinations of the 16 nonperipheral channels. Intervals were set from 500 ms before the cue to 500 ms after the feedback.

We first calculated the mean error (deviation from the required finger pressure) over all trials from the recording session. Individual trials were then classified as accurate (trial error less than mean error) or inaccurate (error greater than mean error).

ERC patterns during a 375-ms interval centered 687 ms postcue (spanning the late contingent negative variation–CNV), regardless of subsequent accuracy, involved left prefrontal sites, as well as appropriately lateralized central and parietal sites. Inaccurate performance by the right hand was preceded by a very simple pattern (Fig. 2a), while inaccurate performance by the left hand was preceded by a complex, spatially diffuse pattern (Fig. 2b). The relative lack of ERCs preceding inaccurate right-hand performance may simply reflect inattention on those trials, while the strong and complex patterns preceding inaccurate performance with the left hand may reflect effortful, but inappropriate, preparation by the right-handed subjects.

ERC patterns related to feedback about accurate and inaccurate performances were similar immediately after the onset of feedback, but began to differ in an interval centered at 281 ms, that spanned the early P3 peak (P3E) (Fig. 3). The ERC patterns for feedback to accurate performance by the two hands were very similar (bootstrap correlation =  $0.91 \pm 0.01$ ), involving midline antero-central, central, anteroparietal, parietal, and antero-occipital sites, left anteroparietal and antero-central sites, and right parietal, anteroparietal, antero-central, and frontal sites. These accurate patterns involved many long-delay (32–79 ms) ERCs. The waveforms of the frontal and antero-central sites consistently lagged those of more posterior sites. For feedback to inaccurate performance, patterns for both hands were also very similar (bootstrap correlation =  $0.90 \pm 0.02$ ), and involved most of the same sites as the accurate patterns, with the striking exception of the left and midline frontal sites. Again, frontal waveforms lagged those of the more posterior sites with which they covaried. There were even more long-delay ERCs than in the accurate patterns.

We suggest that our prestimulus ERC patterns characterize a distributed preparatory neural set that is related to the accuracy of subsequent task per-

electrodes (Fig. 1): the midline precentral electrode that overlays the premotor and supplementary motor cortices was the focus of all movement-related ERC patterns, and the other most significant ERCs involved pre- and postcentral sites that were appropriately contralateral to the responding hand. Moreover, the positive sign of the ERCs between midline precentral and lateralized precentral sites and the negative sign between midline precentral and postcentral sites are consistent with the sharply focused current sources and sinks spanning the hand areas of somatosensory and motor cortices.

While these ERC patterns appear to reflect neatly the functional coordination of the immediately underlying cortical areas, we must again emphasize that their actual neural sources are, in fact, not yet known. Some caution should therefore be exercised in interpreting the patterns too literally.

### 3 Preparation and Feedback During Simple Visuomotor Judgment Tasks

#### 3.1 The First Two Experiments

In a series of four experiments, we attempted to characterize distributed networks of cortical function during simple tasks. In the first experiment (Gevins et al. 1981), we measured event-related cross-correlations between 91 pairwise combinations of recordings from 15 electrodes during performance of two simple tasks, one requiring a spatial judgment and the other a numeric judgment. A cue before each trial indicated the type of task to be performed. The cross-correlation patterns of the two tasks differed during the last 300 ms of the cue interval. These differences, which included midline frontal, parietal, and occipital electrode sites, suggested that neural networks associated with preparation were both task specific and spatially detailed. These "preparatory networks" were better visualized in a second experiment, which extracted event-related cross-correlations that distinguished two similar spatial tasks (Gevins et al. 1983, 1985). Spatially distributed, task-specific "preparatory networks" were found again. This time, the midline frontal (Fz) electrode was the only site that showed a task-dependent difference during the last 300 ms of the cue interval.

#### 3.2 The Third Experiment

We designed a third experiment based on these encouraging results. We wished to manipulate preparatory sets more explicitly, and to investigate feedback about performance accuracy (Gevins et al. 1987, 1989b). Along with a new experimental design, we had to develop new signal processing procedures that more robustly measured event-related covariance between electrode sites.

Seven healthy, right-handed, male adults participated in this study. A visual cue, slanted to the right or to the left, prompted the subject to prepare to make a response pressure with the right or left index finger. One second later, the cue



Fig. 3. Most significant (top two largest standard deviations) early P3 (P3E) feedback ERC patterns for feedback to accurate and inaccurate performance by the right hand. Same subjects and task as Fig. 1 and 2. Same scale as Fig. 1. Both the ERCs and amplitude maps are derived from a 187-ms-wide interval, centered at 281 ms after feedback onset, on seven-subject averaged waveforms. A major difference between accurate and inaccurate patterns occurs at the left and midline frontal sites, which are only involved in the inaccurate patterns. The involvement of these sites may reflect the fact that greater processing is required following inaccurate performance in order to update the preparatory set for the next trial.

formance. This network appears to involve distinctive cognitive (frontal), integrative-motor (midline precentral), and lateralized somesthetic-motor (central and parietal) components. The involvement of the left frontal site is consistent with clinical findings that preparatory sets are synthesized and integrated in prefrontal cortical areas, and with experimental and clinical evidence indicating involvement of the left dorsolateral prefrontal cortex in delayed response tasks. A midline antero-central integrative motor component is consistent with known involvement of premotor and supplementary motor areas in initiating motor responses. The finding of an appropriately lateralized central and parietal component is consistent with evidence from primates and humans for neuronal firing in motor and somatosensory cortices prior to motor responses.

Since ERC feedback patterns of accurate or inaccurate performance (involving either hand) were more similar than those between accurate and inaccurate patterns for one hand, we infer that the feedback patterns were related more to performance accuracy than to the hand used. The fact that ERC patterns following disconfirming feedback involved more frontal sites than did patterns following confirming feedback is consistent with the idea that greater resetting of performance-related neural systems is required following disconfirming feedback. Likewise, the front focus of these differences is consistent with the importance of the frontal lobes in the integration of sensory and motor activities (Fuster 1984; Stuss and Benson 1986).

about 25 200-400 ms intervals spanning each 4- to 6-s task trial. Each trial consists of a cue, stimulus, response, and feedback about performance accuracy; the intervals are time registered to the evoked potential peaks elicited by these events. (In February, 1988, we completed the expansion to 128 channels).

Much of our effort has dealt with developing various spatial and temporal signal enhancement techniques, of which the method of event-related covariance (ERC) is the latest. This method provides a window, albeit limited, on the dynamic functional neural networks which produce simple goal-directed behaviors. ERCs measure two features of short segments of event-related potentials (ERPs): the similarity of waveform and the timing between electrodes. ERC analysis is based on animal studies which showed that when a brain region becomes involved in stimulus-related processing, synchronization of a subset of neurons in that region is manifested as a change in the form of the region's extracellularly recorded, low-frequency macropotentials (reviewed in Gevins and Bressler). Covariance and correlation can measure waveform similarity and timing of macropotentials from different areas of the brain, so these measurement techniques may characterize the spatial organization of coordinated functional activity of the areas involved in a goal-directed behavior. Of course, recording at the scalp, rather than within the brain, introduces some complications into this simple idea. Although for the specific cases we have measured ERCs seem to reflect the coactivation of underlying cortical areas, the net effect of these complications is that we cannot yet definitively say whether this is true in general. Our current research is focused on resolving this issue in some important paradigmatic cases.

## 2.2 Computing Event-Related Covariances (ERCs)

There are ten steps in computing ERCs (Gevins et al. 1987; Gevins and Bressler): the first four reduce spatial smearing and select intervals and trials that contain task-related information in order to enhance the signal-to-noise ratio and reduce the amount of data. The next six steps measure ERCs on bandpass-filtered, enhanced averages computed from the reduced data set.

The ten steps involve:

1. Recording at least 100 trials of each task condition of the experiment, using at least 24 electrodes
2. Applying the Laplacian operator to the potential distribution of each electrode not located at the edge of the scalp, in order to remove the effect of choice of reference electrode and reduce spatial blur from volume conduction through the skull and scalp
3. Removing data that were contaminated with artifact
4. Finding trials with consistent event-related signals, and computing enhanced averages from these trials (optional)
5. Selecting digital bandpass filters and intervals for analysis by examining ERPs, amplitude distribution maps, and (optional) Wigner time-frequency distributions
6. Computing the multilag cross-covariance functions between all pairwise (by channel) combinations of the interval's enhanced averages

ing flexor digitorum muscle potentials, electrocardiogram, and respiration. Three-axis magnetic resonance image scans were made of three of the five subjects.

Grand-average (over the five subjects) ERPs were time-locked to the presentation of the numeric stimulus. Spatiotemporal neuroelectric patterns were then quantified by measuring ERCs between all 153 pairwise combinations of the 18 nonperipheral electrodes in the common subset of 33 channels. ERCs were measured on the grand-average ERPs across a 500-ms interval, centered 312 ms before the numeric stimulus. During this interval, subjects were maintaining the last two visually presented numbers in working memory, and preparing for the next stimulus.

Complex, but distinct ERC patterns characterized the subsequently accurate and inaccurate data sets (Fig. 4). The patterns differed both in overall magnitude ( $t = 3.3$ ,  $df = 48$ ,  $P < 0.01$ ) and in topographic distribution (bootstrap correlation =  $0.37 \pm 0.14$ ), the accurate preparation having stronger ERCs overall. Midline central (607), midline precentral (377), left posteroparietal (257), and right parietal (204) electrodes had the largest summated ERCs in the accurate data set. For the inaccurate data set, the four largest summated ERCs were at midline central (569), midline precentral (392), left frontal (322), and right antero-central (316). Deferring discussion of the implications of the shift from posterior to anterior ERC foci, we note here that the ERC differences preceding accurate and inaccurate performance of each trial of the visuomotor memory task provide another example of the importance of task-specific, preparatory cortical networks in correct action.

## 4 Conclusions

### 4.1 Methodological

Event-related covariance analysis seems to represent a useful improvement over topographic brain electrical activity maps by showing what may prove to be signs of functional interrelations between areas of the cerebral cortex. Furthermore, differences between conditions, which are evident in ERC patterns of preparatory sets, are not apparent on the corresponding topographic maps (Fig. 2) (Gevins et al. 1989a). In our current research we are trying to determine the distributed sources in the brain that produce the ERC patterns at the scalp.

### 4.2 Brain Model

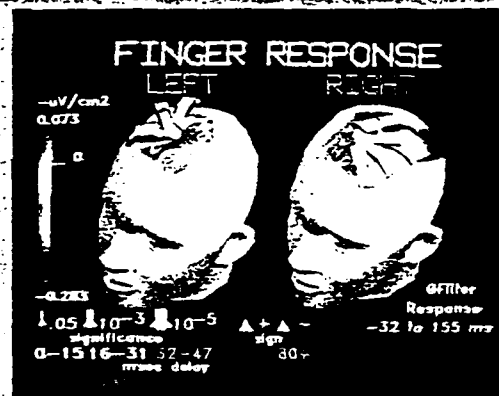
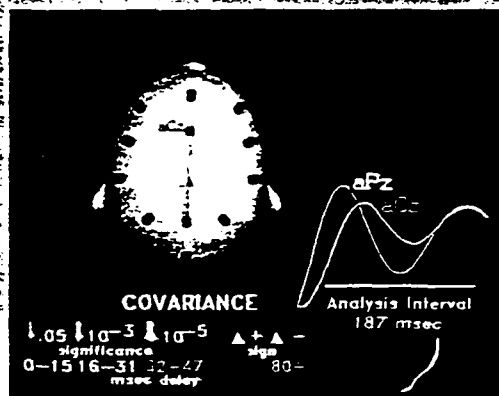
Although it is convenient to describe brains using the language of computer science, our brains are not actually like computers. They are not stimulus-response machines that passively await stimuli, process them according to fixed algorithms, and then make responses. Rather, we know from introspection, observation, and inference that our brains continuously maintain and update detailed representations (models) of what we imagine our self- and world-states to be at

- Gevins AS, Doyle JC, Cutillo BA, Schaffer RE, Tannehill RS, Ghannam JH, Gilcrease VA, Yeager CL (1981) Electrical potentials in human brain during cognition: new method reveals dynamic patterns of correlation. *Science* 213:918-922
- Gevins AS, Schaffer RE, Doyle JC, Cutillo BA, Tannehill RL, Bressler SL (1983) Shadows of thought: shifting lateralization of human brain electrical patterns during brief visuomotor task. *Science* 220:97-99
- Gevins AS, Doyle JC, Cutillo BA, Schaffer RE, Tannehill RS, Bressler SL (1985) Neurocognitive pattern analysis of a visuospatial task: rapidly-shifting foci of evoked correlations between electrodes. *Psychophysiology* 22(1):32-43
- Gevins AS, Morgan NH, Bressler SL, Cutillo BA, White RM, Illes J, Greer DS, Doyle JC, Zeitlin GM (1987) Human neuroelectric patterns predict performance accuracy. *Science* 235:580-585
- Gevins AS, Cutillo BA, Fowler-White RM, Illes J, Bressler SL (1988) Neurophysiological patterns of operational fatigue: Preliminary results. NATO/AGARD conference Proceedings 432:22-22-7
- Gevins AS, Bressler SL, Morgan NH, Cutillo BA, White RM, Greer DS, Illes J (1989a) Event-related covariances during a bimanual visuomotor task. Part I: Methods and analysis of stimulus- and response-locked data. *Electroencephalogr Clin Neurophysiol* 74(1):58-75
- Gevins AS, Cutillo BA, Bressler SL, Morgan NH, White RM, Illes J, Greer DS (1989b) Event-related covariances during a bimanual visuomotor task. Part II: Preparation and feedback. *Electroencephalogr Clin Neurophysiol* 74(2):147-160
- Stuss DT, Benson DF (1986) *The frontal lobes*. Raven, New York



G. Pfurtscheller / F. H. Lopes da Silva  
(Editors)

# Functional Brain Imaging



Hans Huber Publishers  
Toronto · Lewiston N.Y. · Bern · Stuttgart

# Functional Topography of the Human Brain

*A. S. Gevins and S. L. Bressler*

To represent the distributed cortical network involved in goal-directed behaviors, it is necessary to quantify event-related processing in, as well as relations between, the functional centers of the network. This paper discusses the idea that appropriately processed, scalp-recorded event-related potentials can index the activity of cortical regions involved in cognitive task performance. It also presents a set of procedures, called Event-Related Covariance (ERC) Analysis, that we use to measure patterns of statistical relationship between neuroelectric time-series recorded at different scalp sites. Applying ERC Analysis to simple cognitive tasks produced clear-cut results. These were consistent with prior neuropsychological models of the rapidly shifting cortical network accompanying expectancy, stimulus registration and feature extraction, response preparation and execution, and "updating" to feedback about response accuracy.

In studies of higher cognitive functions of the human brain, there currently is a renaissance of interest in measuring spatial aspects of brain activity. One sign of this is the reawakened concern with dipole source localization in the brain. Yet, if this resurgence is to flourish, advances in psychophysiology and the technologies of brain signal measurement and analysis will have to be utilized with a more sophisticated approach. While the localization of single equivalent-dipole generators may be quite informative in the case of sensory and motor events, it is of dubious utility in the case of higher cognitive processes. In fact, it is well known from clinical studies that even simple cognitive functions must require integrated processing in a network involving a number of distributed, specialized cortical areas (Mesulam, 1981). So, although it is convenient, it may not always be a good idea to

compact all the data into a single equivalent dipole.

Rather, it seems more desirable to characterize the dynamic topology of this distributed network to determine which areas are active at any instant of time and which areas are statistically related to each other. This is an idea that has been evolving over the past four decades (Walter & Shipton, 1951; Barlow & Brazier, 1954; Adey et al., 1961; John et al., 1973; Callaway & Harris, 1974; Livanov, 1977; Tucker et al., 1986; Gevins et al., 1981, 1983, 1987; Gevins, 1987a; Bressler, 1987a,b). Our current approach is based on the hypothesis that when regions of the brain are functionally related, their event-related potential (ERP) components are related in shape and line up in time, perhaps with some delay. The idea is that the ERP waveform delineates the course of event-related mass neural activity of a population, so that if two populations are functionally related, their ERPs should line up. If

---

EEG Systems Laboratory, 1855 Folsom Street, San Francisco, CA 94103

The study of fatigue emerged from the collaboration of researchers from: (1) The USAF School of Aerospace Medicine, San Antonio (James Miller); (2) Systems Technology Inc., Hawthorne, California (Henry Jex and James Smith); (3) Washington University, St. Louis (John Stern); and (4) The EEG Systems Laboratory.

This research was supported by The U.S. Air Force Office of Scientific Research, The U.S. Air Force School of Aerospace Medicine, The National Institutes of Neurological and Communicative Diseases and Strokes, and The National Science Foundation. Thanks to Judith Gumbiner, Jennifer Strouher and Kris Dean for manuscript preparation.

so, and if the relations are linear, this could be measured by computing the lagged covariance between the ERPs, or portions of the ERPs, from different regions—a measure we call event-related covariances (ERCs). As we shall see later, initial results of this approach have been quite promising. We must caution, however, that the hypothesis that ERCs measure functional relationships between cortical areas has not yet been proven.

The measurement of ERCs is part of a set of signal processing procedures called "Neurocognitive Pattern Analysis" (NCP Analysis) that we have developed to extract task-related spatiotemporal patterns from the unrelated electrical activity of the brain (Figure 1). In the past 10 years, these procedures have become increasingly sophisticated as the capabilities of computers have expanded. They now measure spatiotemporal task-related processes from up to 64 scalp electrodes in each of up to 25 fraction-of-a-second intervals spanning a 4–6 second period extending from before a cue, through stimulus and response, to presentation of feedback about performance accuracy. This paper describes first the basis for our approach to characterizing the functional topography of the brain, and then the current state of procedures that we are developing to carry out that characterization.

### Neurophysiological Basis for the Measurement of Functional Topography

The representation of neocortex as a distributed neural network of interacting functional centers is a legacy of the Sherringtonian tradition (Sherrington, 1906). The pioneering work of Freeman (1975) has been crucial in reconciling this traditional view with more recent concepts of neural networks of individual neurons, by redefining the functional center as a cooperative domain of interconnected neuronal populations, rather than simply an anatomical pool of neurons. Freeman has demonstrated a systematic order between pulse probabilities of individual neurons and macroscopic forms of cooperative neural activity (macropotentials), showing that macro-

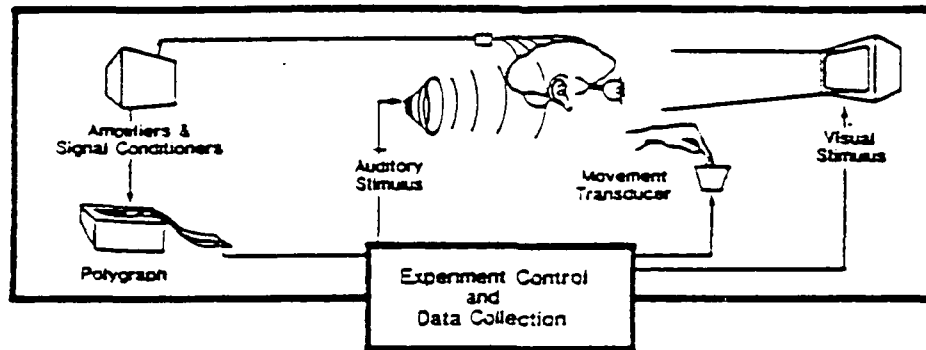
potentials reflect the emergence of dynamic self-organizing order in neuronal populations, lasting from tens to hundreds of milliseconds (Freeman, 1987). These ideas are consistent with the findings of Elul (1972), who concluded that extracellularly recorded cortical macropotentials result from summation of dendritic activity of the synchronized portion of a neuronal population, and of Petsche et al. (1984), who demonstrated the importance of the close relation between macropotentials and local cortical architectonics.

In laying the foundation for the concept of distributed cortical networks, studies on the emergent nature of macropotentials have been complemented by animal experiments focusing on field potential co-synchronization (Adey et al., 1961; Boudreau, 1966; Livanov, 1977). Dumenko (1970) found in dogs that correlation between extracellular potentials of visual and motor cortices increased with conditioning to a visual stimulus and was highest at the time of the conditioned stimulus and response. The finding that high correlation was specific to particular regions of motor and visual cortices was similar to the observation of Bressler (1987a,b) that high correlation between olfactory bulb and cortex in rabbits was specific to particular regions of each. Measures of similarity between field potentials have also been applied to averaged event-related potentials. John et al. (1973) measured the relatedness of waveforms recorded from different conditioned responses and demonstrated differential generalization of neural activity based on waveform similarity.

Given this view of distributed functional cortical networks, and given the sensitivity of ERPs to rapid changes in brain state associated with performance of complex behavioral tasks, we hypothesize that appropriately processed ERPs may reflect the activation of rapidly-shifting, widely distributed functional aggregates of underlying neuronal populations. In the tradition of Lashley (1958) and John (1967), we have sought to characterize the "functional topography" of distributed cortical networks by looking for consistent statistical relations between field potentials recorded over different areas of cortex during performance of highly controlled cognitive tasks.

# ADIEEG IV NEUROCOGNITIVE PATTERN RECOGNITION SYSTEM

## RECORD DATA



## PREPARE DATA

Neurophysiological Data

Behavioral Data

- Perform signal conditioning
- Perform artifact detection and filtering
- Inspect averaged evoked time series

- Select sets of trials balanced between experimental conditions for stimulus, cognitive, performance and response-related variables

## SPATIOTEMPORAL SIGNAL ENHANCEMENT

- Reduce volume conduction smearing with Laplacian operator or spatial deconvolution
- Use a nonlinear, layered-network pattern recognition algorithm to determine subsets of trials, intervals, and channels with event-related information

## EXTRACT SPATIOTEMPORAL EVENT-RELATED INFORMATION

- Compute Wigner distributions
- Determine and apply digital filters
- Estimate covariance and time delay between channels

## MODEL SOURCES OF EVENT-RELATED PATTERNS

- Perform least-squares multiple source localization
- Derive time-varying multi-source models

Figure 1. ADIEEG-IV system for quantification of event-related brain signals. Separate subsystems perform on-line experimental control and data collection, data selection and evaluation, signal processing and pattern recognition. Current capacity is 128 channels. Spherical-head spatial deblurring modules have been implemented, and multiple source modeling algorithms are being developed. Digital tapes of magnetic resonance images or of electrophysiological data from other laboratories are converted into the ADIEEG data format using gateway programs; they are then processed using the same program modules as data collected in the EEG Systems Laboratory. (adapted from Gevins, 1987c)

## CLASSIFIER-DIRECTED ARTIFACT DETECTION

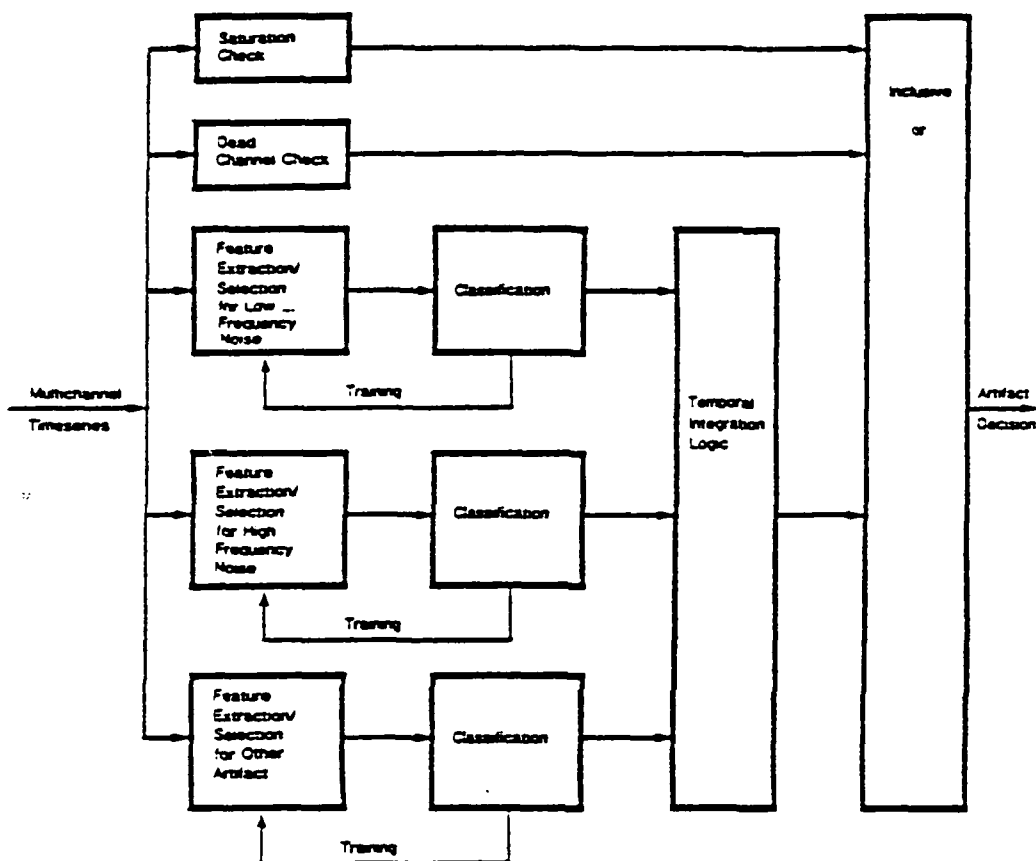


Figure 2. Classifier-directed artifact detection. A system consisting of five parallel detectors is used to find contaminants. Three of the detectors incorporate layered-network classifiers to choose and weigh feature combinations. In this way, a precise automated procedure replaces sole reliance on ad hoc waveform detectors and manually set thresholds. (adapted from Gevins & Morgan, 1986)

In practice, we have measured timeseries covariances (formerly correlations) between scalp potentials from pairs of channels, either on sets of single-trial data (Gevins et al., 1981, 1983, 1985), or on enhanced filtered averages (Gevins et al., 1987, submitted a.b. in prep). The results provide interesting new information about brain function, and suggest that these measures are worth further development. The scalp patterns we have measured have been consistent with the known functional neuroanatomy of the cerebral cortex, as determined from other lines of evidence. As

predicted by neuroanatomical theory and clinical neuropsychological studies, ERC patterns corresponding to visual stimulus processing involved posterior sites that led anterior parietal sites and premotor sites, and ERC patterns at the time of a finger pressure involved the midline precentral electrode that overlies the premotor and supplementary motor cortices. Although the problem of identifying the generators of these patterns is the focus of current research, it has not yet been solved. However, the tendency of the scalp sites involved in these patterns to be spatially separated, with-

out intervening sites, seems to rule out volume-conducted activity from just one or two cortical or subcortical generators.

## Procedures for Measurement of Functional Topography

### Current Computer System

The current computer system is a 32-bit multiprocessor system with 3 computing modes, a 12-MFLOP floating point capability and a 3500 megabyte on-line disk capacity. The current data acquisition system is capable of sampling up to 256 channels at up to 2 kHz sampling rates per channel. (Current amplification capabilities are 128 channels.) Trial presentation, which is performed by a PC controlled by the host computer, is automatically delayed until eye blinks, amplifier setting from eye blinks, and gross body movements have all died down. Up to 70 channels of EEG and non-EEG channels are monitored at a time on a color graphics screen for electrode problems. Other channels are bank-switchable to the monitor. Averages can also be viewed on-line to check for event-registered artifacts. Artifacts such as eye movement and muscle potential contamination are automatically marked by multiple, layered-network pattern classification programs (Figure 2) (Gevins & Morgan, 1986).

### Spatial Sampling

The use of 64 scalp channels provides uniform scalp coverage with an interelectrode distance of about 3.5 cm on a typical adult head. Figure 3 shows a subject wearing a stretchable 64-channel EEG recording cap. The electrodes are placed on the cap according to an expanded version of the 10-20 system (Figure 4).

We are currently extending EEG recordings to 128 channels with interelectrode distances of about 2.25 cm. The desirability of recording from so many sites is evident since regional cerebral blood flow studies suggest that "cortical fields" of 1-3 square centime-



Figure 3. Subject wearing 64 channel EEG cap. (adapted from Gevins, 1988)

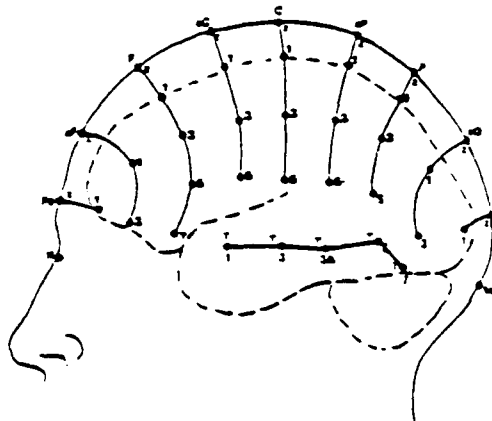


Figure 4. Expanded 10-20 system of electrode position nomenclature. Additional coronal rows of electrodes interpolated between the International 10-20 System coronal rows have the letter "a" for "anterior" added to the designation for the next row posterior, e.g., aPz for anterior parietal midline electrode. With 64 electrodes, the average distance between electrodes is about 3.25 cm. (adapted from Gevins, 1987c)

ters are activated during a wide variety of cognitive tasks (Roland, 1985a,b). Yet, while the possibility of extracting more detailed spatial information has been clearly demonstrated with the MEG (see Williamson & Kaufman, 1987 for discussion and bibliography), it is not widely appreciated that such information can be obtained from appropriately processed EEGs. Examination of spatial spectra has shown that, if information is available from the entirety of an adult's scalp, adequate sampling would require more than 128 electrodes at 2 cm intervals (Gevins, 1988).

In Figure 5, we can see the effect of an increasing number of EEG electrodes on the electric field distribution of a right index fin-

ger flexion. Note the false impression of localization with 16 electrodes, and the correct appearance of a left central focus with 27 and 51 electrodes. Although there is much current discussion about what form of interpolation is best to use in making colored EEG potential maps, it would seem that the more compelling issue is the need for more electrodes.

#### *Rejecting Artifact-Contaminated EEG Signals*

An interactive graphics trial editing program is used by an operator to check the decisions of the automatic artifact detectors (Gevins & Morgan, 1986). In practice, editors have be-

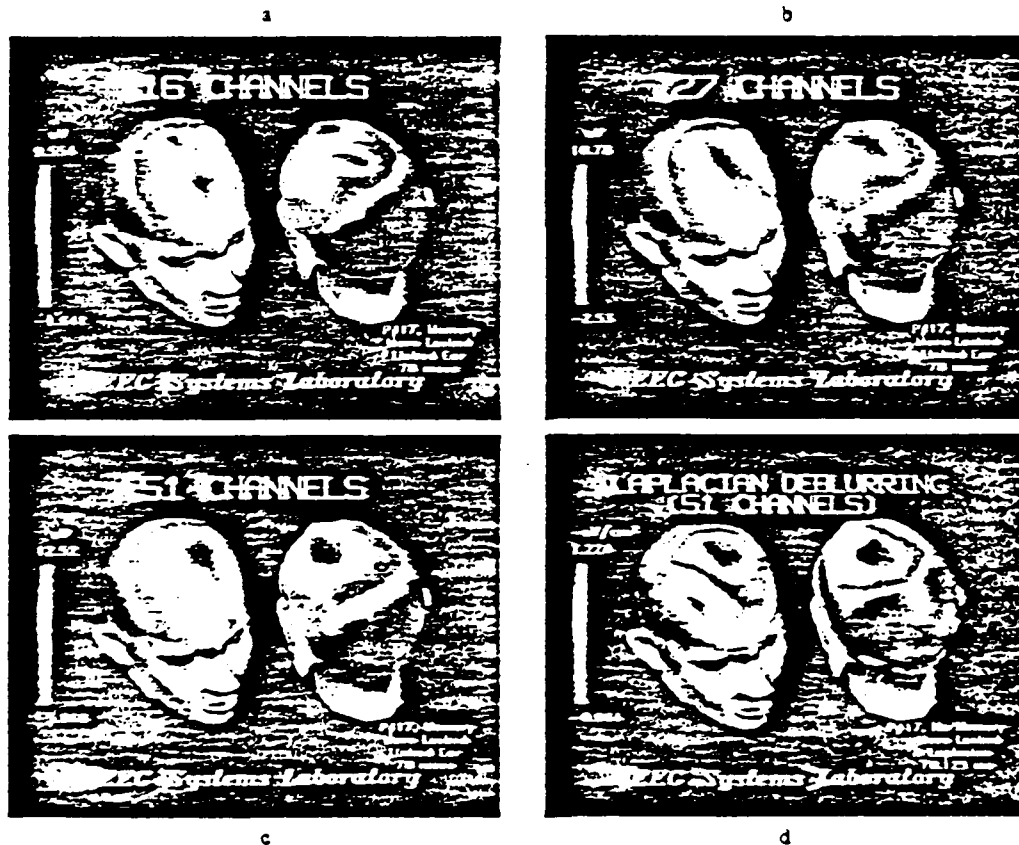


Figure 5. Movement-locked average ERPs at 78 ms after start of right-index-finger flexion, recorded against a linked-ears reference with (A) 16 channels, (B) 27 channels, (C) 51 channels and (D) after application of a Laplacian operation to the 51 channel ERPs. There is a false localization with 16 channels due to insufficient spatial sampling. The 27- and 51-channel ERP recordings show the true potential distribution with increasing resolution. Improvement in topographic localization with the Laplacian is self-evident. (adapted from Gevins, 1988)

come sufficiently skilled to check the single trials of a 64-channel recording in roughly twice the time that it takes to run the experiment. Algorithms are under development to recover trials with non-saturating artifacts. Eye blinks or eye movements, for example, can be removed using least squares noise cancellation, given EOG reference electrodes near the eyes.

#### *Finding Trials with Discernible Event-Related Signals*

We have developed a simple method for finding trials with event-related signals which does not assume that event-related signals are discernible in every trial, and which has minimal assumptions about the statistical properties of signal and noise (Gevins, 1984; Gevins et al., 1986). This method is useful for increasing the signal-to-noise ratio of average ERPs, and for accentuating the differences between averages from two conditions having subtle cognitive differences. However, it is not an essential step when these benefits are not required. First, a mild lowpass filter is applied (3 dB point at 14 Hz and 20 dB down at 32 Hz) and the data, originally sampled at 128 Hz, are decimated by a factor of 3 digitizing points. Then, a "noise" set is formed, composed of segments of single trials for each channel that are randomly timed with respect to stimulus and response events. The number of points in each segment corresponds to that of the ERP interval to be investigated, typically 3 decimated points for a 125 ms interval.

The artificially-formed "noise" data set is then compared with sets of single trial segments which are properly time-registered to stimulus or response events. This comparison produces equations characterizing the event-related signal and determines a list of trials with detectable event-related signals. A pattern classification algorithm constructs the equations that discriminate between sets of single-trial event-related and noise segments for each channel. The equations consist of weighted combinations of the filtered and decimated waveform amplitude values within the interval. Three leave-out-one-third-of-the-trials validations are used, and the average test-set classification is compared with the bi-

nomial distribution for significance. If the equations are significant on validation data, a consistent event-related signal has been found in many of the trials. ERPs that are averaged over these selected trials are called "enhanced" averages, because the signal characteristics have been accentuated (Figure 6).

#### *Controlling for Irrelevant Between-Condition Variables*

In comparing data from two conditions, it is important to balance the two data sets for stimulus-, response-, or performance-related variables that have differences unrelated to the intended comparison. For each between-condition comparison, the two sets of event-related, signal-bearing trials are statistically balanced for each subject by eliminating trials that have outlying values for these irrelevant variables (Gevins et al., 1981, 1983, 1985, 1987, submitted a,b, in prep).

First, a program automatically calculates the largest subset of trials that behaviorally balance the two conditions being compared, for a requested subset of behavioral variables. The set of about 50 behavioral variables includes response time, pressure, velocity, acceleration, duration and error, as well as stimulus parameters, indices of muscle activity and "arousal" (integrated energy in the Pz electrode, computed in 500-ms epochs before and after the onset of each event). This is followed by an interactive program that displays the means, Student's *t*-tests and histograms of the requested variables using a convenient, window-oriented user interface. It is used to check the automatic split of the distributions and to allow their correction if necessary. Between-condition balance is achieved when Student's *t* for each behavioral variable of comparison has a significance of  $p < 0.2$ .

#### *Reducing Blur Distortion at the Scalp*

Because potentials generated by sources in the brain are volume conducted through brain, cerebrospinal fluid, skull and scalp to the recording electrodes, potentials from a localized source are spread over a considerable area of scalp. Potentials measured at a scalp site thus represent the summation of signals from many



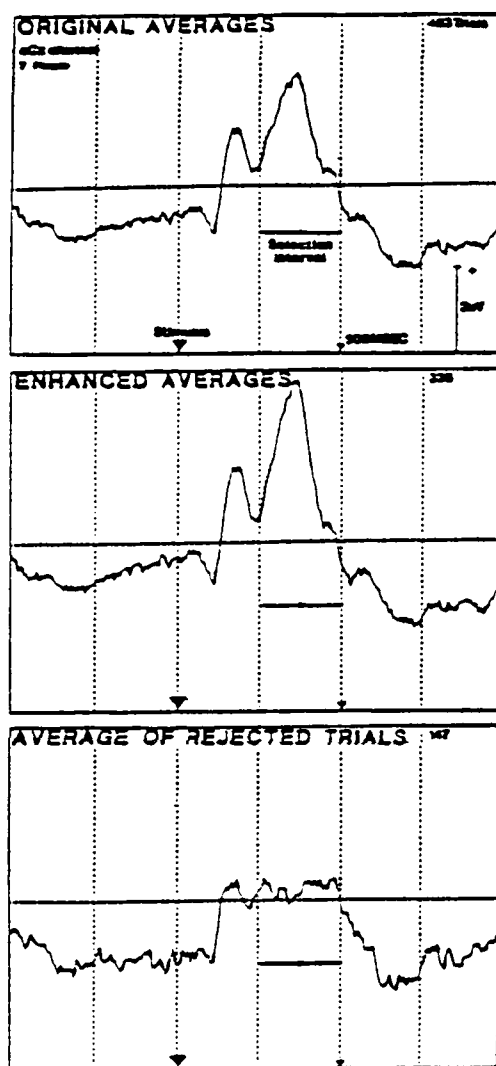


Figure 6. Use of pattern recognition analysis to remove trials without detectable task-related signals from a set of single-trial ERPs. This results in an average ERP with a higher signal-to-noise ratio obtained from fewer trials. (A) An original average ERP formed from 483 presentations of a visual numeric stimulus. (B) Average of 336 trials with consistent event-related signals in the P3 interval. Trials were selected from the original set of 483 by applying a pattern recognition algorithm to distinguish a 250 ms, P3 timeseries segment from a pre-cue "baseline" segment. Note the greatly increased size of the event-related peaks and lower frequency wave forms. (C) Average of 147 trials which did not have consistent event-related signals in the P3 interval. Note the relative lack of event-related activity in the P3 interval. (adapted from Gevins et al., 1986)

sources over much of the brain. (In the context of a 4-shell spherical head model, we have estimated the amount of spread, the "point spread," for a radial equivalent dipole source in the cortex to be about 2.5 cm—Doyle & Gevins, 1986). This spatial low-pass blurring makes source localization difficult, even for nearby cortical sources, and causes the potentials from local sources to be mixed with those from more distant generators. By modeling the tissues between brain and scalp as surfaces with different thicknesses and resistances, we can perform a deblurring operation that, in principle, makes the potential appear as it would if it were recorded just above the level of the brain surface. This operation can be performed without imposing assumptions as to the actual (cortical or subcortical) source locations. The deblurring, however, requires detailed modeling of the tissues, which is a great deal of work when the exact shape of the head is taken into account. Furthermore, there is as yet no good solution to the problem of precisely estimating the local resistances of skull and scalp. When the EEG scalp electrodes are no closer together than about 2.5–3.0 cm, a simpler, model-free deblurring method provides results comparable to the more complex procedure.

This simpler technique, called the Laplacian operator, consists of computing the second derivative in space of the potential field at each electrode. This converts the potential into a quantity proportional to the current entering and leaving the scalp at each electrode site, and eliminates the effect of the reference electrode used during recording. An approximation to the Laplacian, introduced by Hjorth (1975, 1980), assumes that electrodes are equidistant and at right angles to each other. Although this approximation is fairly good for electrodes near the midline, such as Cz, it becomes increasingly poor at the periphery. An optimal estimate of the Laplacian requires precise knowledge of the electrode positions in three dimensions, information which can be obtained by direct measurements from the head (Greer & Gevins, in prep). A properly computed Laplacian operator can produce a dramatic improvement in the spatial topographic detail of ERP components (see Figure 5D).

### *Choosing Filters and Analysis Windows with Wigner Time-Frequency Distributions*

The ERP waveform is a function of time and does not provide explicit frequency information. Yet, the instantaneous frequency is not constant for different ERP components. For each component, the instantaneous frequency must be determined to isolate that component with digital filtering, and the duration over which that frequency is stable must be determined to define the length of the analysis interval. Power spectra of ERP waveforms provide frequency information but obscure time-dependent phenomena. A view of the spectrum as it changed over time would give a new view of the evolution of different frequency components of the ERP. A simple but ineffective approach would be to compute the spectrum over highly overlapped windows of the average ERP. A preferable method is to compute a general function of time and frequency, called the Wigner Distribution, which approximates the instantaneous energy for a given time and frequency. In practice, enhanced ERPs show strong enough energy "peaks" in the Wigner Distribution that very simple interpretations of the time and frequency locations of signal energy are valid (Morgan & Gevins, 1986; Figure 7). From visual inspection of Wigner Distributions, it is a simple matter to specify digital filter characteristics that produce optimal time-frequency resolution for a given ERP component, and to determine the frequency-stable interval for that component. This procedure need not be implemented for each experiment. For example, a filter and interval defined for the N100 in one experiment may be sufficient for analyzing the N100 in another experiment.

### *Computing Event-Related Covariances (ERCs) Between Channels*

To summarize, these preliminary steps are followed before computing ERCs:

1. Record a sufficient amount of data using as many electrodes as possible.
2. Remove data with artifact contamination.
3. Find trials with consistent event-related signals (optional).

4. Select the pair of conditions to be compared, and eliminate trials with extreme values of behavioral variables to obtain behaviorally balanced trial sets.
5. Apply the Laplacian operator to the potential distribution of each non-peripheral scalp electrode location.
6. Compute Wigner Distribution on average ERP (optional) and determine digital filter characteristics and analysis intervals.

Once the data sets have been prepared in this way, the next step is to compute the enhanced, filtered and decimated, averaged Laplacian ERP for each condition. Then, multi-lag crosscovariance functions are computed between all pairwise channel combinations of these averaged ERPs in each selected analysis window. The magnitude of the maximum value of the crosscovariance function and its lag time are the features used to characterize the ERC. The covariance analysis interval is the width of one period of the band-center frequency of each filter. Down-sampling factors are determined by the 20 dB rejection point, and the covariance function is computed up to a lag-time of one-half period of the high frequency for each band. For example, we often use a filter with 3 dB cutoffs at 4 and 7 Hz, and with 20 dB attenuation at 1.5 and 9.5 Hz. The filtered timeseries are decimated from 128 Hz to 21 Hz for each covariance calculation. Covariance is estimated over a 187-ms window, which corresponds to one period of a 5.5 Hz sinusoid. Each window is lagged by up to 8 lags at the original undecimated sampling rate, i.e., 1/128 s per lag.

Estimating the significance of ERCs requires an estimate of the standard deviation of the "noise" ERC. First, random intervals in each single trial of the ensemble are averaged. Then, ERC analysis is performed on a filtered and decimated version of the resulting "noise" averages, yielding a distribution of "noise" ERCs. Because of the large number of channel pairs, some spurious significant covariances may be found. Therefore, the threshold for significance is reduced according to the dimensionality of the data with Duncan's correction procedure. The number of channels is used as a conservative estimate of the number of independent dimensions. The most signifi-

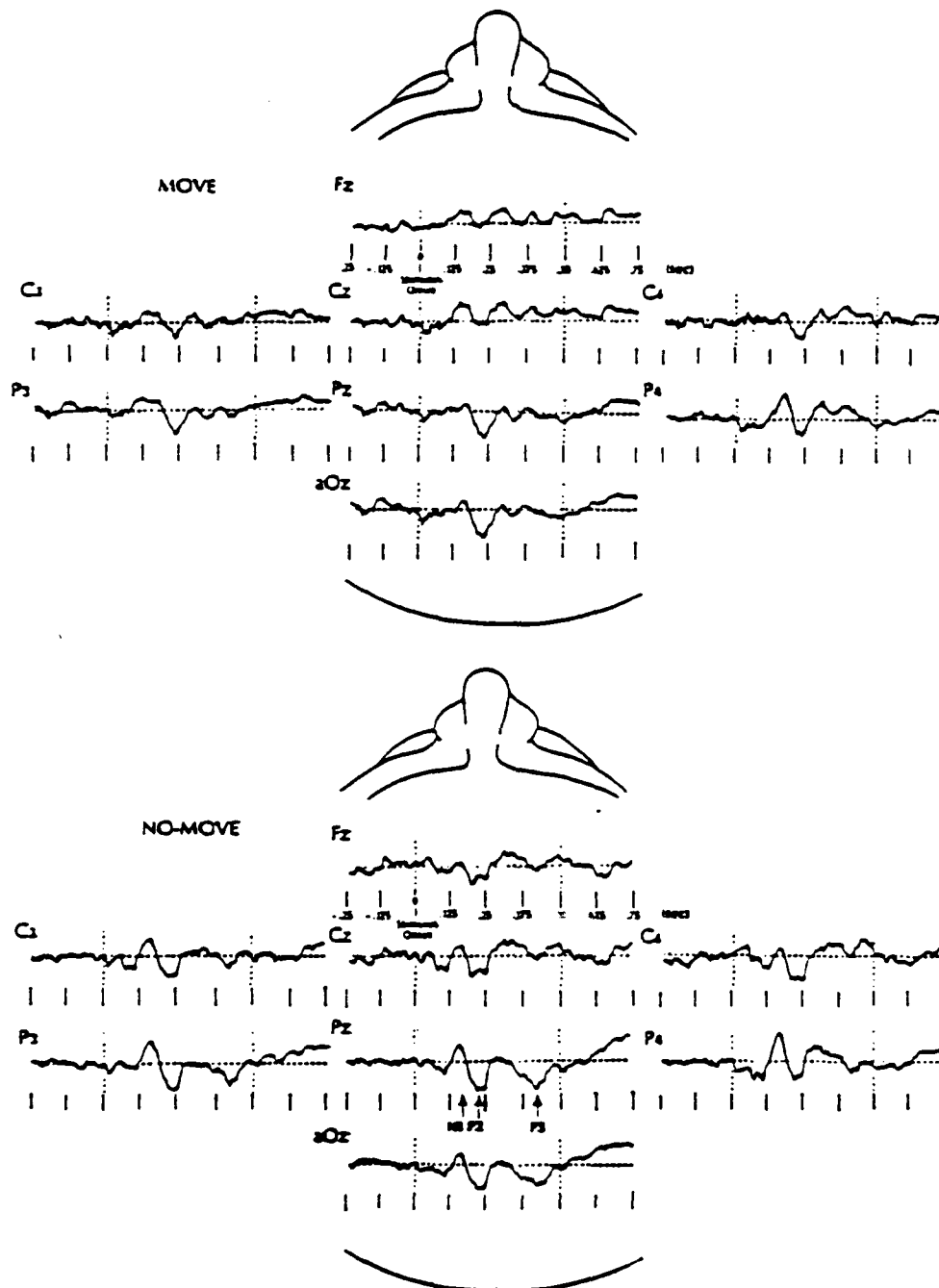
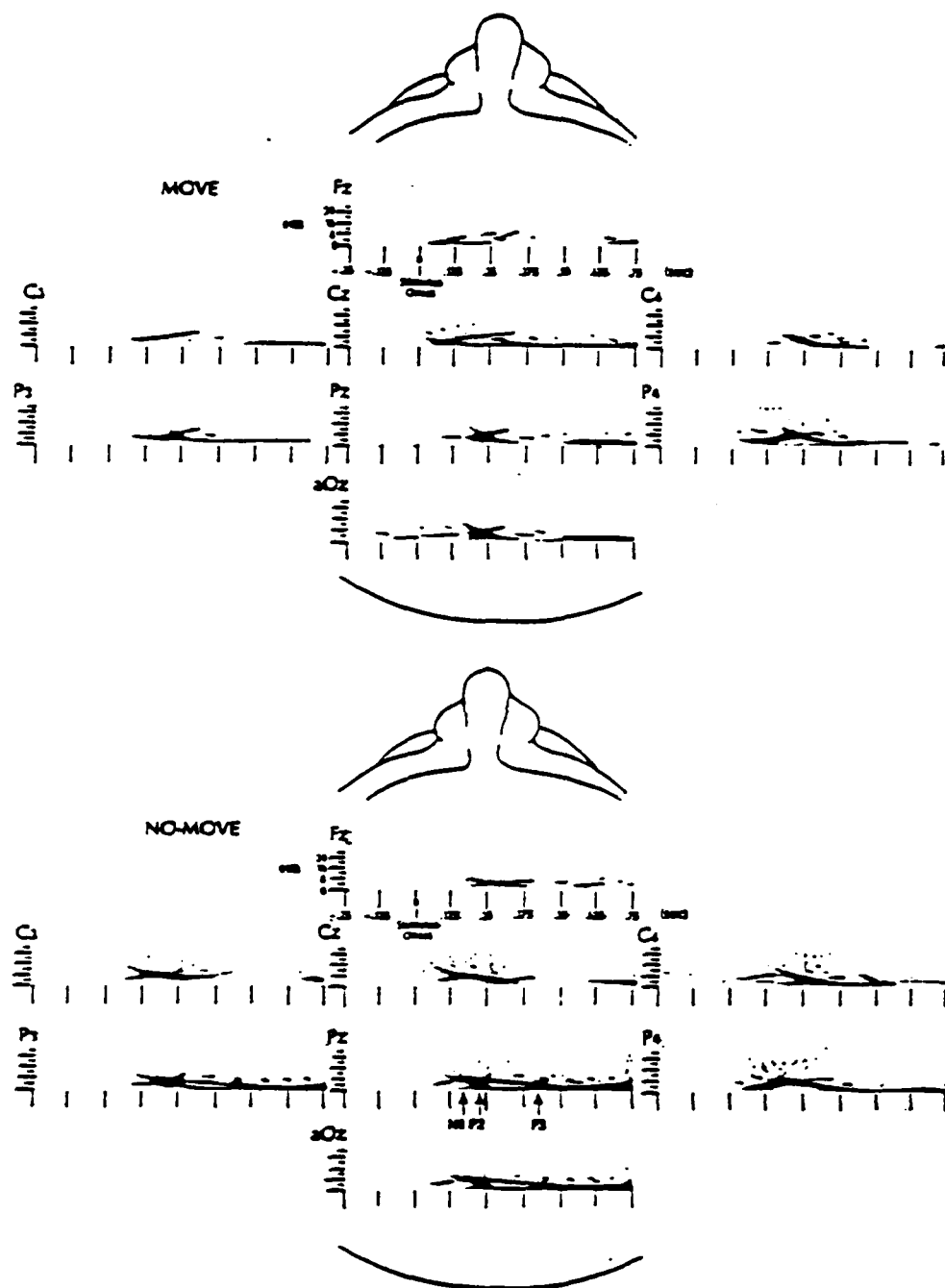


Figure 7. Two representations of eight average ERP channels for "move" and "no-move" cognitive tasks. The view is of the top of the head, with the nose at the top of each set of eight channels. (A) Average time-series of 40 no-move and 37 move trials. Three of the most commonly studied ERP peaks N1, P2, P3 are indicated on the Pz channel of the no-move task. Of these, the P3 peak is larger in the infrequently occurring no-move trials.



(B) The pseudo-Wigner distribution of the analytic signal of the same data. This representation shows that the event-related processes are changing rapidly in both time and frequency. The first moment along the time axis for each frequency is the group delay, while the first moment along the frequency axis is the instantaneous frequency. There is a buildup in energy after the stimulus, and a general increase in frequency until the energy concentration between the time of the N1 and P2 peaks begins to fall off (most prominent in the Pz channel). Then there is a glide down in frequency in the no-move task (most prominent in the Pz and aOz channels), which culminates in a concentration of energy around the time of the P3 peak. (adapted from Gevins 1984)

cant ERCs in each interval are graphed (Figure 8).

To compare ERC maps between conditions, the differences in means of significant ERCs between conditions are tested with an ANOVA and post-hoc t-tests. The similarity between two multivariate ERC maps is measured with an estimate of the correlation between them. The estimate comes from a distribution-independent "bootstrap" Monte Carlo procedure (Efron, 1970), which generates an ensemble of correlation values from randomly selected choices of the repeated measures. This also yields a confidence interval for the estimates.

#### *Validating Significance of ERCs*

We test the between-subject variability of ERC patterns by determining whether each pair of experimental conditions of a particular subject can be distinguished using discriminating equations generated on the other subjects. Likewise, we determine within-subject reliability by attempting to discriminate the experimental conditions for each session using equations generated on that subject's other sessions. These tests are performed on sets of single trials to quantify the extent to which the condition-specific patterns from the ERC analysis of the average ERPs are observable in each trial. Although this procedure could be done with any type of discriminant analysis, we have developed the use of distribution-independent, "neural network" pattern classification algorithms for this purpose (Gevins et al., 1979a,b,c, 1981, 1983, 1985, 1986, 1987; Gevins & Morgan, 1986; Gevins, 1980, 1984, 1987b). We have shown that this method has better sensitivity and specificity than stepwise or full-model linear or quadratic discriminant analysis (Gevins, 1980). The pattern recognition approach has the advantage of testing how well a subject's individual trials conform to those of the group in discriminating two behavioral conditions of interest. In the same way, the trials of each session of a subject are tested by conformity to trials from the other sessions of that subject. Requiring trial-by-trial discriminability is a strict condition for deciding between-subject variability and within-subject reliability.

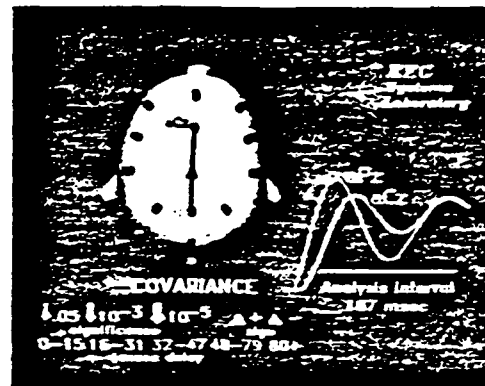


Figure 8. Schematic diagram showing the relationship of an event-related covariance (ERC) line on a top-view of a model head (left) to the theta-band-filtered, averaged event-related Laplacian derivation waveforms (right). ERCs were computed over the indicated 187-ms analysis interval from the aPz and aCz electrode sites. The width of an ERC line indicates the significance of the covariance between two waveforms, with the scale appearing above the word "significance." The color of the line indicates the time delay in ms (lag time of maximum covariance) as shown in the scale above "ms delay." The color of the arrow indicates the sign of the covariance (same color as line = positive; skin color = negative). The arrow points from leading to lagging channel, unless there is no delay, in which case a bar is shown. The covariance between aPz and aCz is significant at  $p < 10^{-5}$ . The aPz waveform leads the aCz waveform by about 16–31 ms (green line), and the covariance is positive (arrow also green). (from Gevins et al., submitted a)

Each subject's classification yields a score, which is the percent of trials that are correctly classified by the group discrimination equations. The score is assessed for significance by comparison to the binomial distribution (Gevins, 1980). A significant classification score for a subject indicates that the group equations are successful in discriminating the two conditions in his or her trials.

Within-subject (between-session) reliability is tested in a similar manner. The trial set (consisting of the two conditions) from each of a subject's sessions is tested with equations developed on the trial sets from his or her other sessions. The single-trial ERC values come from channel pairs that are significant in the ERC pattern formed from the average

over all his or her sessions. Post-hoc comparisons are valuable in determining whether effects of learning and/or habituation are evident over sessions, by indicating which sessions are alike, and where transitions occur between sessions.

## Application of ERC Analysis

### *Study of Visuomotor Performance*

*Procedure* (Gevins et al., 1987, submitted a,b).

Seven healthy, right-handed male adults participated in this study. A visual cue, slanted to the right or to the left, indicated to subjects to prepare to make a response pressure with the right or left index finger. One second later, the cue was followed by a visual numeric stimulus (number 1–9) indicating that a pressure of 0.1 to 0.9 kg should be made with the index finger of the hand indicated by the cue. Feedback indicating the exact response pressure produced was presented as a two-digit number one second after the peak of the response pressure. On a random 20% of the trials, the stimulus number was slanted opposite to that of the cue, and subjects were to withhold their responses on these "catch trials." The next trial followed 1 s after disappearance of the feedback. Subjects each performed several hundred trials, with rest breaks as needed.

Twenty-six channels of EEG data, as well as vertical and horizontal eye-movements and flexor digitorum muscle activity from both arms, were recorded. All single-trial EEG data were screened for eye movement, muscle potential and other artifacts. Contaminated data were discarded.

Intervals used for ERC analysis were centered on major ERP peaks. ERCs were computed between averaged Laplacian ERPs from each of the 120 pairwise combinations of the 16 nonperipheral channels in intervals from 500 ms before cue to 500 ms after the feedback.

Data sets were separated into trials in which subsequent performance was either accurate or inaccurate. Accurate and inaccurate performance trials were those in which the er-

ror (deviation from required finger pressure) was less than or greater than, respectively, the mean error over the recording session.

### Results and Discussion

The ERC pattern for the interval at the peak of the finger pressure (Figure 9) closely corresponded to prior functional neuroanatomical knowledge, lending a first level of validation for the patterns associated with higher-order cognitive activity. The midline precentral electrode, overlying the premotor and supplementary motor cortex, was the focus of all movement-related patterns, and the patterns for the two hands were appropriately lateralized, clearly reflecting the sharply focused current sources and sinks spanning the hand areas of motor cortex.

ERC patterns during a 375-ms interval centered 687-ms post-cue (spanning the late Contingent Negative Variation; CNV) were distinct from those related to overt finger responses. The pattern associated with subsequently accurate right-hand performance involved predominantly left hemisphere sites, particularly left frontal and appropriately la-

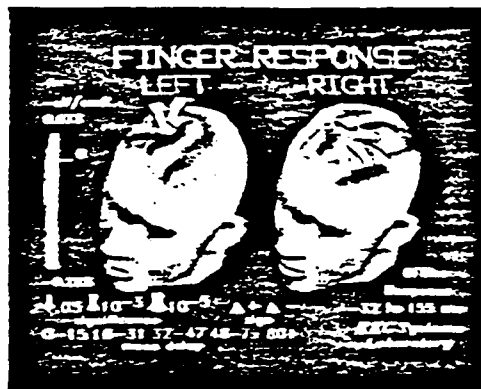


Figure 9. Most significant (top standard deviation) ERC patterns at the peak of the finger pressure for right and left hand trials from seven people, superimposed on maps of Laplacian response potential amplitude. Note that the anterior midline precentral (aCz) electrode is the focus of all covariances, with 16–31 ms time delays between aCz and Fz. The patterns are distinctly lateralized according to responding hand. The sign of the aCz covariances is positive for lateral frontal, and negative for lateral central and anterior parietal electrodes.

teralized central and parietal sites (Figure 10A). The pattern preceding accurate left-hand performance involved predominantly right hemisphere sites, in addition to the left frontal site. Inaccurate performance by the right hand (Figure 10B) was preceded by a highly simplified pattern, while inaccurate performance by the left hand was preceded by a complex, spatially diffuse pattern.

When the trials of each of the 7 subjects were classified by equations developed on the trials of the other 6 subjects, the overall discrimination was 59% ( $p < 0.01$ ) for right hand and 57% ( $p < 0.01$ ) for left-hand performance. For the subject with the most trials, average classification of 68% ( $p < .001$ ) for subsequent right- and 62% ( $p < .01$ ) for subsequent left-hand performance was achieved by testing a separate equation on each fifth of his trials, formed from the other four-fifths.

We suggest that our pre-stimulus ERC patterns characterize a distributed preparatory neural set related to the accuracy of subsequent task performance. This set appears to involve distinctive cognitive (frontal), integrative-motor and lateralized somesthetic-motor components. The involvement of the left-frontal site is consistent with clinical findings that

preparatory sets are synthesized and integrated in prefrontal cortical areas, and with experimental and clinical evidence indicating involvement of the left dorsolateral prefrontal cortex in delayed response tasks. A midline precentral integrative motor component is consistent with known involvement of premotor and supplementary motor areas in initiating motor responses. The finding of appropriately lateralized central and parietal components is consistent with evidence from primates and humans for neuronal firing in motor and somatosensory cortices prior to motor responses.

#### *Study of Incipient Fatigue*

Procedure (Gevins et al., in prep)

After learning and practicing a battery of tasks until their performance was stable on one day, each of five right-handed, healthy male subjects returned to the laboratory the next morning and performed the tasks for about 6 hours. Following a dinner break, they resumed task performance for an additional 6 to 8 hours.

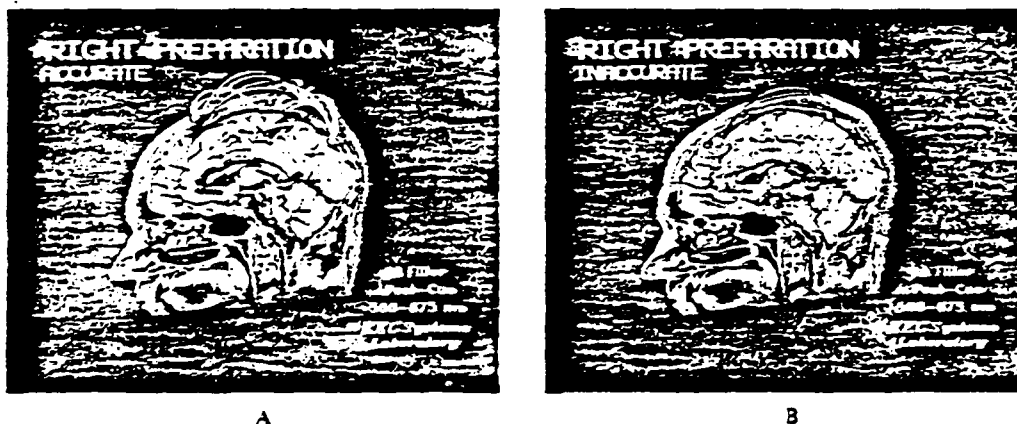


Figure 10. View of the significant ( $p < 0.05$ ) Contingent Negative Variation (CNV) ERC patterns, superimposed on a mid-sagittal Magnetic Resonance image of a subject's cranium. Measurements are from an interval 500 to 875 ms after the cue for subsequently accurate (A) and inaccurate (B) right-hand visuomotor task performance by seven right-handed men. The thickness of an ERC line is proportional to its significance (from .05 to .005). A yellow line indicates the ERC is positive, while a red line is negative. Covariances involving left frontal (F3), left central (C3), left parietal (P3), and left antero-parietal (aP1) electrode sites, all contralateral to the subsequently responding hand, are the most prominent sites in the pattern for subsequently accurate performance. Only two covariances characterize subsequently inaccurate performance: left frontal (F3) with left parietal (P3), and left frontal with left antero-parietal (aP1) sites.

There were four tasks in the battery, including easy and difficult continuous and discrete visuomotor tracking tasks, a simple numeric memory task, and a difficult visuomotor memory task (VMMT). Since we expected that early neural signs of fatigue would be most evident during demanding tasks, we analyzed the VMMT first. This task required subjects to remember two continuously changing numbers, in the presence of numeric distractors, in order to produce precise finger pressures. Each trial consisted of a warning symbol followed by a single-digit visual stimulus to be remembered, followed by the subject's finger-pressure response to the stimulus number presented two trials earlier, followed by a 2-digit feedback number indicating the accuracy of the response. For example, if the stimulus numbers in five successive trials were 8, 6, 1, 9, 4, the correct response would be a pressure of 0.8 kg when seeing the 1, 0.6 kg for the 9, and 0.1 kg for the 4. To increase the task difficulty, subjects were required to withhold their response on a random 20% of the trials. These "no-response catch trials" were trials in which the current stimulus number was identical to the stimulus two trials earlier.

Trials early in the recording session with accurate finger pressures formed the "Alert" data set. Trials from early in the evening, when performance was just starting to decline, formed the "Incipient Fatigue" data set. For each subject, trials with relatively inaccurate responses were then deleted from the Incipient Fatigue data set so that the final Alert and Incipient Fatigue data sets consisted of trials with equivalently accurate performance. This crucial step allowed measurement of neuroelectric patterns associated with incipient fatigue while controlling for those due to variations in performance accuracy.

EEGs were recorded with either 33 or 51 channels with a nylon mesh cap. Vertical and horizontal eye movements were also recorded, as were the responding flexor digitorum muscle potentials, electrocardiogram and respiration. Three-axis Magnetic Resonance Image scans were made of 3 of the 5 subjects.

Grand-average (over the five pilots) ERPs were time-locked to presentation of the numeric stimulus. Incipient-Fatigue ERPs were subtracted from Alert ERPs in order to high-

light changes due to fatigue. Spatiotemporal neuroelectric patterns were then quantified by measuring ERCs between all 153 pairwise combinations of the 18 nonperipheral electrodes. ERCs were measured across brief segments of grand-average Alert-minus-Incipient-Fatigue subtraction ERPs. The first ERC interval was 500 ms wide and was centered 312 ms before the numeric stimulus. The next two ERC intervals were 187 ms wide and were positioned with respect to the N125 peak elicited by the numeric stimulus, and the P380 ERP peak elicited by the infrequent, no-response catch-trial stimuli.

## Results and Discussion

A number of significant Alert-minus-Incipient-Fatigue ERCs were found during the 500-ms prestimulus interval. Significance was determined by comparison to a distribution of "noise" ERCs, and corrected with Duncan's procedure, following the description above ("Computing Event-Related Covariances Between Channels"). Midline central, left parietal, left anteroparietal, right anteroparietal and right posterior parietal electrodes were the major ERC foci. There were no significant ERCs in the interval centered at 62 ms post-stimulus. The ERCs computed over the P380 no-response difference ERP were focused on the midline precentral, and right anterior and posterior parietal electrodes.

The ERC changes with Incipient Fatigue suggest that dynamic functional neural networks associated with specific cognitive functions are selectively affected during early fatigue. During the prestimulus interval, when subjects were maintaining the last two visually presented numbers in working memory and preparing for the next stimulus, ERCs decreased in number in the Incipient Fatigue condition. The lack of ERC differences between Alert and Incipient Fatigue conditions during the interval centered at 62 ms suggests that the "exogenous" stages of visual stimulus processing are relatively unaffected by early fatigue. However, during the later post-stimulus interval of trials requiring an inhibition of the response, ERCs again decreased in number with Incipient Fatigue.



The results suggest that although neural systems responsible for primary visual stimulus processing are relatively unaffected by Incipient Fatigue, cortical associative areas responsible for higher cognitive functions such as working memory rehearsal, preparation, and motor inhibition are altered prior to appreciable degradations in performance.

### Conclusions

The idea of distributed processing networks in the brain has been well established in the literature, dating back to Sherrington. This powerful concept has been under-utilized in neurocognitive studies, perhaps because of the difficulty of measuring activity patterns. Recent attempts at constructing "parallel distributed processing" models of cognition (Rumelhart et al., 1986) aim to derive computational principles from knowledge of the brain's own distributed processing networks. These efforts are encouraging, yet they depend on continued characterization of those networks. Measurement of the dynamic functional topography of the brain, the time-varying statistical relations among the field potentials from a distributed set of recording sites, is an empirical means of accomplishing this. It has been shown that patterns of event-related covariance, measuring functional topography, are related to cognitive processing, and thus may represent active states of a distributed processing network.

At least three major factors have contributed to our ability to begin characterizing the functional topography of the human brain. First was the use of sufficiently controlled cognitive tasks to allow inference of the cognitive processes taking place during brief analysis intervals. Along with this was the production of computer programs to choose trials from two experimental conditions that are balanced for important behavioral variables. This factor created the functional context for topographic measurements. Second was the ability to record from a sufficient number of channels to adequately sample the available re-

coding surface of the head. Indications are that even with 64 evenly spaced scalp electrodes, there is potentially more information to be gained from greater spatial sampling. This factor allowed the topography to be represented spatially. Third was the application of sophisticated signal processing techniques to the analysis of event-related potentials. This factor was necessary to appropriately measure the inter-regional relations comprising the functional topography.

Neurocognitive Pattern (NCP) Analysis and Event-Related Covariance (ERC) Analysis should be distinguished from brain electrical activity maps, which are usually color topographic displays interpolated from 16–20 channels of averaged ERPs or EEG spectra, or the difference between such measures and a set of normative data. We use more extensive signal processing and pattern recognition algorithms to reduce volume conduction effects and to extract event-related signals from unrelated background noise of the brain, compute between-channel ERC patterns, and display their scalp distribution in 3-D perspective graphics of the head and brain. Subtle aspects of neurocognitive function, such as the measurement of preparatory sets that precede accurate performance, are revealed by these ERC patterns but are not necessarily apparent on topographic maps (Gevins et al., submitted b). ERC Analysis is currently undergoing further development. The value of scalp patterns could be greatly expanded by a more adequate understanding of their sources. The difficult problem of determining the distributed source network in the brain producing the scalp ERC patterns is crucial, and is the focus of our ongoing work.

It is a testimony to the ingenuity of cognitive psychologists, psychophysicists, neurologists and psychiatrists that so much has been learned about the timing of neurocognitive processes using very modest recording equipment and analysis techniques. It is, therefore, almost certain that when more advanced recording methods and more powerful analytic tools are widely available, rapid advances in understanding the neural basis of human cognitive functions will take place.

## References

- Adey WR, Walter DO, Hendrix CE (1961) Computer techniques in correlation and spectral analysis of cerebral slow waves during discriminative behavior. *Exp Neurol*, 3, 501-524.
- Barlow JS, Brazier, MAB (1954) A note on a correlator for electroencephalographic work. *Electroenceph clin Neurophysiol*, 6, 321-325.
- Boudreau JC (1966) Computer measurements of hippocampal fast activity with chronically implanted electrodes. *Electroenceph clin Neurophysiol*, 20, 165-174.
- Bressler SL (1987a) Relations of olfactory bulb and cortex. I: Spatial variation of bulbo-cortical interdependence. *Brain Research*, 409, 285-293.
- Bressler SL (1987b) Relations of olfactory bulb and cortex. II: Model for driving of cortex by bulb. *Brain Research*, 409, 294-301.
- Callaway E, Harris P (1974) Coupling between cortical potentials from different areas. *Science*, 183, 373-375.
- Doyle JC, Gevins AS (1986) *Spatial filters for event-related potentials*. EEG Systems Laboratory Technical Report-0011.
- Dumenko VN (1970) Electroencephalographic investigation of cortical relationships in dogs during formation of a conditioned reflex stereotype. In Rusinov, V.S. (Ed.) *Electrophysiology of the nervous system*. Plenum Press, New York, 107-117.
- Efron B (1970) *The jackknife, the bootstrap, and other resampling plans*. SIAM, Philadelphia.
- Elul R (1972) The genesis of the EEG. *Int Rev of Neurobiol*, 15, 227-272.
- Freeman WJ (1975) *Mass action in the nervous system*. Academic Press, New York.
- Freeman WJ (1987) Analytic techniques used in the search for the physiological basis of the EEG. In Gevins AS, Remond A (Eds.) *Methods of analysis of brain electrical and magnetic signals* (Handbook of electroencephalography and clinical neurophysiology, Vol. 1). Elsevier, Amsterdam, 583-664.
- Gevins AS (1980) Pattern recognition of human brain electrical potentials. *IEEE Trans Pattern Analysis Mach Intel PAMI-2*(5), 383-404.
- Gevins AS (1984) Analysis of the electromagnetic signals of the human brain: Milestones, obstacles and goals. *IEEE Trans Biomed Engr BME-31*(12), 333-350.
- Gevins AS (1987a) Correlation analysis. In Gevins AS, Remond A (Eds.) *Computer analysis of brain electrical and magnetic signals* (Handbook of electroencephalography and clinical neurophysiology, Vol. 1). Elsevier, Amsterdam, 171-193.
- Gevins AS (1987b) Statistical pattern recognition. In Gevins AS, Remond A (Eds.) *Computer analysis of brain electrical and magnetic signals* (Handbook of electroencephalography and clinical neurophysiology, Vol. 1). Elsevier, Amsterdam, 541-582.
- Gevins AS (1987c, in press) Recent advances in neurocognitive pattern analysis. In Basar, E. (Ed.) *Dynamics of sensory and cognitive processing of the brain*. Springer-Verlag, Berlin.
- Gevins AS (1988, in press) Analysis of multiple lead data. In Rohrbaugh J, Johnson R, Parasuraman R (Eds.) *Event-related potentials of the brain*. Oxford University Press, New York.
- Gevins AS, Morgan NH (1986) Classifier-directed signal processing in brain research. *IEEE Trans Biomed Engr BME-33*(12), 1054-1068.
- Gevins AS, Zeitlin GM, Yingling CD, Doyle JC, Dedon MF, Schaffer RE, Roumasset JT, Yeager CL (1979a) EEG patterns during "cognitive" tasks. I. Methodology and analysis of complex behaviors. *Electroenceph clin Neurophysiol*, 47, 693-703.
- Gevins AS, Zeitlin GM, Doyle JC, Schaffer RE, Callaway E (1979b) EEG patterns during "cognitive" tasks. II. Analysis of controlled tasks. *Electroenceph clin Neurophysiol*, 47, 704-710.
- Gevins AS, Zeitlin GM, Doyle JC, Yingling CD, Schaffer RE, Callaway E, Yeager CL (1979c) Electroencephalogram correlates of higher cortical functions. *Science*, 203, 665-668.
- Gevins AS, Doyle JC, Cutillo BA, Schaffer RE, Tannehill RS, Ghannam JH, Gilcrease VA, Yeager CL (1981) Electrical potentials in human brain during cognition: New method reveals dynamic patterns of correlation of human brain electrical potentials during cognition. *Science*, 213, 918-922.
- Gevins AS, Schaffer RE, Doyle JC, Cutillo BA, Tannehill RS, Bressler SL (1983) Shadows of thought: Shifting lateralization of human brain electrical patterns during brief visuomotor task. *Science*, 220, 97-99.
- Gevins AS, Doyle JC, Cutillo BA, Schaffer RE, Tannehill RS, Bressler SL (1985) Neurocognitive pattern analysis of a visuomotor task: Rapidly-shifting foci of evoked correlations between electrodes. *Psychophysiol*, 22, 32-43.
- Gevins AS, Morgan NH, Bressler SL, Doyle JC, Cutillo BA (1986) Improved ERP estimation via statistical pattern recognition. *Electroenceph clin Neurophysiol*, 64, 177-186.
- Gevins AS, Morgan NH, Bressler SL, Cutillo BA, White RM, Illes J, Greer DS, Doyle JC, Zeitlin GM (1987) Human neuroelectric patterns predict performance accuracy. *Science*, 235, 580-585.

- Gevins AS, Bressler SL, Morgan NH, Cutillo BA, White RM, Greer DS, Illes J (submitted a) Event-related covariances during a bimanual visuomotor task, Part I: Methods and analysis of stimulus- and response-locked data. *Electroenceph din Neurophysiol*.
- Gevins AS, Cutillo BA, Bressler SL, Morgan NH, White RM, Illes J, Greer DS (submitted b) Event-related covariances during a bimanual visuomotor task, Part II: Preparation and feedback. *Electroenceph din Neurophysiol*.
- Gevins AS, Bressler SL, Cutillo BA, Morgan NH, Illes J, White RM, Greer DS (in prep.) *Neuroelectric changes precede impairment of prolonged task performance*.
- Greer, DS, Gevins AS (in prep.) *Spatial deblurring of scalp recorded brain potentials using an optimal Laplacian operator*.
- Hjorth B (1975) An on-line transformation of EEG scalp potentials into orthogonal source derivations. *Electroenceph din Neurophysiol*, 39, 526-530.
- Hjorth B (1980) Source derivation simplifies topographical EEG interpretation. *Am J EEG Technol*, 20, 121-132.
- John ER (1967) *Mechanisms of memory*. Academic Press, New York.
- John ER, Bartlett F, Schimokaochi M, Kleinman D (1973) Neural readout from memory. *J Neurophysiol*, 36, 893-924.
- Lashley, K.S. (1958) Cerebral organization and behavior. *Proc Assoc Res Nervous Mental Disease*, 36, 1-18.
- Livanov MN (1977) *Spatial organization of cerebral processes*. Wiley, New York.
- Mesulam MM (1981) A cortical network for directed attention and unilateral neglect. *Ann Neurol*, 10, 309-325.
- Morgan NH, Gevins AS (1986) Wigner distributions of human event-related brain signals. *IEEE Trans Biomed Engr*, BME-33(1), 66-70.
- Petsche H, Pockberger H, Rappelsberger P (1984) On the search for the sources of the electroencephalogram. *Neuroscience*, 11, 1-27.
- Roland PE (1985a) Cortical organization of voluntary behavior in man. *Human Neurobiology*, 11, 216.
- Roland PE (1985b) In Solokoff L (Ed.) *Brain imaging and brain function*. Raven Press, New York.
- Rumelhart DE, McClelland JL, PDP Research Group (1986) *Parallel distributed processing: Explorations in the microstructures of cognition*. MIT, Cambridge.
- Sherrington CS (1906) *The integrative action of the nervous system*. Yale University Press, New Haven, CT.
- Tucker DM, Roth DL, Bair, TB (1986) Functional connections among cortical regions: Topography of EEG coherence. *Electroenceph din Neurophysiol*, 63, 242-250.
- Walter W, Shipton H (1951) A new toposcopic display system. *Electroenceph din Neurophysiol*, 3, 281-292.
- Williamson SJ, Kaufman L (1987) Analysis of neuromagnetic signals. In Gevins AS, Remond A (Eds.) *Methods of analysis of brain electrical and magnetic signals* (Handbook of electroencephalography and clinical neurophysiology, Vol 1). Elsevier, Amsterdam, 405-448.

EEG 03389

## Event-related covariances during a bimanual visuomotor task. I. Methods and analysis of stimulus- and response-locked data<sup>1</sup>

A.S. Gevins, S.L. Bressler, N.H. Morgan, B.A. Cutillo, R.M. White,  
D.S. Greer and J. Illes

*EEG Systems Laboratory, 51 Federal Street, San Francisco, CA 94107 (U.S.A.)*

(Accepted for publication: 4 April 1988)

**Summary** A new method that measures between-channel, event-related covariances (ERCs) from scalp-recorded brain signals has been developed. The method was applied to recordings of 26 EEG channels from 7 right-handed men performing a bimanual visuomotor judgment task that required fine motor control. Covariance and time-delay measures were derived from pairs of filtered, laplacian-derived, averaged wave forms, which were enhanced by rejection of outlying trials, in intervals spanning event-related potential components. Stimulus- and response-locked ERC patterns were consistent with functional neuroanatomical models of visual stimulus processing and response execution. In early post-stimulus intervals, ERC patterns differed according to the physical properties of the stimulus; in later intervals, the patterns differed according to the subjective interpretation of the stimulus. The response-locked ERC patterns suggested 4 major cortical generators for the voluntary fine motor control required by the task: motor, somesthetic, premotor and/or supplementary motor, and prefrontal. This new method may thus be an advancement toward characterizing, both spatially and temporally, functional cortical networks in the human brain responsible for perception and action.

**Key words:** Event-related covariances; Event-related potentials; Laplacian derivation; Spatio-temporal maps; N100; P300; Response potentials; Functional cortical networks

This study was undertaken to test the hypothesis that human task performance involves coordinated processing of information by different areas of the brain. Prior studies have shown that when a brain region becomes involved in a task, some subset of neurons in that region becomes synchronized, and the synchronization is manifested as a change in the wave shape of its extracellularly

recorded macropotential (John 1967; Elul 1972; Freeman and Skarda 1985; Freeman 1987). Low-frequency components, in particular, have been shown to be important for visuomotor and cognitive tasks (Legewie et al. 1969; Ishihara and Yoshi 1972; Doyle et al. 1974; Komisaruk 1977; Gevins et al. 1979a,b,c). We hypothesize, therefore, that during performance of such tasks, coordinated processing will be reflected in the similarity of low-frequency potential wave shape among the regions involved. Since wave shape similarity of macropotentials from different areas of the brain can be measured by covariance and correlation (reviewed in Gevins 1987; Gevins and Bressler 1988), these techniques can characterize the spatial organization of coordinated low-frequency activity.

Both animal and human studies provide further evidence for this reasoning. Animal studies using

<sup>1</sup> A part of the results concerning the covariance pattern of the response event reported here, has been summarized in Gevins et al. 1987. This paper presents a detailed description of the complete experimental design, the methods of analysis, ERP and event-related covariance results of 'exogenous' and 'endogenous' stimulus-locked data and response-locked data, and a discussion relating these results to other psychophysiological research.

*Correspondence to:* A.S. Gevins, EEG Systems Laboratory, 51 Federal Street, San Francisco, CA 94107 (U.S.A.).

behavioral conditioning, for example, have shown that the functional coordination of neuronal populations is reflected in the synchronization of their macropotentials (possibly with time delay) specifically in the theta (4–7 Hz) frequency band (Adey et al. 1961; Efremova and Trush 1973; Livanov 1977). Dumenko (1970) found that the correlation between extracellular potentials of visual and motor cortices in dogs increases with conditioning to a visual stimulus, and is highest at the time of the conditioned stimulus and response. John et al. (1973) measured the relatedness of wave forms recorded from multiple brain locations of cats that were learning 2 different conditioned responses. On the basis of wave form similarity, he demonstrated differential generalization of neural activity. Bressler (1987) reported that correlations between the gamma band of the olfactory bulb and cortex in rabbits are specific to particular regions of each.

In studies of human performance, Livanov (1977) found that correlation levels among scalp electrodes were higher during motor and mental activity than during rest. Callaway and Harris (1974) used a mutual information approach to successfully measure the degree of relatedness between cortical areas during mental tasks. Our own work with human subjects to date has been aimed at improving the precision of spatial, temporal, and behavioral measurements by using more modern recording and signal processing technologies. In one study (Gevins et al. 1981), distinct, complex, and rapidly changing patterns of evoked brain potential correlation distinguished sets of single trials of several visuomotor tasks that differed only in type of spatial or numerical judgment. In a later study of a brief spatial judgment task (Gevins et al. 1983, 1985), the site of maximum differences between the correlations of response and no-response evoked potentials shifted during sequential stimulus-locked intervals, in a manner consistent with neuropsychological models of the task.

Major methodological improvements over our previous studies are reported here. More robust and complete methods for measuring event-related, between-channel covariation were developed and applied to discern differences in each

stage of a 4 sec long task. The methods included: (a) the use of laplacian derivations to reduce spatial smearing, (b) rejection of outlying trials by a pattern classification procedure, (c) interactive statistical procedures for adjusting the distributions of behavioral variables to create highly controlled data sets, and (d) analysis of inter-electrode wave form covariance and time delay in numerous brief intervals.

The task involved cued preparation, stimulus evaluation, response execution of precise right- and left-hand finger pressures, and evaluation of feedback about response accuracy (Fig. 1). Spatial patterns of wave form covariance and timing were derived from short intervals (Fig. 2) of averaged event-related potentials recorded from multiple scalp electrodes. Here we describe our methods and their application to stimulus- and response-locked wave forms, averaged across subjects, as a test of whether they produce results consistent with functional neuroanatomical models found in the literature. Part II (Gevins et al. 1989) of this paper presents the prestimulus and feedback-evoked results.

### General methods and materials

Seven male adults were selected for participation in this study. All were right-handed according to the Edinburgh Inventory (Oldfield 1971). None had any history of psychiatric or neurologic disease.

Stimuli for this experiment were presented visually on a Videographics II amber CRT monitor, placed 70 cm from the subject's eyes, and subtended a visual angle of  $<1.5^\circ$ . Stimuli had a duration of 315 msec and an illumination of 0.5 log fL against a background of  $-1.5$  log fL. One second before the stimulus appeared, a cue ('V') was presented at a fixation point at center screen. The cue was slanted to the right or left to indicate the responding hand (Fig. 1). In 'response' trials (80%), a stimulus number from 1 to 9 was presented, slanted in the same direction as the cue; the subject was to respond quickly with the index finger of the indicated hand, with a pressure of 0.1–0.9 kg, according to the stimulus number. A

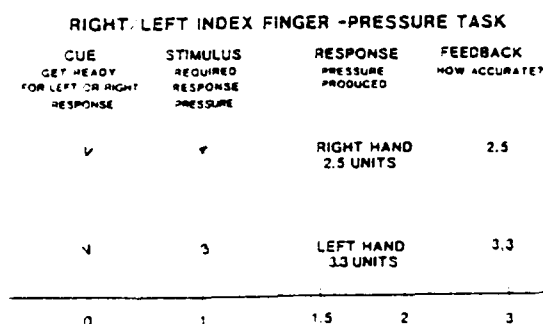


Fig. 1. Sequence of events in the bimanual visuomotor task. The right-cued, right-hand response condition is shown above, while the left-cued, left-hand response condition is shown below. The abscissa shows time in seconds. One second following a cue (a slanted letter 'V'), a slanted 1-digit stimulus was presented. If the direction of slant (right or left) of the stimulus number was the same as the cue, the subject had to produce a precise pressure with his right or left index finger (depending on the direction of slant) in proportion to the magnitude of the stimulus number. One second following completion of the response, a 2-digit feedback number indicated the finger pressure that the subject actually produced. On a random 20% of the trials, the stimulus number was slanted in the opposite direction from the cue (not shown). On those 'catch' trials, the subject had to inhibit his finger response.

random 20% of the trials were miscued. In these 'no-response' trials, the stimulus was slanted in the direction opposite to the cue, and the subject was to withhold his response.

As feedback for response trials, a 2-digit score that indicated the response pressure to a tenth of a unit, was presented 1 sec after the peak of the response pressure. Response error was the difference between the response pressure and the stimulus number. For each hand, an adaptive error tolerance was determined as the moving average of response error for the preceding 5 response trials. If the response error was less than the error tolerance level, the feedback number was underlined to indicate a 'win' and the subject earned a bonus of about 5 cents. This was implemented to equalize task difficulty across the session and between hands, and to provide an index of current performance level for each hand. If response onset was longer than 1.5 sec the feedback 'OO' was presented. The feedback 'OK' was presented 1.5 sec after the stimulus when the subject correctly withheld his finger response on no-response trials.

If the subject incorrectly responded to a miscued (no-response) stimulus, he received the feedback 'XX' and was penalized 10 cents.

Trials were presented in blocks of 17, with the task types (right and left, response and no-response) randomly ordered, except that the first 2 trials were never 'no-response' trials. The subject initiated a block by pressing a button, and the 17 trials followed automatically at 1.5 sec intervals. After each block, a summary of the subject's average response accuracy for each hand, the number of incorrect responses, and the monetary bonus earned appeared on the monitor.

Each subject practiced the task in a pre-recording session until his performance error reached an asymptote. He then performed between 800 and 1000 trials in a recording session that lasted approximately 5 h, including short rest periods. The adaptive error tolerance, as well as post-hoc procedures described below, were used to control for learning and fatigue.

EEGs from 26 scalp electrodes referenced to the midline antero-parietal (aPz) electrode (placed halfway between Pz and Cz), vertical and horizontal eye movements (EOGs), and potentials from responding flexor digitorum muscles (EMGs) recorded with bipolar electrodes, were digitized at 128 samples/sec from 0.75 sec before the cue to 1.0 sec after feedback. Approximately 8500 trials of data were collected from the 7 subjects and were edited by 2 independent raters to remove artifacts evident on EEG, EOG, and EMG polygraph channels. Additional trials were eliminated in which the response was slow, biphasic or delayed beyond 1.25 sec, or in which there was some EMG activity in the non-responding hand or in the cue-to-stimulus epoch. No-response trials with EMG activity were also eliminated.

### Analysis

Prior to computation of event-related covariances (ERCs), analytic procedures were employed to reduce spatial blurring, to select trials with consistent event-related signals, and to control for task-irrelevant factors. First, the laplacian operator was applied to the potential distribution from

the electrodes that were not located at the periphery of the scalp. Second, a trial-selection method increased the signal-to-noise ratio of the subsequent averaged event-related potential (ERP), and accentuated differences between the pair of conditions to be compared. Third, trials with extreme behavioral values were eliminated to obtain behaviorally balanced trial sets.

Averaged ERPs were formed from these laplacian-enhanced, balanced trials, then digitally filtered and appropriately down-sampled. Analysis windows were selected to span the major ERP peaks (Fig. 2). Multitap cross-covariance functions were computed between all pairwise (by channel) combinations of the averaged ERPs in each window. The individual steps will now be presented in detail.

*Reducing volume conduction distortion using the laplacian derivation (LD)*

Potentials which arise from localized sources in the brain become considerably blurred as they are volume-conducted through the skull and scalp.

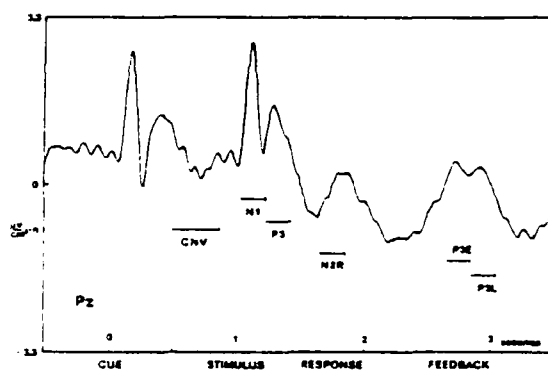


Fig. 2. A representative averaged wave form, from the midline parietal channel (Pz) of 1 subject, showing the major ERP components of this task and the corresponding event-related covariance (ERC) analysis intervals: pre-stimulus CNV, post-stimulus N1 and P3, response N2R, and feedback P3E and P3L. The response onsets of the individual trials forming the average varied, and the average was time-locked to the onset of the cue; the resulting time smear attenuated the ERP components of the response in this figure. This is also true for feedback components, since the feedback was timed to the end of the response. This was not a problem for the overall analysis, since separate response and feedback averages were computed, time-locked to their respective onsets.

Consequently, they are considerably spread by the time they reach the scalp (Rush and Driscoll 1969). In order to reduce this smearing and to remove the effect of the reference electrode, we used the LD to estimate the current source density from the scalp potential distribution. This technique compensates for the spread of potential and improves the spatial resolution of scalp-recorded signals by approximating the local spatial second derivative of the potential field at a point on the scalp. This derivative is proportional to the density of current exiting or entering the scalp at that point (Nunez 1981). (Determining the actual current would require knowledge of the local resistivities of CSF, skull, and scalp.)

Hjorth (1975, 1980) originally proposed a formulation of the LD at a particular electrode site using surround electrodes at hypothetically uniform distances and at right angles. Since inter-electrode distances can vary considerably between people, we improved the original Hjorth technique by measuring the distances between electrodes, as did Thickbroom et al. (1984), who proposed the formulation

$$f_{LD}(i) = \frac{\sum_{j \in S_i} \frac{V_j}{d_{ij}}}{\sum_{j \in S_i} \frac{1}{d_{ij}}}$$

where  $f_{LD}(i)$  is the LD of electrode  $i$ ,  $V_j$  is the voltage at electrode  $j$ ,  $d_{ij}$  is the distance between electrodes  $i$  and  $j$ , and  $S_i$  is the set of electrodes surrounding electrode  $i$ . Electrode positions were measured in 3 dimensions using a 3-D digitizer before and after each recording session (Gevins 1988). The distances  $d_{ij}$  were the ellipsoid arc lengths between pairs of electrodes. We have recently improved this technique further by using the exact angles of surround electrodes as well (Greer and Gevins in prep.).

We excluded the 10 electrodes at the periphery of the recording montage from further analysis because there was inadequate sampling of the surrounding potential at these sites. (Representation of the spatial second derivative of potential at a point depends on measurement of the change of potential in 2 orthogonal directions at the surface.)

Examination of the LD wave forms confirmed that the signal-to-noise ratios were low (poor signal representation) at these peripheral sites compared to the other sites. Sixteen non-peripheral electrodes remained: left and right frontal (F3, F4), midline frontal (Fz), left and right antero-central (aC3, aC4), midline antero-central (aCz), left and right central (C3, C4), midline central (Cz), left and right antero-parietal (aP1, aP2), midline antero-parietal (aPz), left and right parietal (P3, P4), midline parietal (Pz) and midline antero-occipital (aOz). The antero-central electrodes were halfway between the corresponding central and frontal sites, the antero-parietal electrodes were halfway between the parietal and central sites, and the antero-occipital electrodes were halfway between the occipital and parietal sites.

The peaks in LD topographies were at different locations than the ERP topographies and were more spatially localized (cf., Fig. 3A and B). In most cases, this localization was valuable in distinguishing overlapping components. The polarity of most event-related LD peaks changed across the scalp, in correspondence to sources and sinks (regions of emerging and entering 'equivalent current'). Thus, they were labeled by the standard ERP terminology (e.g., N1) according to their latency.

#### *Eliminating trials that lacked detectable event-related signals*

We developed a simple method for choosing and averaging only those trials that had detectable task-related signals (Gevins et al. 1986). Rather than selecting trials that conformed to a fixed model of the shape of the event-related signal (e.g., matched filtering or 'Weiner' filtering — see reviews in Gevins 1984; McGillem and Aunon 1987), we used a pattern classification algorithm to select trials that were statistically different from noise. Trials that could not be distinguished from noise were not included in the averaged wave forms.

A set of event-related data consisted of EEG segments from a brief time interval (125 or 250 msec), time-locked to the event of interest. This set was compared to a set of noise data, composed

of EEG segments of the same length, but randomly timed with respect to stimulus and response events. The distributions of the event-related and noise sets had, on the average, similar statistical properties. Therefore, a sophisticated mathematical pattern classification algorithm was needed to discriminate the 2 sets based on the fact that the event-related segments were non-stationary and the noise segments were stationary (Gevins and Morgan 1986).

The algorithm constructed equations that discriminated the 2 sets on a channel-by-channel basis. Averaged ERPs for each channel were formed from trials containing event-related segments that were correctly discriminated from noise. 'Selected trial sets' for each subject were formed from trials containing segments that were correctly discriminated from 'noise' in the majority of channels with significant ( $P < 0.01$ ) event-related signals.

The procedure was performed for individual subjects and channels, using low-pass filtered data (17-point linear-phase finite-impulse response, 3 dB attenuation at 7 Hz, 20 dB attenuation at 16 Hz), down-sampled from 128 to 32 Hz. Trial selection of stimulus-locked data used a 250 msec wide interval centered 375 msec after the stimulus. Trial selection of response-locked data used a 125 msec wide interval, centered on the peak of the response-related wave form for each subject. This peak latency varied from 38 to 86 msec after response onset, as measured from the finger-pressure transducer channel.

#### *Controlling for irrelevant between-condition variables*

It was important to balance the data set from 2 conditions for stimulus-, response- or performance-related variables that were different from, but unrelated to, the intended comparison. For example, it was important that the pressure of left- and right-handed responses did not differ. For each between-condition comparison for each subject, the 2 sets of event-related, signal-bearing trials were statistically balanced by eliminating trials that had outlying values of irrelevant variables (Gevins et al. 1981, 1985). This procedure involved an interactive program that displayed the



TABLE I

Numbers of original and final trials for stimulus-locked and response-locked data (averaged across 7 subjects).

	Stimulus-locked				Response-locked	
	Right-cued		Left-cued		Right-cued	Left-cued
	Response	No-response	Response	No-response		
Original trials	1345	539	1284	537	1395	1219
Final trials	790	354	717	339	1079	906

means, Student's *t* tests, and histograms of about 50 behavioral variables, such as response time, pressure, velocity, acceleration, duration and error, as well as stimulus parameters, indices of muscle activity and 'arousal' (integrated energy measured from the Pz electrode, and computed in 500 msec epochs before and after the onset of each event). Between-condition balance was achieved when the Student's *t* test for each variable of comparison had a significance of 0.2 or greater. 'Enhanced' averages of these event-related time series were then computed for each condition from the LD, signal-bearing, balanced trial sets of each subject.

For stimulus-locked wave forms, data sets of right- and left-hand responses were balanced for pressure, duration, velocity, acceleration (when possible), and error of response. Data sets of each individual subject were pruned of trials that had high reaction times ( $> 3$  S.D.s), but were not balanced between hands because of inherent hand differences. No-response (miscued) sets were balanced with the corresponding response sets (according to cued hand) by pruning no-response trials that contained outlying indices of prestimulus 'arousal.' No-response sets were then compared between hands and did not require further balancing. The numbers of trials in the original and final data sets are given in Table I.

Response-locked sets for each subject were pruned of trials with reaction times  $> 3$  S.D.s and balanced between hands for the other response variables listed above. Reaction time and EMG indices were not balanced, because of hand differences within subjects, but mean reaction time across the 7 subjects was almost the same between hands (right hand mean =  $611 \pm 136$  msec, left hand mean =  $619 \pm 137$  msec). The onset of the

EMG occurred, on the average, 60 msec before initiation of the response. The numbers of original and final trials are given in Table I.

#### Between-channel covariance measures

The prestimulus events of enhanced averages were bandpass filtered with a delta band filter (for the low-frequency contingent negative variation) and the other events were filtered with a theta band filter (Fig. 3C). Each filter was a gaussian FIR type, with no side lobes in the time response for the delta case, and 1 side lobe for the theta case. This lobe limited the time smear to the minimum possible smear for each passband and.

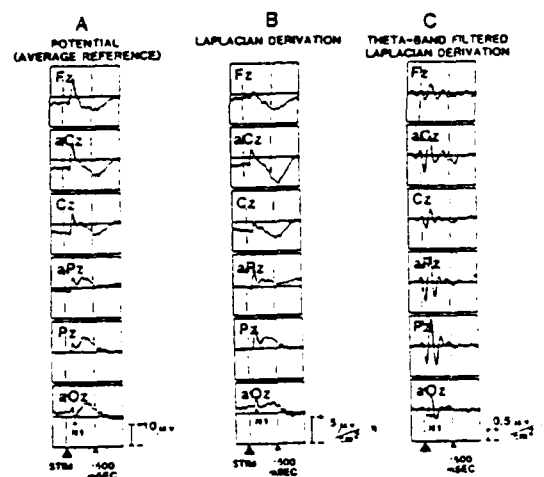


Fig. 3. A: stimulus-locked averages (of all 7 subjects;  $N = 790$ ) of potentials from midline electrode sites under right-hand response conditions. B: unfiltered laplacian derivations (LDs). C: theta band filtered LDs. Positive potential is up for A; emerging 'equivalent current' is up for B and C. The term  $\eta$  in the units for the LD indicates that for each electrode, the voltages at the neighboring electrodes were weighted by the mean of the distances to those neighbors. The post-stimulus N1 is shown for the midline antero-occipital (aOz) electrode.

in particular, ensured that analysis windows did not include major contributions from other peaks. Also, since the filters were zero phase, they did not introduce any time shifts. Nonetheless, we compared filtered and unfiltered averages to ensure that the filtering did not differentially distort the relative amplitudes and latencies of the analyzed peaks.

Multi-lag covariance functions were computed for the enhanced, filtered averages (Fig. 4). The covariance analysis interval used for computing each covariance function was the width of 1 period of the band-center frequency of each filter. Down-sampling factors were determined by the 20 dB rejection point, and covariance functions were computed up to a lag time of one-half period of the high frequency for each band. The interval length for the theta (4–7 Hz) band was 187 msec, corresponding to one period at 5.5 Hz. The theta-filtered data, originally sampled at 128 Hz, were down-sampled by 6, and the covariance function computed to 8 lags ( $\pm 62$  msec). The interval length for the delta (0.1–3 Hz) band was 375 msec, corresponding to one period at 2.5 Hz. Delta-filtered data were down-sampled by 8, and the covariance function computed to 16 lags ( $\pm 125$  msec). The covariance measure was defined as the maximum absolute value of the covariance function, and the time delay as the lag time of that maximum. (Note that the covariance is not normalized by signal strength and is therefore sensitive to the amplitude, as well as to the shape, of time series from the 2 channels.)

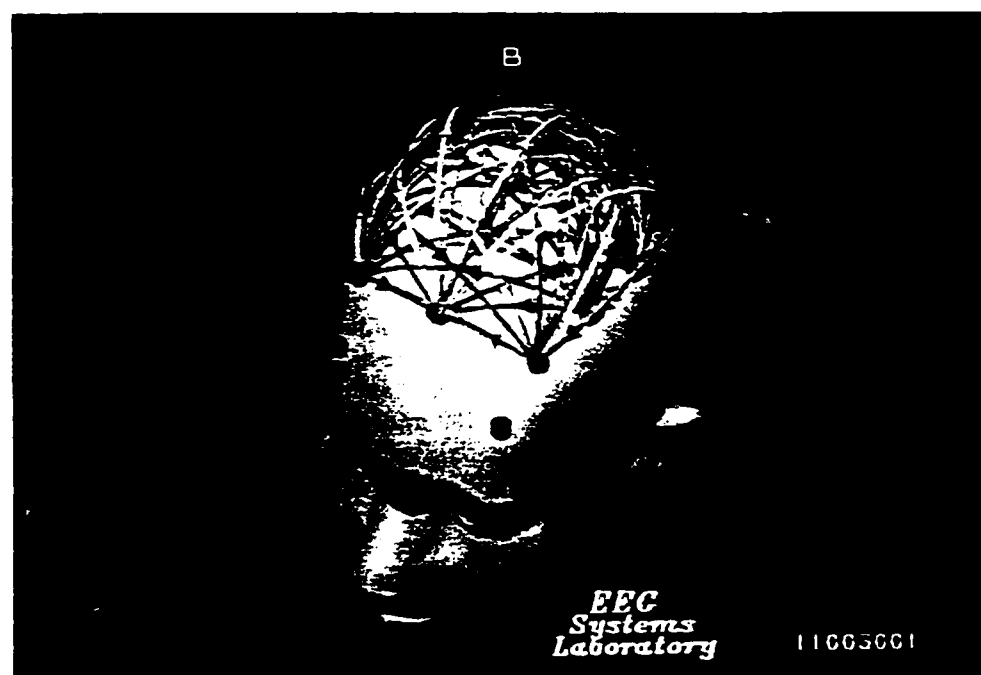
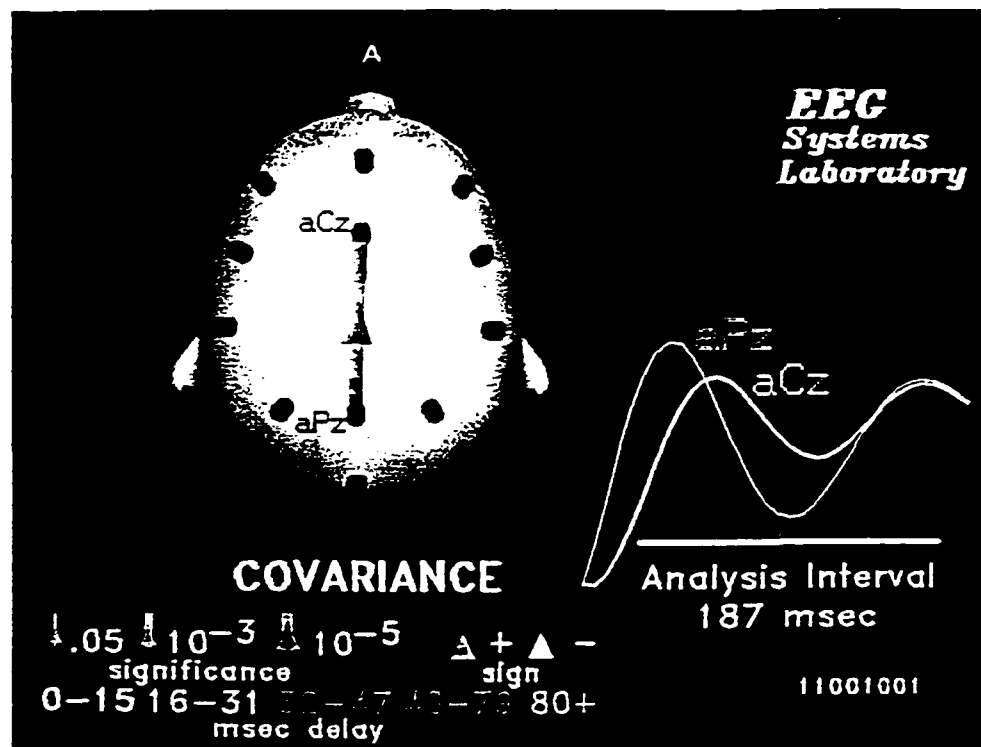
Covariance measures were converted to significance scores (after square root transformation was

used to approximately normalize the signal-squared covariance distribution) by comparing them with the noise median and with Tukey's biweight estimate of noise variance (Iglewicz 1983). Tukey's biweight estimate was computed from sample distributions of zero-lag covariances between intervals centered around data points with a minimum energy envelope. For  $N$  data points, the covariances have  $N - 1$  degrees of freedom. Thus the theta band covariances were computed from 5 down-sampled time points, and had 4 degrees of freedom. Despite this low value, significances frequently reached  $P < 0.00001$ . Adjustment for multiple comparisons within an interval (120 pairings of 16 non-peripheral channels) was done by a Duncan procedure, in which the number of channels was taken as a conservative approximation of the number of independent covariance pairs.

To test the mean difference between the ERC patterns under 2 conditions, the Student's  $t$  test was applied to the distributions of all significant ERCs for each condition. Similarity between 2 ERC patterns, irrespective of the magnitudes of the ERCs, was measured with an estimate of the correlation, and its confidence interval was produced by the distribution-independent 'bootstrap' Monte Carlo procedure (Efron 1982). This generated an ensemble of correlation values, each computed for a sample of the ERC distribution formed by random selection with replacement.

To show the most prominent results, all significant ERCs within 1 S.D. from the maximum value in that interval were displayed (Fig. 4). Diagrams of ERCs within 2 S.D.s were also examined for additional information. Both time series contrib-

Fig. 4. A: schematic diagram on a top view of a model head, showing the relationship of an ERC line (left) to the ERP wave forms from the 2 corresponding electrode sites (right). The ERC was computed over the indicated 187 msec analysis interval from the theta band-filtered, averaged, response-locked LD ERP segments. In the ERC diagram, the width of a line connecting 2 sites indicates the significance of the covariance between the ERP wave forms from those sites, with the scale appearing above the word 'significance.' The color of the line indicates the time delay in msec (lag time of maximum ERC) as shown in the scale above 'msec delay.' The color of the arrow indicates the sign of the ERC (same color as line = positive; tan = negative). The arrow points from the leading to the lagging channel, unless there is no delay, in which case a bar is shown. The ERC between aPz and aCz is significant at  $P < 10^{-5}$ . The aPz wave form leads the aCz wave form by about 16–31 msec (green line), and the ERC is positive (arrow also green). B: schematic diagram showing all possible ERC lines between pairs of the 16 non-peripheral electrode sites. All 26 electrode sites are indicated as red disks, but computation of an adequate estimate of the LD was not actually possible at the 10 peripheral sites. Since a ring of peripheral electrodes must be expended in order to estimate the LD at the interior sites, there are still large unrecorded scalp areas even when recordings are made with 26 electrodes.



uting to each significant ERC were examined to ensure that the ERC was due to the primary ERP component, and not to any interactions resulting from the unavoidable time smear caused by narrow-band filtering (Fig. 3C). The most prominent electrode site was the one that covaried significantly with the most other sites. Other prominent sites covaried with more than one-half the number of sites of the most prominent site.

## Results

### Stimulus-locked wave forms

The unfiltered LD response and no-response wave forms, averaged over all 7 subjects, contained peaks at different sites; these peaks corresponded to N1 at 130–140 msec and P2 at 230–240 msec (Fig. 5). The entering current, corresponding to N1, was greatest at the lateral parietal sites (not shown). There were 2 sites of maximal exiting current: the midline antero-central and midline antero-parietal sites, corresponding to the anterior and posterior fall-off of the potential field. It is likely that N1 at the anterior sites involved resolution of the contingent negative variation (CNV; Tecce 1972).

Right- and left-hand response wave forms contained a P3 wave, approximately 250 msec wide, centered near 350 msec, with maximal emerging current at Pz (Fig. 5, left). The infrequent no-response wave forms had a much larger P3 wave, with maximal emerging current at aCz (Fig. 5, right). The response P3 wave had the posterior maximum characteristic of the task-relevant 'P300' peak reported in the literature (e.g., Squires et al. 1977). The no-response P3 had the larger amplitude characteristic of the probability-sensitive 'P300,' and the anterior maximum characteristic of the 'no-go' P3a (Squires et al. 1975).

In response wave forms, a slow shift corresponding to response preparation began after P2, and peaked at about 600 msec (Fig. 5, left). Entering current was largest at aCz, with larger amplitude at central sites contralateral to the responding hand (not shown). (For the right response, the amplitude of C3 was approximately 9 times greater than the amplitude of C4; for the left response,

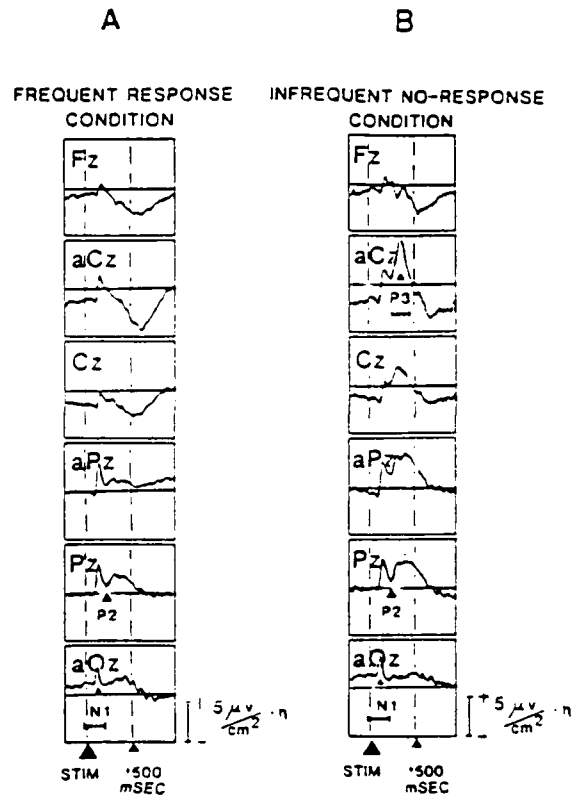


Fig. 5. Right-hand response (A,  $N = 790$ ) and right-hand no-response (B,  $N = 354$ ) averaged, unfiltered, 7-subject, stimulus-locked, LD wave forms from midline electrode sites. The N1 peak and corresponding ERC analysis interval are shown for the aOz electrode, the P2 peak is shown for the Pz electrode, and the P3 peak and interval are shown for the aCz (midline antero-central) electrode. The difference between conditions is highlighted by the large P3 peak (maximal at aCz) in the infrequent no-response condition. Emerging 'equivalent current' up.

the amplitude of C4 was about 2.5 times greater than the amplitude of C3.) In no-response trials, a broad 'slow wave' peaked at 550 msec at Fz and 700 msec at aCz, then extended past 1 sec (Fig. 5, right). The slow wave had large entering current at midline central and frontal sites (maximal at aCz), but was small elsewhere.

Theta filtering emphasized the early peaks, including the no-response anterior P3 wave, and eliminated the slower response preparation and slow wave components. It also resolved the wide posterior P3 wave into 2 theta band peaks.

### Stimulus-locked ERCs

ERCs were computed for the theta band-filtered data in a series of 187 msec wide intervals centered before and after the stimulus. ERC patterns were highly consistent over the early intervals, reflecting the high degree of synchrony of the filtered N1 and P2 peaks. In a representative interval centered 62 msec after the stimulus (Fig. 6), there was a common pattern for both the right and left response stimulus conditions at the threshold of 1 S.D. It consisted of ERCs of the midline antero-parietal site with midline parietal and antero-central sites. In these early intervals, the right-slanted stimulus patterns, but not the left, also involved the right parietal site (P4). At 2 S.D.s from the maximum ERC, however, the left stimulus patterns included both P3 and P4, whereas the right stimulus patterns included P4 and aC3, but not P3. In these early intervals, the patterns for response and no-response conditions were also the same.

In order to test the significance of the between-condition difference observed in the patterns of Fig. 6, we used the Student's *t* test to compare the distributions of all the significant ERCs ( $P < 0.05$ ) of the right and left stimulus patterns. The distributions of right and left stimulus ERC patterns were significantly different at  $P < 0.05$  ( $t = 2.1$ ,  $df = 238$ ). The bootstrap correlation was  $0.86 \pm 0.02$ . Thus, although the distributions were significantly different in overall scale, they had a similar underlying pattern.

The ERC patterns of response and no-response trials diverged by the interval centered at 281 msec (not shown). As characterized by the 312 msec centered pattern (Fig. 7, right), the Pz site was prominent in the response patterns and had significant ERCs with right parietal and antero-parietal, midline and left antero-central and right frontal sites. The midline antero-central site was prominent in the no-response patterns and covaried with Pz, F3, Fz, and aC4 (Fig. 7, left). The aCz-Fz ERC, with aCz leading by 48–79 msec, was particularly characteristic of the no-response patterns during the intervals from 281 to 375 msec. The difference between the distributions of all significant ERCs ( $P < 0.05$ ) that corresponded to the response and no-response patterns observed

in Fig. 7 was highly significant at  $P < 0.001$  ( $t = 11.3$ ,  $df = 238$ ). The bootstrap correlation was  $0.50 \pm 0.02$ . Therefore, the scale difference between the response and no-response distributions was highly significant, but they had some common ERCs.

The response patterns underwent another change at the 375 msec centered interval, as the intervals approached the onset of the response. The patterns became more complex, with more ERCs involving more electrode sites. By the 500 msec interval, the right- and left-hand response patterns involved the same sites, with prominent involvement of aCz. The no-response patterns did not undergo any major changes from the 281 to 500 msec centered intervals except that they diminished in complexity. By 500 msec, the only significant no-response ERC (at either the 1 or 2 S.D. thresholds) was aCz-Fz, with aCz leading by 48–79 msec for both hands.

### Response-locked wave forms

The unfiltered LD wave forms (Fig. 8) contained a slowly increasing shift that corresponded to the readiness potential (RP). It was maximal before the onset of the response and was characterized by an increase in slope that peaked 62 msec after the response began ('N2R'), and by a component that peaked 187 msec after the response began ('P2R'). The N2R peak was localized to only a few midline sites, and to sites contralateral to the responding hand. Current sinks were anterior (maximum at aCz). Current sources were posterior: the only sources were C3, aP1 and P3 for the right hand, and the homologous right-hemisphere sites for the left hand.

Left- and right-hemisphere maxima were at aP1 and aP2, respectively; therefore, there was an anterior-posterior inversion of polarity, but no inversion along the midline.

The P2R component was present at only a few electrode sites: it was absent at aCz, where the RP and N2R were strongest. For the right-hand response, the maximum current sink was at C3, and principal sources were at Cz and F3. For the left-hand response, the maximum sink was at C4; the sources were at Cz, F4, and aC4. Theta band filtering removed the RP and enhanced N2R and P2R.

*Response-locked ERCs*

ERCs were computed for a series of 187 msec wide intervals centered on the theta band-filtered,

response-locked averaged LD wave form before and after onset of the response. In the interval centered 187 msec before the response, the ERC

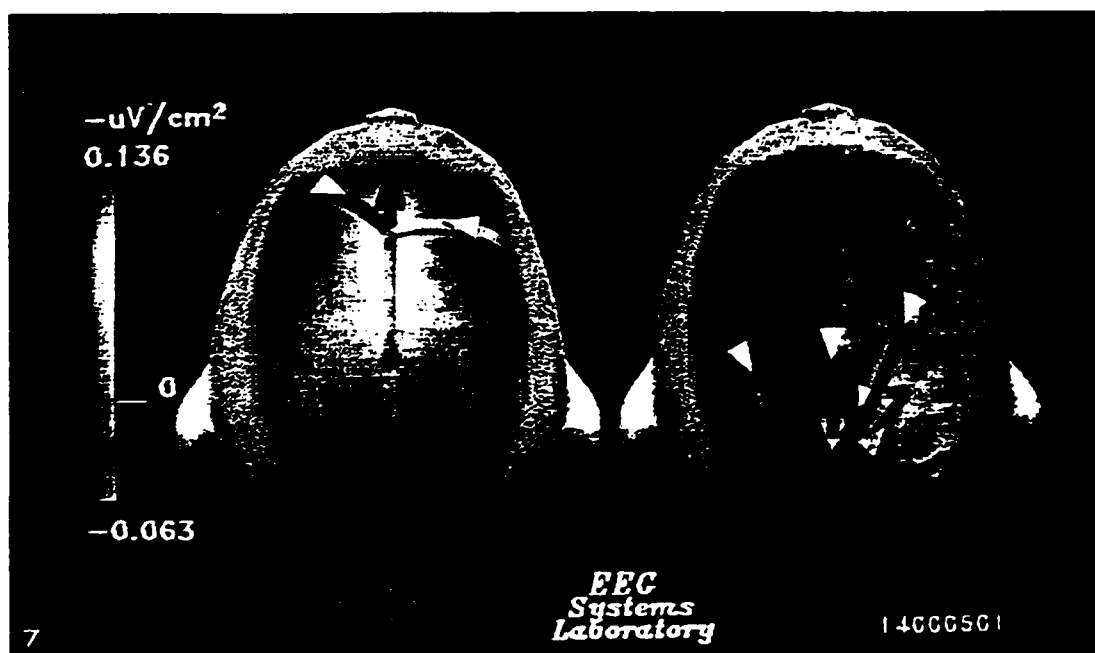
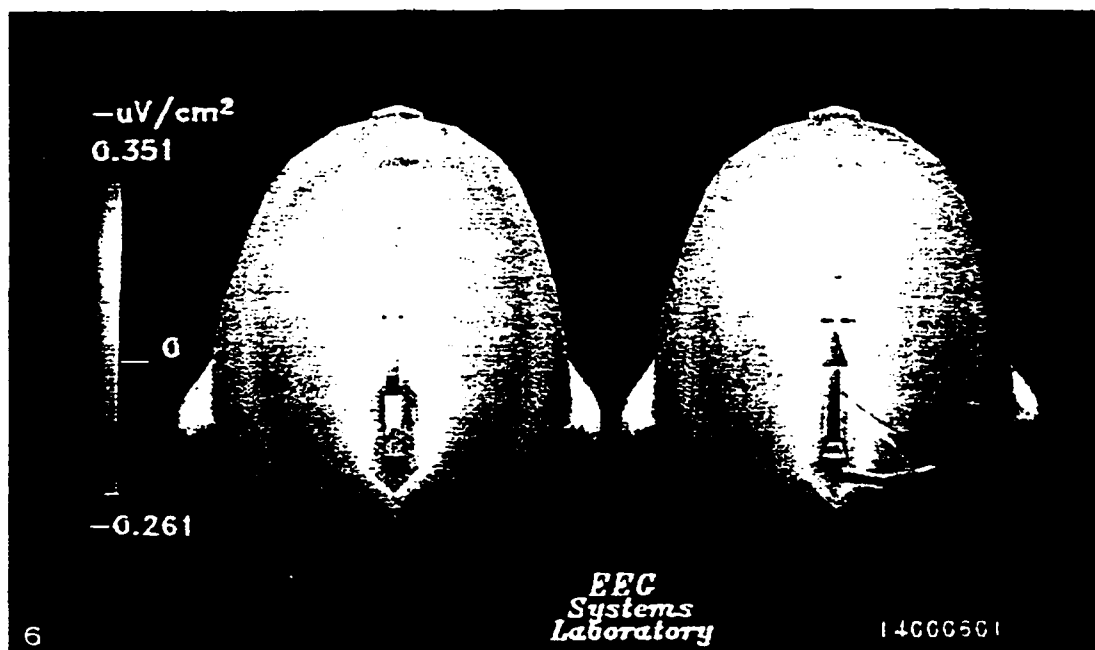


Fig. 6. View of the most significant (within 1 S.D. of largest value) ERCs from the stimulus-locked, LD N1 wave of the response condition, superimposed on colored maps of N1 wave amplitude. ERCs were measured during a 187 msec wide interval, centered 62 msec after left (left) and right (right) stimulus onset, from the theta band-filtered averages over all 7 subjects. The ERC diagram conforms to the significance, sign, and delay scales of Fig. 4A. The color scale at the left, representing wave amplitude, covers the range from the minimal to maximal values of the 2 maps. For both left- and right-handed conditions, there is a maximum of wave amplitude occipitally and a minimum at the midline antero-central (aCz) site. Common ERCs for both left- and right-hand conditions exist between midline parietal (Pz) and antero-parietal (aPz), and between midline antero-parietal and antero-central sites. Additional ERCs for the right-hand condition, involving the right parietal (P4) site, reflect the lateralization of the N1 peak at parietal sites.

Fig. 7. View of the most significant (top standard deviation) P3 ERC patterns superimposed on colored maps of integrated P3 amplitude. Measurements were made from theta band-filtered averages over all 7 subjects, during an interval 218–405 msec after onset of the right-cue stimulus, for pressure response (right) and no-response (left) conditions. The midline parietal site is prominent in the pattern for the response condition, and the midline antero-central site is prominent in the infrequent no-response condition. Pz lags most other sites in the response condition, while aCz lags in the no-response condition.

#### INDEX FINGER PRESSURE

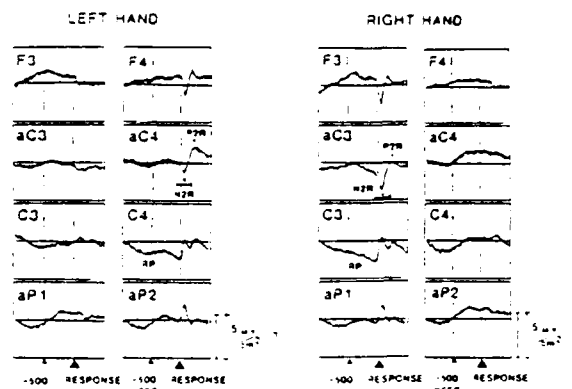


Fig. 3. Response-locked, unfiltered, LD wave forms of lateral electrode sites for left- and right-hand index finger responses. The RP (readiness potential), 'N2R' and 'P2R' components are indicated, as is the N2R ERC interval. Note the reversals of polarity in N2R and P2R between C3 and aC3 (right hand), and between C4 and aC4 (left hand). Emerging 'equivalent current' up.



Fig. 9. View of the most significant (top standard deviation) ERCs from the N2R wave superimposed on colored maps of the amplitude of that wave for left- (left,  $N = 906$ ) and right-hand (right,  $N = 1079$ ) index finger responses. N2R ERCs were measured during a 187 msec interval centered on the peak of left-hand and right-hand index finger pressures from theta band-filtered averages over all 7 subjects. The ERC diagram conforms to the significance, sign, and delay scales of Fig. 4A. The maximal wave amplitude is at lateralized central (C4 and C3) and antero-parietal (aP4 and aP3) sites, while the minimal amplitude is at the midline antero-central (aCz) site. Note that the aCz site is involved in all ERCs in this interval. The patterns are distinctly lateralized according to responding hand. The sign of ERCs involving aCz is positive for lateral frontal sites, and negative for lateral central and antero-parietal sites. Note the 16–31 msec lag between aCz and Fz.

patterns were weak and did not differ appreciably between hands. The ERC patterns became strong and contralateral to the responding hand beginning with the interval centered at the response onset.

Right- and left-hand patterns within the threshold of 1 S.D. were nearly mirror images in the N2R interval (Fig. 9), centered 62 msec after response onset. The aCz site was involved in all ERCs in both patterns. This site covaried with short delay (0–15 msec) with the antero-parietal, central and frontal sites contralateral to the responding hand (and with the left antero-central site for the right-hand pattern), and with the midline central site. Additionally, aCz led Fz by 16–31 msec. The ERCs of aCz with aP1 and C3 for the right hand, and with aP2 and C4 for the left, were negative. ERCs were positive for aCz with aC3 and F3 for the right hand, and with F3 for the left. Additional ERCs, which were included at the 2 S.D. threshold, were all contralateral to the responding hand. The only other sites involved were P3 for the right-hand pattern, and P4 and aC4 for the left. Right- and left-hand patterns in the interval centered at 187 msec, at both 1 and 2 S.D.s, involved the same sites as in the 62 msec centered interval. The lags increased from the 0–31 msec to the 16–47 msec range.

The distributions of all significant response-related ERCs during the 62 msec centered interval differed significantly between right and left hands at  $P < 0.02$  ( $t = 2.6$ ,  $df = 192$ ). The bootstrap correlation was  $0.06 \pm 0.12$ . Thus, not only were the distributions significantly different from each other, they were also uncorrelated.

## Discussion

This study suggests that the method of event-related covariance (ERC) can measure signs of the dynamic functional cortical networks underlying goal-directed behaviors at the scalp. Indeed, the distinct, rapidly changing spatial patterns of wave form synchronization seen in event-related covariance maps correspond to clinical neuropsychological models of a simple numerical judgment task that requires visual stimulus processing followed by response execution. Furthermore, having found

specific task-related time differences between wave forms within a given analysis interval, we suggest that functional cortical networks may be characterized by the time relations of activity at their nodes. While the ERC patterns suggest functional co-involvement of underlying cortical regions, we must reiterate that the actual generators are in fact unknown, and further studies will be needed to determine what they are. With this caveat in mind, we present a discussion of the functional neuro-anatomical implications of the results.

### *Response-related ERPs and ERCs*

Since ERC patterns for the robust N2R and P2R components of response-related wave forms were simple and clear cut, they will be discussed first. There were several main findings. First, the midline antero-central electrode site (aCz), overlying premotor and supplementary motor cortices thought to be involved in planning and execution of precise finger control (Ingvar and Philipson 1977; Foit et al. 1980; Roland et al. 1982), was central to all response-related patterns. Second, response-related ERC patterns reflected an inversion of polarity in the filtered LD wave forms between the lateralized central and the lateralized antero-central and/or frontal sites. The polarity reversal, possibly extending across the central sulcus, may reflect a single dipole source generator in the finger region of the motor cortex. However, if this were the case, the 2 poles of the generator would be highly covariant, that is, there would be high covariance between lateral, antero-central, and central sites. Since this was not so, we favor the interpretation that there are 2 closely spaced generators, 1 motor (antero-central) and 1 somesthetic (post-central). Third, midline ERCs of the antero-central site with the frontal and central sites were response features common to both hands. The ERC between the antero-central and central sites had a short-lag delay and may reflect volume-conducted activity from a single generator. The longer-lag delay (16–31 msec) between the antero-central and frontal sites suggests the presence of 2 distinct generators, although additional studies are required to rule out a 'rotating' single generator as the source of the covariance (Fender 1987).



The findings reported here thus support the conclusion that during the N2R and P2R components of a voluntary, skilled, ballistic finger response, there are at least 4 primary cortical generators: one midline in premotor and/or supplementary motor cortices; another midline in prefrontal cortex; a third in the hand region of motor cortex contralateral to the responding hand; and a fourth in the contralateral hand region of the somesthetic cortex. These areas are the same as those determined by studies of direct cortical recordings of motor potentials in humans and monkeys (Arezzo and Vaughan 1975; Pieper et al. 1980), although prefrontal involvement was absent in monkeys.

#### *Stimulus-related ERPs and ERCs*

The stimulus-related patterns displayed several characteristic features. For example, the patterns of intervals within the first 250 msec differed according to the slant of the stimulus. There were short-delay ERCs involving the midline antero-parietal site, midline antero-central site, and midline parietal site in the patterns of all the conditions. This suggests that perceptual processing in parietal areas was coordinated with motor initiation control in supplementary motor and/or premotor areas that had been 'primed' for response by the cue.

The right parietal site was a salient feature of the ERC patterns for the right-slanted stimulus, regardless of cue. For the left-slanted stimulus, there was weak involvement of both the right and left parietal sites (both of which were only evident at the 2 S.D. threshold). Therefore, the right parietal site was involved regardless of the stimulus and was stronger when the stimulus was slanted to the right. The left parietal site was involved when the stimulus was slanted to the left. The appearance of the right parietal site in patterns for both right and left hands may reflect the importance of that region for humans performing attentional tasks (Mesulam 1981). Our result may be compared with the finding of Heilman and Van den Abell (1980) that the right parietal lobe is focally activated by stimuli projected into either visual field, whereas the left is only activated by stimuli projected into the right field. The fact that

the component that changed hemisphere in our ERC patterns was ipsilateral, rather than contralateral to the stimulus direction, may be explained by a contralaterally activated, but obliquely oriented generator that projects its field ipsilateral to the slant of the stimulus. Even though the stimulus subtended only a small visual angle, its tilt into one-half of the visual field may have evoked an obliquely oriented generator population, possibly buried in the parieto-occipital sulcus. Such a 'paradoxical' ipsilateral posterior peak of potential in response to foveal visual stimulation has been reported by Barrett et al. (1976).

The ERC patterns began to differ according to the type of response after the early intervals, while differences related to the physical characteristics of the stimulus disappeared. By the interval centered at 312 msec after the stimulus, which spanned the P3 wave, the ERC patterns clearly differed according to the subjective interpretation of the stimulus, rather than to the stimulus per se. The difference between the anterior (aCz) concentration of ERCs in the no-response condition, and the posterior (Pz) concentration in the response condition, is consistent with other studies of go/no-go tasks (see summary in Tueting 1978).

There has been considerable interest in the neural substrates of the P3 component, with evidence of widespread cortical and subcortical sources (Halgren et al. 1980; Wood et al. 1980; Okada 1983; Glover et al. 1986; Velasco et al. 1986). The complex pattern of covariance and delay for the P3 wave in the infrequent no-response condition suggests that more than one source is responsible for its generation. In particular, the long-lag delays (48–79 msec) of the midline antero-central with the midline and left frontal sites, as well as the concurrent short delays (< 31 msec) of the midline antero-central with right antero-central and midline parietal sites, are difficult to reconcile with the notion of a single generator.

The ERC between Fz and aCz was prominent in later intervals of both response and no-response stimulus-locked patterns. Examination of the filtered wave forms showed that aCz and Fz changed shape in the period from 375 to 500 msec post stimulus, so that the aCz site led Fz with

short delay in the response condition and with long delay in the no-response condition. This apparent condition-dependent adjustment in the timing of the wave forms, along with the significance of their ERC, suggests that the relation of these 2 sites is an important sign of the subjective decision to execute or withhold the finger press. Since aCz was a prominent site in all response patterns, its short-delay timing relation to Fz may reflect a higher order cognitive control process for the initiation of response. The midline frontal electrode site overlies the prefrontal cortex, which is known to be involved in the temporal organization of behavior (Ingvar 1985; Stuss and Benson 1986).

#### *ERC method: advances, remaining issues*

The methods presented here represent a significant advance over those of our previous studies (Gevins et al. 1981, 1983, 1985), in that we have now found task-specific scalp patterns of mass neural integration that conform to a priori predictions based on the presumed function of underlying cortical areas. It is unlikely that volume conduction blurring played a significant role in the resulting scalp ERC patterns. First, the LD greatly reduced the effect of blurring from the spatial spread of potential. Second, because we considered only the most significant ERCs, we reduced any global effects due to potential spread. Third, although volume conduction cannot be ruled out as the basis for ERCs between neighboring sites, ERCs due to volume conduction would tend to be greatest for nearby sites and would decrease uniformly with distance in all directions. Volume-conduction blurring is not considered to be a major factor in determining the ERC patterns since the patterns presented here were highly localized and involved ERCs between sites with non-covarying intervening sites.

Although we cannot rule out subcortical sources, the same reasoning makes it seem unlikely that they are directly responsible for the ERC patterns. Subcortical sources would tend to produce diffuse scalp patterns in which all intervening sites covaried. We should emphasize, however, that even if all the sources of the scalp ERC patterns are cortical, the ERCs do not necessarily result from direct communication between cortical

regions. There are numerous pathways, involving subcortical and other cortical structures, that could account for the measurement of similar wave forms from any 2 cortical regions.

Determination of the actual sources of these ERC patterns awaits further studies using combined electrical, magnetic, and radiological data, as well as intracerebral data from human patients and non-human primates. Since these studies may require a separate analysis of each subject, we are concerned with the issue of inter-subject variability. The variability of ERC patterns between subjects for the pre-stimulus interval of the present experiment has been discussed elsewhere (Gevins et al. 1987) and will be summarized in part II. We are currently investigating the inter-subject variability of the other events (Gevins et al. in prep.).

The measurement of event-related covariances is currently the only practical means of identifying narrow-band, fraction-of-a-second patterns of wave shape similarity and timing differences between event-related signals recorded from different scalp sites. Measurements of spectral coherence, as are conventionally estimated from smoothed periodograms or autoregressive models, have not yet achieved a similar degree of temporal and frequency resolution (reviewed in Gersch 1987). Likewise, measures of mutual information, used to estimate the degree of relatedness between 2 averaged event-related time series (Mars and Lopes da Silva 1987), require a substantially longer data segment. By definition, topographic maps of potential or metabolic activity do not show this type of information.

#### **Conclusion**

Our findings suggest that a network model, 'connectionist,' approach to human brain function is feasible. There are indications, from the stimulus-locked ERC intervals, for example, that cortical processing of the meaning of the stimulus evolves into processing the choice of response at approximately 300 msec post stimulus. This finding is consistent with models of cortical information processing (John and Schwartz 1978) that distinguish between early exogenous and later en-

ogenous processes. The response-related ERC patterns agree with multi-component neurophysiological and radiological models of the cortical activity that accompanies voluntary responses (Roland et al. 1982; Deecke et al. 1985). Taken together, the results presented here clearly suggest that intelligible signs of task-specific coordination are available from the distributed mass neural processes of the brain (Freeman 1975, 1987). In part II of this report, we present the application of the ERC method to higher cognitive functions.

This research was supported by The Air Force Office of Scientific Research, The National Science Foundation, The National Institutes of Neurological and Communicative Disorders and Strokes, and The Office of Naval Research.

Thanks to Drs. Marta Kutas, Robert Knight, Walton Roth and Ray Johnson for critical review of the manuscript, to Jhaine Salzman and Daniel Orzech for technical assistance, and to Kns Dean, Jeanne Toal, and Judith Gumbiner for manuscript preparation. In addition to some of the authors, computer programming and other scientific and engineering support was performed by Dr. Joseph Doyle, Mr. Robert Tannehill and Mr. Gerald Zeitlin.

## References

- Adey, W.R., Walter, D.O. and Hendrix, C.E. Computer techniques in correlation and spectral analysis of cerebral slow waves during discriminative behavior. *Exp. Neurol.*, 1961, 3: 501-524.
- Arezzo, J. and Vaughan, H.G. Cortical potentials associated with voluntary movements in the monkey. *Brain Res.*, 1975, 88: 99-104.
- Barrett, G., Blumhardt, L., Halliday, A., Halliday, E. and Kniss, A. A paradox in the lateralization of the visual evoked response. *Nature*, 1976, 261: 253-255.
- Bressler, S.L. Relation of olfactory bulb and cortex. I. Spatial variation of bulbo-cortical interdependence. *Brain Res.*, 1987, 409: 285-293.
- Callaway, E. and Harris, P.R. Coupling between cortical potentials from different areas. *Science*, 1974, 183: 873-875.
- Deecke, L., Kornhuber, H.H., Lang, W., Lang, M. and Schreiber, H. Timing function of the frontal cortex in sequential motor and learning tasks. *Hum. Neurobiol.*, 1985, 4: 143-154.
- Doyle, J., Ornstein, R. and Galin, D. Lateral specialization of cognitive mode. II. EEG frequency analysis. *Psychophysiology*, 1974, 11: 567-578.
- Dumenko, V. Electroencephalographic investigation of cortical relationships in dogs during formation of a conditioned reflex stereotype. In: V. Rusinov (Ed.), *Electrophysiology of the Central Nervous System*. Plenum, New York, 1970: 107-117.
- Efremova, T.M. and Trush, V.D. Power spectra of cortical electric activity in the rabbit in relation to conditioned reflexes. *Acta Neurobiol. Exp. (Warsz.)*, 1973, 33: 743-755.
- Efron, B. *The Jackknife, The Bootstrap, and Other Resampling Plans*. Society for Industrial and Applied Mathematics, Philadelphia, PA, 1982.
- Elul, R. The genesis of the EEG. *Int. Rev. Neurobiol.*, 1972, 15: 227-272.
- Fender, D.H. Source localization of brain electrical activity. In: A.S. Gevins and A. Rémond (Eds.), *Methods of Analysis of Brain Electrical and Magnetic Signals. Handbook of Electroencephalography and Clinical Neurophysiology*, Vol. 1. Elsevier, Amsterdam, 1987: 355-403.
- Foit, A., Larsen, B., Hattori, S., Skinhøj, E. and Lassen, N.A. Cortical activation during somatosensory stimulation and voluntary movement in man: a regional cerebral blood flow study. *Electroenceph. clin. Neurophysiol.*, 1980, 50: 426-436.
- Freeman, W.J. *Mass Action in the Nervous System*. Academic Press, New York, 1975.
- Freeman, W.J. Analytic techniques used in the search for the physiological basis of the EEG. In: A.S. Gevins and A. Rémond (Eds.), *Methods of Analysis of Brain Electrical and Magnetic Signals. Handbook of Electroencephalography and Clinical Neurophysiology*, Vol. 1. Elsevier, Amsterdam, 1987: 583-664.
- Freeman, W.J. and Skarda, C.A. Spatial EEG patterns, nonlinear dynamics and perception: the neo-sherringtonian view. *Brain Res. Rev.*, 1985, 10: 147-175.
- Gersch, W. Non-stationary multichannel time series analysis. In: A.S. Gevins and A. Rémond (Eds.), *Methods of Analysis of Brain Electrical and Magnetic Signals. Handbook of Electroencephalography and Clinical Neurophysiology*, Vol. 1. Elsevier, Amsterdam, 1987: 261-296.
- Gevins, A.S. Analysis of the electromagnetic signals of the human brain: milestones, obstacles and goals. *IEEE Trans. Biomed. Eng.*, 1984, BME-31: 833-850.
- Gevins, A.S. Correlation analysis. In: A.S. Gevins and A. Rémond (Eds.), *Methods of Analysis of Brain Electrical and Magnetic Signals. Handbook of Electroencephalography and Clinical Neurophysiology*, Vol. 1. Elsevier, Amsterdam, 1987: 171-193.
- Gevins, A.S. Analysis of multiple lead data. In: J. Rohrbaugh, R. Johnson and R. Parasuraman (Eds.), *Event Related Potentials of the Brain*. Oxford University Press, New York, 1988: in press.
- Gevins, A.S. and Bressler, S.L. Functional topography of the human brain. In: G. Pfurtscheller and F. Lopes da Silva (Eds.), *Functional Brain Imaging*. Hans Huber, Bern, 1988: 99-116.
- Gevins, A.S. and Morgan, N.H. Classifier-directed signal processing in brain research. *IEEE Trans. Biomed. Eng.*, 1986, BME-33: 1054-1068.
- Gevins, A.S., Zeitlin, G.M., Yingling, C., Doyle, J., Dedon, M., Henderson, J., Schaffer, R., Roumasset, J. and Yeager, C. EEG patterns during 'cognitive' tasks. I. Methodology and analysis of complex behaviors. *Electroenceph. clin. Neurophysiol.*, 1979a, 47: 693-703.

- Gevins, A.S., Zeitlin, G., Doyle, J., Schaffer, R. and Callaway, E. EEG patterns during 'cognitive' tasks. II. Analysis of controlled tasks. *Electroenceph. clin. Neurophysiol.*, 1979b, 47: 704-710.
- Gevins, A.S., Zeitlin, G.M., Doyle, J.C., Schaffer, R.E., Yingling, C.D., Yeager, C.L. and Callaway, E. EEG correlates of higher cortical functions. *Science*, 1979c, 203: 665-668.
- Gevins, A.S., Doyle, J., Cutullo, B., Schaffer, R., Tannehill, R., Ghannam, J., Gilcrease, V. and Yeager, C. Electrical potentials in human brain during cognition: new method reveals dynamic patterns of correlation of human brain electrical potentials during cognition. *Science*, 1981, 213: 918-922.
- Gevins, A.S., Schaffer, R.E., Doyle, J.C., Cutullo, B.A., Tannehill, R.S. and Bressler, S.L. Shadows of thought: shifting lateralization of human brain electrical patterns during brief visuomotor task. *Science*, 1983, 220: 97-99.
- Gevins, A.S., Doyle, J.C., Cutullo, B.A., Schaffer, R.E., Tannehill, R.S., Bressler, S.L. and Zeitlin, G. Neurocognitive pattern analysis of a visuomotor task: low-frequency evoked correlations. *Psychophysiology*, 1985, 22: 32-43.
- Gevins, A.S., Morgan, N., Bressler, S., Doyle, J. and Cutullo, B. Improved event-related potential estimation using statistical pattern classification. *Electroenceph. clin. Neurophysiol.*, 1986, 64: 177-186.
- Gevins, A.S., Morgan, N.H., Bressler, S.L., Cutullo, B.A., White, R.M., Illes, J., Greer, D.S., Doyle, J.C. and Zeitlin, G.M. Human neuroelectric patterns predict performance accuracy. *Science*, 1987, 235: 580-585.
- Gevins, A.S., Cutullo, B.A., Bressler, S.L., Morgan, N.H., White, R.M., Illes, J. and Greer, D.S. Event-related covariances during a bimanual visuomotor task. II. Preparation and feedback. *Electroenceph. clin. Neurophysiol.*, 1989, 74(2): in press.
- Gevins, A.S., Cutullo, B.A., Bressler, S.L., Morgan, N.H., White, R.M., Illes, J. and Greer, D.S. Event-related covariances during a bimanual visuomotor task: individual differences. In prep.
- Glover, A.A., Onofri, M.C., Ghilardi, M.F. and Bodis-Wollner, I. P300-like potentials in the normal monkey using classical conditioning and an auditory 'oddball' paradigm. *Electroenceph. clin. Neurophysiol.*, 1986, 65: 231-235.
- Greer, D.S. and Gevins, A.S. Spatial deblurring of scalp recorded brain potentials using an optimal Laplacian operator. In prep.
- Halgren, E., Squires, N., Wilson, C., Rohrbaugh, J., Babb, T. and Crandall, P. Endogenous potentials generated in the human hippocampal formation and amygdala by unexpected events. *Science*, 1980, 210: 803-805.
- Heilman, K.M. and Van den Abell, T. Right hemisphere dominance for attention: the mechanism underlying hemispheric asymmetries of inattention (neglect). *Neurology*, 1980, 30: 327-330.
- Hjorth, B. An on-line transformation of EEG scalp potentials into orthogonal source derivations. *Electroenceph. clin. Neurophysiol.*, 1975, 39: 526-530.
- Hjorth, B. Source derivation simplifies topographical EEG interpretation. *Am. J. EEG Technol.*, 1980, 20: 121-132.
- Iglewicz, B. Robust scale estimators and confidence intervals for location. In: D.C. Hoaglin, F. Mosteller and J.W. Tukey (Eds.), *Understanding Robust and Exploratory Data Analysis*. Wiley, New York, 1983: 404-429.
- Ingvar, D.H. 'Memory of the future': an essay on the temporal organization of conscious awareness. *Hum. Neurobiol.*, 1985, 4: 127-136.
- Ingvar, D.H. and Philipson, L. Distribution of cerebral blood flow in the dominant hemisphere during motor ideation and motor performance. *Ann. Neurol.*, 1977, 2: 230-237.
- Ishihara, T. and Yoshi, N. Multivariate analytic study of EEG and mental activity in juvenile delinquents. *Electroenceph. clin. Neurophysiol.*, 1972, 33: 71-80.
- John, E.R. *Mechanisms of Memory*. Academic Press, New York, 1967.
- John, E.R. and Schwartz, E.L. The neurophysiology of information processing and cognition. *Ann. Rev. Psychol.*, 1978, 29: 1-29.
- John, E.R., Bartlett, F., Shimokaochi, M. and Kleinman, D. Neural readout from memory. *J. Neurophysiol.*, 1973, 36: 893-924.
- Komisaruk, B.R. The role of rhythmical brain activity in sensorimotor integration. *Progr. Psychobiol. Physiol. Psychol.*, 1977, 7: 55-90.
- Korn, G.A. and Korn, T.M. *Mathematical Handbook for Scientists and Engineers*. McGraw-Hill, New York, 1968.
- Legewie, H., Simonova, O. and Creutzfeldt, O.D. EEG changes during performance of various tasks under open- and closed-eyed conditions. *Electroenceph. clin. Neurophysiol.*, 1969, 27: 470-479.
- Livanov, M.N. *Spatial Organization of Cerebral Processes*. Wiley, New York, 1977.
- Mars, N.J. and Lopes da Silva, F.H. EEG analysis methods based on information theory. In: A.S. Gevins and A. Rémond (Eds.), *Methods of Analysis of Brain Electrical and Magnetic Signals. Handbook of Electroencephalography and Clinical Neurophysiology*, Vol. 1. Elsevier, Amsterdam, 1987: 297-307.
- McGill, G.D. and Aunon, J.I. Analysis of event-related potentials. In: A.S. Gevins and A. Rémond (Eds.), *Methods of Analysis of Brain Electrical and Magnetic Signals. Handbook of Electroencephalography and Clinical Neurophysiology*, Vol. 1. Elsevier, Amsterdam, 1987: 131-169.
- Mesulam, M.M. A cortical network for directed attention and unilateral neglect. *Ann. Neurol.*, 1981, 10: 309-325.
- Nunez, P.L. *Electric Fields in the Brain: the Neurophysics of EEG*. Oxford University Press, New York, 1981.
- Okada, Y. Inferences concerning anatomy and physiology of the human brain based on its magnetic field. *Nuovo Cimento*, 1983, 2: 379-409.
- Oldfield, R.C. The assessment and analysis of handedness: the Edinburgh inventory. *Neuropsychologia*, 1971, 9: 97-113.
- Pieper, C., Goldring, S., Jenny, A. and McMahon, J. Comparative study of cerebral cortical potentials associated with voluntary movements in monkey and man. *Electroenceph. clin. Neurophysiol.*, 1980, 48: 266-292.
- Roland, P.E., Meyer, E., Shibasaki, T., Yamamoto, Y.L. and

- Thompson, C.J. Regional cerebral blood flow changes in cortex and basal ganglia during voluntary movements in normal human volunteers. *J. Neurophysiol.*, 1982, 48: 467-480.
- Rush, S. and Driscoll, D.A. EEG electrode sensitivity — an application of reciprocity. *IEEE Trans. Biomed. Eng.*, 1969, BME-16: 15-22.
- Squires, K.C., Donchin, E., Herning, R.I. and McCarthy, G. On the influence of task relevance and stimulus probability on event-related potential components. *Electroenceph. clin. Neurophysiol.*, 1977, 42: 1-14.
- Squires, N.K., Squires, K.C. and Hillyard, S.A. Two varieties of long-latency positive waves evoked by unpredictable auditory stimuli in man. *Electroenceph. clin. Neurophysiol.*, 1975, 38: 387-401.
- Stuss, D.T. and Benson, D.F. *The Frontal Lobes*. Raven Press, New York, 1986.
- Tecce, J.J. Contingent negative variation (CNV) and psychological processes in man. *Psychol. Bull.*, 1972, 77: 73-108.
- Tueting, P. Event-related potentials, cognitive events, and information processing: A summary of issues and discussion. In: D. Otto (Ed.), *Multidisciplinary Perspectives in Event-Related Brain Potential Research*. U.S. Government Printing Office, Washington, DC, 1978: 159-169.
- Thickbroom, G.W., Mastaglia, F.L., Carroll, W.M. and Davies, H.D. Source derivation: application to topographic mapping of visual evoked potentials. *Electroenceph. clin. Neurophysiol.*, 1984, 59: 279-285.
- Velasco, M., Velasco, F., Velasco, A.L., Almanza, X. and Olvera, A. Subcortical correlates of the P300 potential complex in man to auditory stimuli. *Electroenceph. clin. Neurophysiol.*, 1986, 64: 199-210.
- Wood, C., Allison, T., Goff, W., Williamson, P. and Spencer, D. On the neural origin of P300 in man. In: H. Kornhuber and L. Deecke (Eds.), *Motivation, Motor and Sensory Processes of the Brain: Electrical Potentials, Behavior and Clinical Use*. Progress in Brain Research, Vol. 54. Elsevier, Amsterdam, 1980: 51-56.

EEG 03390

## Event-related covariances during a bimanual visuomotor task.

### II. Preparation and feedback<sup>1</sup>

A.S. Gevins, B.A. Cutillo, S.L. Bressler, N.H. Morgan, R.M. White,  
J. Illes and D.S. Greer

*EEG Systems Laboratory, 51 Federal Street, San Francisco, CA 94107 (U.S.A.)*

(Accepted for publication: 4 April 1988)

**Summary** Event-related covariance (ERC) patterns were computed from pre-stimulus and feedback intervals of a bimanual visuomotor judgment task performed by 7 right-handed men. Late contingent negative variation (CNV) ERC patterns that preceded subsequently accurate right- or left-hand responses differed from patterns that preceded subsequently inaccurate responses. Recordings from electrodes placed at left frontal, midline antero-central, and appropriately contralateral central and parietal sites were prominent in ERC patterns of subsequently accurate performances. This suggests that a distributed cortical 'preparatory network,' composed of distinct cognitive, integrative motor, somesthetic, and motor components, is essential for accurate visuomotor performance.

ERC patterns related to feedback about accurate and inaccurate responses were similar to each other in the interval immediately after feedback onset, but began to differ in an interval spanning an early P300 peak. The difference became even greater in an interval spanning a late P300 peak. For both early and late P300 peaks, ERC patterns following feedback about inaccurate performance involved more frontal sites than did those following feedback about accurate performance.

Together with the stimulus- and response-locked results presented in part I, results of this study on the preparatory and feedback periods suggest that ERCs show salient features of the rapidly shifting, functional cortical networks that are responsible for simple cognitive tasks. ERCs thus provide a new perspective on information processing in the human brain in relation to behavior — a perspective that supplements conventional EEG and ERP procedures.

**Key words:** Event-related covariances; Event-related potentials; Contingent negative variation; P300; Spatiotemporal mapping; Preparatory networks; Feedback networks; Performance accuracy

As a step towards characterizing the distributed functional cortical networks that underly higher cognitive functions, we have been measuring the spatial synchronization of event-related potentials

(ERPs) (Gevins et al. 1981, 1983, 1985, 1987). In this experiment, we measured the spatial synchronization of ERPs related to preparation, stimulus processing, response execution and feedback about response accuracy during a 4 sec long bimanual visuomotor task. The results reported in part I (Gevins et al. 1989) showed that event-related covariance (ERC) patterns of stimulus processing and response execution correspond to existing models of the spatial and temporal organization of cortical function. The results presented in this second report show that the ERCs of pre-stimulus and feedback intervals are related to the accuracy of performance and are also consistent with recognized neurocognitive models. ERCs provide a new

<sup>1</sup> A part of the preparation results reported here have appeared in abbreviated form in Gevins et al. 1987. In addition to a more complete description of cue-locked ERPs, this paper presents the ERPs and ERCs for the feedback-locked event, and a discussion relating the contingent negative variation (CNV)- and P300-interval results to each other and to other psychophysiological research.

*Correspondence to:* A.S. Gevins, EEG Systems Laboratory, 51 Federal Street, San Francisco, CA 94107 (U.S.A.).

means of characterizing performance-related aspects of neural processing and thereby open new avenues for understanding the CNV and P300 waves.

## Methods

### *Subjects, task and recordings*

Detailed methods of this study were presented in part I and will be reviewed briefly here.

EEGs were recorded from 7 right-handed, healthy male adults while they performed a well-practiced visuomotor task. Each trial of the task began with a cue symbol ('V'), which was slanted to the right or left to indicate with which hand the subject should respond. One second after this cue, a visual stimulus (no. 1-9) appeared. In 'response' trials, the stimulus was slanted in the same direction as the cue. The subject had to respond quickly with the index finger of the indicated hand, by producing a pressure from 0.1 to 0.9 kg linearly related to the stimulus number. In a randomly distributed 20% of the trials, the stimulus was slanted in the direction opposite to the cue. In these 'no-response' catch trials, the subject had to withhold the finger response.

Feedback was presented visually 1 sec after the subject's peak response pressure in response trials. Feedback indicated the actual pressure (to a tenth of a stimulus unit) the subject made. If the response was sufficiently close to the required response (according to a continuously updated tolerance of adaptive error), the feedback number was underlined to indicate a 'win.' The purpose of the adaptive error tolerance was to adjust the margin for winning as performance fluctuated. The error tolerance was computed for each hand separately as a function of performance during the previous 5 trials. Subjects earned a bonus of 5 cents for each win and were penalized 10 cents for each response to a 'no-response' catch trial. Summaries of performance and the amount of money earned were presented at the end of each block of 17 trials. Together with frequent rest breaks, these procedures were intended to help subjects remain alert during the 5-7 h recording session.

Using visual editing, we discarded trials that contained physiological or instrumental artifact, slow, hesitant, or delayed responses, or any sign of EMG in the non-responding hand or in the cue-to-stimulus epoch in the responding hand.

### *Performance accuracy*

In order to identify neuroelectric patterns associated with preparation and quality of performance, each subject's trials were sorted according to hand and response accuracy. 'Accurate' and 'inaccurate' data sets contained trials in which the response error (deviation from required finger pressure) was less or greater, respectively, than the mean error calculated over each subject's entire recording session. Accurate and inaccurate trials were distributed uniformly across the session and, therefore, did not differ because of learning or possible systematic shifts in arousal across the session.

Trials were also sorted according to hand and accuracy during feedback-locked intervals. Behavioral variables such as response time, pressure, and duration were carefully balanced to eliminate the possibility that differences in post-response activity, unrelated to our neurophysiological hypotheses, might extend to the onset of feedback.

### *Laplacian derivation wave forms and event-related covariances*

Sixteen laplacian derivation (LD) channels were computed from recordings by a total of 26 scalp electrodes. The 16 were the non-peripheral scalp electrodes with adequate sampling of surrounding potential. Enhanced, averaged, event-related, LD time series were formed from sets of trials that contained detectable event-related signals (Gevins et al. 1986). A positive peak in the LD wave form represented the emerging current at the scalp and is referred to as a 'current source.' (This terminology should not be confused with an actual neural source or 'generator.') Since most LD peaks changed polarity across the scalp, all peaks were labeled according to standard ERP terminology (e.g., CNV, P300).

ERCs for each of the 120 pairwise combinations of the 16 non-peripheral channels were computed from the enhanced, filtered, 7-person aver-

aged LD wave forms (see part I). A delta (0.1–3 Hz) bandpass filter and a covariance interval width of 375 msec were used to emphasize the low-frequency, late post-cue CNV component of the LD wave form. A theta (4–7 Hz) bandpass filter and a 187 msec wide covariance interval were used to analyze the post-feedback LD components. Measuring the covariance between narrow bandpass-filtered wave forms was equivalent, in principle, to computing the magnitude of the cross-spectrum in the frequency domain. However, working in the time domain made it easier to derive the optimal trade-offs between time and frequency resolution in our data. Working in the time domain also made computations efficient, since we could calculate only over the band of interest, and not over the entire spectrum.

All ERCs with significance of  $P < 0.05$  were displayed for pre-stimulus CNV intervals. Time delays could not be computed for the CNV, because an interval wide enough to allow an adequate estimate of the delay would have included components related to processing of the cue and would thus have not related solely to the CNV. ERCs within 2 S.D.s of the maximum ERC value were displayed for the feedback intervals, because of the many highly significant ERCs. As described in part I, ERC patterns were compared for differences in magnitude by the Student's  $t$  test, and for differences in pattern by the 'bootstrap' correlation method (Efron 1982).

We used pattern classification procedures to determine how well the pre-stimulus ERCs could predict the subsequent performance accuracy, and to assess differences between subjects. A non-linear, 2-layered 'neural network' pattern classification algorithm (Viglione 1970; Gevins 1980) classified each trial for subsequent performance accuracy by forming weighted combinations of the pre-stimulus ERCs. Classification equations that consisted of weighted combinations of the decisions of discriminant functions were computed using a recursive procedure. The discriminant functions themselves consisted of weighted combinations of a subset of the ERCs shown in Fig. 2. We validated this procedure by classifying the trials of each subject by equations developed on the trials of the other 6 subjects. We used a

binomial distribution to determine the significance of the average of the 7 validations. A more detailed discussion of the application of pattern classification procedures to neuroelectric signals can be found in Gevins (1980, 1987) and Gevins and Morgan (1986, 1988).

## Results

### *Behavioral analysis*

For accurate trials, the mean deviation of response pressure from the required pressure was  $0.035 \pm 0.020$  kg for the right hand, and  $0.039 \pm 0.020$  kg for the left hand. The comparable values for inaccurate performance were  $0.162 \pm 0.066$  kg for the right hand and  $0.166 \pm 0.076$  kg for the left hand. Mean reaction times for the 4 performance conditions in the final data sets ranged consistently from 610 to 618 msec.

### *Cue-locked wave forms*

Although visual inspection of the pre-stimulus CNV in the 7-person averaged, delta-filtered LD wave forms (Fig. 1) suggested differences in amplitude that were related to condition, such differences were not statistically significant. The mean squared amplitude (over channels) of the CNV wave form, thought to be related to preparatory set (Walter 1967; reviewed in Tecce 1972), was measured for 375 msec wide intervals (corresponding to covariance analysis intervals) under subsequently accurate and inaccurate, right- and left-hand conditions. In the interval centered at 687 msec post cue (covering the late peak of the CNV), the amplitudes of the CNV wave form for subsequently accurate and inaccurate performances did not differ significantly for either hand. The similarity of the late CNV amplitudes was also confirmed by the bootstrap correlation procedure. When we compared the distributions of amplitude of the 687 msec interval of subsequently accurate and inaccurate trials, the correlations were  $0.84 \pm 0.16$  for right-hand trials and  $0.83 \pm 0.14$  for left-hand trials. Thus, the late CNVs under conditions of accurate and inaccurate performance did not differ either in magnitude or in spatial pattern.



### CUE TO PREPARE FOR AN INDEX FINGER RESPONSE

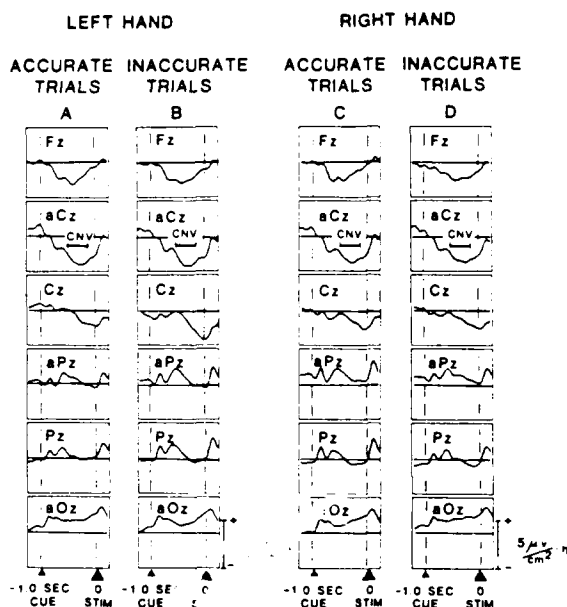


Fig. 1. Laplacian derivation (LD) wave forms from midline electrode sites, showing the contingent negative variation (CNV), and the event-related covariance (ERC) analysis interval centered at 687 msec post-cue in the cue-to-stimulus period. The mean late CNV amplitudes, from low-pass filtered (below 3 Hz) averages of 7 subjects, are not significantly different for the comparison of left-accurate (A) with left-inaccurate (B) conditions, or right-accurate (C) with right-inaccurate (D) conditions.

In contrast to the non-specific CNV amplitude patterns that were seen across all LD channels, there were differences in the CNV amplitude of the left and right antero-central (motor-related)

TABLE I

Mean absolute amplitude of the laplacian derivation wave form from a 375 msec wide interval centered at 750 msec post cue on the late CNV. The left and right antero-central sites (aC3 and aC4) are thought to overly primary motor areas. The antero-central CNV was larger contralateral to the hand indicated by the slant of the cue preceding accurate and inaccurate performance. The asymmetries that preceded inaccurate performance tended to be larger. Values are expressed in units of  $\mu\text{V}/\text{cm}^2$ .

Electrodes	Accurate		Inaccurate	
	Right cue	Left cue	Right cue	Left cue
aC3	0.63	0.15	0.83	0.14
aC4	0.18	0.36	0.14	0.50

sites. The results summarized in Table I show that the absolute amplitude of the late CNV, for the 375 msec wide interval centered at 750 msec post cue, was appropriately lateralized to the hemisphere contralateral to the corresponding hand for both accurate and inaccurate performance. For the right hand, the left antero-central amplitude was greater than the right by more than 4:1. For the left hand, the right antero-central was greater than the left by 2:1 or more. If CNV amplitude lateralization is taken as a sign of response preparation, it is surprising that the asymmetries preceding inaccurate performance tended to be larger.

#### Cue-locked ERCs

ERCs were computed from delta band-filtered, averaged LD wave forms in each of several intervals during the 500 msec preceding the stimulus. Visually distinct and statistically reliable performance-related differences were first clearly apparent in the interval centered 687 msec post cue,

Fig. 2. View of the significant ( $P < 0.05$ ) late CNV ERC patterns (colored lines), superimposed on maps of late CNV amplitude. Both ERCs and CNV amplitude measurements are from an interval 500–875 msec after the cue for subsequently accurate and inaccurate right-hand (A,B) and left-hand (C,D) visuomotor task performance by 7 right-handed subjects. The thickness of an ERC line is proportional to its significance (from 0.05 to 0.005). A violet line indicates that the ERC is positive, while a blue line indicates that the ERC is negative. Because of the short ERC analysis interval, time delays could not be computed for the CNV. The color scale at the left of each picture represents wave amplitude and covers the range from the minimal to maximal values of the 2 maps. ERCs involving left frontal and appropriately contralateral central and parietal electrode sites are prominent in patterns for subsequently accurate performance by both hands. The magnitude and number of ERCs that precede subsequently inaccurate left-hand performance are greater and are more widely distributed compared to the accurate pattern. For the right hand, fewer and weaker ERCs characterize subsequently inaccurate performance. The amplitude maps are very similar for the 4 conditions and do not indicate any of the specific differences evident in the ERC patterns.

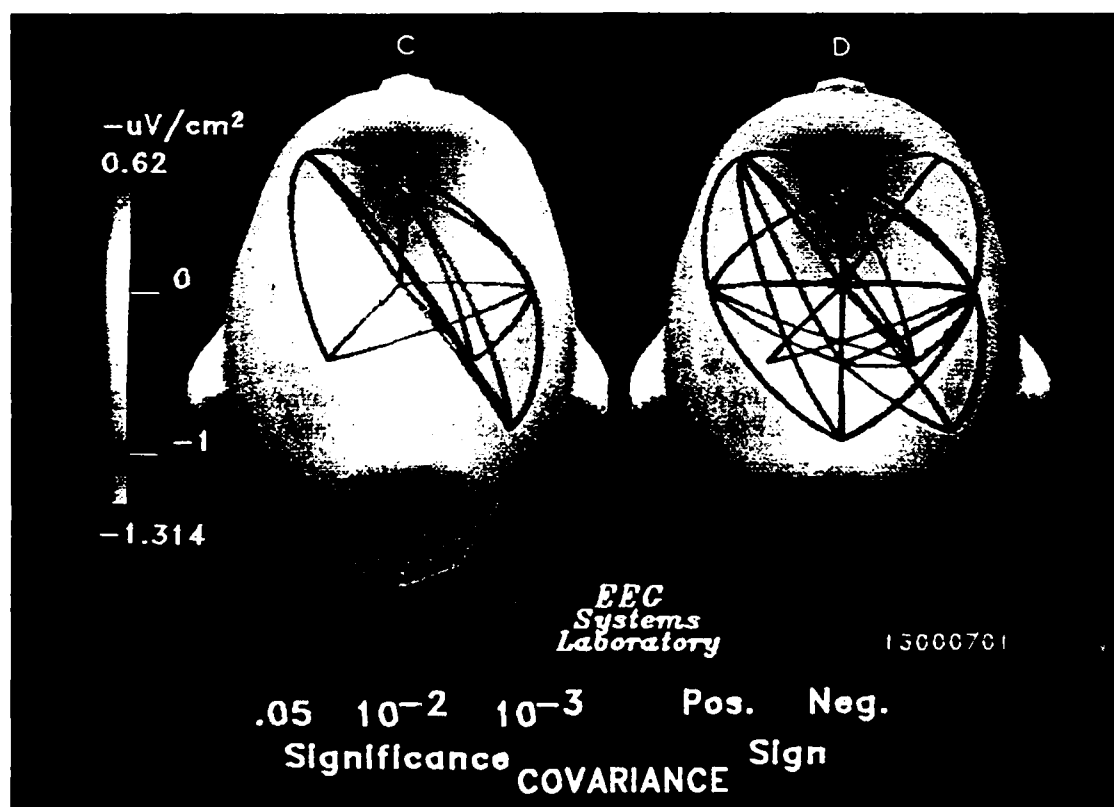
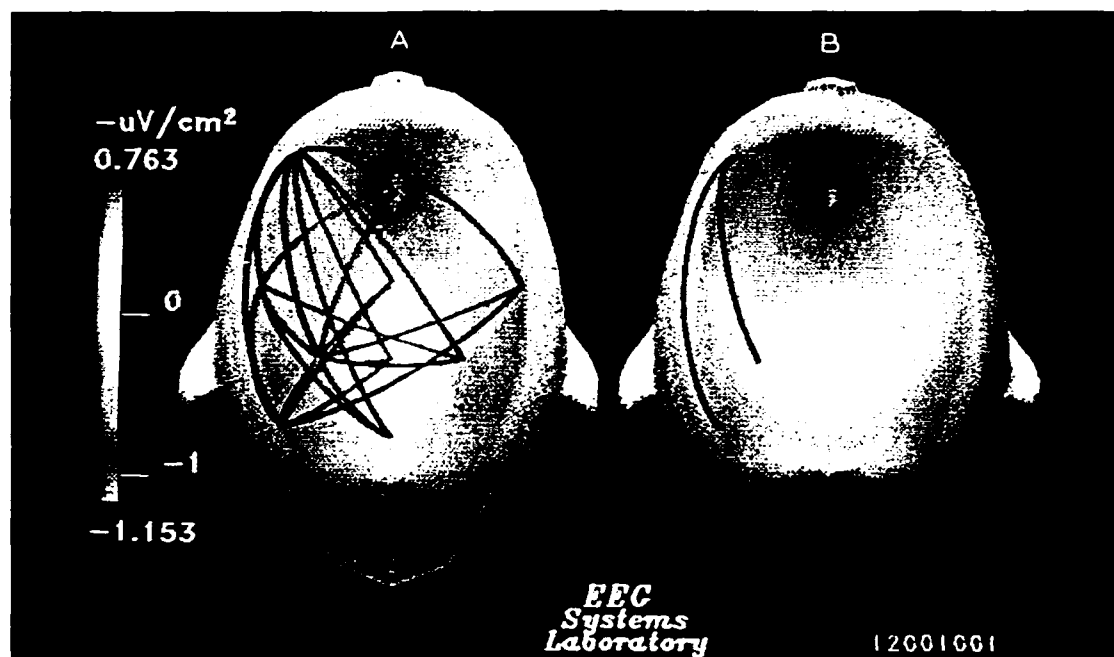


TABLE II

Location of maximum exiting (+) and entering (−) current, and peak latency and amplitude at that site for the 2 P3 waves elicited by feedback in accurate and inaccurate trials. Note that the site of maximum exiting current for accurate performance shifts from midline antero-central (aCz) to midline antero-parietal (aPz) in going from the early peak to the later component. Note also the larger amplitude of the early wave for feedback to accurate performance and the late wave for feedback to inaccurate performance.

Condition	Early P3 ('P3E')			Late P3 ('P3L')		
	Site of maximum	Latency (msec)	Amplitude ( $\mu\text{V} \cdot \text{cm}^2$ )	Site of maximum	Latency (msec)	Amplitude ( $\mu\text{V} \cdot \text{cm}^2$ )
<i>Accurate</i>						
Right hand	aCz +	320	4.7	aPz +	461	3.4
	F4 −	289	−2.3	F4 −	400	−2.0
Left hand	aCz +	328	4.6	aPz +	430	2.9
	F4 −	305	−1.9	F4 −	500	−1.9
<i>Inaccurate</i>						
Right hand	aCz +	305	3.6	aCz +	460	4.2
	F4 −	305	−2.2	F4 −	500	−1.4
Left hand	aCz +	328	3.5	aCz +	460	3.8
	F4 −	305	−2.2	F4 −	500	−2.1

i.e., 313 msec pre stimulus (Fig. 2). These ERC patterns were quite distinct from those related to overt finger response pressures (part I).

During the period between the cue and the stimulus, the averaged event-related muscle potential (right and left EMG) and eye movement (vertical and horizontal EOG) channels were at the noise level and did not differ between conditions. These low levels confirmed that the ERCs were neural in origin and were not associated with overt movements (Fig. 3).

In the 687 msec centered interval, ERCs associated with subsequently accurate right-hand performance involved sites primarily over the left hemisphere (Fig. 2A). All 24 significant ERCs involved left-sided sites and 18 (75%) of these were exclusively left-sided. The most significant ERCs involved left frontal, central, and parietal sites.

The 687 msec centered pattern of subsequently accurate left-hand performance involved a greater proportion of right hemisphere sites than did the accurate right-hand pattern (Fig. 2C). Of 18 significant ERCs, 13 (72%) involved electrode sites over the right hemisphere. There was only 1 left-sided intrahemispheric covariance, between aP1 and F3.

During this same interval, there were only 2 significant ERCs associated with subsequently in-

accurate, right-hand performance, namely left parietal and antero-parietal to left frontal (Fig. 2B). ERCs for subsequently inaccurate left-hand performance (Fig. 2D) were more bilaterally symmetric and complex than those for subsequently accurate left-hand performance.

For right-hand performances, the mean magnitude of event-related covariance in the 687 msec centered interval was significantly larger when performance was subsequently accurate ( $4.86 \pm 0.34$ ) than when it was subsequently inaccurate ( $3.90 \pm 0.41$ ) (Student's  $t = 7.7$ ,  $df = 23$ ,  $P < 5 \times 10^{-8}$ ). By contrast, the mean ERC preceding accurate left-hand performance ( $4.10 \pm 0.68$ ) was smaller than that preceding inaccurate left-hand performance ( $4.93 \pm 0.73$ ) ( $t = 5.6$ ,  $df = 38$ ,  $P < 5 \times 10^{-6}$ ).

We calculated the bootstrap correlation between the distributions of significant ERCs of accurate or inaccurate conditions, to assess the similarity of ERC patterns irrespective of the difference in magnitude. Right-hand, subsequently accurate and inaccurate ERC patterns were correlated at  $0.57 \pm 0.09$ , while the correlation for the left hand was  $0.10 \pm 0.14$ . Thus, accurate and inaccurate preparatory patterns differed in both magnitude and pattern for both hands. The right-hand correlation was quite high (0.57), given that

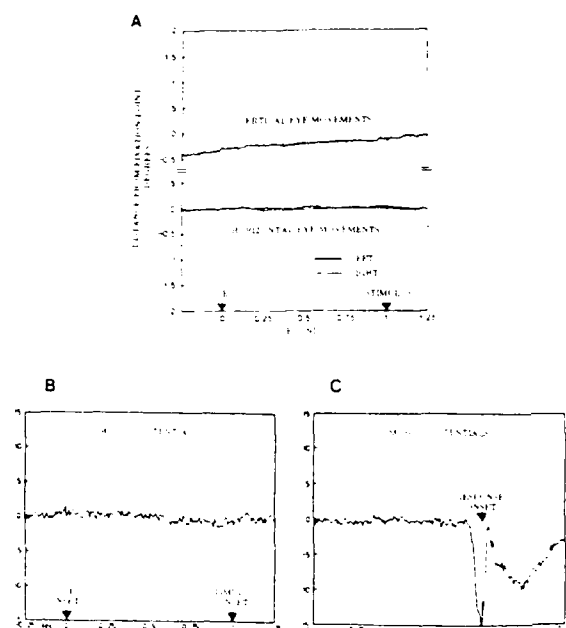


Fig. 3. Averaged vertical and horizontal eye movement signals during the period between the cue and the stimulus for right- and left-hand trials from 7 subjects (A). Averaged muscle potential signals from right flexor digitorum during the cue-to-stimulus epoch (B). Muscle potentials during overt movements were many times larger (C). Averaged muscle potential signals from left flexor digitorum showed the same relation. Since there is no evidence of eye or muscle movements during preparation of either the right- or left-hand, the ERC patterns in Fig. 2 are not the result of overt movements.

there were only 2 significant ERCs in the right inaccurate pattern (Fig. 2B). This indicates that the ordering of the non-significant ERCs in that pattern was roughly similar to that of the accurate pattern, and that the difference in magnitude was the overriding effect.

We used statistical pattern classification of ERCs during the interval between the cue and the stimulus to assess how well the ERCs discriminated subsequent performance on a trial-by-trial basis, and to measure differences between subjects. These results have been described elsewhere (Gevins et al. 1987) and are summarized here.

ERCs from 6 of the subjects were used to discriminate the subsequent accuracy of the remaining subject's performance. This was repeated

7 times. The ERCs shown in Fig. 2 were the variables that we submitted to these discriminations. Using this leave-out-one-person validation, both left- and right-hand overall classifications (57% and 59% respectively) were significant at  $P < 0.01$ . Six of the 7 subjects had similar patterns for right-hand discriminations, while there were 2 distinct groups for left-hand discriminations. For the subject with the most trials, the single-subject classification was 68% ( $P < 0.001$ ) for subsequent right- and 62% ( $P < 0.01$ ) for subsequent left-hand performance (as determined by 5 leave-out-one-fifth replications). Thus, the subjects' preparatory patterns for both accurate and inaccurate right-hand performances were very similar, while their left-hand patterns distinguished the subjects into 2 groups. More detailed analysis of individual sub-

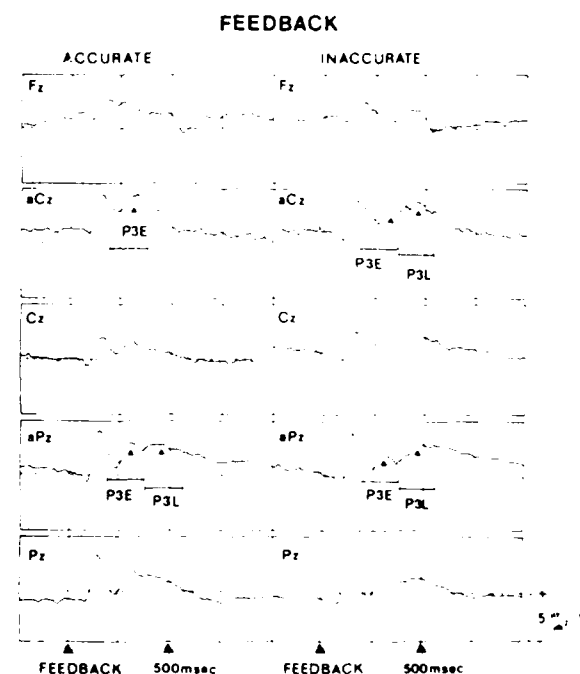
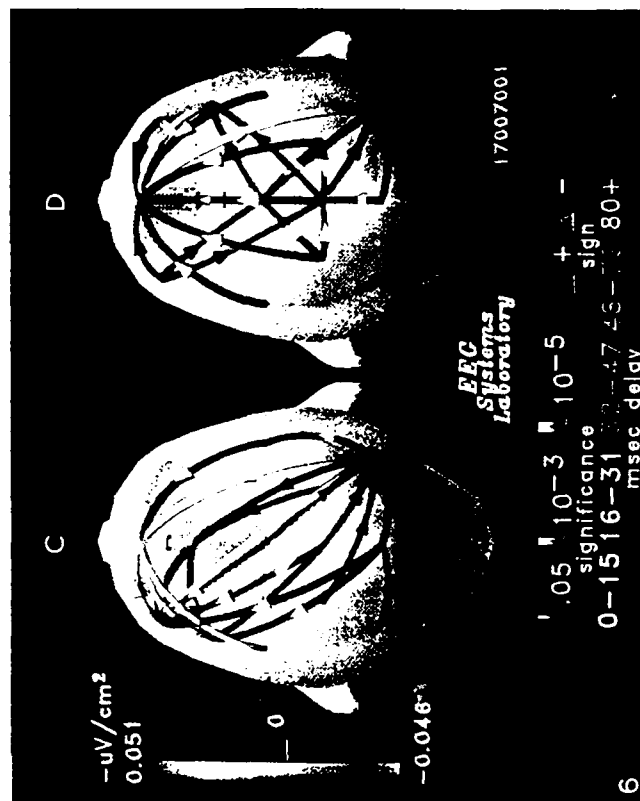
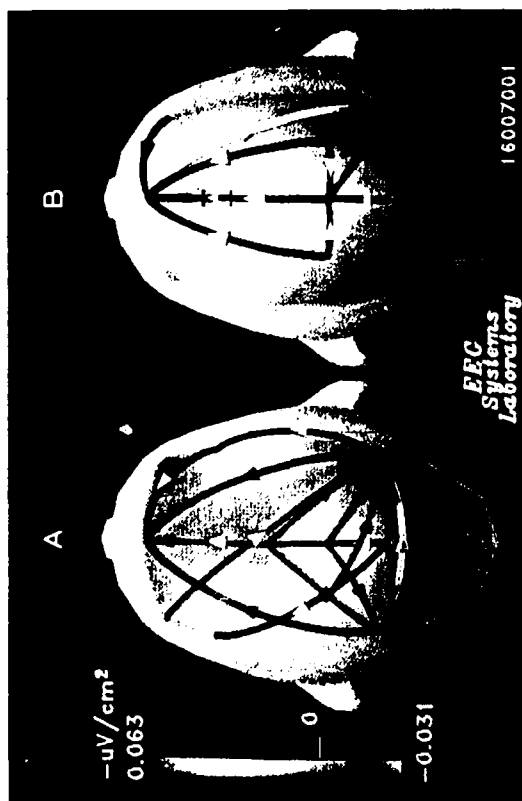


Fig. 4. Feedback-evoked LD wave forms at midline sites for left-hand accurate and inaccurate performance trials, showing early and later, more long-lasting, P3 waves. The early P3 (P3E) is larger for feedback about accurate than for feedback about inaccurate performance, while the later P3 (P3L) is larger for feedback about inaccurate performance. Both components can be seen clearly at some sites, including aPz. This demonstrates that there are in fact 2 separate components and not a single P3 whose latency is shifted at different sites.



0.05 10-3 10-5 + -  
significance  
0-15 16-31 32-47 48-63 80+  
msec delay

ject data will be presented elsewhere (Gevins et al. in prep.).

#### *Feedback-locked wave forms*

The 7-person averaged, unfiltered LD wave forms (Fig. 4) contained early peaks before 200 msec after the feedback. They corresponded to N1 and P2 and were similar to those seen in the stimulus event (see part I). A small peak, corresponding to the N2 wave, was distinguishable at about 250 msec, with entering current at the midline antero-occipital site and exiting current at the lateral parietal sites (not shown).

Two closely overlapping late LD peaks, corresponding to positive potentials, had differing topographies in the different experimental conditions. Theta band filtering accentuated the condition-specific differences of these wave forms by removing the delta band portion of the wave form. Table II shows the sites of the maxima for current sources and sinks of the positive peaks during feedback about accurate and inaccurate right- and left-hand performances.

There was a robust early 'P3E' peak at 281–328 msec during feedback about accurate performance, with emerging current at all midline sites and lateral parietal sites (maximal at the midline antero-central site), and entering current at lateral frontal sites (maximal at the right frontal site). The later, wider 'P3L' peak at 430–500 msec had its maximal current source at the midline antero-parietal site, and its maximal sink at the right frontal site. The amplitude of the P3E peak was larger than that of the later P3L.

Feedback about inaccurate performance was also characterized by 2 peaks that occurred between 300 and 600 msec. The P3E peak, at 305–328 msec, was similar in topography to that of the accurate performance, but had a lower overall amplitude. The later P3L, at 460–600 msec, was larger than that of the accurate performance. The site of maximal exiting current for the P3L was more anterior, at the midline antero-central site, and its amplitude was larger than the amplitude of the P3E.

For both accurate and inaccurate performance, peak amplitudes at 500 msec during feedback about right-hand performance were larger at the left central and left antero-central sites than at corresponding sites of the right hemisphere. Similarly, amplitudes at 500 msec for feedback about left-hand performance were larger at the right antero-central site for accurate performance, and larger at the right central site for inaccurate performance.

#### *Feedback-locked ERCs*

In the interval spanning the early 'exogenous' N1 and P2 feedback peaks, ERCs from theta band-filtered, averaged LD wave forms did not differ according to accuracy of each hand and resembled the early stimulus-locked patterns shown in part I.

Differences between accurate and inaccurate conditions began to emerge in the interval centered at 281 msec that spanned the early P3 peak (P3E). When the ERC patterns for feedback to accurate and inaccurate performance were compared, the

Fig. 5. Most significant (top 2 S.D.s; within 2 S.D.s of largest value) early P3 (P3E) feedback ERC patterns for feedback about accurate and inaccurate performance by the right hand (A and B) and left hand (C and D). ERC patterns are superimposed on color maps of wave amplitude. The thickness of an ERC line is proportional to the negative log of its significance (from 0.05 to 0.00005). The color scale at the left of each picture represents wave amplitude and covers the range from the minimal to maximal values of the 2 maps. Both the ERCs and amplitude maps are derived from a 187 msec wide interval, centered at 281 msec after the onset of feedback, on theta band-filtered wave forms averaged over all 7 subjects. A major difference between accurate and inaccurate patterns is that the left and midline frontal sites are only involved in the inaccurate patterns. The involvement of these sites may reflect the fact that greater processing is required after inaccurate performance, in order to improve subsequent performance.

Fig. 6. Most significant (top 2 S.D.s) late P3 ERC patterns for feedback to accurate and inaccurate performance by the right hand (A and B) and left hand (C and D). Both the ERCs and amplitude maps are derived from a 187 msec wide interval, centered at 468 msec after feedback onset, on theta band-filtered 7-subject averaged wave forms. Involvement of the left parietal site, greater involvement of the right parietal site, and absence of the right frontal site distinguished the accurate patterns from the inaccurate.

bootstrap correlation was  $0.36 \pm 0.35$  for right- and  $0.73 \pm 0.05$  for left-hand performance. The ERC patterns for feedback about accurate performance by the two hands (Fig. 5A and C) were highly similar (bootstrap correlation =  $0.91 \pm 0.01$ ), and involved midline antero-central, central, antero-parietal, parietal and antero-occipital sites, left antero-parietal and antero-central sites, and right parietal, antero-parietal, antero-central, and frontal sites. These accurate patterns involved many long-delay (32–79 msec) ERCs. The wave forms of the frontal and antero-central sites consistently lagged those of more posterior sites.

The ERC patterns during feedback about inaccurate performance by the left and right hands (Fig. 5B and D) were also very similar (bootstrap correlation =  $0.90 \pm 0.02$ ). They involved most of the same sites as the accurate patterns, with the striking exception of the left and midline frontal sites. Again, frontal wave forms lagged those of the more posterior sites with which they covaried. There were even more long-delay ERCs than in the accurate patterns.

In the interval centered at 468 msec, spanning the late P3 peak (P3L), the patterns for accurate and inaccurate performance were still very different (bootstrap correlation =  $-0.38 \pm 0.27$  for right- and  $0.13 \pm 0.08$  for left-hand performance). The patterns during feedback about right- and left-hand accurate performance had many sites in common (e.g., midline parietal, antero-parietal, central, antero-central, and frontal sites, bilateral parietal sites, and left antero-central and frontal sites), although they were less similar than in the early P3 interval (bootstrap correlation =  $0.58 \pm 0.06$ ) (Fig. 6A and C). The absence of the right frontal site from these patterns was conspicuous, considering its prominence in the accurate patterns from the early P3 interval. The inaccurate patterns were also less similar than in the early P3 interval (bootstrap correlation =  $0.77 \pm 0.04$ ). They differed from the accurate ones, particularly in that the right frontal site was involved, the left parietal site was absent, and the right parietal site was less involved (Fig. 6B and D).

Feedback patterns about left-hand accurate and inaccurate performance had more ERCs than did patterns during feedback about right-hand perfor-

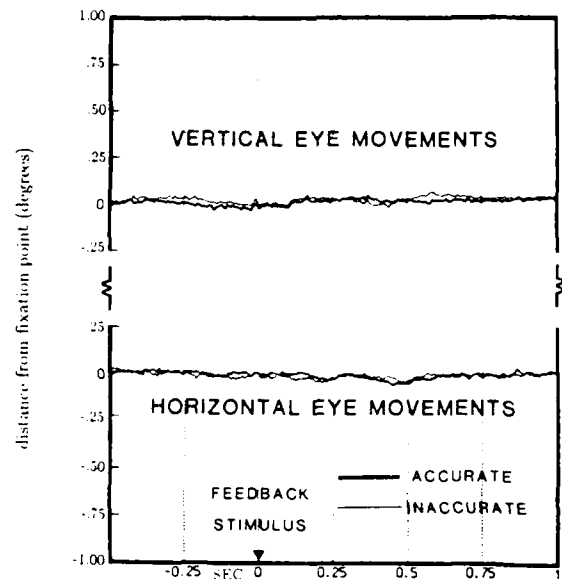


Fig. 7. Averaged vertical and horizontal eye movement signals from 7 subjects during feedback about accurate and inaccurate left-hand performance.

mance. As was the case during the P3E interval, the similarity of P3L ERC patterns between the 2 hands, regardless of performance accuracy, was greater than between accurate and inaccurate patterns for either hand. This implies that the feedback ERC patterns in both intervals were related more to performance accuracy than to the hand used.

Vertical and horizontal EOG channels were at the noise level for all conditions of accuracy and handedness (Fig. 7).

## Discussion

Although the event-related preparatory and feedback covariance patterns reported here appear to represent signs of 'functional coordination' between nodes within a cooperative cortical network, we must again caution that such an interpretation is speculative until the generators of these patterns are determined. With this in mind, we offer the following comments on the results of this study.

### Preparation

The prominence of the left frontal site in our preparatory patterns prior to actual response ex-

ecution by either hand is consistent with clinical evidence that prefrontal cortical areas are involved in the synthesis of preparatory sets (Luria 1966), and that the left dorsolateral prefrontal cortex is specifically involved in cued delayed response tasks (Jacobsen 1935; Pribram et al. 1977; Shallice 1982; Fuster 1984). Similarly, the prominence of the midline central and antero-central sites suggests the presence of an integrative motor component. The involvement of these sites in the preparatory patterns is consistent with clinical evidence for involvement of the premotor and supplementary motor regions when existing motor schemes are initiated, or when new ones are established (Penfield and Jasper 1959; Goldman-Rakic 1984; Milner and Petrides 1984; Goldberg 1985; Stuss and Benson 1986). The integrative motor component, strong in the pattern preceding accurate left-hand performance and weaker in the pattern preceding accurate right-hand performance, may indicate that a greater degree of motor control is necessary when strongly right-handed subjects execute a fine motor response with their left hands. The existences of appropriately lateralized somesthetic and motor preparatory components are supported by experimental evidence for distinct firing patterns of neurons in the motor and premotor cortices preceding motor responses in non-human primates (Evarts et al. 1984). The difference between ERC patterns corresponding to preparation and to actual response execution (see part I) suggests that they reflect different organizations of neural activity.

The detailed spatial organization and interelectrode covariance of the late CNV clearly reveal several anatomically and functionally distinct processes. Although traditional CNV studies have tended to view the CNV as a unitary brain process that reflects anticipation of a response based on the contingency between 2 stimuli (S1 and S2) (Walter 1967; reviewed in Tecce 1972), there has been growing evidence that the CNV is a multi-component process (Ruchkin et al. 1986; Loveless et al. 1987). There has also been some debate as to whether the CNV reflects only motor preparation, or whether there is also a cognitive component related to the expected stimulus (S2) (Gaillard 1977 (reviewed in Gevins and Cuttillo 1986);

Rohrbaugh et al. 1980; Ruchkin et al. 1986). As discussed above, the present results support the idea that preparation is a multi-component process that includes not only motor-somesthetic preparation but also cognitive and high-level integrative motor components. Finally, inconsistent results of previous studies that related the CNV to the quality of subsequent performance could be attributed, at least in part, to insufficient spatial sampling and analysis (for recent examples, see Macar and Vitton 1982; Macar and Besson 1986).

Our preparatory findings are consistent with 'continuous flow' models of the temporal organization of human cognition (Erikson and Schultz 1979; Coles et al. 1985). The temporal evolution of the ERC patterns that follow the cue indicates that response preparation begins with evaluation of the cue, well before stimulus presentation. Like previous workers (Rohrbaugh et al. 1976; Coles and Gratton 1986), we found a slightly larger CNV amplitude over motor areas contralateral to the subsequently responding hand. The paper by Coles and Gratton demonstrated that the response is more likely to be made with the correct hand when the CNV is lateralized contralaterally, rather than ipsilaterally, to the hand indicated by the stimulus. The ERC patterns appear to be more sensitive to preparatory set than do amplitude patterns; they clearly distinguished subsequent near-target (accurate) from far-from-target (inaccurate) index finger pressures, both of which were performed with the correct hand.

#### *Feedback*

The ERC patterns of both the early and late P3 peaks in the feedback interval appeared to reflect a difference between 'confirming' (following accurate performance) and 'disconfirming' (following inaccurate performance) feedback, with a greater difference for the later peak. In the early interval, the main difference between the confirming and disconfirming patterns was that all frontal sites were involved in disconfirming feedback, whereas the left and midline frontal sites were absent for confirming feedback. For the late peak, the left and midline frontal sites, as well as the left parietal site, became involved in the pattern for confirming feedback, and the right frontal site was no longer



involved. The patterns from the late interval for disconfirming feedback were quite different from those of the early interval, although the changes were different for the 2 hands.

ERC patterns for P3 peaks that followed disconfirming feedback involved more frontal sites than did patterns that followed confirming feedback. We would expect a greater resetting of performance-related neural systems following disconfirming feedback, as well as a strong frontal involvement, given the importance of the frontal lobes for the integration of sensory and motor activities (Fuster 1984; Stuss and Benson 1986). The difference between right- and left-hand patterns was greater for the late than for the early peak, with both left-hand patterns having a greater number of ERCs than the right-hand patterns. This suggests that in the right-handed subjects of this study, resetting these systems after left-hand performance required more processing during the late peak.

Prior experiments dealing with feedback-evoked potentials have shown differences in P3 latency between confirming and disconfirming feedback to auditory stimuli, with confirming feedback eliciting a short-latency P3, and disconfirming feedback eliciting a long-latency P3 (Squires et al. 1973). The latency of our early P3, however, did not vary with feedback conditions as it did in previous studies, and our late P3 for disconfirming feedback was delayed only about 30 msec. Rather, the late P3 LD peak at the site of maximum exiting current was larger than the early P3 peak during feedback about inaccurate responses, but was smaller during feedback about accurate responses (Fig. 4). The major difference between confirming and disconfirming feedback wave forms in our study, therefore, was related to the relative amplitudes of the early and late P3 peaks, rather than to their latency.

The P3 peaks in our data relate to late positive waves reported in other studies on feedback about accuracy. From studies of time estimation, Johnson and Donchin (1978, 1985) concluded that the early P3 is associated with the identification and classification of the feedback, while the later P3 is associated with the utilization of feedback information in the reinforcement or revision of the

response (time estimate). In other studies, particularly those in which monetary bonuses served as an incentive for good performance (e.g., Poon et al. 1974; Steinhauer 1981), the second positive wave was attributed in part to additional processing (such as assessing current assets), once the nature of the feedback has been determined. Likewise, Stuss and Picton (1978) suggested that serial processing, i.e., recognizing the meaning of a feedback stimulus, followed by using that information, is reflected in a P3 component followed by a long-latency, broad duration, later component (which they termed 'P4'). The increasing divergence over time of confirming and disconfirming feedback ERC patterns is consistent with the general conclusion of these researchers that the second late positive wave is related to utilization of information extracted from the feedback stimulus.

### Conclusion

Using modern recording and signal processing technologies, we have attempted to improve the spatial, temporal, and neurocognitive specificity of earlier studies. In the spatial domain, we increased the number of channels recorded simultaneously and reduced volume conduction blurring. Even with these advancements, the specificity of the results suggests that a further increase in spatial sampling will be beneficial. In the temporal domain, we measured shifts on the order of tens of milliseconds between event-related peaks of different channels. Since the analysis was restricted to specific frequency bands, there is a wealth of data in other frequency regions and their accompanying time intervals, that has yet to be explored.

We have isolated specific cognitive processes related to different events in the 4 sec trial, using highly controlled tasks. The time evolution of ERC patterns over the course of the whole 4 sec trial should provide deeper insight into the neurocognitive processing involved. In light of the striking findings reported here and in part I, determining the generators of scalp-recorded event-related covariance patterns is the next essential step in characterizing the dynamic functional cortical networks that underly cognition and behavior.

This research was supported by grants and contracts from the Air Force Office of Scientific Research, the National Institutes of Neurological and Communicative Diseases and Strokes, the National Science Foundation, and the Office of Naval Research.

Thanks to Drs. Marta Kutas, Robert Knight, and Walton Roth for critical review of the manuscript, to Jhaine Salzman and Daniel Orzech for technical assistance, to Kris Dean, Jeanne Toal, and Judith Gumbiner for manuscript preparation, and to Dr. Joseph Doyle, Mr. Gerald Zeitlin, Mr. Robert Tannehill and Mr. Bryan Costales for programming and other scientific and engineering support.

## References

- Coles, M.G. and Gratton, G. Cognitive psychophysiology and the study of states and processes. In: G. Hockey, A. Gaillard and M. Coles (Eds.), *Energetics and Human Information Processing*. Nijhoff, Dordrecht, 1986.
- Coles, M.G., Gratton, G., Bashore, T.R., Eriksen, C.W. and Donchin, E. A psychophysiological investigation of the continuous flow model of human information processing. *J. Exp. Psychol.: Hum. Percept. Perform.*, 1985, 11: 529-553.
- Efron, B. *The Jackknife, The Bootstrap, and Other Resampling Plans*. Society for Industrial and Applied Mathematics, Philadelphia, PA, 1982.
- Erkson, C.W. and Schultz, D.W. Information processing in visual search: a continuous flow conception and experimental results. *Percept. Psychophys.*, 1979, 25: 249-263.
- Evarts, E., Shinoda, Y. and Wise, S. *Neurophysiological Approaches to Higher Brain Functions*. Wiley, New York, 1984.
- Fuster, J.M. Behavioral electrophysiology of the prefrontal cortex. *Trends Neurosci.*, 1984, 7: 408-414.
- Gaillard, A.W.K. The late CNV wave: preparation versus expectancy. *Psychol. Physiol.*, 1977, 14: 563-568.
- Gevins, A.S. Pattern recognition of human brain electrical potentials. *IEEE Trans. Patt. Anal. Mach. Intell.*, 1980, PAMI-2: 383-404.
- Gevins, A.S. Statistical pattern recognition. In: A.S. Gevins and A. Rémond (Eds.), *Methods of Analysis of Brain Electrical and Magnetic Signals. Handbook of Electroencephalography and Clinical Neurophysiology*, Vol. 1. Elsevier, Amsterdam, 1987: 541-582.
- Gevins, A.S. Analysis of multiple lead data. In: J. Rohrbaugh, R. Johnson and R. Parasuraman (Eds.), *Event-Related Potentials of the Brain*. Oxford University Press, New York, 1988: in press.
- Gevins, A.S. and Cuttillo, B.A. Signals of cognition. In: F. Lopes da Silva and A. Rémond (Eds.), *Applications of Computer Analysis to EEG. Handbook of Electroencephalography and Clinical Neurophysiology*, Vol. 2. Elsevier, Amsterdam, 1986: 335-381.
- Gevins, A.S. and Morgan, N.H. Classifier-directed signal processing in brain research. *IEEE Trans. Biomed. Eng.*, 1986, BME-33: 1054-1068.
- Gevins, A.S. and Morgan, N.H. Applications of neural-network (NN) signal processing in brain research. *IEEE ASSP Trans.*, 1988, 36: 1152-1161.
- Gevins, A.S., Zeitlin, G.M., Doyle, J.C., Yingling, C.D., Schaffer, R.E., Callaway, E. and Yeager, C.L. Electroencephalogram correlates of higher cortical functions. *Science*, 1979, 203: 665-668.
- Gevins, A.S., Doyle, J., Cuttillo, B., Schaffer, R., Tannehill, R., Ghannam, J., Gilcrease, V. and Yeager, C. Electrical potentials in human brain during cognition: new method reveals dynamic patterns of correlation. *Science*, 1981, 213: 918-922.
- Gevins, A.S., Schaffer, R.E., Doyle, J.C., Cuttillo, B.A., Tannehill, R.S. and Bressler, S.L. Shadows of thought: rapidly changing, asymmetric brain-potential patterns of a brief visuomotor task. *Science*, 1983, 220: 97-99.
- Gevins, A.S., Doyle, J.C., Cuttillo, B.A., Schaffer, R.E., Tannehill, R.S., Bressler, S.L. and Zeitlin, G. Neurocognitive pattern analysis of a visuomotor task: low-frequency evoked correlations. *Psychophysiology*, 1985, 22: 32-43.
- Gevins, A.S., Morgan, N.H., Bressler, S., Doyle, J. and Cuttillo, B. Improved event-related potential estimation using statistical pattern recognition. *Electroenceph. clin. Neurophysiol.*, 1986, 64: 177-186.
- Gevins, A.S., Morgan, N.H., Bressler, S.L., Cuttillo, B.A., White, R.M., Illes, J., Greer, D.S., Doyle, J.C. and Zeitlin, G.M. Human neuroelectric patterns predict performance accuracy. *Science*, 1987, 235: 580-585.
- Gevins, A.S., Bressler, S.L., Morgan, N.H., Cuttillo, B.A., White, R.M., Illes, J. and Greer, D. Event-related covariances during a bimanual visuomotor task. I. Methods of analysis of stimulus- and response-locked data. *Electroenceph. clin. Neurophysiol.*, 1989, 74: 58-75.
- Gevins, A.S., Cuttillo, B.A., Bressler, S.L., Morgan, N.H., White, R.M., Illes, J. and Greer, D. Event-related covariances during a bimanual visuomotor task: individual differences. In prep.
- Goldberg, G. Supplementary motor area structure and function: review and hypotheses. *Behav. Brain Sci.*, 1985, 8: 567-616.
- Goldman-Rakic, P. The frontal lobes: uncharted provinces of the brain. *Trends Neurosci.*, 1984, 7: 425-429.
- Jacobsen, C.F. Functions of the frontal association area in primates. *Arch. Neurol. Psychiat.*, 1935, 33: 558-569.
- Johnson, R. and Donchin, E. On how P300 amplitude varies with the utility of the eliciting stimuli. *Electroenceph. clin. Neurophysiol.*, 1978, 44: 424-437.
- Johnson, R. and Donchin, E. Second thoughts: multiple P300s elicited by a single stimulus. *Psychophysiology*, 1985, 22: 182-194.
- Loveless, N.E., Simpson, M. and Näätänen, R. Frontal negative and parietal positive components of the slow wave dissociated. *Psychophysiology*, 1987, 24: 340-345.
- Luna, A.R. *Higher Cortical Functions in Man*. Basic Books, New York, 1966.
- Macar, F. and Besson, M. Contingent negative variation in processes of expectancy, motor preparation and time estimation. *Biol. Psychol.*, 1986, 21: 293-307.

- Macar, F. and Vitton, N. An early resolution of contingent negative variation (CNV) in time discrimination. *Electroenceph. clin. Neurophysiol.*, 1982, 47: 213-228.
- Milner, B. and Petrides, M. Behavioral effects of frontal-lobe lesions in man. *Trends Neurosci.*, 1984, 7: 403-407.
- Penfield, W. and Jasper, H. *Epilepsy and the Functional Anatomy of the Human Brain*. Little and Brown, Boston, MA, 1959.
- Poon, L.W., Thompson, L.W., Williams, R.B. and Marsh, G.R. Changes of anteroposterior distribution of CNV and late positive component as a function of information processing demands. *Psychophysiology*, 1974, 11: 660-673.
- Pribram, K., Plotkin, H., Anderson, R. and Leong, D. Information sources in the delayed alternation task for normal and 'frontal' monkeys. *Neuropsychologia*, 1977, 15: 329-340.
- Rohrbaugh, J.W., Syndulko, K. and Lindsley, D.B. Brain components of the contingent negative variation in humans. *Science*, 1976, 191: 1055-1057.
- Rohrbaugh, J.W., Syndulko, K., Sanquist, T.F. and Lindsley, D.B. Synthesis of the contingent negative variation brain potential from non-contingent stimulus and motor elements. *Science*, 1980, 208: 1165-1168.
- Ruchkin, D.S., Sutton, S., Mahaffey, D. and Glaser, J. Terminal CNV in the absence of motor response. *Electroenceph. clin. Neurophysiol.*, 1986, 62: 445-463.
- Shallice, T. Specific impairments of planning. *Phil. Trans. Roy. Soc. Lond.*, 1982, 298: 199-209.
- Squires, K.C., Hillyard, S.A. and Lindsay, P.H. Cortical potential evoked by confirming and disconfirming feedback following an auditory discrimination. *Percept. Psychophys.*, 1973, 13: 25-31.
- Steinhauer, S.R. *Emitted and Evoked Pupillary Responses and Event-related Potentials as a Function of Reward and Task Involvement*. Doctoral Dissertation. City University of New York, 1981.
- Stuss, D.T. and Benson, D.F. *The Frontal Lobes*. Raven Press, New York, 1986.
- Stuss, D.T. and Picton, T.E. Neurophysiological correlates of human concept formation. *Behav. Biol.*, 1978, 23: 135-162.
- Tecce, J. Contingent negative variation (CNV) and psychological processes in man. *Psychol. Bull.*, 1972, 77: 73-108.
- Viglione, S.S. Applications of pattern recognition technology. In: J.M. Mendel and K.S. Fu (Eds.), *Adaptive Learning and Pattern Recognition Systems*. Academic Press, New York, 1970: 115-161.
- Walter, W.G. Slow potential changes in the human brain associated with expectancy, decision and intention. *Electroenceph. clin. Neurophysiol.*, 1967, Suppl. 26: 123-130.

# Applications of Neural-Network (NN) Signal Processing in Brain Research

ALAN S. GEVINS, SENIOR MEMBER, IEEE, AND NELSON H. MORGAN, SENIOR MEMBER, IEEE

(Invited Paper)

**Abstract**—This paper reviews the application of neural-network (NN) signal processing methods to neurological waveform detection and pattern analysis. NN methods are shown to be an excellent way of incorporating expert knowledge about the brain into a mathematical framework with minimal assumptions about the statistics of signals and noise. Constrained by expert knowledge, NN algorithms can search for optimal or near-optimal connections between, and weightings of, application-specific features in data spaces for which human knowledge is incomplete.

Applying NN algorithms to electrical signals noninvasively recorded from the human brain, the neurological effects of different types of sleeping pills have been differentiated, and insights have been gained as to how our brains produce higher cognitive functions. Other signal processing problems with highly dimensioned noisy data may be amenable to similar solutions. However, the importance of application-specific constraints in solving real-world problems should not be underestimated.

## INTRODUCTION

**E**XTRACTING useful information from neuroelectric data recorded at the scalp requires a complex, and often unknown, series of processing operations. This is a multidimensional signal processing problem in which the signal and noise have unknown but similar statistics, in which the noise generally is significantly stronger than the signal, and in which the signal dimensions are smeared because of spatial crosstalk.

Because of the difficulty of brain signal analysis, conventional open-loop analyses are often insufficiently sensitive. Prior selection of the signal features either solely by "blind" application of statistical procedures or solely from expert opinion may not differentiate disease processes or discriminate the conditions of an experiment. In the former case, statistical features which maximize some criteria, such as the amount of variance explained, may be irrelevant for distinguishing clinical categories or experimental conditions whose means overlap. In contrast, while expert knowledge is invaluable for the initial choice of appropriate measurements and for the final interpretation of results, features chosen by experts may be highly

correlated with each other and therefore not effective in combination. While experts may have a good intuitive grasp of multidimensional patterns, they cannot determine the best combinations of features from a superset of features to characterize thousands of millions of data samples. Furthermore, the brain's actual computational algorithms underlying experts' decisions (as opposed to experts' English language descriptions of the rules they use) are not often available for inspection since they are coded in the "wetware" of the brain.

We have found iterative neural-network (NN) procedures to be useful in overcoming these limitations when analyzing neuroelectric signals from the human brain [2]–[5]. Constrained by expert knowledge, these techniques search for optimal or near-optimal connections of, and weightings between, application-specific features in data spaces for which human knowledge is incomplete [18]. However, in our experience, it is not useful to feed large sets of data into a neural net without constraints or guidance since our noisy, multidimensional data require the determination of combinations of a relatively small number of features (feature subsets) in order to generalize classification past the training data set. "Hidden units" in NN explicitly test combinations of features for discriminative power, but a combinatorial explosion is encountered when exhaustively selecting a small number of features from a larger set. A fully connected Hopfield-type network seemingly obviates the need for feature selection, but practical experience with noisy and time-varying experimental data suggests that resultant classification networks are likely to be far from optimal. In particular, Hopfield networks are likely to settle into local minima in these instances, even when simulated annealing methods are used. Multilayer perceptrons employing gradient search methods are prone to similar difficulties.

Our approach has been to use NN's to select combinations of application-specific features from larger sets chosen by experts (or expert systems) [6]–[13]. Big problems, such as discriminating the brain state corresponding to good and poor performance, are divided into subproblems. Small candidate sets of features are selected for the subproblems by reference to brain anatomy and neurophysiology. NN's are then sequentially applied to each of the feature sets. Network topology is determined by propagation of classification error back to connections and

Manuscript received February 22, 1988. This work was supported by the National Institute of Neurological and Communicative Diseases and Stroke, the U.S. Air Force Office of Scientific Research, and the National Science Foundation.

The authors are with the EEG Systems Laboratory, San Francisco, CA 94103.

IEEE Log Number 8821367.

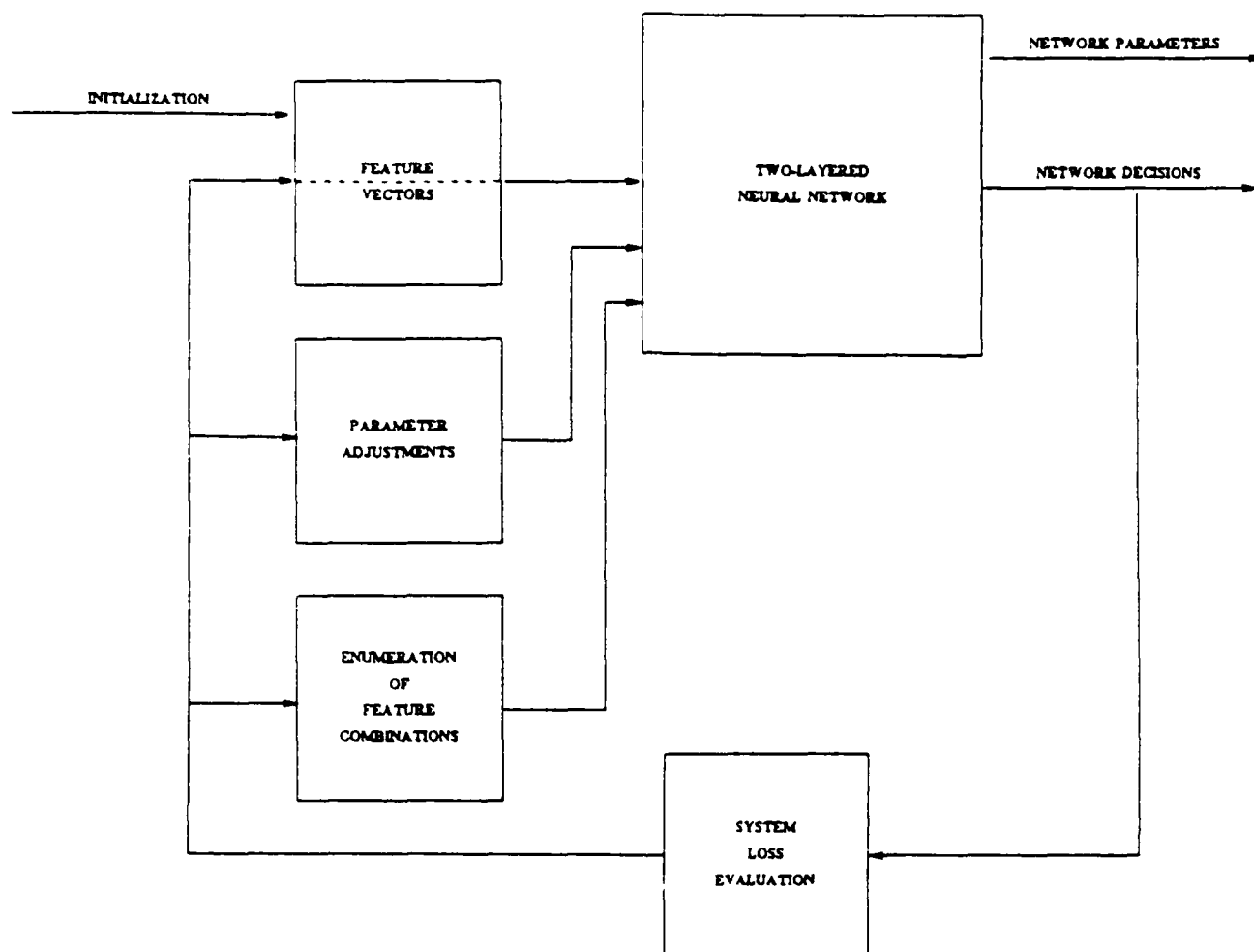


Fig. 1. Neural network (NN) for feature extraction and classification. Performance of this network is fed back to guide feature selection.

weighting of hidden units during training mode operation [16], [19]. To generate each network, the algorithm iterates a two-step procedure (Fig. 1). First a "network loss" is calculated for a two-layered network consisting of hidden threshold logic units (TLU's) previously chosen and each possible new hidden unit. Candidate TLU's are generated by the exhaustive enumeration of all feature subsets of a given size and computing a simple statistical classifier for each. The network loss is a function defined to reflect both the quantity and severity of classification errors. Error correction is propagated back to network parameters by minimizing this measure of the difference between desired and actual output. This process iterates until adding more units does not result in significant improvements. For most of the applications described here, several hundred patterns are used to select a final set of about six hidden units for each of up to several hundred subproblems. Independent data are then passed through the network to test the validity of the final network equations. The significance of this test is determined by the binomial distribution and by comparison to results obtained when data of random class are passed through the

network. The performance of each network is fed back to guide feature selection. Several hundred thousand of these network configurations are trained to test possible feature subsets for each subproblem of each application. The final network parameters frequently yield useful information about the relevance of each feature for classification.

While larger networks (such as a three-layer perceptron with backward propagation and a sigmoid nonlinearity) can generate more complicated decision surfaces, we have found the critical practical problem to be the estimation of network parameters from noisy data. This problem is not solved by a more complex network, but can instead be treated with classifier-directed feature selection methods. Evaluation of hundreds of thousands of simpler classifiers results in small feature subsets which generalize well to new data in the presence of noise.

#### APPLICATIONS OF NEURAL-NETWORK SIGNAL PROCESSING TO BRAIN RESEARCH

Over the last ten years, we have found this approach to be useful in our multidimensional signal processing work with signals of unknown characteristics and signal-to-

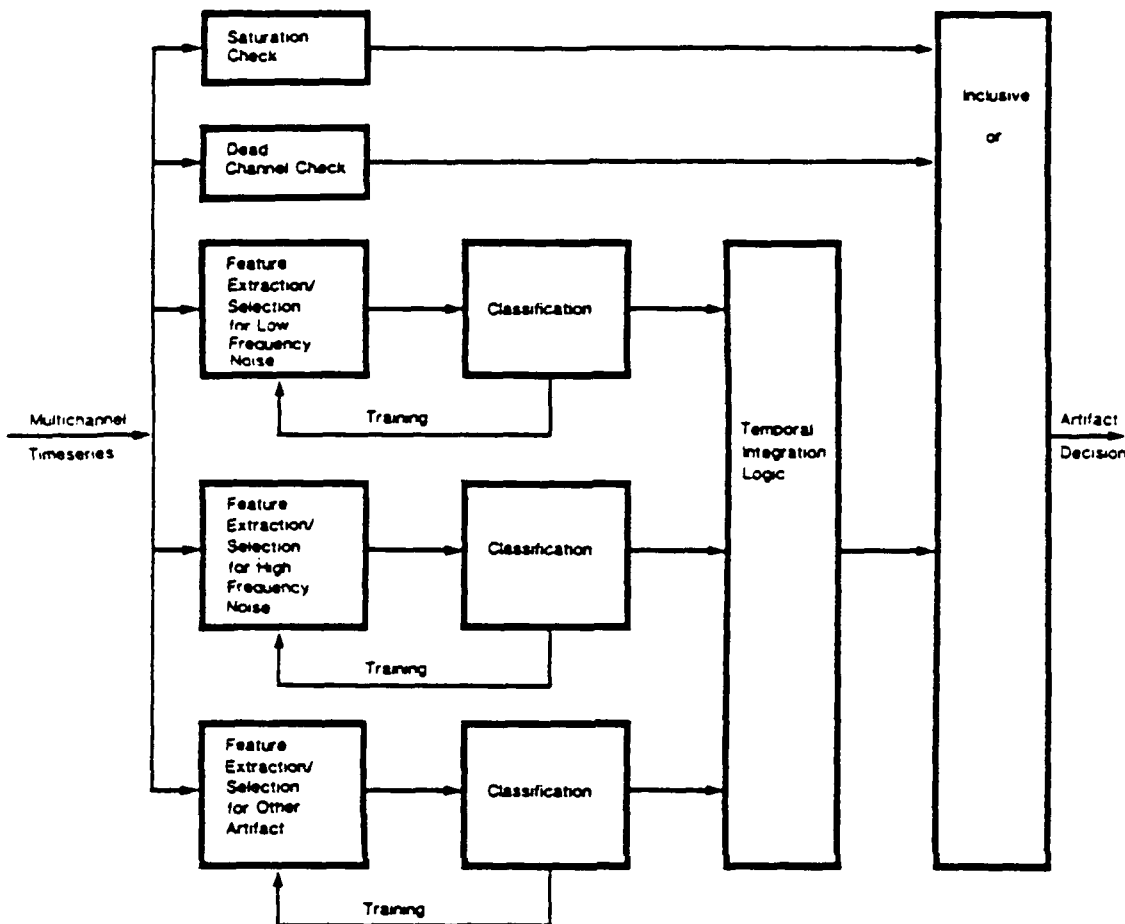


Fig. 2. NN artifact (contaminant) detection. A system consisting of five parallel detectors is used to find contaminants.

noise ratios well below one. We now review some of these applications.

#### A. Waveform Detection

1) *Contaminant Detection—Replacing ad hoc Detectors:* The characterization of infrequent, morphologically variable transient events, such as contaminants arising from eye blinks, eye movement, or muscle potentials, is an essential component of neuroelectric signal analysis. Accordingly, a great deal of energy has been expended over the years in efforts to automatically detect these phenomena, but with mixed results (see review in Barlow [1]).

We have implemented an NN system for automatic rejection of contaminants of neuroelectric signals [5]. Expert knowledge of contaminant types is represented by training data which have been hand marked, rather than by explicit descriptions of the features a human uses to detect these events. These hand-marked data are used to train multilayered networks which are used to distinguish clean from contaminated data.

Parallel layered-network detectors are each specialized for a different type of contaminant (Fig. 2). Three of the detectors incorporate the layered NN classifier of Fig. 1 to choose and weight feature combinations. In this way,

sole reliance on ad hoc waveform detectors and manually set thresholds is replaced by a precise automated procedure. One detector uses low-frequency, neuroelectric signal power spectral density, cross-spectral density between neuroelectric signals and horizontal and vertical eye movement signals, and correlation coefficient between neuroelectric signals and vertical eye movement signals as features to detect eye blinks and eye-movement contamination. Another layered-network detector uses neuroelectric signal power spectral density, zero-lag autocorrelation, and the first-order AR predictor coefficient as candidates for muscle potential and steady-state high-frequency instrumental contamination. An optional third detector uses the same type of features for other types of contaminant that users wish to train the machine to reject. Features are evaluated over half-second intervals every 125 ms of the time series. Classification decisions are made every 125 ms using a nonlinear interpolation of neighboring decisions. Several thousand segments are used for each training class, and an equal number for each test class.

For each detector, the final feature subset was determined by an exhaustive search for subsets of plausible features. Each possible subset was trained and then tested on independent sets of hand-marked data from one or more

subjects. The resulting networks were then used for classification with other data from the same or new subjects. The system frequently finds contaminants which would be difficult to detect with any static setting of signal amplitude thresholds. Fig. 3 shows a sample eye-blink contaminant and two channels of time series which were marked by the system. While the first channel could easily be rejected by a simple fixed-amplitude threshold detector, the second contains contaminated variance "buried" in the neuroelectric signals.

In practice, the automated system performs a first pass through the data, replacing one of the two human scorers who formerly hand marked the data. A human scorer then rapidly reviews the system's decisions. Routine use of this system over the last two years has reduced by a factor of 15 the man hours required to edit contaminated data from recordings with up to 64 channels.

**2) Evoked Potential Estimation:** Evoked potentials (also called event-related potentials or ERP's) are neuroelectric signals which are time registered to an experimental stimulus or a subject's response. Because the amplitude of these stimulus or response-related neuroelectric signals can be smaller than the neuroelectric activity unrelated to the experimental events, signal processing must be used to extract estimates of their waveforms. For those cases where the timing and morphology of each evoked potential has some similarity over many stimulus presentations (trials), a simple average will improve the signal-to-noise ratio by a factor of the square root of the number of trials. However, real evoked potentials frequently vary significantly in both respects, leading to a requirement of many stimulus repetitions before a useful average can be obtained. Many methods exist for computing improved estimates of averaged event-related potentials, given some assumptions about the underlying signal characteristics [17]. For many of our experiments on higher cognitive brain functions, we cannot assume that stimulus-related signals are measurable in every trial nor can we presume much knowledge about statistical properties of event-related signal and unrelated "noise." We have developed a method using NN's for averaged ERP estimation without the first assumption, and with minimal assumptions about signal and noise properties [9]. In particular, we assume that the noise process is roughly stationary, and the non-stationary signal process can be time registered to an external event. We can then synthesize a stationary noise process with statistics very close to those of the actual noise by randomizing the start point of the analysis interval for each trial. Since the nonevent-related potentials are stationary and the power in an individual trial is primarily nonevent-related ( $SNR \ll 1$  over the trial), the synthesized ensemble has statistics quite close to those of the "noise." Discriminability of the time-registered trials from this ensemble can be taken as a measure of signal strength.

We have used NN procedures to select trials with discriminable event-related signals in a defined time interval by attempting to discriminate the set of time-registered

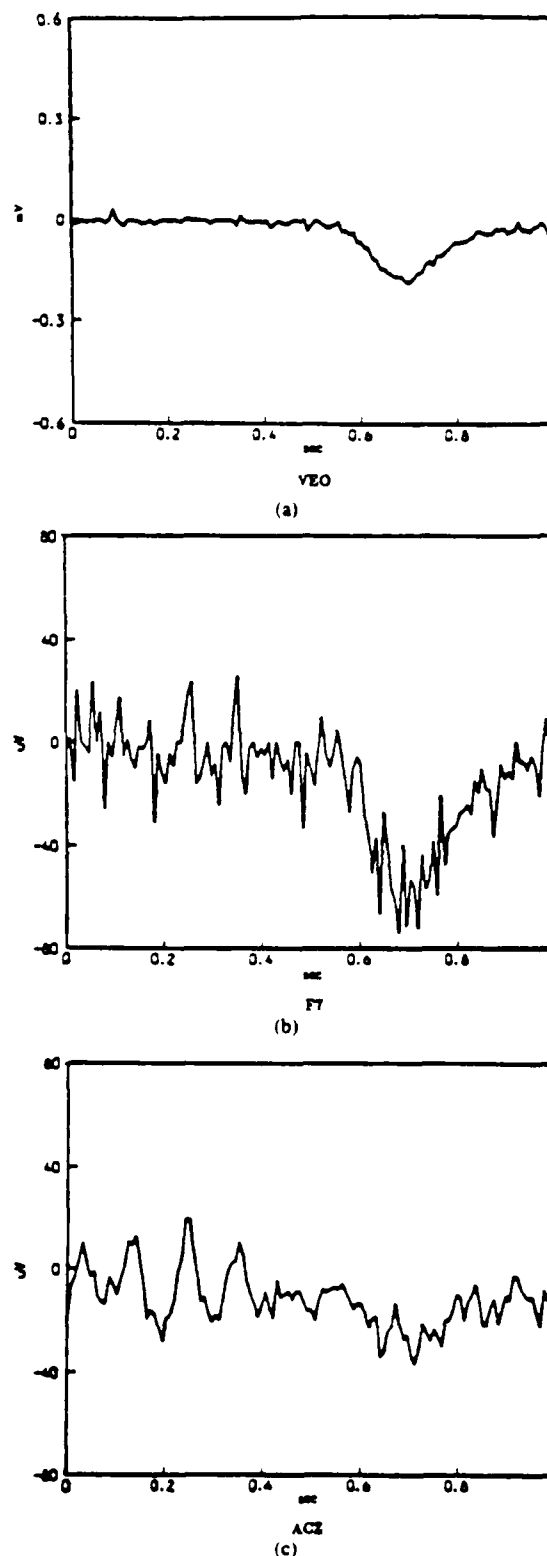


Fig. 3. Three channels of neuroelectric time series with eye blink contaminant detected by NN system of Fig. 1. (a) The vertical eye movement time series (VEO) clearly shows a blink 0.6–0.8 s past the stimulus onset. (b) Left frontal neuroelectric channel (F7) shows a large eye-contaminant wave which could easily be detected with a simple fixed-threshold algorithm. (c) Anterior midline precentral neuroelectric channel (ACZ) is also contaminated by the eye blink, but the maximal or integrated amplitudes would not trigger an amplitude threshold device since the just-prior uncontaminated signal has a larger amplitude than the contaminant.

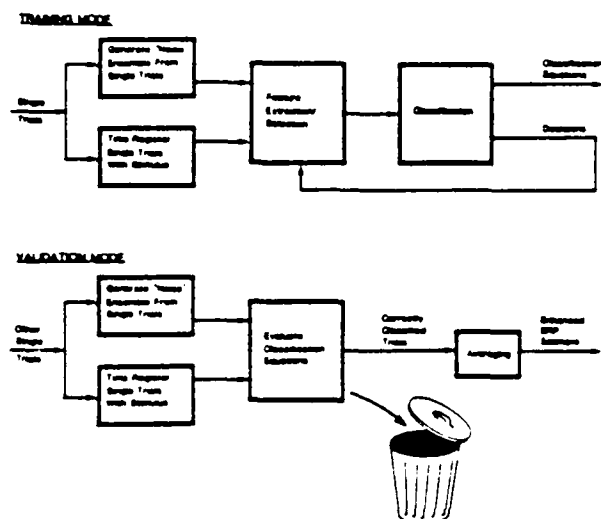


Fig. 4. NN event-related potential (ERP) estimation.

trials from the set of artificially made "noise" trials (Fig. 4). The layered-network classifier of Fig. 1 is used to find those trials (time registered to a stimulus) which have a consistent event-related signal in an interval of interest. This is done by comparing the ensemble of candidate trials to the ensemble of "noise" trials synthesized from the same data. "Enhanced" averages are then formed from the selected signal-bearing trials.

For each neuroelectric signal channel, an equation was derived which discriminates the "noise" trials by applying the NN algorithm to a prelabeled training set consisting of two-thirds of the total trials. The equation was tested on the remaining third of the trials. This procedure was repeated for each third of the data (using the remaining two-thirds for training). This multiple partitioning, or jackknife cross validation, reduced sampling error due to test set selection. If overall classification was significant, trials which were classified as containing event-related signals were then selected. The averages computed from these trials show enhancement of evoked potential peaks in the chosen interval (Fig. 5). In the example shown in the figure, the positive peak 391 ms after the stimulus (P391) is 31 percent larger in the enhanced average. The averages of unselected trials are relatively flat in that interval.

Thus, using an NN procedure to reject realizations with a low signal-to-noise ratio, the estimate of a consistent signal component may be enhanced without prior assumptions about the statistical properties of the signal and noise inherent in techniques such as minimum mean-square error (MMSE) filtering. When knowledge of the signal is limited, this approach can still be used to pick realizations which maximally differ from the ongoing noise.

### B. Feature Extraction

Neuroelectric signals are sensitive indexes of the central nervous system effects of psychotropic medications, and have proven useful in distinguishing broad classes of

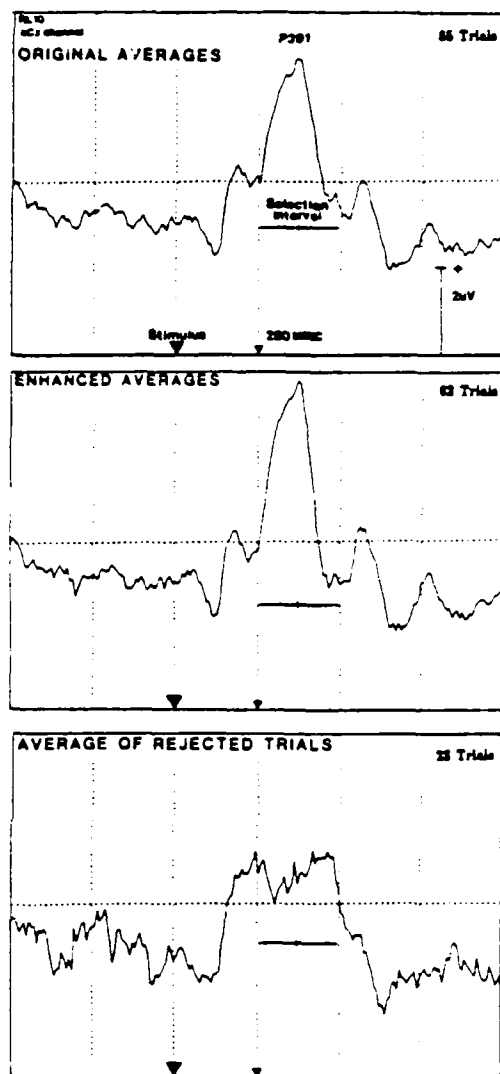


Fig. 5. Averaged stimulus-registered visual ERP waveforms obtained by presenting a stimulus 85 times (top), enhanced average resulting from NN selection of those stimulus trials with detectable event-related brain signals (center), and average of trials without detectable signals (bottom).

drugs such as stimulants, sedatives, antipsychotics, etc., [14], [15]. The problem of distinguishing subtypes of the same class of drugs is more difficult, however. As in other applications, the major problem is choosing the most effective subset of signal features from a large candidate population. As a contribution to this area, we have used NN techniques to select subsets of neuroelectric spectral features which could distinguish each of three benzodiazepine sedative hypnotic drugs (sleeping pills) from a placebo [5]. This resulted in a set of feature "signatures" which characterize the effects of each of these drugs.

The effects of multiple therapeutic doses of three benzodiazepines (quazepam, triazolam, and flurazepam) on periods of slow wave, nonrapid-eye-movement sleep were assessed. Such periods from all-night sleep recordings of eight healthy men were spectral analyzed, and the data of



each drug were compared to the placebo using the NN algorithm described above. Equations were developed and validated which characterized the effects of the drugs on the eight subjects.

Spectral bins from 0.5 to 15.5 Hz in 0.5 Hz steps represented the average spectral intensity for a specific frequency component during a given 16 s interval. Fig. 6 shows stacked spectral displays for the three drugs and the placebo from one of the eight subjects. A decrease of the delta and theta bands (0.5–3.5 and 4–7.5 Hz, respectively) and increase of the sigma band (12–14.5 Hz) spectral intensity existed for all drugs. However, it is difficult to make precise comparisons between the drugs from this sort of visual display, and the eight subjects differed considerably. Furthermore, the mean spectral intensities were not significantly different between drugs.

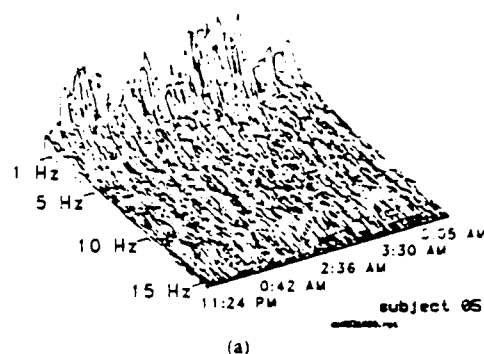
Using the layered-network algorithm described above, we determined which of the seven 0.5 Hz components of each of three conventional frequency bands (called delta, theta, and sigma) were optimal for discriminating each drug from placebo. Then the seven best frequency components (three delta, two theta, two sigma) were combined in a single analysis called the "full-spectrum" analysis.

For each of the four sets of spectral measures (delta, theta, sigma, full spectrum), for each of the nine hypotheses (each of the three drugs versus placebo in each third of the evening), each subject's drug and placebo spectral intensity observations were converted into standard scores (0 mean and unit variance) in order to reduce the effect of irrelevant differences in overall signal amplitude between subjects. Each standardized spectral estimator for each drug was then discriminated from the placebo, yielding a percent accuracy of discrimination. The discriminating equations were validated using three leave-out-one-third replications as described in the section on evoked potential estimation. The significance of the classification accuracies was determined by reference to the mean and variance of nine "pseudoclassifications." A pseudoclassification consisted of attempting to discriminate the placebo spectral observations of one-third of the night from those of another third. An index of a drug's effect, from 0 to 100 percent, was formed by subtracting the expected placebo-versus-placebo from the drug-versus-placebo classification accuracy, and then dividing the maximum possible drug-versus-placebo minus placebo-versus-placebo accuracy. For example, if the drug-versus-placebo accuracy was 75 percent, and if the placebo-versus-placebo accuracy was 51 percent, then the percent drug effect would be  $(75-51)/(100-51) = 49$  percent.

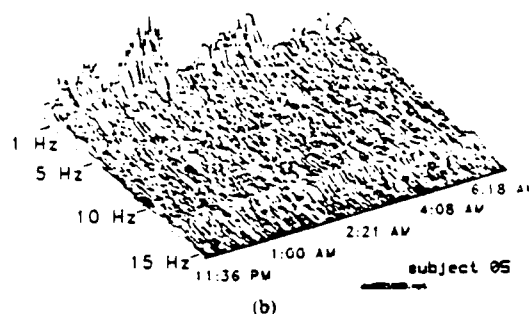
The spectral signature of each drug was determined by extracting the weightings given to the individual frequency components of significant drug-versus-placebo equations. This was done by weighting each feature in an equation by: 1) the relative size of its discriminant function term, 2) the relative size of its TLU, and 3) the negative log of the significance of the equation.

All three drugs differed markedly from the placebo dur-

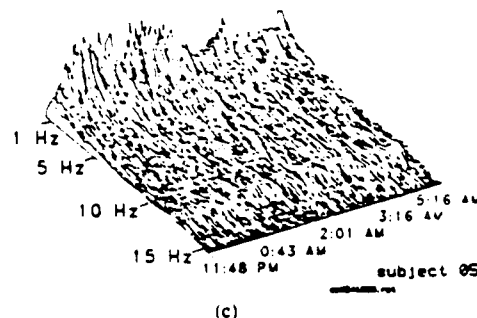
## Placebo



## Quazepam



## Triazolam



## Flurazepam

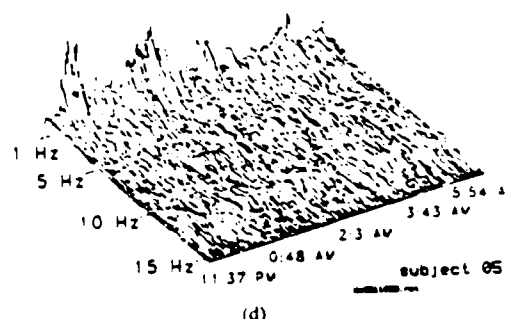


Fig. 6. Stacked spectral display of slow-wave sleep of Subject 5 after administration of a placebo (a), and three benzodiazepine sleeping pills (b)–(d). Each spectral line represents 16 s of slow-wave sleep.

ing each third of the evening. Flurazepam had the largest effect on the full spectrum of neuroelectric frequency components; quazepam and triazolam had smaller, equal effects. All drugs reduced delta and theta band, and increased sigma band spectral intensity, but to differing degrees and with their own characteristic spectral signatures. For instance, quazepam's signature (Fig. 7) was a predominant increase in the 12 Hz and a decrease in the 7.5 Hz components. The derivation of such a "spectral signature" as well as a single index of the overall drug effect is characteristic of NN signal processing analysis methods; the features chosen for discrimination can themselves be as instructive as the resulting classification. In particular, since the candidate features were transformed to standard scores, the feature weights suggest the relative importance of each feature.

### C. Pattern Classification and Brain State Prediction

The measurement of spatiotemporal neuroelectric patterns related to higher cognitive brain functions is a particularly difficult signal processing problem. The essential difficulty is a low SNR confounded by a plethora of possible signal features. In applying NN techniques, the goal is to physically interpret the selected features, the classification equations, and the relative classification performance between spatial and temporal constraint groups. When NN's are used to study the brain mechanisms of higher cognitive functions, interpretation of the classification equations can be more important than optimizing the accuracy of classification for differing cognitive tasks.

In our current use of NN to study cognitive functions, inputs to the networks consist of parameters derived from brain signals measured at up to 64 locations on the scalp of people playing specially contrived video-type games. In a typical experiment, about a gigabyte of raw brain data is recorded, from which several thousand replications of a thousand or so signal features are computed. Outputs of the networks consist of decisions as to which functional brain state the brain signal parameters represent. The connections and weights of the networks are interpreted to answer hypotheses about brain function. Neurological interpretation of the network parameters is made possible by using specific constraints, based on the anatomy of the cerebral cortex, for each of the networks. These constraints also permit an exhaustive search for globally optimal TLU's by reducing the number of combinations of brain signal features to a computable amount.

Fig. 8 shows the results of this analysis in a recent experiment [10], [12]. By extracting just those brain signals related to subjects' preparation to react to a number on a video screen, we found that certain areas of the brain appeared to be coordinating themselves in anticipation of the forthcoming numeric stimulus. We call these patterns "preparatory neural networks," and they are shown in Fig. 8 as hatched lines connecting different points on the head. The areas of the brain that appear to be important

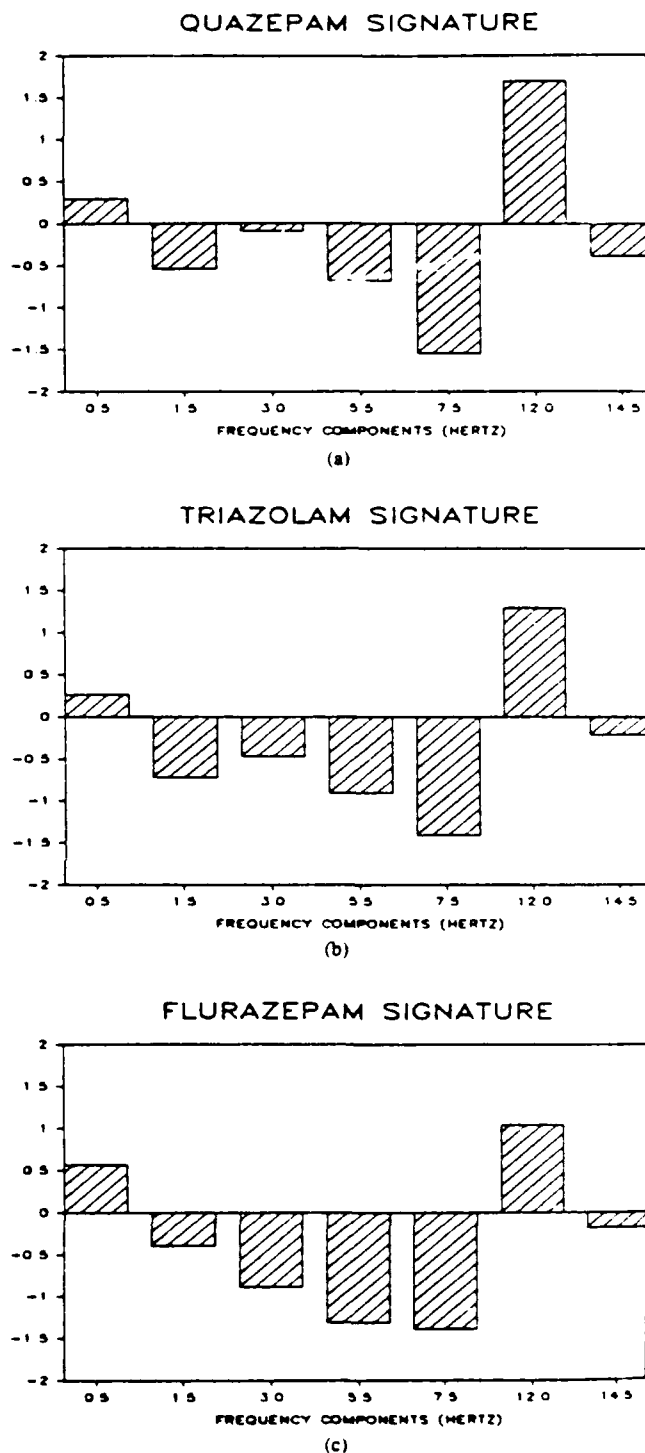


Fig. 7. (a)-(c) Characteristic spectral signatures of drug effects obtained for each drug from the coefficients of the classification equations. Ordinate is dimensionless relative weighting of spectral features.

in preparing for good performance are known as the left prefrontal cortex (the "cognitive sequencing" area), the midline premotor cortex (the area which is the "executive" of all voluntary movements), and the motor and parietal cortices (areas involved in controlling finger movements and feeling the pressure of the response but-

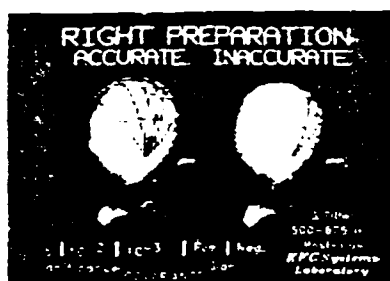


Fig. 8. Patterns of "preparatory neural networks" showing apparent coordination of certain areas of the brain in anticipation of a forthcoming numeric stimulus.

ton against the finger). When these areas are not involved or not well coordinated during preparation, the subject's performance is likely to be inaccurate. Many errors, it seems, are predetermined by the failure to establish a proper preparatory network during the split second before the task. These preparatory networks are thus an indication of the importance of the human brain's ability to create and constantly update models of itself and the external world.

Obtaining this result required using the NN procedure in a number of ways. First, trials with detectable signals were selected using the evoked potential enhancement technique described earlier. After a spatial Laplacian was calculated for each channel, between-channel covariances were computed across 375 ms intervals for trials low pass filtered at 3 Hz. Covariances for decimated time points prior to the stimulus in each trial were considered possible features to distinguish subsequent performance accuracy. The combinatorial problem of selection of a subset of these features was reduced to only considering those covariances which were statistically significant in a previous analysis of filtered, enhanced averages. Analyses were done for seven subjects, both as a group (equations formed from six of the subjects, and tested on the seventh), and as individuals (classification of one-fifth of the trials using equations from the other four-fifths, repeated over all fifths). The overall discrimination of subsequently accurate from subsequently inaccurate trials for the group was 59 percent, which was significant at the 0.01 level for the number of feature patterns used. For the one subject with most trials, the average correct classification was 68 percent, which was significant at the 0.001 level. In other words, given a general superset of likely features, the NN algorithm was able to choose features which in combination would predict subsequent accuracy of performance on the task up to about two-thirds of the time. Both the significant levels of these classifications and the spatial specificity of the features selected to achieve the classification were consistent with a view that specific, spatially coordinated "neural preparatory sets" are an important determinant of the accuracy of human visuomotor performance.

In another experiment, we found neuroelectric pattern changes which preceded deterioration of performance as

subjects performed difficult concentration tasks for many hours [13]. Five fighter test pilots performed difficult visuomotor-memory tasks during a 10–14 h period. The NN pattern classification methods described above were used to measure the effects of prolonged concentration, and particularly to search for neuroelectric indicators which predicted the onset of deteriorating performance. The time series for each single trial was processed with a spatial Laplacian, and with a temporal low-pass filter with a cut-off of 3 Hz. Decimated intervals of length 0.5 s from each channel's time series were used to compute covariances between all pairwise combinations of the 18 neuroelectric signal channels. In the pilot with the most data, leading indicators were found which distinguished fully alert and incipiently impaired sets of trials with equally accurate performance 81 percent of the time (average of five leave-out-one-fifth validations). This initial result suggested that similar methods could be used to develop an on-line warning system so that people engaged in hazardous or critical work would be alerted to the possibility of impaired performance due to mental fatigue.

## DISCUSSION

We have described several applications of NN signal processing methods in which success of the application required more than a clever NN algorithm. In particular, expert specification of application-specific constraints, statistical procedures for generating reference noise distributions, and statistical procedures for checking validity and reliability were required. NN algorithms, when coupled with these and other analogous methods, may prove to be generally useful in signal processing. They can also serve as an explicit description of the parallel implementation of pattern recognition algorithms for a hardware realization.

In considering these methods, we should not confuse the term "neural network" with how a human brain actually works. The human brain accomplishes its prodigious feats of perceiving, thinking, and acting with somewhere between  $10^{11}$ – $10^{12}$  processing elements (neurons). A substantial subset of these elements (the pyramidal cells of the neocortex with their complex processing capabilities and connections with up to 50 000 other neurons) are more comparable to mainframe computers than they are to the op-amp model neurons of current NN algorithms. The human brain's processing elements are organized into several hundred major divisions, each comprised of millions to billions of neurons. These divisions are in turn organized into a few dozen major functional systems that perform such functions as analysis of light and sound and pressure to the body surface, control of muscles, linguistic encoding and decoding, and generation of models of self and world. Adaptive, purposive behavior is found at all levels of organization of the brain, down to the individual neurons themselves. Roughly three-fourths of the

brain is concerned with higher associative and executive functions not directly connected with processing sensory data and executing motor responses.

Consideration of the human brain thus suggests the need for quotation marks when referring to NN signal processing and pattern recognition systems as being "brain-like." Although there is no harm in giving anthropomorphic names to our algorithms and systems, it is not helpful in the long run to lose sight of the vast difference in scale and capability between the machines we create and the apparatus with which we create them. Our AI and our NN systems have "intelligence" in the same sense that a broad jumper could said to be flying (Chomsky, personal communication, 1984).

The lesson from real brains for designing better NN signal processing systems is the apparent necessity of devoting a major amount of resources in a self-organizing system to higher level executive functions that generate models of the system and the world external to it. In practical terms, this suggests a union of AI and NN systems, the context and goal direction being specified by the former and feature extraction and pattern recognition by the latter. In a limited way, such a union was required to make each of the sample applications reported here work well enough to be practical.

### CONCLUSIONS

We have reported four applications in brain research of NN signal processing and feature analysis:

- 1) contaminant detection for replacement of ad hoc detectors,
- 2) waveform detection for evoked-potential estimation,
- 3) feature extraction for identification of characteristic "signatures" of different sleeping pills,
- 4) pattern classification and state prediction for measuring human cognitive brain functions.

Analyses in these areas have traditionally depended heavily upon either expert selection of features or on rote application of statistical methods. The major significance of NN methods is that they provide an effective way of incorporating expert knowledge in a mathematical framework. The resulting blend has solved problems that were difficult to solve previously. The approach described here may well be applicable to many problems in signal interpretation.

Finally, we summarized the implications of current knowledge about brain function for computer engineers interested in using artificial neural network signal processing.

1) 10 000 op-amps do not make a brain. A better electronic analogy of a human brain would be a hundred billion mainframes, essentially globally connected, each running the correct program.

2) While low-level networks are important for both neural systems and engineering applications, the example of the human brain suggests that self and world models

generated by high-level executive systems are critical to system function.

### REFERENCES

- [1] J. S. Barlow, "Artifact processing (rejection and minimalization) in EEG data processing," in *Handbook of Electroencephalography and Clinical Neurophysiology, Vol. 2: Clinical Applications of Computer Analysis of EEG and Other Neurophysiological Signals*, F. H. Lopes da Silva, W. Storm van Leeuwen, and A. Remond, Eds. Amsterdam, The Netherlands: Elsevier, 1986, pp. 15-55.
- [2] A. S. Gevins, "Pattern recognition of human brain electrical potentials," *IEEE Trans. Pattern Anal. Machine Intell.*, vol. PAMI-2, pp. 383-404, Sept. 1980.
- [3] —, "Analysis of the electromagnetic signals of the human brain: Milestones, obstacles, and goals," *IEEE Trans. Biomed. Eng.*, vol. BME-31, pp. 833-850, Dec. 1984.
- [4] —, "Statistical pattern recognition," in *Handbook of Electroencephalography and Clinical Neurophysiology, Vol. 1: Methods of Analysis of Brain Electrical and Magnetic Signals*, A. Gevins and A. Remond, Eds. Amsterdam, The Netherlands: Elsevier, 1987, pp. 541-582.
- [5] A. S. Gevins and N. H. Morgan, "Classifier-directed signal processing in brain research," *IEEE Trans. Biomed. Eng.*, vol. BME-33, pp. 1054-1068, Dec. 1986.
- [6] A. S. Gevins, G. Zeitlin, J. Doyle, C. Yingling, R. Schaffer, E. Callaway, and C. Yeager, "Electroencephalogram correlates of higher cortical functions," *Science*, vol. 203, pp. 665-668, 1979.
- [7] A. S. Gevins, J. Doyle, B. Cutillo, R. Schaffer, R. Tannehill, J. Ghannam, V. Gilcrease, and C. Yeager, "Electrical potentials in human brain during cognition: New method reveals dynamic patterns of correlation of human brain electrical potentials during cognition," *Science*, vol. 213, pp. 918-922, 1981.
- [8] A. S. Gevins, R. E. Schaffer, J. C. Doyle, B. A. Cutillo, R. S. Tannehill, and S. L. Bressler, "Shadows of thought: Shifting lateralization of human brain electrical patterns during brief visuomotor task," *Science*, vol. 220, pp. 97-99, 1983.
- [9] A. S. Gevins, N. H. Morgan, B. Cutillo, J. Doyle, and S. Bressler, "Improved ERP estimation via statistical pattern recognition," *EEG Clin. Neurophysiol.*, vol. 64, pp. 177-186, 1986.
- [10] A. S. Gevins, N. H. Morgan, S. L. Bressler, B. A. Cutillo, R. M. White, J. Illes, D. S. Greer, J. C. Doyle, and G. M. Zeitlin, "Human neuroelectric patterns predict performance accuracy," *Science*, vol. 235, pp. 580-585, 1987.
- [11] A. S. Gevins, G. M. Zeitlin, C. D. Yingling, J. C. Doyle, M. F. Dedon, R. E. Schaffer, J. T. Roumasset, and C. L. Yeager, "EEG patterns during 'cognitive' tasks. I. Methodology and analysis of complex behaviors," *EEG Clin. Neurophysiol.*, vol. 47, pp. 693-703, 1979.
- [12] A. S. Gevins, S. L. Bressler, N. H. Morgan, B. A. Cutillo, R. M. White, D. S. Greer, and J. Illes, "Event-related covariances during a bimanual visuomotor task. Part I: Methods and analysis of stimulus and response-locked data," *EEG Clin. Neurophysiol.*, in press, 1988.
- [13] A. S. Gevins, B. A. Cutillo, R. M. Fowler-White, J. Illes, and S. L. Bressler, "Neurophysiological patterns of operational fatigue. Preliminary results," in *Proc. NATO Aerosp. Med. Panel Symp.*, Trondheim, Norway, 1987.
- [14] W. M. Hermann, Ed., *Electroencephalography in Drug Research*. New York: Gustav Fischer, 1982.
- [15] W. M. Hermann and E. Schaefer, "Pharmacology-EEG: Computer EEG analysis to describe the projection of drug effects on a functional cerebral level in humans," in *Handbook of Electroencephalography and Clinical Neurophysiology, Vol. 2: Clinical Applications of Computer Analysis of EEG and Other Neurophysiological Signals*, F. H. Lopes da Silva, W. Storm van Leeuwen, and A. Remond, Eds. Amsterdam, The Netherlands: Elsevier, 1986, pp. 15-55.
- [16] R. D. Joseph, "Contributions to perception theory," Ph.D. dissertation, Cornell Univ., Ithaca, NY, 1961.
- [17] G. D. McGillem and J. I. Aunon, "Analysis of event-related potentials," in *Handbook of Electroencephalography and Clinical Neurophysiology, Vol. 1: Methods of Analysis of Brain Electrical and Magnetic Signals*, A. S. Gevins and A. Remond, Eds. Amsterdam, The Netherlands: Elsevier, 1987, pp. 131-169.
- [18] N. Morgan and A. S. Gevins, "Ignorance-based signal estimation given multiple noisy realizations," in *Proc. Int. Conf. Acoust. Speech, Signal Processing (ICASSP'86)*, Tokyo, Japan, 1986.

- [19] S. S. Viglione, "Applications of pattern recognition technology," in *Adaptive Learning and Pattern Recognition Systems*, J. M. Mendel and K. S. Fu, Eds. New York: Academic, 1970, pp. 115-161.



Alan S. Gevins (M'73-SM'79) was educated at the Massachusetts Institute of Technology, Cambridge, and pursued research in pattern recognition of EEG's at the University of California School of Medicine in San Francisco.

He has been the Director and Chief Scientist of the EEG Systems Laboratory, San Francisco, CA, since 1974. He is known for both engineering work in signal processing and for basic science studies of human higher brain functions.



Nelson H. Morgan (S'76-M'80-SM'87) received the Ph.D. degree in electrical engineering and computer science from the University of California, Berkeley, in 1980 where he conducted research into discrete-time signal processing methods.

He is the Chief Engineer of the EEG Systems Laboratory, San Francisco, CA. He directed speech and signal processing research at National Semiconductor and joined the EEG Systems Laboratory in 1984. His research and publications in the last five years have focused on the application of pattern recognition techniques to a variety of signal processing problems. He is also the author of a recent book on techniques for producing synthetic speech.

## Human Neuroelectric Patterns Predict Performance Accuracy

ALAN S. GEVINS, NELSON H. MORGAN, STEVEN L. BRESSLER, BRIAN A. CUTILLO, ROSEANN M. WHITE,  
JUDY ILLES, DOUGLAS S. GREER, JOSEPH C. DOYLE, AND GERALD M. ZEITLIN

## Human Neuroelectric Patterns Predict Performance Accuracy

ALAN S. GEVINS, NELSON H. MORGAN, STEVEN L. BRESSLER,  
BRIAN A. CUTILLO, ROSEANN M. WHITE, JUDY ILLES,  
DOUGLAS S. GREER, JOSEPH C. DOYLE, GERALD M. ZEITLIN

In seven right-handed adults, the brain electrical patterns before accurate performance differed from the patterns before inaccurate performance. Activity overlying the left frontal cortex and the motor and parietal cortices contralateral to the performing hand preceded accurate left- or right-hand performance. Additional strong activity overlying midline motor and premotor cortices preceded left-hand performance. These measurements suggest that brief, spatially distributed neural activity patterns, or "preparatory sets," in distinct cognitive, somesthetic-motor, and integrative motor areas of the human brain may be essential precursors of accurate visuomotor performance.

**P**REPARATORY SET FOR HUMAN VISUOMOTOR performance, defined as a state of readiness to receive a stimulus or make a response (1), has been studied by a variety of disciplines. Temporal properties of preparatory sets have been measured in information-processing studies, but such studies have not focused on the underlying neural systems (2). Spatial properties of preparatory sets measured in cerebral blood flow studies have revealed increased metabolic activity for sensory-specific focus of attention in superior prefrontal, midfrontal, and anterior parietal cortices (3). These studies have been limited, however, by the temporal resolution (1 minute or longer) of blood flow measurement techniques. Clinical neuropsychological studies have demonstrated that behaviors requiring preparatory sets (4) rely on intact lateral frontal regions (5), but variability in size and location of lesions has limited the spatial specificity of such studies in localizing normal function. And although scalp-recorded brain electrical and magnetic recordings provide both spatial and temporal information on neural activity underlying preparatory sets, studies of the contingent negative variation (CNV), an event-related brain potential component thought to be related to preparatory set, have often yielded controversial or ambiguous results (6).

Recording from 26 electrodes and using several signal-enhancing procedures, we

measured the rapidly changing spatial patterns of mass neuroelectric activity associated with preparation and execution of precise right- and left-hand finger pressures in response to visual numeric stimuli. We found differences occurring during the prestimulus period between patterns associated with subsequently accurate and inaccurate performance. These group differences allowed discrimination of subsequent performance accuracy for both hands of individual subjects. Thus, a spatially specific, multicomponent neural preparatory set, composed of an invariant left frontal component and hand-specific central and parietal components, may be essential for accurate performance of certain types of difficult visuomotor tasks.

Seven healthy, right-handed male adults were recruited from the community and paid for their participation. They were required to exert rapid, precisely graded pressures (forces from 0.1 to 0.9 kg) followed by immediate release, with right- and left-hand index fingers in response to visual numeric stimuli (numbers 1 to 9). The stimulus was presented randomly on successive trials 1 second after a cue (the letter V lasting 0.3 second) that was slanted at a 30° angle to the right or left to indicate the required response hand (7). In "respond" trials, the

EEG Systems Laboratory, 1855 Folsom Street, San Francisco, CA 94103

stimulus was slanted in the same direction as the cue, and the subject was to respond quickly with finger pressure of the indicated hand, with a force corresponding to the stimulus number on a linear scale from 1 to 9. In a random 20% of the trials, the stimulus was slanted opposite to the cue and the subject was to make no response. These miscued "catch" trials ensured that subjects attended to the cues and stimuli. To help subjects calibrate their responses, the pressure produced was displayed 1 second after completion of each response (8).

Brain potentials from 26 scalp electrodes (9), vertical and horizontal eye movement potentials, and flexor digitorum muscle potentials were recorded onto magnetic tape at 128 Hz from 0.75 second before the cue to 1 second after feedback (10). The Laplacian operator, a spatial pattern enhancement technique, was applied to the brain potentials at every time point to reduce the blur distortion that results as potentials are transmitted from the brain to the scalp (11). Two independent raters edited the data for artifacts by visual inspection of brain, eye movement, and muscle potential polygraph channels. Trials with artifacts due to eye movement, head or electrode movement, or scalp muscle contamination were eliminated, as were trials with slow, bimodal, or delayed responses, or with flexor digitorum activity between the cue and the stimulus.

The remaining trials (60%) were then sorted for response accuracy, and the two sets of trials were balanced according to a number of criteria to avoid confounding performance variations due to transitory and longer lasting changes in arousal and learning with inaccuracy per se. Accurate and inaccurate data sets consisted of trials in which the error (deviation from required pressure) for each subject was, respectively, less and greater than his mean error over all remaining trials (12). Mean reaction time, averaged across all subjects, was consistent among hand and accuracy conditions (610 to 618 msec).

To quantitate the electrical activity of the brain, we measured the covariance (similarity of wave shape) between different pairs of electrodes over brief segments (187 or 375 msec) of event-related (cue, stimulus, response, feedback) waveforms averaged from the seven subjects (13-15). Covariances between each of the 120 combinations of the 16 Laplacian-transformed channels were computed from enhanced (16) and filtered average waveforms. We determined the covariance for each electrode pair by computing the cross-covariance function between their waveform segments, with the lag time for one channel with respect to the other varying from 0 to 125 msec. The value of

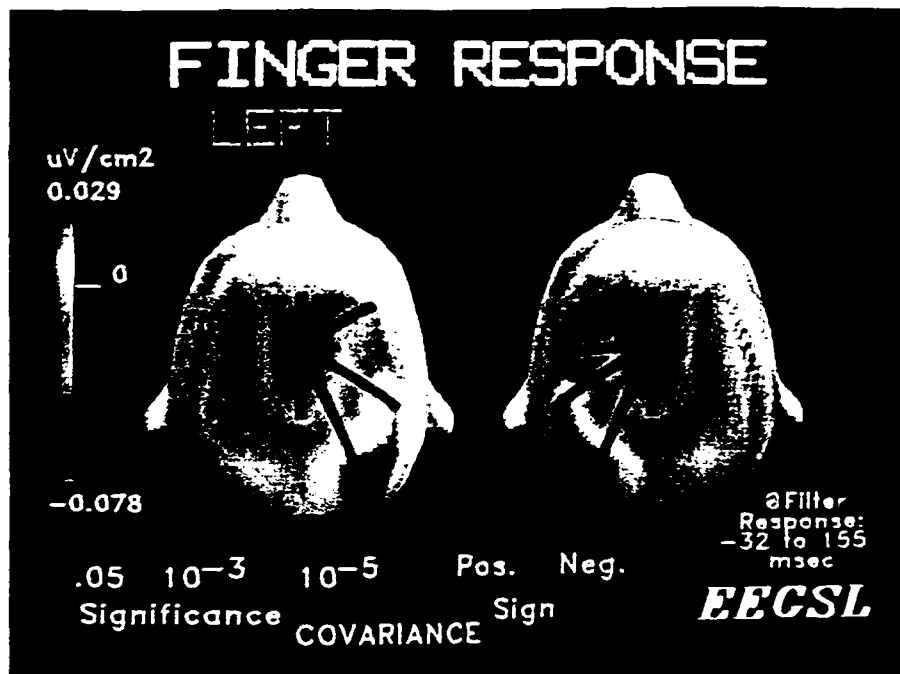


Fig. 1. Most significant, between-channel covariance patterns (colored lines), looking down at the top of the head, from the wave at the peak of the response superimposed on colored maps of that wave's amplitude. The motor-related wave was measured during a 187-msec interval centered on the peak of left-hand and right-hand index finger pressures from seven right-handed men (19). The thickness of a covariance line is proportional to the negative logarithm of its significance (from 0.05 to 0.00005) (17). A violet line indicates a positive covariance (motor-related waves with the same polarity), and a blue line indicates a negative covariance (motor-related waves with opposite polarities). The color scale at the left, representing wave amplitude, covers the range from the minimum to maximum values of the two maps. All covariances refer to the site overlying supplementary and premotor cortices. There is a strong lateralization of frontal, central, and antero-parietal covariances over the hemisphere contralateral to the responding hand, a result consistent with the lateralization of the amplitude maps.

covariance was the maximum absolute value of that function. For the wave at the peak of the response, covariances were analyzed to determine whether they were significantly different from noise values (17, 18); we could then compare the levels of significance of each electrode pair under different experimental conditions.

To validate the analysis in a known case, this procedure was applied to waveforms time-registered to the onset of the finger pressure response. The most significant left- and right-hand covariances occurred between electrodes overlying cortical regions involved in motor execution (Fig. 1) (19). These patterns of covariance presented much more spatially discrete information than their corresponding amplitude maps (20). In the 187-msec interval centered on the peak of the response (62 msec after response onset), right- and left-hand covariance patterns were nearly mirror images. In both patterns all covariances involved the midline antero-central site overlying the premotor and supplementary motor cortices. Covariances between this site and the left frontal, antero-central, central, and antero-parietal sites for right-hand responses, and between corresponding right-hemisphere

sites (except right antero-central) for the left hand, were all consistent with known motor-related cortical areas.

The procedure was then applied to the cue-to-stimulus period to study preparatory sets (21). Statistical comparison of the CNV amplitudes (Fig. 2) during an interval 500 to 875 msec after the cue did not reveal significant differences between accurate and inaccurate conditions (22). During this same period, however, well-defined between-channel covariance patterns related to subsequent accuracy were discovered. They first appeared in the interval centered 500 msec after the cue and became well differentiated between accurate and inaccurate conditions in the 500- to 875-msec interval (centered 313 msec before stimulus onset) spanning the late component of the CNV. The lack of muscle potential and eye movement signals in these intervals confirmed that these patterns were neural in origin (Fig. 3).

Covariance patterns during the period between the cue and the stimulus (Fig. 4) were distinct from those related to overt finger responses. During the interval from 500 to 875 msec after the cue onset, covariance patterns associated with subsequent



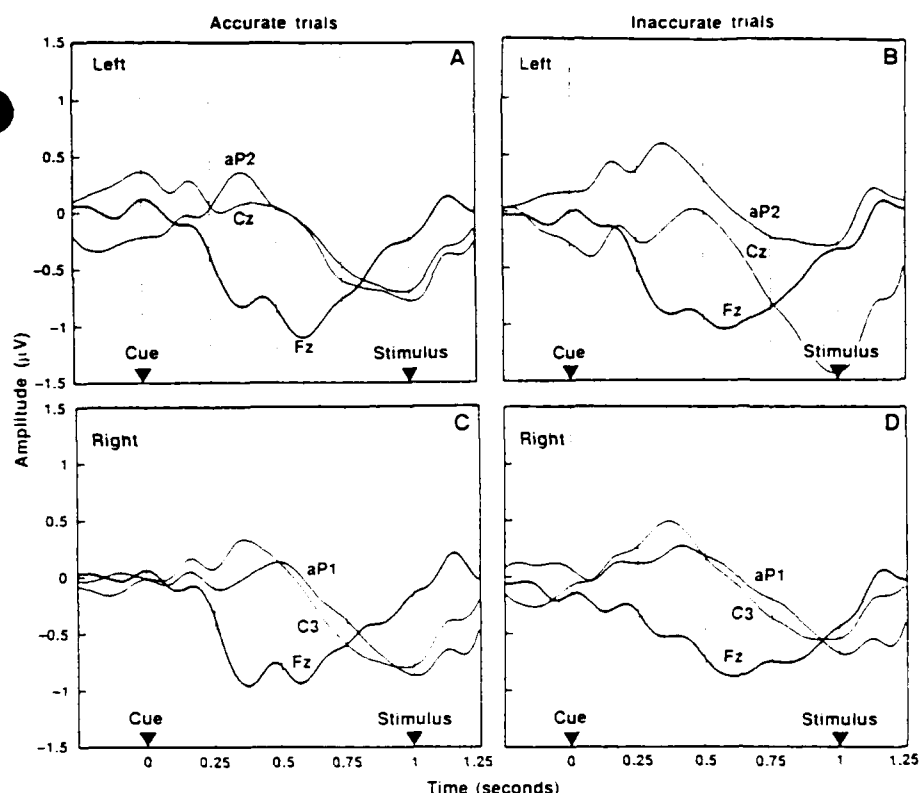


**Fig. 2.** Amplitudes of the CNV computed during the cue-to-stimulus period. Amplitudes between low-pass filtered (below 3 Hz), event-related Laplacian waveforms, averaged from seven subjects, are not significantly different for the comparison of (A) left-accurate (252 to 274 trials) with (B) left-inaccurate (254 to 284 trials) conditions, or (C) right-accurate (291 to 309 trials) with (D) right-inaccurate (282 to 304 trials) conditions.

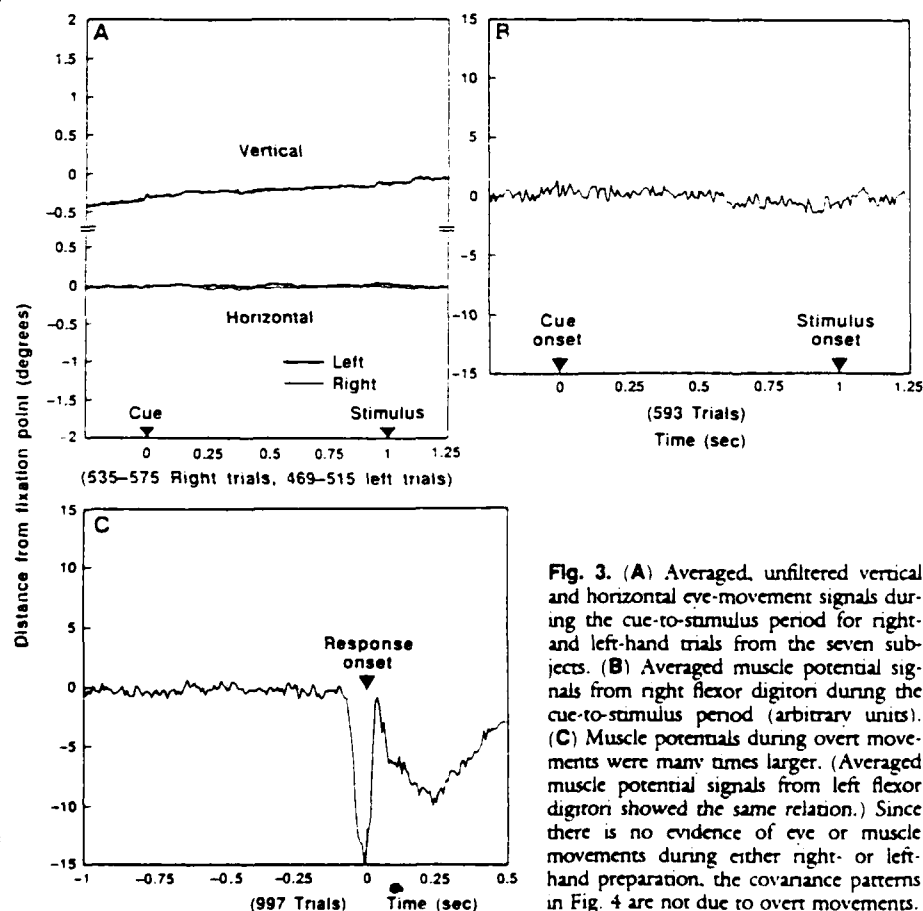


**Fig. 3.** (A) Averaged, unfiltered vertical and horizontal eye-movement signals during the cue-to-stimulus period for right- and left-hand trials from the seven subjects. (B) Averaged muscle potential signals from right flexor digitorum during the cue-to-stimulus period (arbitrary units). (C) Muscle potentials during overt movements were many times larger. (Averaged muscle potential signals from left flexor digitorum showed the same relation.) Since there is no evidence of eye or muscle movements during either right- or left-hand preparation, the covariance patterns in Fig. 4 are not due to overt movements.

accurate right-hand performance involved predominantly left hemisphere sites, particularly left frontal, central, parietal, and antero-parietal sites (23). All 24 significant covariances involved sites on the left side, and 18 (75%) of these were exclusively on the left side. The covariance pattern preceding subsequently accurate left-hand performance for this interval involved predominantly right-hemisphere sites. Of 18 significant covariances in this pattern, 13 (72%) involved right hemispheric sites. The right-sided central, parietal, and antero-parietal sites were most prominent, compared with corresponding prominent contralateral sites for the right-hand accurate pattern. The left frontal site was prominent before both left- and right-hand performance. The midline central and antero-central sites were prominent in the left-hand pattern but were not among the most prominent in the right-hand pattern.

Only two significant covariances were related to subsequently inaccurate right-hand performance in this interval, namely, left parietal with left frontal and antero-parietal with left frontal. In contrast, the subsequently inaccurate covariance pattern for the left hand was more bilateral and complex than the subsequently accurate pattern. The patterns for the two accuracy conditions differed both in scale and pattern for the left hand, but only in scale for the right hand (24). Unlike the between-channel covariance patterns, the CNV amplitude maps were highly similar for both accuracy conditions and hands and were not useful in determining what areas would covary.

Through the use of statistical pattern classification procedures, covariances shown in Fig. 4 were considered possible variables to distinguish subsequent performance accuracy. The trials of each of the seven subjects were classified by equations developed on the trials of the other six subjects (25). The overall discrimination of subsequently accurate from subsequently inaccurate trials was 59% ( $P < 0.01$ ) for right-hand and 57% ( $P < 0.01$ ) for left-hand performance. Discrimination of subsequent right-hand performance accuracy was above 57% for six subjects but was 50% for the seventh. For left-hand performance, discrimination for three subjects ranged from 56% to 67%, and was 53% or below for four subjects (who had fewer trials overall). Average classification of each fifth of the trials from the four subjects with lowest left-hand discrimination, calculated from equations developed from the other four-fifths, was 61% ( $P < 0.001$ ). This suggests that the four subjects had similar covariance patterns before left-hand performance, which differed from those of the other three subjects. The

Fig. 4. View of the significant ( $P < 0.05$ ) between-channel CNV covariance patterns, looking down at the top of the head, superimposed on maps of CNV amplitude. Measurements are from an interval 500 to 875 msec after the cue for subsequently accurate and inaccurate left-hand (top) and right-hand (bottom) visuomotor task performance by seven right-handed men. The thickness of a covariance line is proportional to the negative logarithm of its significance (from 0.05 to 0.001). A violet line indicates the covariance is positive, while a blue line is negative. Covariances involving left frontal and appropriately contralateral central and parietal electrode sites are prominent in patterns for subsequently accurate performance of both hands. The magnitude and number of covariances are greater before subsequently inaccurate left-hand performance by these right-handed subjects and are more widely distributed than the left-hand accurate pattern. For the right hand, fewer and weaker covariances characterize subsequently inaccurate performance. The amplitude maps are similar for the four conditions and do not indicate any of the specific differences evident in the covariance patterns.



greater uniformity for right- over left-hand discrimination suggests that there are similar covariance patterns among the strongly right-handed subjects preceding accurate and inaccurate right-hand performance, and a divergence of patterns preceding left-hand performance. Although there were differences in discriminative power between individuals, overall the group preparation patterns were effective in deciding an individual's subsequent performance accuracy. For the one subject with the most trials, an average classification of 68% ( $P < 0.001$ ) for subsequent right-hand and 62% ( $P < 0.01$ ) for subsequent left-hand performance was achieved by testing a separate equation on each fifth of his trials, formed from the other four-fifths.

Although the origin of these event-related, between-channel covariance patterns of preparatory sets is unknown (26), our results suggest that preparation for accurate performance in a visuomotor task involves several brain components (27): a cognitive component manifested by invariant activity at the left frontal covariance site, a hand-specific somesthetic-motor component manifested by the contralateral central and parietal sites, and an integrative motor component manifested by activity at the midline central and antero-central sites. The last component was strong in the pattern preceding accurate left-hand performance and weaker in the pattern preceding accurate right-hand performance. For both hands, preparatory covariance patterns were different from those accompanying actual response execution. Covariance patterns preceding inaccurate performance by each hand differed markedly. The relative lack of significant covariances preceding inaccurate right-



hand performance may be interpreted as evidence for a weakened preparatory set. By contrast, the complex, anatomically diffuse but strong patterns in the left-hand condition suggest that inaccurate performance by the nondominant hand of strongly right-handed subjects may result from erroneous, possibly confounded, preparatory sets.

Our evidence for distributed, coordinated preparatory components of human visuomotor performance is consistent with earlier studies of this behavior. The involvement of the left frontal site is consistent with evidence that preparatory sets in humans are synthesized and integrated in left dorsolateral prefrontal cortices (4, 5). The finding of

an appropriately lateralized parieto-central somesthetic-motor component is consistent with data that show neuronal firing patterns before motor responses in the motor cortex of nonhuman primates and localized potentials in the somesthetic cortex of humans at the same time (1, 28). Finally, a midline antero-central integrative motor component is consistent with known involvement of premotor and supplementary motor regions in initiating existing motor schemes and establishing new ones (3, 29).

Our results demonstrate that the human brain, unlike a fixed-program computer, dynamically "programs" its distributed, specialized subsystems in anticipation of the

need to process certain types of information and take certain types of action. When these preparatory sets are incomplete or incorrect, subsequent performance is likely to be inaccurate.

# REFERENCES AND NOTES

1. E. V. Evars, Y. Shinoda, S. P. Wise, *Neuropsychological Approaches to Higher Brain Functions* (Wiley, New York, 1984).
2. M. Posner, *Chronometric Explorations of the Mind* (Erlbaum, Hillsdale, NJ, 1978).
3. P. E. Roland, *J. Neurophysiol.* 48, 744 (1982); *Human Neurosci.* 4, 155 (1985); in *Brain Imaging and Brain Function*, L. Sokoloff, Ed. (Raven, New York, 1985), pp. 87-104.
4. D. T. Stuss and D. F. Benson, *The Frontal Lobes* (Raven, New York, 1986).
5. A. R. Luna, *Higher Cortical Functions in Man* (Basic Books, New York, 1966); H. L. Teuber, in *The Frontal Granular Cortex and Behavior*, J. M. Warren and K. Akert, Eds. (McGraw-Hill, New York, 1964); B. Milner and M. Petrides, *Trends Neurosci.* 7, 43 (1984); P. S. Goldman-Rakic, *ibid.*, p. 419.
6. J. J. Tecce, *Psychol. Bull.* 77, 73 (1972); J. W. Rohrbaugh, K. Svendsen, T. F. Sanquist, D. B. Lindsley, *Science* 208, 1165 (1980); A. W. K. Gaillard and W. Rutter, Eds., *Advances in Psychology*, vol. 10, *Tutorials in Event-Related Potential Research* (Elsevier, Amsterdam, 1983); A. Gevins and B. Cutillo, in *Application of Computer Analysis to EEG: Handbook of Electroencephalography and Clinical Neurophysiology*, F. Lopes da Silva, S. Van Leeuwen, A. Remond, Eds. (Elsevier, Amsterdam, 1987), vol. 2.
7. The cue, stimulus, and feedback were presented on a Videograph-11 cathode ray tube monitor located 70 cm from the subject and were of equal duration and visual angle (under 1°).
8. Feedback indicating exact response pressure to one-tenth of a stimulus unit was presented as a two-digit number 1 second after the peak of response. The feedback number was underlined to indicate a "win" when the response error was less than the recent performance level, which was updated on-line after each trial as the average error from the preceding five trials for each hand separately. This criterion made it harder for the subject to win the monetary bonus (5 cents) paid for "win" trials as performance improved. This technique and rest breaks minimized possible systematic changes in arousal. Monetary penalties (10 cents) were deducted only for responding to missed "catch" trials. Each subject performed between 900 and 1000 trials over a period of 5 to 6 hours, with frequent rest breaks. Subjects practiced the task, learning the motor control and the conditions of reward and penalty, in a pretesting session that continued until performance approached a stable asymptote.
9. Electrodes were placed according to an expanded version of the standard 10-20 electrode system, in which additional coronal rows of electrodes were interposed between the original rows. The anterior midline parietal electrode was used as reference.
10. The band pass had a 6-decibel/octave roll-off below 0.1 Hz and a 24-decibel/octave roll-off above 50 Hz. The roll-off below 0.1 Hz was gradual enough to allow sensitivity to ultralow-frequency brain potential components.
11. B. Hjorth, *EEG Clin. Neurophysiol.* 39, 526 (1975); *Am. J. EEG Technol.* 20, 121 (1980); P. L. Nunez, *Electric Fields in the Brain: The Neurophysics of EEG* (Oxford Univ. Press, New York, 1981). This operation removed the effect of the reference channel. Peripheral channels were not transformed because application of the Laplacian operator to an electrode requires surrounding electrodes, which are absent for channels at the edge of a recording array. Sixteen channels remained: left and right frontal (F3 and F4); midline frontal (Fz); left and right antero-central (aC3 and aC4); midline antero-central (aCz); left and right central (C3 and C4); midline central (Cz); left and right antero-parietal (aP1 and aP2); midline antero-parietal (aPz); left and right parietal (P3 and P4); midline parietal (Pz); and midline antero-occipital (aOz).
12. For right- and left-hand accurate performance, mean error was 0.35 (range, 0.24 to 0.52), and 0.39 (range, 0.28 to 0.51), respectively. For right- and left-hand inaccurate performance, mean error was 1.62 (range, 1.18 to 1.96) and 1.66 (range, 1.40 to 2.18), respectively. Classifying performance separately for each individual compensated for between-subject performance differences; hence, each data set contained trials from each subject. Outlying trials on the distribution of recent performance level were eliminated to ensure that accurate and inaccurate data sets did not differ from each other according to factors that could be related to transitory changes in arousal. Accurate and inaccurate trials were evenly distributed throughout the recording session.
13. This approach is based on the hypothesis that when areas of the brain are functionally related, the wave shapes of their macropotentials are consistently similar [M. N. Livanov, *Spatial Organization of Cerebral Processes* (Wiley, New York, 1977); W. Freeman, *Mass Action in the Nervous System* (Academic Press, New York, 1975); in (14); A. Gevins et al., *Psychophysiology* 22, 32 (1985)].
14. A. Gevins and A. Remond, *Handbook of Electroencephalography and Clinical Neurophysiology* (Elsevier, New York, in press), vol. 1, chap. 8.
15. A. Gevins et al., *Science* 213, 918 (1981); A. Gevins et al., *ibid.* 220, 97 (1983).
16. Enhanced averages were formed from sets of trials selected as follows: for each channel, sets of single-trial data samples in a 250-msec interval centered 750 msec after the cue were submitted to a mathematical pattern classification program. The program attempted to discriminate the event-related trials from a "noise" data set with statistical properties similar to the ongoing electroencephalogram in corresponding channels. In each interval, significantly distinguished channels ( $P < 0.05$ ) were tabulated for each person. The enhanced averages were formed from those trials in which a majority of the tabulated channels were significantly classified [A. Gevins, N. Morgan, S. Bressler, J. Doyle, B. Cutillo, *EEG Clin. Neurophysiol.* 64, 177 (1986)].
17. The maximum absolute value of covariance was converted to a significance (after square-root transformation) by comparison with a noise median and an estimate of noise variance through the use of a Tukey bivariate scale estimate. These statistics were determined from sample distributions of the square root of zero-lag covariances between intervals centered around samples with the minimum energy envelope derived from the Hilbert transform. Duncan's correction procedure was used to control for the 120 comparisons within each interval. Detailed signal-processing methods and analyses of stimulus-, response-, and feedback-related patterns have been developed (18).
18. A. Gevins et al., in preparation.
19. D. H. Ingvar and L. Philipson, *Ann. Neurol.* 2, 230 (1977); C. F. Pieper, S. Goldring, A. B. Jennv, J. P. McMahon, *EEG Clin. Neurophysiol.* 48, 266 (1980); A. Foit, B. Larsen, S. Harton, E. Skunhoj, N. A. Lassen, *ibid.* 50, 426 (1980); P. E. Roland, B. Larsen, N. A. Lassen, E. Skunhoj, *J. Neurophysiol.* 43, 118 (1980). The major peak in the Laplacian waveform during the response was centered 62 msec after response onset and was approximately 190 msec wide; therefore, a 4- to 7-Hz bandpass filter and a covariance interval of 187 msec were used. Given the high signal strength of overt movement and the resulting large number of significant response-related covariances, only the top standard deviation of significant covariances could be shown in Fig. 1 without creating an overly complex display. If all significant covariances are considered, left-sided covariances were significantly greater than the comparable right-sided ones by the  $t(78) = 18.5$ ,  $P < 0.0001$  for the right-hand response. Significant right-sided covariances were significantly greater than the left-sided ones  $t(78) = 21.5$ ,  $P < 0.001$  for the left-hand response. The right antero-central electrode site did not appear in the left-hand pattern in Fig. 1 because its significance was slightly below the 1-SD cutoff.
20. We made amplitude maps by determining the average amplitude of the Laplacian waveform for each electrode site over the same interval used to calculate covariances and interpolating between sites. Amplitude was represented on a color scale, with red representing the maximum and violet the minimum.
21. A delta filter (low-pass cutoff at 3 Hz) and a covariance interval width of 375 msec were used to study the low-frequency CNV component.
22. Comparison by the  $t$  test of mean-squared amplitude, measured on each Laplacian waveform over the same 500- to 875-msec-centered postcue interval as was used for the between-channel covariance between subsequently accurate and inaccurate conditions of each hand, was not significant at  $P < 0.05$ . Similarity between the sets of CNV amplitudes, or the two covariance maps, was measured with an estimate of the correlation and its confidence interval. Correlation was not used in this context to assess linear dependence. For the small number of repeated measures, a normal distribution could not be confirmed. Therefore, robust, resistant estimates were calculated with a distribution-independent "bootstrap" Monte Carlo procedure [B. Efron, *The Jacarite, The Bootstrap, and Other Resampling Plans* (Society for Industrial and Applied Mathematics, Philadelphia, 1982)], which generates an ensemble of correlation values from randomly selected choices of the repeated measures. When the distributions of CNV amplitudes from subsequently accurate and inaccurate conditions were compared according to this procedure, the correlations were  $0.84 \pm 0.16$  before right-hand performance and  $0.83 \pm 0.14$  before left-hand performance. Thus, it is not possible to discriminate between subsequently accurate and inaccurate waveforms on the basis of the mean-squared amplitude of the averaged event-related CNV waveforms.
23. These four sites were the most prominent in that the numbers of significant covariances in which they were involved each exceeded half of the maximum number of any site (none for the antero-parietal site). The other sites in the pattern were involved in one-third or fewer of that maximum. The same criterion was used to judge which sites were most prominent in the left-hand pattern.
24. In addition to the cue-to-stimulus period, the post-stimulus and postfeedback periods also differed in accuracy, but the response period did not (18). The signal strength of prestimulus covariances was much smaller than those during overt responses, that is, the scale of significance was three orders of magnitude smaller. The smaller number of prestimulus covariances allowed all significant covariances to be shown in Fig. 4. Comparison by  $t$  test of the sets of subsequently accurate and inaccurate covariances was significant at  $P < 0.001$  for both left- $t(38) = 5.57$  and right-hand  $t(23) = 7.70$  comparisons. The bootstrap correlation (22) between covariance patterns before subsequently accurate and inaccurate performance from channel pairs that were significant for either condition was  $0.57 \pm 0.09$  for the right hand and  $0.10 \pm 0.14$  for the left hand. The  $t$  test and bootstrap correlation results, taken together, suggest that the left-hand accurate and inaccurate conditions differ both in scale and in pattern, whereas right-hand results differ only in scale.
25. The classifier was a nonlinear, two-layered, adaptive decision network (15); A. Gevins et al., *Science* 203, 665 (1979); A. Gevins et al., *Psychophysiology* 22, 32 (1985) that decided whether subsequent performance was accurate or inaccurate from CNV interval, between-channel covariances of each trial. This algorithm produced, by a recursive procedure, classification equations consisting of weighted combinations of the decisions of discriminant functions, which themselves consisted of weighted combinations of a subset of the covariance values of Fig. 4. Cross-validation of the equations was performed by testing equations on data that were not used to derive them. Significance was determined according to the binomial distribution. Details of the application of pattern classification procedures to the analysis of brain signals have been presented [A. Gevins, *IEEE Trans. Pattern Anal. Mach. Intell.* 2, 282 (1980); in (14), chap. 17, and N. Morgan, *IEEE Trans. Biomed. Eng.*, in press]. These conservative procedures notwithstanding, we must caution that the degree of generalization of these results to the population at large is unknown and can be determined only by additional studies with new subjects.
26. Previous studies that measured interelectrode correlation have suggested a cortical origin for these patterns (13-15). The difficult problem of identifying the generators of these patterns is the focus of current work. At present, the focal, spatially separated patterns tend to rule out volume-conducted activity from one or two cortical or subcortical generators.
27. D. Ruchkin, S. Sutton, D. Mahaffey, *EEG Clin. Neurophysiol.* 63, 445 (1986).
28. V. B. Mountcastle, *J. R. Soc. Med.* 71, 14 (1978); B. Lee, H. Luders, R. Lesser, D. Dinner, H. Morris, *Ann. Neurol.* 20, 32 (1986).
29. G. Goldberg, *Behav. Brain Sci.* 8, 567 (1985).
30. Supported in part by grants and contracts from the Air Force Office of Scientific Research, the Air Force School of Aerospace Medicine, the National

Science Foundation, and the National Institutes of Neurological and Communicative Disorders and Strokes, National Institutes of Health. We thank G. Zeitlin, R. Tannehill, and B. Costales for programming, J. Salzman for data analysis, K. Dean and J. Toal for manuscript preparation, and D. F. Benson, J. Halliday, M. Kutas, R. Parasuraman, C. Rebert,

W. Rutter, and J. Rohrbaugh for comments on earlier versions of this manuscript. This report is dedicated to the memory of Samuel Sutton for his seminal contributions to the study of human psychophysiology.

20 May 1986; accepted 10 October 1986

---

## CHAPTER 11

# Signals of Cognition

ALAN S. GEVINS and BRIAN A. CUTILLO

*EEG Systems Laboratory, 1855 Folsom Street, San Francisco, CA 94103 (U.S.A.)*

### 11.1. Introduction

#### 11.1.1. OVERVIEW

Brain potentials have been widely used for studying brain activity associated with *higher mental functions* in humans, either as continuous EEG or as averaged event-related potentials (ERPs). Although over 50 years old, human 'psycho-neurophysiology' is still in its infancy, awaiting development of more powerful tools for measuring the minute signals of neurocognitive processes and locating their sources in the brain. Such tools include recordings with many channels, event-related magnetic field (ERMF) measurements, and advanced signal processing techniques. However, even with the most advanced techniques currently available, the best we can hope to do is observe some signs of the timing and location of mass neural activity associated with cognition. The advantages of non-invasiveness and fine temporal resolution are motivating the development of better recording and analytic techniques.

#### 11.1.2. EEG STUDIES OF COGNITION

The first report of an EEG phenomenon associated with cognition was Hans Berger's observation that the alpha rhythm decreased in amplitude during mental arithmetic (Berger 1929). There have been many subsequent EEG studies of cognition, with recent emphasis on hemispheric specialization (reviewed in Gevins and Schaffer 1980; Gevins 1983; Butler and Glass 1986). The major limitation in EEG studies is that the long EEG segments required make it impossible to resolve the split-second stages of cognitive processing.

### 11.1.3. EVENT-RELATED POTENTIALS (ERPs) AND COGNITION

ERPs are a valuable tool for studying the mass neural activity generated during cognitive processes. They are usually studied by averaging a number of brief EEG segments time-registered to a stimulus or response in simple cognitive tasks. Averaging enhances signals correlated in time with the stimulus and subsequent task processing and suppresses unrelated background activity. An averaged ERP waveform consists of a series of positive and negative waves. A significant change in latency or amplitude of a peak, between experimental conditions which differ in a specific cognitive aspect of task performance, is assumed to reflect differences in the mass neural activity associated with that cognitive process. Since the avera-

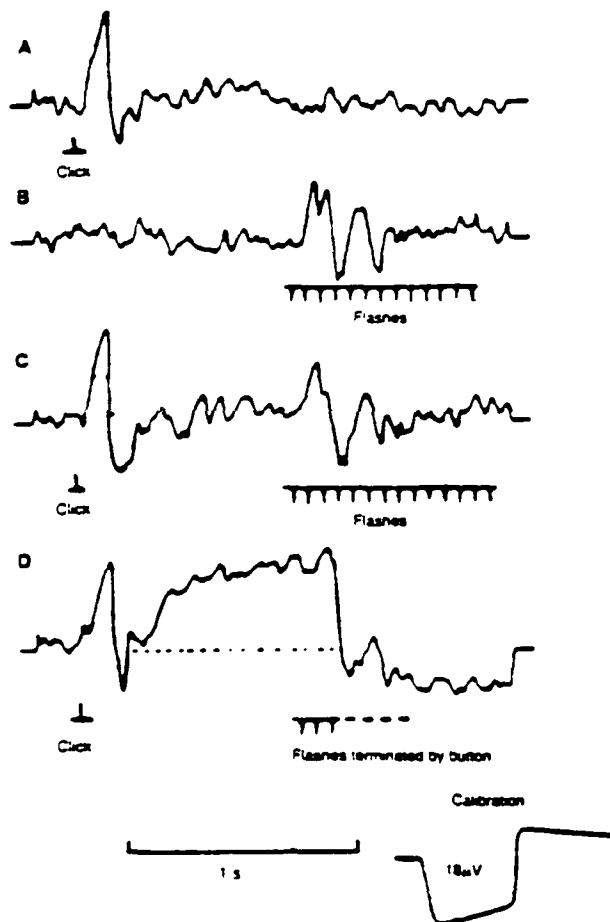


Fig. 1. The contingent negative variation (CNV), reported to be related to expectation in the interval between warning and imperative stimuli, from original report of W.G. Walter et al. (1964). Averaged waveforms (from vertex electrode referenced to mastoid) to unpaired click (A) and flash (B) stimuli, paired click and flash stimuli 1 sec apart with no task-relevant contingency (C), and CNV in the 1 sec interval between the paired stimuli when they are made contingent by requiring a button press to the second stimulus (D).

ged ERP is synchronized to a stimulus or response, it is possible to make inferences about the sequence and timing of task-associated processes, such as pre-stimulus expectation or preparation, encoding of stimulus features, evaluation of the 'meaning' of the stimulus, and response selection and execution. ERP components which are influenced primarily by physical stimulus properties are called 'exogenous,' while those which covary mainly with cognitive factors are called 'endogenous.' In actuality, most components are sensitive to both exogenous and endogenous factors.

In the mid-sixties, two separate teams of researchers discovered that certain ERP components are related not just to 'exogenous' factors, such as stimulus properties or motor activity, but also to cognitive ('endogenous') factors. In 1964, W.G. Walter, Cooper, Aldridge, McCallum and Winter reported an ERP event related to expectation (Walter et al. 1964). This 'contingent negative variation' (CNV) is a slowly increasing negative shift preceding an expected stimulus, often visible in the unaveraged EEG (Fig. 1). The CNV was found to vary during stages of conditioned learning, with motivation, attention and distraction, and other cognitive factors (reviewed in Tecce 1972).

At almost the same time, Sutton, Braren, Zubin and John discovered a positive wave peaking about 300 msec after infrequent task-relevant stimuli (Sutton et al. 1965; Fig. 2). This 'P300' or 'P3' peak is considered endogenous because its scalp topography and behavior do not depend on physical stimulus properties *per se*, but on their 'meaning' in the context of the task. P300 is evoked by many types of paradigms (see Roth 1978; Tueting 1978; Donchin 1979; and Duncan-Johnson and Donchin 1982 for reviews), but the most common factors which influence its behavior are stimulus frequency and task relevance. An especially cogent finding

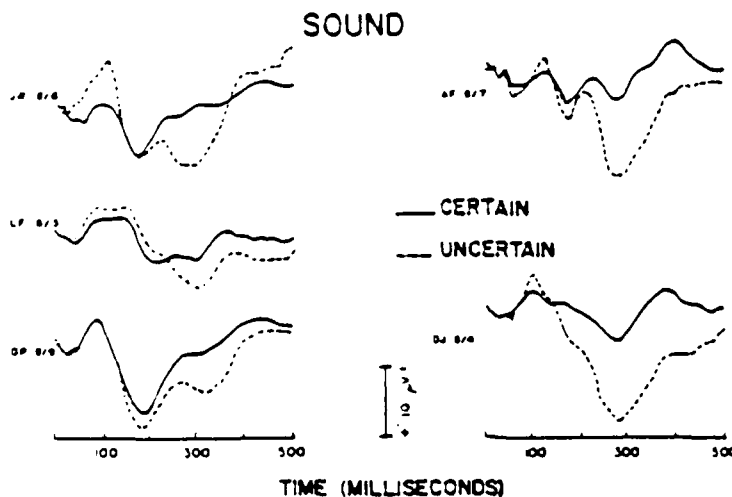


Fig. 2. Illustration of P300 ERP from the original report of Sutton et al. (1965). ERP waveforms from 5 persons elicited by infrequent unexpected ('uncertain') and frequent expected ('certain') auditory stimuli. P300 is the large positive wave peaking about 300 msec post stimulus.

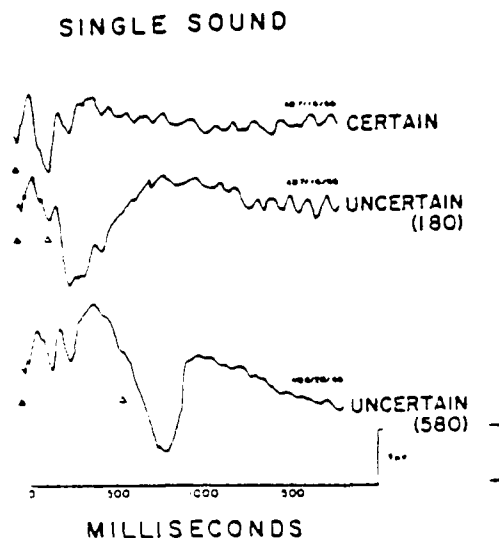


Fig. 3. Missing stimulus ERP or 'emitted potential' elicited by infrequent omissions of the second stimulus in regularly spaced pairs of auditory stimuli. The 'missing stimulus potential' is visible in the 2 lower waveforms as a large positive wave peaking about 300 msec after the time when the missing stimulus was expected (indicated by the rightmost triangle). The preceding solid triangles indicate the presentation times of actual auditory stimuli. (Adapted from the original report of Sutton et al. 1967.)

was the elicitation of P300 by the *absence* of a stimulus in a regularly timed sequence of stimuli. This 'missing stimulus ERP,' obtained by averaging the brain potentials registered to the time the missing stimuli should have occurred, lacks early exogenous peaks such as N100 and P200, but contains P300 and other endogenous waves (Sutton et al. 1965, 1967; Ruchkin et al. 1975) (Fig. 3).

## 11.2. Basic assumptions of the ERP method

### 11.2.1. COGNITION CAN BE MEASURED

#### 11.2.1.1. *Cognitive factors can be isolated*

Mental events cannot be measured directly; we can only observe behavioral and neural activity associated with them. Psychological studies use behavioral measures such as reaction time to define component stages of cognitive processing and make inferences about their nature and timing. The validity of any cognitive study depends on the effectiveness of experimental design and controls in manipulating a specific cognitive factor while holding all other factors constant. For example, a typical 'memory task' involves not only memory, but also expectation and preparation, encoding of stimulus features, comparison with memory, and selection and



execution of a response. The study of brain signals associated with cognition is further complicated by their more complex sensitivity to physical aspects of stimuli and response movements.

*11.2.1.2. The timing of neurocognitive processes is consistent*

The averaged ERP method assumes that task-related cognitive processes do not vary much in timing from trial to trial. If neurocognitive functions were truly 'hard wired,' this might be a reasonable assumption, but there is little evidence to support such an idea. Trial-to-trial variations in the timing of neurocognitive processes affect both the latency and the amplitude of an ERP component, since latency and the amplitude in the averaged waveform are interdependent. Measures of the integrated amplitude ('area') of a wave are sometimes used to alleviate the excessive sensitivity of peak amplitude measures to these variations, and latency correction for particular peaks has been attempted by adjusting the single-trial data in time (Woody 1967; Aunon 1978; see Section 11.6.1 in this chapter, and Chapter 5 in Vol. 1). However, without careful filtering (Aunon et al. 1981), the amplitude increase produced by latency correction procedures may be influenced by unrelated EEG activity, usually an alpha frequency component (Chase et al. 1984). The disappearance of an experimental effect after latency correction has been reported (Kutas et al. 1977), suggesting that the amplitude results of other studies could be due to differences in variance of the timing of task-related signals between conditions.

The measurement of peak latency is another important consideration, especially in chronometric studies (see Sections 11.4.2.2-3 and 11.5.1-2, below). Latency is measured with respect to a peak chosen either by visual inspection or automated programs which choose the point of largest amplitude within a (usually broad) latency range. However, the presence of high frequency activity can cause spurious variability in latencies determined by automated programs, especially for broad peaks, due to tiny 'peaklets' which are clearly not the center of the wave. In this case low-pass filtering, or measuring the latency as the center of gravity of the wave may be appropriate. Even with visual choice of peaks, the close overlap of two separate peaks of slightly different distribution can cause confusion. For a discussion of the methods of latency measurement see Callaway et al. (1983).

*11.2.1.3. Learning and automatization are not appreciable*

The issues of learning, automatization and habituation must be considered when stimuli and tasks are repeated hundreds of times. For example, in one study a reduction in P300 amplitude was attributed to fatigue after 12 h of continuous task performance (Mane et al. 1983). In such a case, follow-up recordings in an unfatigued state should be made to determine whether the effect was actually due to fatigue rather than automatization, since reduction of P300 amplitude with extensive task performance has been reported (Kramer et al. 1983; Woods and Courchesne 1983). Signs of habituation have been observed in many ERP components

(Callaway 1973; Megela and Teyler 1979), including the CNV (reviewed in Loveless 1979) and the P300 (Courchesne 1978; reviewed in Roth 1973 and Verbaten 1983).

#### 11.2.2. OVERLAPPING COMPONENTS CAN BE RESOLVED

The averaged ERP waveform is assumed to be a linear composite of spatially and temporarily overlapping 'components' generated in distinct neural systems. However, it is naive to consider that peaks in the averaged ERP are distinct components, and precise measurement of the overlapping components in the composite waveform is problematic (see Discussion in Callaway et al. 1978). In some cases, relatively simple experimental or analytic methods may be effective in distinguishing separate components. One example is the 'selective attention effect' initially attributed to the N100 peak (Hillyard et al. 1973). The amplitude of N100 was observed to be larger for 'attended' stimuli, which were selected on the basis of simple physical properties, than for those which were 'ignored.' However, it was subsequently shown, by manipulation of inter-stimulus intervals and by subtracting the ERP for 'ignored' stimuli from the ERP for 'attended' stimuli, that the amplitude increase was actually due to a broad, low-amplitude negative wave ('processing negativity') which overlapped the N100 peak (Hansen and Hillyard 1980; Näätänen et al. 1978) (Fig. 4). Another example is the clarification of the relationship of P300 latency to reaction time in a study by Friedman et al. (1978). Some studies

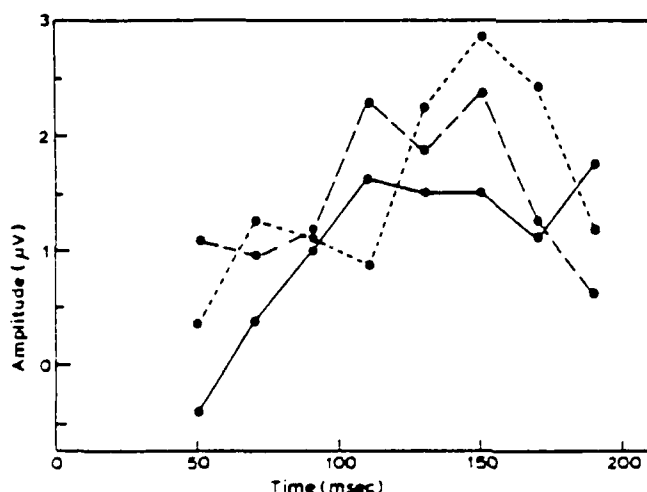


Fig. 4. The 'N100 selective attention effect': an example of overlapping event-related waves. The apparent amplitude increase of the N100 peak in the averaged ERP for 'attended' stimuli is actually due to a broad, low amplitude negative wave ('Nd' or 'processing negativity') which overlaps N100. This was demonstrated by manipulating the length of the inter-stimulus interval, and by subtracting the ERPs for 'unattended' from the ERPs for 'attended' stimuli. The illustration shows the subtraction ERPs for inter-stimulus intervals of 250 msec (dashed line), 300 msec (solid line) and 2000 msec (dotted line). (Adapted from Näätänen et al. 1982.)

reported moderate correlations of P300 latency and reaction time, while the results of other studies were negative (reviewed in Donchin et al. 1978). By dividing their data into reaction time quartiles, Friedman and colleagues distinguished 4 overlapping peaks in the P300 range, only one of which was related to reaction time (Fig. 5), suggesting that this might account for the inconsistent findings of other studies.

It is not often possible to distinguish overlapping components by such simple methods. As a more general solution to this problem, it was proposed that independent components could be mathematically defined by principal components analysis (PCA; see Donchin and Heffley 1978). This method was used to demonstrate the independence of P300 and CNV (Donchin et al. 1975), and has become a fairly common practice in ERP studies. PCA determines statistically independent factors representing different sources of variance in the data by forming linear combinations of the ERP amplitude values at each sampled timepoint. These factors are maximally uncorrelated with each other and account for most of the variance in the data (see Chapters 3, 5, 16 and 17 in Vol. 1). Usually, 4–10 factors will account for more than 90% of the variance, depending on the complexity of the sources of variance (Donchin and Heffley 1978; Kavanagh et al. 1978). In spite of its popularity, the PCA method has inherent limitations. In particular, it is difficult to determine which experimental variable or 'source of variance' a particular factor reflects (Rosler and Manzey 1981; Wood and McCarthy 1984). Other difficulties and possible alternatives to PCA are discussed in Section 11.6.2 (below), and Vol. 1, Chapter 14.

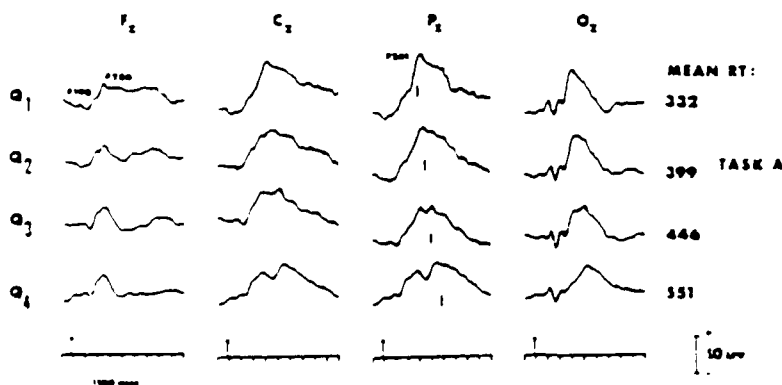


Fig. 5. Separation of overlapping waves in the averaged ERP in a visual discrimination task by computing subaverages of trials according to reaction-time quartiles. Vertical lines in the parietal (Pz) channel mark mean reaction times (RT), time scale is 110 msec per division, and arrow marks stimulus onset. Comparison of central (Cz) and parietal (Pz) waveforms from short to long RT quartiles reveals that the late positive complex is composed of several overlapping peaks. Since only the longest-latency peak is correlated with RT ( $r=0.99$ ), it becomes clearly distinct (at about 525 msec) in the longest RT quartile. (Adapted from Friedman et al. 1978.)

### 11.3. Methodological requirements of neurocognitive studies

Methodological requirements for neurocognitive studies have been discussed in several books and review articles (Donchin et al. 1977; Thatcher and John 1977; Gevins and Schaffer 1980; Gevins et al. 1985). As in any experiment, it is essential to control all factors not directly related to the intended experimental manipulation. Special attention to experimental control is required in neurocognitive studies, since brain signals are very sensitive to many factors, and neurocognitive signals are small in relation to 'background' activity. Only a few of the more important issues are discussed below.

#### 11.3.1. ELIMINATION OF ARTIFACTS

Contamination of brain signals by non-neural potentials is a serious problem. The major sources of physiological artifacts are eye movements and blinks, and muscle activity, particularly of the scalp muscles. Artifacts are usually eliminated by visual inspection of polygraph tracings or automated algorithms which reject trials exceeding preset voltage levels. However, small undetected eye movements or muscle activity which may be related in time to the stimulus or response will summate in averages and could cause spurious results. It is possible that task-related eye and muscle activity, however slight, accompanies all cognitive processing. Lateral eye movements (saccades) and blinks have been shown to be correlated with cognitive processes (Just and Carpenter 1976; Stern et al. 1984), and activity of the facial and scalp muscles has been used to distinguish different cognitive tasks (Cacioppo et al. 1983). Other sources of artifactual muscle potentials include response movements and subvocalization. Digital algorithms for removing the effects of eye movements have been developed for averaged ERPs (Verleger et al. 1982; Gratton et al. 1983), and single-trial data (Gasser et al. 1983; Bonham et al. unpublished manuscript). They seem effective in removing task-related artifacts, and further evaluation of their performance, as well as extension of such methods to muscle potential contaminants, is eagerly awaited. (See also Chapter 1 of this volume.) Contamination by physiologic artifacts is also a serious problem in brain magnetic field recordings and has not yet been systematically studied.

#### 11.3.2. CONTROL OF PHYSIOLOGIC AND EXPERIMENTAL FACTORS

##### 11.3.2.1. Arousal

One aspect of experimental control concerns general physiologic factors. Brain signals vary with age, handedness, gender, level of autonomic arousal, fatigue, and use of caffeine, nicotine, alcohol and various drugs. Autonomic arousal is a special problem which has not received adequate attention. Indirect indices, such as pupil size, have been used to measure the phasic arousal of the central nervous system during cognitive tasks (Kahneman 1973). More direct measures of CNS 'activa-

tion,' such as EEG spectral intensity, have been used to measure gross differences in global arousal (Loomis et al. 1938; Daniel 1966; Rechtschaffen and Kales 1973; Simon et al. 1977), and there is no fundamental obstacle to an EEG index of phasic 'activation' (Gevins et al. 1977). However, it is more difficult to distinguish effects associated with specific 'information processing' from those which reflect the overall level of activity of the central nervous system (Khachaturian and Gluck 1969; Khachaturian et al. 1973). These two types of activity are not totally distinct, but are aspects of the integrated functioning of the brain. Until technological advances provide better means of distinguishing the two, control of these factors must be attempted by manipulation of task difficulty, motivation and general physiological factors.

#### 11.3.2.2. *Isolating cognitive processes*

The essential issue of experimental design and control bears on the validity of assuming that the experimental conditions actually manipulate a specific neurocognitive process, and that the results are not due to factors not directly related to that process. Tasks should be simple and short to reduce the possibility of trial-to-trial variation in performance and 'strategy,' but challenging enough to engage full attention. The conditions of an experiment should be controlled for irrelevant stimulus, physiological-state and response-related factors by experimental design and *a posteriori* balancing of data sets. Such factors include the physical properties, frequency and ordering of stimuli, task difficulty, automatization, and the timing, force, duration, hand and nature of response movements (Gevins et al. 1979a, b; 1980, 1981). Task difficulty should be adjusted according to changes in performance, as indexed by behavioral measures such as reaction time and error. Behavioral measures should be made on each trial to verify that the task is properly performed, and to form balanced sets of trials differing only in the variable(s) under study prior to hypothesis testing (Gevins and Schaffer 1980; Gevins 1983; Gevins et al. 1985, 1986). If ERP peak amplitudes are measured with respect to a pre-stimulus baseline, the effects of expectancy must be considered, especially when inter-stimulus intervals are constant.

Finally, the hypotheses, paradigms, and electrode locations should be designed with careful consideration of the information about localized neurocognitive functions obtained from clinical observations, metabolic scanning techniques (regional blood flow and positron emission tomography), intracranial recording and stimulation studies, and primate models.

#### 11.4. ERP events associated with cognition: two major lines of research

##### 11.4.1. SIGNALS OF PREPARATION: THE CONTINGENT NEGATIVE VARIATION AND THE READINESS POTENTIAL

###### 11.4.1.1. *Cognitive factors*

The contingent negative variation (CNV) is a slowly increasing negative potential which occurs between two stimuli in tasks involving a contingency or association of paired stimuli (see Fig. 1). It is best seen when the stimuli are separated by a regular interval with a response required after the second stimulus. About 200 msec after the second stimulus, there is a sharp positive deflection, termed the 'CNV resolution.' The psychological conditions which reliably elicit the CNV are of 4 general types (Hillyard 1973): (1) holding a motor response ready, (2) preparation for a perceptual judgment, (3) anticipation of reinforcement or feedback, and (4) preparation for a cognitive decision. The CNV was initially considered a signal of 'expectancy' (Walter 1964), but subsequent studies demonstrated that it is affected by many cognitive factors including attention, distraction, preparation for cognitive tasks, anticipation of information, ambiguity and task difficulty, and also by non-cognitive factors such as stimulus intensity, modality and timing, reaction time and magnitude of movement, motivation, positive or negative reinforcement, noxious stimuli, arousal, age, fatigue, various types of drugs, and clinical disorders including learning disability, senility, neurosis, anhedonia, depression and schizophrenia (reviewed in Tecce 1972; Rockstroh et al. 1982; Rohrbaugh and Gaillard 1983).

The theory that the CNV reflects preparatory processes assumes that the negative potential shift reflects a build-up of 'cerebral potentiality' which is released during the positive-going resolution following the second stimulus (Walter 1964; Rockstroh et al. 1982). The scalp distribution of the CNV is widespread, usually largest at the midline central electrode, but also strong at precentral and frontal sites (Crow et al. 1963). The CNV is thought to reflect depolarization of apical dendrites in frontal and central cortex (Walter 1964), but the theory that this facilitates neuronal action potentials has not been proven (Rebert 1978). The possible involvement of frontal cortex is of particular interest, since it is thought to mediate higher-order functions such as preparation and planning (Fuster 1980; Goldman-Rakic 1984). The theory that the CNV reflects *task-specific* cortical activation has been weakened by failure to elicit localization of amplitude with different types of tasks, such as linguistic, spatial and pattern discriminations (Donchin et al. 1978), or attention to different sensory modalities (see Hillyard 1973). Also, evidence for an inverse relationship of CNV amplitude and reaction time, which would support the 'potentiality' hypothesis, has been inconsistent (reviewed in Tecce 1972), although recent studies indicate that this may have been due to the use of short (less than 2 sec) intervals (Brunia and Vingerhoets 1980).

#### 11.4.1.2. *Sensory and motor aspects of the CNV*

The extent to which the CNV reflects cognitive *association* of two stimuli is still unclear. The CNV was found to consist of two overlapping waves with different topographies and responses to experimental factors (Low et al. 1966). These two components can be seen as separate waves when the inter-stimulus interval is 2 sec or longer (Rohrbaugh et al. 1976). The early CNV, sometimes called the 'orienting wave,' is a frontally maximum negative wave following S1, and the late CNV, which has been called the 'expectancy wave,' is a centrally maximum negative shift preceding S2. A number of researchers believe that the CNV observed at short inter-stimulus intervals is merely a composite of two separate negative waves and is not related to contingent association between two stimuli (Gaillard 1978; Rohrbaugh and Gaillard 1983). Rohrbaugh et al. (1980) synthesized a CNV-like waveform from ERPs accompanying *unassociated* events: the slow negative wave following unpaired stimuli (click or flash), the readiness potential (RP) preceding self-initiated finger movements, and the ERP to another unpaired stimulus (Fig. 6). The synthetic waveform created by adding the voltage timeseries of these 3 ERPs, positioned in time to emulate a 1 sec inter-stimulus interval, resembled the CNV recorded in a traditional paired-stimuli paradigm.

The readiness potential (RP) mentioned above is a centrally maximum negative shift beginning about 500 msec before voluntary motor actions (Kornhuber and Deecke 1965). It responds to some of the same factors as the CNV, such as motivation (reviewed in McAdam 1973), but the CNV is typically stronger at frontal sites and is not usually lateralized (Näätänen and Michie 1979b), whereas the RP is larger over central sites contralateral to the responding hand (Deecke and Kornhuber 1977). The CNV is reported to be larger when a motor response is required to the second stimulus, but also occurs in the absence of response (reviewed in Rockstroh et al. 1982; Rohrbaugh and Gaillard 1983).

Many other researchers believe that the negative waves associated with non-contingent events do not fully account for the behavior of the CNV and favor the view that the CNV does reflect contingency to some extent (Donchin et al. 1974; Ritter et al. 1984). The CNV has been seen to develop when a contingency between two stimuli is learned and then decline when the contingency is removed. CNV amplitude is reduced by distracting stimuli (Tecce 1978), instructions to change 'attentional focus' (McCallum and Walter 1968), and 'equivocation' of contingency through random omission of the second stimulus (Walter et al. 1964; Low et al. 1966). Other evidence for a non-motor aspect comes from paradigms in which a negative shift is sustained through a 7 sec sequence of contingent stimuli (Kutas and Hillyard 1980a, b, c), which has not been observed for the RP. A few studies have reported topographic changes related to modality-specific expectancy, but the effect is small in relation to overall CNV amplitude (Simson et al. 1977a; Ritter et al. 1980; Woods and Courchesne 1983). All considered, it seems that both the CNV and the RP are compound phenomena which reflect neural activity related to many sensory, cognitive and motor factors.

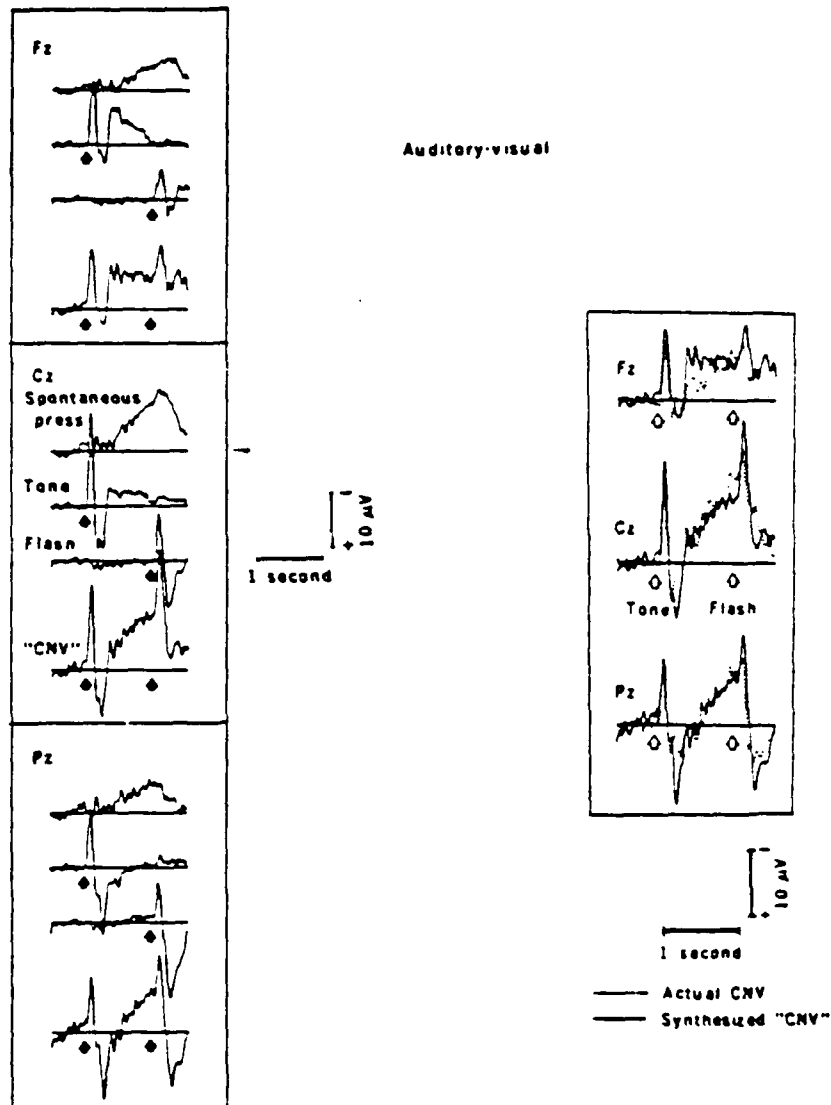


Fig. 6. Synthesis of CNV-like waveform by superimposing ERPs accompanying unassociated events. Left: the readiness potential (RP) preceding self-initiated finger presses and the ERPs elicited by unpaired clicks and flashes were positioned in time to emulate a 1 sec inter-stimulus interval, and their voltage time series were summed to produce the synthesized 'CNV.' Right: comparison of synthesized (solid lines) and actual CNV (dotted lines). Waveforms are from midline frontal (Fz), central (Cz) and parietal (Pz) electrodes referenced to linked ears. (Adapted from Rohrbaugh et al. 1980.)



#### 11.4.2. PROBABILITY AND INFORMATION: P300 AND OTHER LATE POSITIVE PEAKS

Under appropriate conditions, task-relevant visual, auditory or tactile stimuli, or the omission of expected stimuli, elicit a sequence of overlapping positive peaks in the 300–700 msec latency range. This is termed the late positive complex (LPC) and includes the P3a, P3b and slow wave (SW). The P3b peak (usually called 'P300') was first reported in 1965 (Sutton et al. 1965) and has been the subject of many subsequent studies. However, this robust, easily elicited wave has been highly resistant to a precise definition of its relationship to cognition and behavior. Although P300 is influenced by *many* cognitive factors in a complex manner, there are several well-established facts about its behavior (reviewed in Donchin 1979; Pritchard 1981; Duncan-Johnson and Donchin 1982). Task-relevant ('attended') stimuli elicit substantial P300 waves, and its amplitude is larger for infrequent deviant stimuli, as in the popular 'oddball' paradigm, where infrequent 'target' stimuli must be distinguished from frequent 'non-targets.' Its midline distribution is maximal at Pz or Cz and is relatively unaffected by physical stimulus properties, such as modality or intensity, provided that they do not provide task-relevant information (Simson et al. 1976, 1977a, b). The amplitude of P300 is inversely related to the probability of occurrence of stimuli which have different 'meanings' in the context of the task (Tueting et al. 1970). This effect of global probability can be modified by several factors. The ordering of preceding stimuli ('local' or 'subjective' probability) can override the effect of global probability (K. Squires et al. 1976). Similarly, P300 amplitude to feedback stimuli is not related to absolute probability, but to the 'contingent probability' of a particular feedback following a particular response (Campbell et al. 1979). Also, uncertainty ('equivocation') in difficult judgment tasks weakens the effect of global probability on P300 (Ruchkin and Sutton 1978).

P300 is affected by many other factors, and its behavior is usually interpreted in terms of concepts borrowed from the field of cognitive psychology. However, its behavior may fit a particular cognitive model in one study, but in a different paradigm it is often contradictory. There seems to be no simple relationship between P300 and a specific psychological factor, and because of this, a parsimonious model of P300 and cognition has not yet been achieved. The difficulty of interpreting P300 in terms of psychological constructs is discussed in Chase et al. (1984) and Donchin (1984). From a neurophysiological perspective, there is little reason to expect that simple peak amplitude and latency measurements from a few midline electrodes could characterize specific neurocognitive processes. Even so, substantial progress toward understanding neurocognitive processes has been achieved through the ingenuity of the first generation of ERP researchers. We will discuss several prominent lines of research and the evolution of some theories which used to explain the behavior of P300 in order to illustrate the effect of overly simplified ideas about cognitive processing on past ERP research.

#### 11.4.2.1. *P300 and selective attention*

Attempts have been made to relate the behavior of P300 to psychological models of selective attention (reviewed in Donald 1983). Hillyard and colleagues (Hillyard et al. 1973; Hink et al. 1977) interpreted the behavior of the N100 and P300 waves in terms of the 'stimulus-set/response-set' model of selective attention (Broadbent 1970). 'Stimulus-set selection' denotes early selection of stimuli in a particular sensory 'channel' defined by modality, spatial location or gross physical properties, and 'response-set selection' denotes subsequent selection based on higher-order criteria related to choice of appropriate response. However, the 'stimulus-set' effect initially attributed to N100 was found to be due to an overlapping negative wave, the 'Nd' or 'processing negativity' (Näätänen et al. 1978; Hansen and Hillyard 1980), and P300 seems to be relatively unaffected by stimulus-response compatibility (discussed in McCarthy and Donchin 1983), and its latency is not well correlated with reaction time (see next section). Still, there is ample evidence of 'channel selection' in early ERP components and higher-order selection associated with P300, but these effects are not easily explained by any of the early/late selection models derived from psychological studies (see Hillyard 1984; Posner et al. 1984).

#### 11.4.2.2. *P300 and stimulus evaluation*

A more refined theory proposes that P300 latency is related to the time required for stimulus evaluation. If so, its latency might be expected to vary with the difficulty of stimulus evaluation and, therefore, with response time. In relatively difficult judgment tasks, its latency has been reported to be correlated with RT, but only moderately, from  $r = 0.20$  to  $0.66$  (Donchin et al. 1978; McCarthy and Donchin 1983). In simpler tasks with short reaction times, P300 often peaks *after* response initiation. One proposed explanation is that the relationship of P300 and response processes changes according to task requirements and performance strategy (Donchin 1984). For example, when speed of response is emphasized, the correlation of P300 latency and RT is reduced, although P300 latency *per se* is relatively unaffected, but this does not explain its weak correlation with RT in the *same* task, as determined by single-trial measurements (Kutas et al. 1977). Another possible explanation is that P300 is a composite of several overlapping peaks with different relationships to RT, as in the study by Friedman et al. (1978), in which the late positive wave consisted of 4 highly overlapped peaks, only one of which was correlated with RT (see Fig. 5). In fact, the correlation of the one peak was unusually high ( $r = 0.81-0.90$ ), suggesting that the weaker correlations in other studies might be due to failure to distinguish such overlapping components.

Better support for the stimulus evaluation theory is provided by changes in P300 latency resulting from manipulation of factors affecting stimulus evaluation processes. Latency increases have been produced by increasing the difficulty of stimulus discriminability and stimulus categorization. Discriminability factors which increase P300 latency include detection of small variations in simple stimuli (Ritter et al.

1972; N. Squires et al. 1977), stimulus complexity (Ritter et al. 1983b), and degraded, masked or 'noisy' stimuli (McCarthy and Donchin 1981; Ritter et al. 1982). Factors related to categorization difficulty include difficulty of judgment (Ritter et al. 1983b), and number of items in the comparison (memory) set (Ford et al. 1979). However, these factors also affect the N200 waves, which always precede response initiation (Renault et al. 1982) and are better correlated with reaction time (Ritter et al. 1979; Ritter et al. 1983a, b), suggesting that they are more closely associated with the stages of stimulus evaluation (see Section 11.5.1.3).

#### 11.4 2.3. P300 and memory: updating of an 'internal model'

A possible explanation both for the dissociation of P300 latency and reaction time and its relation to stimulus evaluation is that P300 is associated with the updating of an internal schema or memory template *subsequent* to stimulus evaluation (Tuetting 1978; Donchin 1981; McCarthy and Donchin 1983). This theory proposes that the internal schema cannot be updated until the significance of the stimulus has been fully evaluated, while a response can be initiated as soon as the information required for performance of the current trial has been evaluated. Thus P300 latency would be correlated with reaction time indirectly, and the degree of correlation would depend on the stage of stimulus evaluation required for response initiation and context updating in a particular task.

Two aspects of 'context updating' are the amount of updating induced by the *current* stimulus and its effects on 'expectancy' which should be evident in the *succeeding* trial. Since this has not been systematically studied, we will consider evidence from the literature which bears on these issues. The 'amount of updating' aspect is supported by its larger amplitude for infrequent stimuli ('global probability' effect) and longer latency for disconfirming feedback (K. Squires et al. 1973), two instances where more updating would be expected. Evidence for the 'expectancy' aspect is the influence of local probability, which can modulate the effect of global probability on P300 amplitude (K. Squires et al. 1976). The order of preceding stimuli seems to create an expectancy set, resulting in larger amplitudes when an expectation is violated, and the weakening of the effect of local probability at long inter-stimulus intervals suggests the decay of a memory trace. The expectancy theory would also account for the dependence of P300 amplitude for feedback stimuli on the 'contingent probability' with respect to the preceding response, rather than the absolute probability of a particular feedback. The interplay between global and local probability was demonstrated by K. Squires et al. (1976) by using a 50/50 probability of targets and non-targets. Since global probability was equal, P300 amplitude in the averages for targets and non-targets was the same, but when trials were averaged according to the *preceding* stimuli, P300 amplitude was larger for targets which followed non-targets (Fig. 7), and even for *non-targets* which followed targets. Other support comes from studies of 'equivocation,' in which P300 amplitude is directly related to the degree of confidence with which a stimulus can be used in updating (reviewed in Ruchkin and Sutton 1978).

and from 'guessing' paradigms, in which its amplitude is larger when the subject's *prediction* is disconfirmed (Horst et al. 1980).

Another line of evidence linking P300 to memory processes comes from studies of short-term memory search. The most common psychological paradigm for studying short-term memory scanning is Sternberg's memory search task (Sternberg 1969), in which previously designated targets ('memory set') must be identified in a series of random stimuli ('test set'). This is very similar to the 'oddball' paradigm used in many P300 studies, in which the memory set (target) usually consists of one item. Since the target remains the same over many trials, no updating of a memory representation of the target should be required, yet P300 amplitudes are

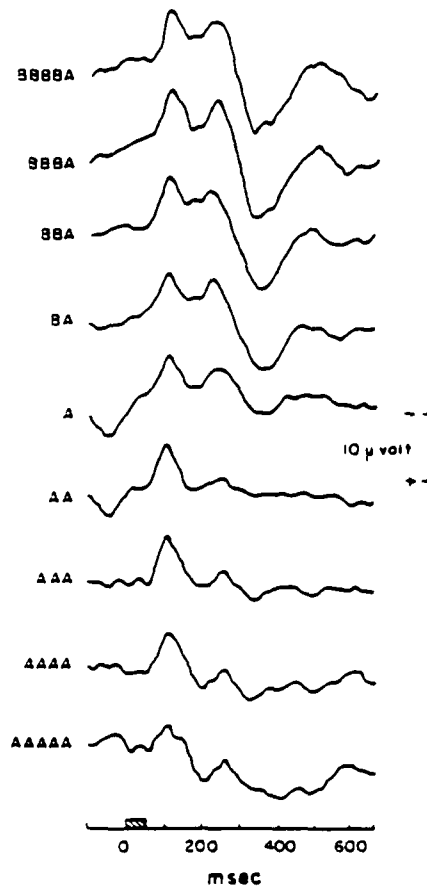


Fig. 7. Effect of stimulus sequence ('local probability') on P300 amplitude in an auditory discrimination task. Since the ratio of targets and non-targets (global probability) was 50/50, P300 amplitude in averaged ERPs for targets and non-targets was the same. However, when averaged according to the sequence of *preceding* stimuli, P300 amplitude for both targets and non-targets increased linearly as a function of the number of dissimilar stimuli preceding it. The first letter at the left of each sequence indicates the letter of the target in that sequence, i.e., 'B' is the target in the first 4 sequences and 'A' is the target in the last 5 sequences. (Adapted from K. Squires et al. 1976.)

larger for stimuli which *match* the target (at target probabilities of 50% or less). Thus the amplitude increase to targets may be related instead to the updating of subjective expectancy regarding the sequence of stimulus events. However, ERP studies using the Sternberg paradigm suggest a relationship between P300 and the actual memory search and comparison process (Marsh 1975; Adams and Collins 1978; Ford et al. 1979). P300 latency to matches was found to increase in a linear manner with the number of items in the memory set (about 25 msec per item). A recent study by Kramer et al. (1983) produced several interesting results. The slope of the linear increase in P300 latency with memory set size for target matches was the same as the slope for the increase in reaction time (RT), but for non-targets (mismatches) the RT slope was steeper, while the latency slope remained the same. This might indicate that the relationship between P300 and the processes leading to response differs for targets and non-targets, although other interpretations for such results are possible (Halliday et al. 1984). P300 amplitude was larger for targets than for non-targets, even when the frequency of targets was 80%, suggesting that the memory match had a stronger effect than probability. In early sessions, P300 amplitudes to memory matches were larger when targets were infrequent, as would be expected, but in later sessions this probability effect was absent for memory matches in the easier 'consistent mapping' condition. This was interpreted as the lack of need for 'memory updating' when task performance is 'automatized.' Considering the behavior of P300 in these and other studies, it is clear that P300 is not simply related to short term memory or updating of an internal model.

#### 11.4.2.4. P300, controlled processing and capacity

The psychological concepts of 'controlled processing' and 'processing capacity' have been applied to the behavior of P300. 'Controlled processing' denotes a limited-capacity central process involving conscious effort (reviewed in Moray 1969; Kahneman 1973), and is distinguished from automatic processing, which does not make demands on 'processing capacity' (Schneider and Shiffrin 1977). Thus an automatic process does not interfere with concurrent automatic or controlled processes. Automatic processes may occur in parallel, while controlled processes are considered serial. Examples of automatic processes are initial encoding of sensory information and the execution of skilled motor actions. Controlled processes include memory rehearsal and search, target detection, and various types of decision or judgment. Prominent P300 peaks are elicited when a task requires controlled processing, and it has been suggested that P300 amplitude is related to the amount of controlled processing required in some tasks (Rosler 1983), although contradictory evidence is provided by many reports of amplitude *reduction* with increasing task difficulty and amplitude *increase* as stimulus probabilities are learned.

When two tasks performed simultaneously both require controlled processing, their interference is evident as a decline in performance measures such as reaction

time and accuracy. If P300 is associated with controlled processing, it should reflect such interference. Studies using dual-task paradigms (Isreal et al. 1980; Wickens et al. 1983) have demonstrated that: P300 amplitude to infrequent targets in an 'oddball' task is reduced when a second task is performed concurrently, and its amplitude to 'oddball' targets varies inversely with the difficulty of the second task only if it requires controlled processing. For example, increasing the difficulty of a well-learned, presumably automatized, tracking task does not reduce P300 amplitude in the concurrent oddball task, but increased difficulty of a monitoring or vigilance task does. Further, P300 amplitudes in the two tasks vary reciprocally as task difficulty is manipulated, suggesting that under these conditions it indexes the distribution of processing capacity between tasks (Wickens et al. 1983).

#### 11.4.2.5. *The slow wave*

Some tasks elicit a long-duration slow wave (SW), which begins as early as 180 msec and peaks between 500 and 700 msec. It has been distinguished from P300 by topography and behavior (reviewed in Ruchkin and Sutton 1983). SW amplitude is larger for all task-relevant stimuli, whether or not they are targets, and thus can occur without P300 (N. Squires et al. 1975). Its amplitude has been reported to be larger for *non-targets* in conditions where they might require more processing than targets (Friedman et al. 1981; Kramer et al. 1983), and to increase with task difficulty, while P300 decreases (Ruchkin et al. 1980a). The SW is thought to be associated with processes subsequent to stimulus evaluation in the context of the current trial, possibly related to task performance over many trials (Ruchkin et al. 1980b; Stuss et al. 1980).

An interesting finding is that SW topography can change with task requirements. Its midline distribution is typically negative at Fz, positive at Pz, and about zero at Cz, but in the 'guess' condition of a detection task, its posterior positivity shifts forward (Ruchkin et al. 1980b). Also, an experimental effect is sometimes seen only in the frontal negative or parietal positive portions. This suggests that the anterior and posterior components of the SW may be generated by different neural processes (Picton and Stuss 1980; Fitzgerald and Picton 1981; Friedman et al. 1981).

### 11.5. The variety of ERP components

This section deals in some detail with several topics in cognitive ERP research in order to illustrate the basic information about cognitive processing which researchers must rely on in applying new methods of signal processing and analysis.

#### 11.5.1. ENDOGENOUS NEGATIVE WAVES

In the past 10 years the number of reported ERP components has increased dramatically. ERP events first thought to be unitary phenomena were later found to

consist of several waves, distinguishable by topography, experimental manipulations and analytic methods. We will discuss several negative waves which peak between 100 and 400 msec post stimulus (reviewed in Näätänen and Michie 1979b).

#### *11.5.1.1. Processing negativity*

The 'processing negativity' (Näätänen et al. 1978), or 'Nd' (Hansen and Hillyard 1980), is a broad negative wave which is larger in amplitude for stimuli which must be selected on the basis of simple physical properties. It is thought to be a sign of early selective attention, sometimes referred to as 'channel selection.' Its onset and duration reflect the nature and difficulty of stimulus selection, and its topography reflects the modality and side of stimulation. Since it begins as early as 60 msec and lasts for 500 msec, it overlaps the N100 peak and causes an apparent increase in N100 amplitude, which initially led researchers to attribute the selective attention effect to N100 (Hillyard et al. 1973). It was distinguished from N100 by its behavior in response to experimental manipulations and by subtracting the averaged ERPs for attended and unattended stimuli (Näätänen et al. 1978, 1981; see Fig. 4, this chapter). The processing negativity itself may be composed of several components with different topographies and relationships to task requirements (Hansen and Hillyard 1983). A sequence of negative peaks in this latency range were reported to respond differentially to selection of visual stimuli on the basis of location, color, spatial frequency or orientation (Harter and Guido 1980; Harter et al. 1982). The relationship of these waves to selective attention and sensory channels is not well understood (discussed in Hillyard 1984, and Posner et al. 1984).

#### *11.5.1.2. Missing stimulus negativity*

The missing stimulus negativity (MSN) is part of the emitted potential elicited by occasional omissions in a regular sequence of stimuli (Klinke et al. 1968). In this case, the earlier 'exogenous' waves are absent, and the purely endogenous MSN begins at the time the stimulus was expected (see Fig. 3). Its amplitude is largest over the appropriate sensory cortex for expected visual, auditory or somesthetic stimuli (Simson et al. 1976, 1977a; Renault 1983), and is relatively independent of attention or task requirements (Näätänen and Michie 1979a). The MSN is similar in topography and behavior to the N200 wave described below.

#### *11.5.1.3. The N200 peaks*

Infrequent stimuli which deviate from the majority elicit a negative wave at about 200 msec (Roth 1973; Squires et al. 1975). The stimuli need not be task-relevant or 'attended' (Snyder and Hillyard 1976), and N200 amplitude is inversely related to the frequency of deviant stimuli (Squires et al. 1975). Since N200 closely overlaps the P200 peak, it is usually measured in the difference waveform by subtracting the ERP to the frequent 'standard' stimuli from the ERP to deviant stimuli.

The N200 wave has been seen to consist of two separate peaks in a number of

studies. The N2a or 'mismatch negativity' (MMN) is elicited by infrequent deviant stimuli, task-relevant or not. Its sensitivity to probability and magnitude of deviation led to the interpretation of N2a as a sign of 'neuronal mismatch' in the orienting response to deviant stimuli, 'an automatic, basic sensory process ... irrespective of, perhaps even unmodified by, the task and subjective factors' (Näätänen 1982). Its modality-specific topography suggests involvement of activity in and around the sensory cortex (Simson et al. 1977a), and its amplitude, onset time, peak latency and duration are affected by physical factors, such as stimulus discriminability, complexity, and nature and magnitude of deviation. The slightly later N2b peak is not sensitive to these factors, but is affected by certain task-related factors such as attention and categorization difficulty (Ritter et al. 1979). N2b has a modality-independent fronto-central distribution similar to P3a, which appears to always follow it (Squires et al. 1975, 1977). A similar pair of peaks have been observed in the missing stimulus negativity (Renault and Lesèvre 1979), and it has been reported that in certain tasks N2b is preceded by a negative peak (termed 'NA'), which differs from N2a in that it is not affected by probability (Ritter et al. 1983a,b).

Since N2a (or 'NA') is affected by exogenous factors, while the behavior of N2b is more endogenous, and since an experimental manipulation which increases the

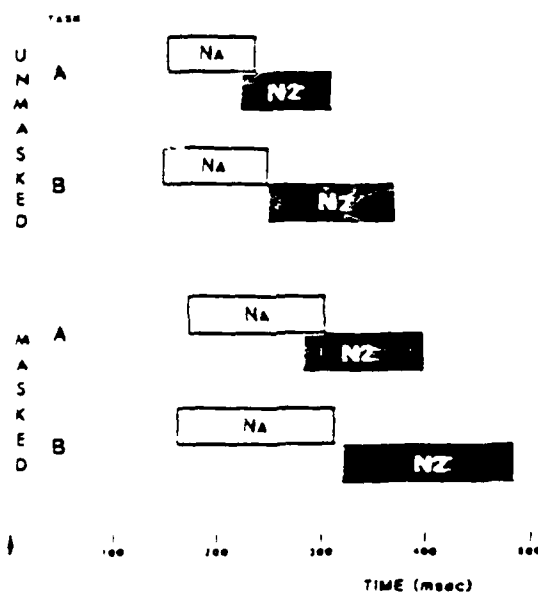


Fig. 8. Differential manipulation of two N200 peaks. The earlier 'NA' wave is influenced by the exogenous factor of stimulus discriminability, while the later 'N2' (N2b) is affected by the endogenous factor of categorization difficulty. The bars connect onset and peak latencies of NA and N2. In both tasks, increasing stimulus discriminability by masking lengthens the onset-to-peak times of NA, which causes an identical delay in the onset of N2. The increase in difficulty of judgment of stimulus category between tasks A and B does not affect the timings of NA, but increases the peak latency and onset-to-peak time of N2. (Adapted from Ritter et al. 1983a.)



latency of the earlier peak produces an identical increase in the timing of N2b (Ritter et al. 1979, 1983a; Renault 1983), they are thought to be associated with successive, contingent stages of information processing. Several two-stage models have been proposed: pattern recognition and stimulus categorization (Ritter et al. 1982, 1983a,b), two stages of the orienting response (Näätänen and Gaillard 1983), automatic and controlled processing (Ritter et al. 1983b), and active perceptual processing ('template matching') leading to evaluation of stimulus significance and response selection (Renault 1983). All these models propose that the earlier wave is associated with automatic feature extraction processes which precede the endogenous processes associated with N2b, and that their peak latency, onset and duration reflect the timing of such processes. High correlations of peak latencies and reaction times have been reported (Renault et al. 1982; Näätänen and Gaillard 1983), and differential manipulation of the amplitude and timing of the two waves by changes in physical ('exogenous') and task-related ('endogenous') factors support this theory (McCarthy and Donchin 1981; Ritter et al. 1982, 1983a,b; Fig. 8 of this chapter).

#### 11.5.2. CHRONOMETRIC MODELS OF ERPs

'Chronometrics' refer to methods for inferring the sequence and timing of component stages of cognitive processing (reviewed in Chase 1984). This approach was pioneered by Donders in the mid-1800's and has been most elegantly applied in the work of Posner (1978). Chronometric analysis is well suited to ERP studies, since the timing of onset, peak latency and duration of the waves associated with various cognitive factors can be used to infer the temporal relationships of processing stages. The short and medium latency peaks in the first 80 msec following a stimulus are highly exogenous: their latency and topography depend on the modality, intensity, and other physical properties of the stimulus. The P100 and N100 peaks are also considered exogenous, generated primarily in sensory cortex, although it is likely that other cortical areas are also involved (Goff et al. 1978; Wood et al. 1980; Allison 1984). They are thought to reflect later stages of feature encoding. The P200 peak which immediately follows N100 is usually considered exogenous, although its topography is less dependent on stimulus modality and not largest over sensory cortex. If the task requires selection of stimuli on the basis of simple physical properties, the long-duration 'processing negativity,' thought to be a sign of early selective attention, may occur in this latency range (Näätänen et al. 1978).

If the stimulus differs from the majority of stimuli, the N2-P3a peak complex occurs in the 200-300 msec range (N. Squires et al. 1975). Task relevance ('attention') is not required, and their amplitudes vary inversely with probability. N200 consists of two successive peaks. The earlier peak, termed N2a, mismatch negativity and NA by various authors, is affected by exogenous factors such as stimulus modality, complexity, discriminability, and nature and magnitude of deviation, whereas N2b is sensitive to higher-order task factors such as difficulty of stimulus

categorization. Also, since the timing of N2b is affected by changes in latency of the earlier wave, and N2b latency is highly correlated with reaction time, N2a (or NA) and N2b are thought to reflect successive, contingent stages of automatic feature recognition (template matching) and subsequent task-related evaluation (see Section 11.5.1.3).

If the stimulus is also *task relevant*, P3a will be followed by the P3b (P300) peak, usually largest over parietal ('association') areas. The behavior of P3b is affected in a complex manner by numerous cognitive factors of a higher order than the preceding waves (see Section 11.4.2). P3b appears to be involved in almost all types of higher cognitive functions. Some tasks elicit later peaks such as the N400, thought to be associated with semantic processing (see Section 11.5.3.1), and the long-duration slow wave, peaking between 500 and 700 msec, which seems associated with processes subsequent to stimulus evaluation in the current trial, possibly related to task performance over many trials.

A typical visual discrimination task might consist of identifying designated target stimuli which occur infrequently in a sequence of 'standard' stimuli, and making a finger movement in response to targets. The averaged ERP for target stimuli might contain a sequence of peaks like those at the top of Fig. 9: P90, N130, P190, N225 (N2a), N250 (N2b), P290 (P3a), P375 (P3b), a slow wave (SW) peaking at 575 msec, and negative movement-related potentials (RP) peaking at 500 msec. The chronology of onset, peak latency and duration of the component waves in this hypothetical waveform, as might be derived by PCA, subtraction, topographic, or other methods, is illustrated in the lower part of Fig. 9. These component waves, which are associated with various aspects of the stimulus and task processing, can be seen to wax and wane in a highly overlapping manner. Since the onset of a particular wave often precedes the peak of the previous wave, it appears that the neural process indexed by the later wave begins before the culmination of the preceding stage, which agrees with evidence from chronometric behavioral studies that cognitive processing involves multiple parallel and sequential stages.

Most models applied to ERPs to describe the flow of information between stages are derived from psychological studies (discussed in Chase et al. 1984). The assumption of strictly sequential processing stages, as in Sternberg's 'additive factor method' (Sternberg 1969), seems unsuited to most ERP phenomena. Several models combining parallel and sequential views have been considered, including McClelland's 'cascade model' (McClelland 1979), the 'asynchronous discrete stage model' of Miller (1982), and others based on similar principles, such as 'continuously available output' (Norman and Bobrow 1976) and 'continuous flow' (Eriksen and Schultz 1979). The approach of Posner, though not expressed as a general model, is perhaps the most promising for chronometric ERP analysis (Posner 1978).

Considering the hypothetical 'components' of the ERP waveform for target stimuli of our visual discrimination task (Fig. 9) in terms of information flow and processing stages, we might speculate that the encoding of stimulus features begins with the mid-latency exogenous waves between 40 and 80 msec and continues

through P90, N130 and P190. The feature codes necessary for identification of target stimuli must be available by the N2a peak at 225 msec, since N2a (or 'NA') is affected by the nature and degree of deviation from the 'standard' (i.e., the mismatch between feature code and internal 'neural template' of the frequent 'standard' stimuli). This idea is supported by the increase in latency and duration of NA caused by degraded or complex stimuli, which may require more processing to generate a utilizable feature code. Such an increase in timing delays the succeeding N2b by the same amount, indicating that processes associated with N2b are contingent on those associated with the earlier wave. N2b itself is sensitive to more

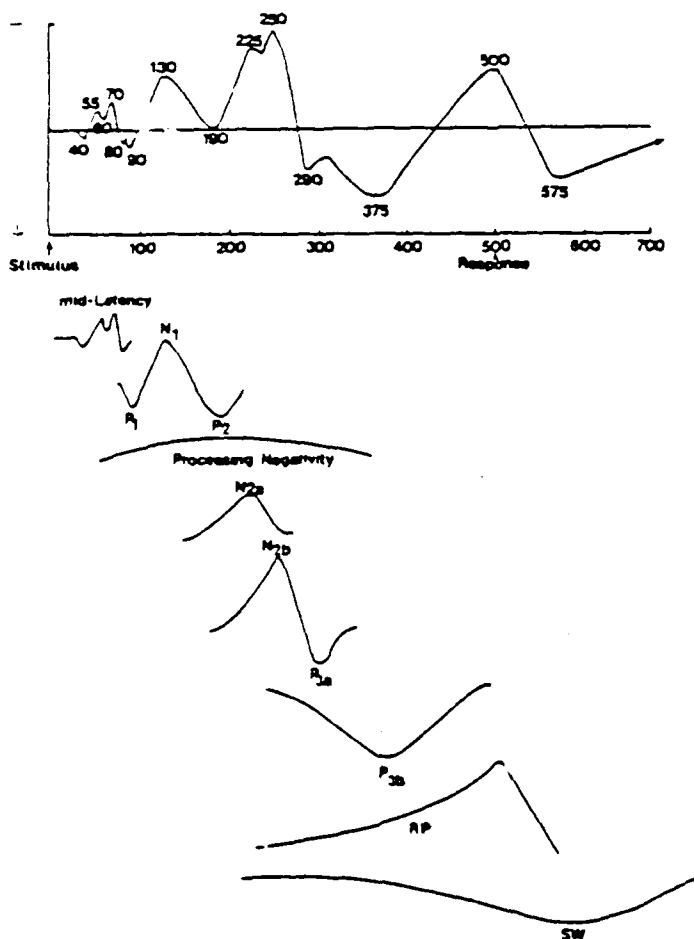


Fig. 9 Top: model averaged ERP waveform for infrequent target stimuli in a hypothetical visual discrimination task, showing mid-latency, P1, N1, P2, N2a, N2b, P3a, P3b and slow wave (SW) peaks, the 'processing negativity,' and the movement-related readiness potential (RP). Bottom: hypothetical 'components' of the waveform, as might be inferred by subtraction, PCA and topographic methods, showing their onset times, peak latencies and durations. Note the high degree of overlap of successive components. (See text for further discussion.)

'endogenous' task-related factors which do not affect N2a. The topographies of N2b and the similarly behaving P3a which follows it are not affected by stimulus modality, suggesting that they are associated with processes involving a modality-independent or 'common code.' The increase in N2b latency caused by categorization difficulty and its high correlation with reaction time suggests that it is associated with evaluation of stimulus information required for response selection. The P3b ('P300') peaks at 375 msec and is elicited only by task-relevant stimuli. Its latency is sometimes (but not always) moderately correlated with N2b latency and reaction time. Its amplitude is larger for stimuli which *match* the memorized target, but also becomes larger as the frequency of target stimuli is reduced. Considered along with its latency behavior (see Sections 11.4.2.2 and 3), P3b appears to be related both to stimulus evaluation in the current trial and also to the updating of an internal schema or expectancy set subsequent to stimulus evaluation. That is, it seems to be contingent on 'common codes' associated with stimulus evaluation (possibly indexed by N2b), but utilizes those codes for updating an internal schema which is involved in task performance over a series of trials. The slow wave also seems related to processes subsequent to stimulus evaluation; it may also be involved in ongoing task performance, perhaps more than P3b, since it is strong for non-targets as well as targets.

### 11.5.3. LANGUAGE AND LATERALIZATION

#### 11.5.3.1. N400

Recently, a negative wave peaking at about 400 msec was reported to be related to 'semantic incongruity' in the reading of sentences (Kutas and Hillyard 1980a, b). This 'N400' wave was elicited by a word which was semantically inappropriate in the context of a sentence. A semantically appropriate word presented in a larger typeface elicited a P300 wave without N400, suggesting that deviation from *semantic* context was required for elicitation of N400. In support of this interpretation, N400 was found to be relatively insensitive to the probability of semantically inappropriate words, and also, violations of grammar did not elicit an N400-like wave (Kutas and Hillyard 1982). Later studies (Kutas et al. 1984) indicated that N400 amplitude was related to semantic expectancy, rather than semantic inappropriateness *per se*: appropriate words with a low degree of semantic expectancy (Cloze probability) also elicited N400, although smaller in amplitude than for inappropriate words. Similar waves have been reported for semantic mismatch in word pairs, for words outside an expected category, and for semantic judgments of picture stimuli (reviewed in Kutas et al. 1984). Such findings led to the hypothesis that N400 reflects priming or facilitation in semantic processing.

Semantic expectancy may not be the only factor which elicits N400. Similar negative waves have been produced by naming single words and pictures, where there is no semantic context, and by non-semantic tasks such as mental rotation and comparison of geometrical figures (Stuss et al. 1983). It has been suggested

that N400 reflects the utilization of short-term working memory in maintaining a task-related context, semantic or otherwise, which would certainly be involved in the processing of long sentences.

#### *11.5.3.2. Lateralization studies*

The right-sided lateralization of N400 (Kutas and Hillyard 1982) is difficult to interpret in view of the abundant neuropsychological evidence for the involvement of certain left-hemisphere cortical areas in linguistic functions. The well substantiated role of the 'language' areas of posterior frontal and temporal cortices of the dominant hemisphere (usually the left hemisphere in right-handed persons) makes language a good choice for studying the localization of neurocognitive processes. Many attempts have been made to measure language-associated lateralization and localization in the EEG and ERP, but the findings have been inconsistent (reviewed in Beaumont 1983; Gevins 1983; Molfese 1983; Rugg 1983; Butler and Glass 1986). Topics which have been addressed include acoustic and phonetic processing (Wood 1975; Molfese 1980), the effect of semantic context on homonyms (Brown et al. 1979), connotative (affective) value (Chapman 1977; Chapman et al. 1980), and lexical and semantic functions (Buchsbaum and Fedio 1970; Brown et al. 1976; Chapman et al. 1978; Molfese 1979). The series of studies by Kutas and colleagues are particularly interesting and include, in addition to the N400 studies mentioned above, studies of natural sentence processing, grammar, and differences between processing of open-class (content) and closed-class (function) words (Kutas and Hillyard 1980a,b,c, 1982; Kutas et al. 1984).

A number of studies have reported language-associated hemispheric lateralization of one or more ERP peaks, often with larger amplitudes over left hemisphere sites of right-handed people. Unfortunately, many of the studies are of questionable validity due to methodological flaws (reviewed in Friedman et al. 1975; Donchin et al. 1977; Gevins et al. 1979c, 1980; Beaumont 1983; Gevins 1983). Common shortcomings include failure to properly isolate the intended linguistic function due to poor experimental design; inadequate control of spurious factors such as stimulus properties, eye movement, response movements, sub-vocalization and task difficulty; and inappropriate location of the reference electrode. Also, anatomical differences between hemispheres in the temporo-parietal region must be taken into account in evaluating interhemispheric differences between electrodes situated over the posterior 'language center' (Wernicke's area). An illustration of the importance of experimental control is provided by two studies of Gevins and colleagues (Gevins et al. 1979a,b,c). The differences in lateralization of EEG spectral power between verbal and non-verbal (spatial) tasks found in the first study were not observed in a subsequent study in which task difficulty, stimulus and movement-related factors were more highly controlled.

Other reasons for the failure to find consistent patterns of lateralization and localization related to linguistic and non-linguistic functions include the use of paradigms based on simplistic neurocognitive models, and inappropriate or in-

adequate brain potential measures and analyses. It is unrealistic to assume that just one or two cortical areas are involved in any specific cognitive function (Luria 1977). In the case of language, regional cerebral blood flow (rCBF) studies have shown that during language tasks the pattern of cortical activation in the *non-dominant* hemisphere is almost a mirror image of the activation of the 'language areas' of the dominant hemisphere (Lassen et al. 1978). Thus the brain potentials associated with this bilateral activation might not exhibit gross lateralization of amplitudes, and the measurement of any subtle hemispheric differences might require more detailed spatial sampling and more sophisticated methods of signal processing and analysis. For example, in a study comparing split-second numeric and spatial judgment tasks, Gevins and colleagues (1981) found no significant lateralizations of peak amplitudes in the averaged ERP. However, when a single-trial measures of waveshape similarity between electrodes (cross-correlation) in brief analysis intervals spanning the major ERP peaks were analyzed by mathematical pattern recognition techniques, they found complex patterns of evoked correlations which differed between tasks. The lateralization of correlations were mixed, although in two intervals they were predominately right or left sided.

#### 11.6. Advances in recording and analysis

A major research challenge is the development of better methods of resolving the complex signals of cognition, which overlap both temporally and spatially at the scalp. Progress is being made in several areas, including ERP estimation, post-processing, spatial sampling and analysis, source localization, and the modeling of neurocognitive processes.

##### 11.6.1. IMPROVED ERP ESTIMATION

Although the averaging technique is useful, its effectiveness is limited by trial-to-trial variability in the timing, shape and strength of event-related signals (see Chapter 5 of Vol. 1). Considerable effort has been directed toward improving methods of event-related signal measurement and ERP estimation, but although some techniques are applicable in particular instances, no single method which can replace averaging has been developed (see review in Gevins 1984). Methods for reducing the effect of 'atypical' trials in averages, such as down-weighting (Gasser et al. 1983) or elimination of outliers (Gevins et al. 1986; see Chapter 5 in Vol. 1) are simple and fairly effective. The use of Wiener filtering (also called 'minimum mean square error,' or MMSE) to improve the event-related signal in the average ERP has been considered (see Chapter 5 in Vol. 1, Chapter 10 of this Volume, and reviews in De Weerd 1981 and McGillem et al. 1981), but their usefulness in studying neurocognitive signals has not been demonstrated. Latency correction procedures have been used to compensate for trial-to-trial variations in the timing of event-related signals by shifting the temporal position of individual trials before averaging (Woody 1967). However, for these procedures to be effective, the event-

related signal must be relatively large with respect to background EEG, and filtering of rhythmic background EEG is necessary (see Section 11.2.1.2). A possible improvement might be the application of latency correction only to trials with distinct event-related signals. Since the timing and shape (i.e., frequency) of individual peaks in the ERP waveform can vary independently, it is clear that the ERP is not a stationary process, and recently developed time-varying filters (see Fig. 1, Chapter 10) may provide more accurate measurement of neurocognitive signals (De Weerd 1981; Yu and McGillem 1983). Significant advances in ERP signal estimation should occur when analytic models with greater neurophysiological fidelity are developed (see 11.6.5 below).

#### 11.6.2. IMPROVED POST-PROCESSING

Another area where improvement is needed is feature extraction, which is the determination of those signal properties which best characterize the cognitive factors defined by the experimental conditions. Heuristic feature extraction, the most common method, consists of manually or automatically measuring the latency and amplitude of an ERP peak of interest. However, overlapping components can render such measures ambiguous, and simple heuristic methods may extract only a small portion of the information in the ERP. PCA is commonly used as an 'objective' method of ERP feature extraction (Harman 1976; see Chapters 3, 16 and 17 in Vol. 1) and has been used in many studies (Donchin 1966, 1979; Thatcher and John 1977; Donchin et al. 1978). However, a number of somewhat arbitrary decisions must be made in applying PCA, including the segment of the time series to transform, the type of filters to be used, the number of channels, experimental conditions and persons to include, and the type of rotation to apply to the extracted components. These decisions are crucial, since mixed sources of variance in the data can cause confusion in interpreting the meaning of the extracted components (Van Rotterdam 1970; Rosler and Manzey 1981; Wood and McCarthy 1984). As a means of statistical feature extraction, the major drawback of PCA is that the small amount of residual variance unaccounted for by the major components might be crucial in characterizing and distinguishing the cognitive functions being studied (see Chapter 17 in Vol. 1). Also, linear combinations of variables may not be as effective as other combinations formed by procedures which do not assume linearity (Gevins 1980, 1984).

As an alternative to the use of PCA for feature extraction, mathematical pattern recognition (PR) procedures have been successfully used to choose ERP features and feature combinations which are good or even optimal for hypothesis testing (see Chapter 17 in Vol. 1). One such algorithm, known as stepwise discriminant analysis (SWDA) (Sampson 1967), is widely available and has been extensively used for feature selection and hypothesis testing (Donchin 1966; D.O. Walter et al. 1967; reviews in Gevins 1980, 1984; McGillem et al. 1981). SWDA first chooses the variable with the greatest ratio of between-condition to within-condition variance and then selects succeeding variables by the same criterion after removing

the variance accounted for by variables already chosen. Despite its popularity, SWDA and other methods which choose variables one at a time have a major limitation: the set of best variables chosen one at a time is unlikely to be as good as a set of variables chosen in *combination* (Cover 1974; Cover and Van Campenhout 1976). The only way to determine the best combination of variables is to try all possible combinations, but this is computationally impractical in most cases. Algorithms which efficiently compute all possible linear subsets of variables have been developed (Furnival and Wilson 1974), but the problem remains when there are many variables or when non-linear combinations are desired. In such cases, carefully considered temporal or anatomic constraints must be used to limit the search for variable subsets. Anatomical constraints can be applied by forming neurophysiologically relevant subsets of electrodes, and temporal constraints can be applied by limiting the search to brief time intervals determined from the major peaks in the averaged ERP (Gevins et al. 1979a, 1981, 1985).

Regardless of the feature extraction procedure used, the underlying problem is that *statistically* independent features are not necessarily neurophysiologically independent. For example, if an experiment causes the event-related activity of several brain systems to covary together, only one statistically independent feature may be required to characterize the activity of the several systems. There is at present no general solution to this problem other than to design experimental conditions which may highlight differences between neural systems, and to organize the data for analysis using *a priori* neuroanatomical and neurophysiological knowledge (Gevins et al. 1979a, 1981, 1985).

### 11.6.3. SPATIAL ANALYSIS

#### 11.6.3.1. Need for more electrodes

The resolution of neurophysiologically distinct 'components' is perhaps the major problem in ERP research. Much effort is devoted to devising variations of a few basic paradigms, but little to increasing the dimensionality of parametrization of event-related brain signals. Small changes in peak amplitude or latency at a few midline electrodes are assumed to be adequate to characterize the mass neural activity of a large number of psychological functions. For example, since the P300 wave is affected by many factors, how can it be determined whether the P300 elicited in one paradigm is the same P300 observed in other paradigms, or a different one associated with different neural processes? The P300 elicited by 'no-go' stimuli in a go/no-go task is more anterior in distribution than the 'typical' P3 (Simson et al. 1977b), and the frontal or 'novelty' P300 elicited by unexpected stimuli is even more anterior (Courchesne et al. 1975). Do such variations reflect changes in the activity of the same neural sources, or the involvement of different sources? Information from a larger number of electrodes, especially lateral ones, could shed some light on this issue, but very few studies use more than the usual 3 or 4 midline sites. For instance, although the midline distribution of P300 is



unaffected by stimulus modality, modality effects in its lateral topography have been reported (Snyder et al. 1980). Studies using up to 50 electrodes indicate that a high degree of spatial sampling is useful in distinguishing ERP components (Lehmann 1981, 1984; Gevins et al. 1984; Lehmann and Skrandies 1984; see also Chapter 12 in Vol. 1).

The spatial patterning of scalp-recorded brain signals is complex, reflecting the activity of many anatomically and functionally differentiated neural systems. Recordings of many EEG channels simultaneously are becoming more common due to advances in technology (Lehmann et al. 1969; Lehmann 1971, 1984; Kavanagh 1972; Kavanagh et al. 1978; Darcey 1979; Darcey et al. 1980; Ary et al. 1981; Gevins et al. 1984). Basic methodological considerations, such as the separation between electrodes required to avoid spatial aliasing must be considered (see Vol. 1, Chapters 3 and 12). With 60 electrodes evenly distributed over the head, the average inter-electrode distance is about 3.25 cm; with 120 electrodes, the distance is about 2.3 cm. Preliminary analyses of the spatial spectrum of endogenous ERPs elicited by unpatterned visual stimuli indicate that a spacing of about 2 cm is necessary to avoid appreciable spatial aliasing (Doyle and Gevins submitted).

#### *11.6.3.2. Removing the effect of the reference electrode*

The location of the reference electrode greatly affects the topography of brain potentials. A P300 peak recorded with mastoid or chest reference has a maximum positive amplitude at Cz or Pz, but is more posterior with a nose reference, and becomes a negative peak with an occipital maximum when a common average reference is used.

The Laplacian derivation (LD) promises to be useful in removing the influence of the reference location, and also in reducing the blurring effect of volume conduction (Hjorth 1975; Nuñez 1981). This technique uses the potentials recorded from a local group of electrodes to compute the curvature of the electrical field at the center electrode, yielding a measure of electrical current perpendicular to the scalp at that site. LD measures are independent of the location of the reference electrode, and are less sensitive to current sources outside the boundary of the local electrode group. The ability of the LD to sharpen spatial detail and enhance weak signals in the EEG has been demonstrated (Spehr 1976; Murray and Cobb 1980; Wallin and Stålberg 1980). It has only recently been applied to ERPs, and seems effective in sharpening the spatial pattern of exogenous components for visual stimuli (Thickbroom et al. 1984), and auditory stimuli and movement-related signals (Gevins et al. 1984). The LD distributions of endogenous components are not as localized, but the overlapping late positive peaks are more distinguishable by their LD topography (Gevins et al. 1984). Computation of the LD amounts to little more than adding the bipolar EEG channels surrounding a particular electrode, each weighted by the inter-electrode distance, but the LD works best when many channels are recorded and the LD cannot be accurately determined for channels on the periphery of the montage. Spatial deconvolution procedures are

also reference independent and provide even more reduction of volume conduction effects than the LD (Doyle and Gevins submitted).

#### *11.6.3.3. Analyzing spatial information*

The first step in spatial analysis is computation of the topographic pattern of ERP voltages (Lehmann et al. 1969; Lehmann 1971; Kavanagh 1972). Topographic maps consist of isopotential contour lines representing the peaks and valleys of potential or current, much like topographic geophysical maps. Since the location of the reference electrode has a strong effect on scalp topography (Lehmann 1984; Lehmann and Skrandies 1984; see Chapter 12 in Vol. 1), voltages should be converted to reference-independent measures by Laplacian derivation or spatial deconvolution. Comparison of topographic patterns across persons is problematic: scalp electrodes positioned by reference to skull landmarks are not precisely coordinated with underlying cortical areas, the variation between a scalp site and a designated cortical area being about 1 cm. In addition, functional neuroanatomy differs among people, so that activity at a particular electrode may not be functionally equivalent across persons. One solution is the use of magnetic resonance imaging (MRI) to determine the relative position of scalp electrodes and cortical areas (Doyle and Gevins submitted).

While valuable insights can be gained by examining topographic maps, statistical methods are needed to quantify spatial information. One approach is to reduce the information for statistical analysis to a few features, such as the location, orientation and magnitude of an 'equivalent current dipole' (Kavanagh 1972; Kavanagh et al. 1978; Darcey 1979; Darcey et al. 1980) or the locations of maximum positive and negative potential values (Lehmann 1971; Lehmann and Skrandies 1980, 1984). Multivariate statistical methods can also be used to evaluate spatial patterns by reference to normative values from control populations (John et al. 1977a, b, 1983; Duffy et al. 1981), or by making comparisons between experimental conditions for each electrode or group of electrodes (Gevins et al. 1979a,b,c, 1981, 1983, 1985). These and other aspects of spatial analysis are discussed in detail in Vol. 1, Chapters 3, 12, 17 and 18 (see also Section 10.5 of Chapter 10).

#### *11.6.3.4. Measurement of inter-channel relationships*

Studies of the inter-relationship of event-related activity between different scalp locations aim to find some indication of 'functional coordination' or 'interdependency' between neural areas. Such information is potentially useful for inferring the presence of several simultaneously active sources. There are two ways of doing this: the characteristics of the ERP waveforms may be quantified for individual channels and the resulting measures compared between channels, or the relationship between channels can be directly quantified by various measures of similarity or interdependence of their activity, with particular emphasis on the time lag between channels. Some of the measures of inter-channel interdependence include: spectral coherence (D.O. Walter 1963; see Chapter 4, Vol. 1); polycoherence

(Saltzberg 1985; see Chapter 4, Vol.1); partial coherence (Gersch and Goddard 1970; see Chapter 10 in Vol. 1); information-theoretic measures (Callaway and Harris 1974; Saito and Harashima 1981; Inouye et al. 1983; Mars and Lopes da Silva 1983; see Chapters 6, 10, and 11 in Vol. 1); correlation (see Fig. 10; reviewed in Livanov 1977; Gevins et al. 1981, 1985; see Chapter 6 in Vol. 1); and multichannel non-stationary autoregressive modelling (Gersch et al. 1983; see Chapter 10, Vol. 1).

Only a few of these methods are applicable to very brief data segments, which is necessary for resolution of the split-second stages of neurocognitive processing. Sometimes it is possible to use sets of short data segments from several trials

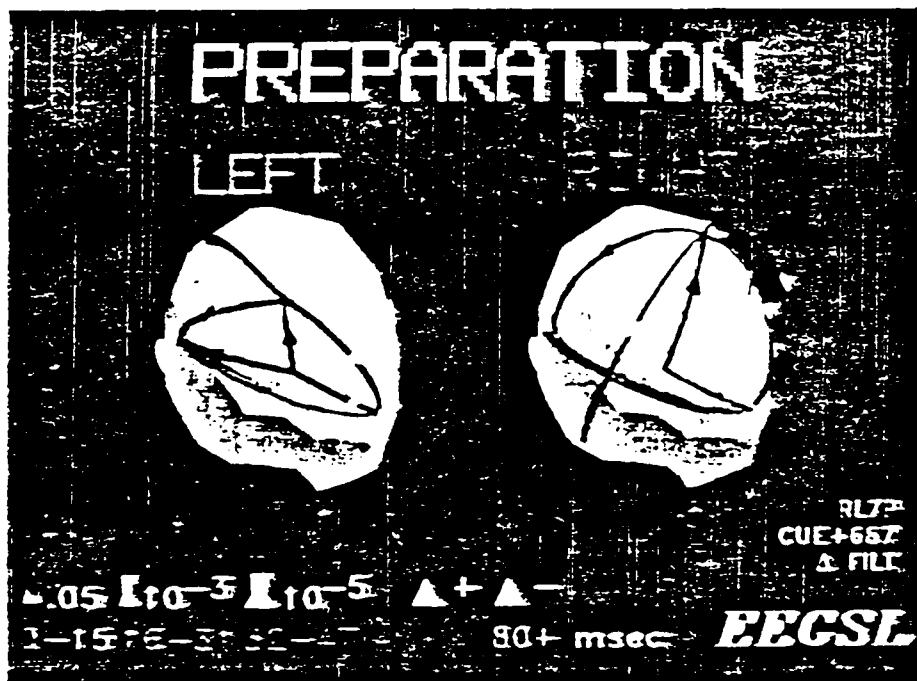


Fig. 10. Measures of the similarity in the shape of event-related potential components recorded from different channels have been used to study spatiotemporal interdependencies between neural systems. In this illustration, the most significant event-related covariance patterns of 7 right-handed adults during an interval from 500 to 875 msec after the presentation of a cue are shown. The cue prepared subjects to make a response with the right or left hand; a visual stimulus appearing 1 sec after the cue indicated the magnitude of the required finger pressure. The thickness of a line is proportional to the negative log of its significance from 0.05 to 0.005. The color of a line indicates the time at which two channels are maximally synchronized (yellow: 0-15 msec; green: 16-31 msec; blue: 32-47 msec; red: 48-79 msec; purple: > 80 msec). These preparatory patterns are focused primarily on left prefrontal and midline precentral electrodes for performance by both hands, and central and parietal electrodes appropriately contralateral to the hand to be used for the response. Since there was no sign of overt muscle or eye movement activity, these patterns suggest that preparatory sets may be composed of cognitive, integrative-motor, somesthetic-motor, and visuo-perceptual components. For details about covariance patterns associated with subsequently accurate or inaccurate performance, see Gevins et al. (1986).

which presumably contain consistent signals of a particular process. Furthermore, for a measure of 'functional coordination' to have anatomical and physiological validity, it must be independent of reference location and should provide information about the *temporal* relationship of inter-channel signals, that is, whether the event-related signals of one channel lead or 'predict' those of another channel.

#### 11.6.4. LOCALIZATION OF NEURAL SOURCES

##### 11.6.4.1. *General considerations*

Determining the sources of scalp-recorded brain activity is a difficult problem, especially in the case of 'endogenous' signals related to cognition. The use of 'equivalent current dipole model' techniques to infer the neural source of a particular pattern of electric or magnetic fields observed at the scalp is appropriate only in special instances which conform to the assumptions of the model (Kavanagh et al. 1978; Darcey et al. 1980; Ary et al. 1981; Nuñez 1981; Williamson and Kaufman 1981a,b; Cohen and Cuffin 1983; Okada 1983; see Chapter 9 in this volume, and Chapters 13 and 14 in Vol. 1 regarding dipole modeling for the visual system).

The assumption of single generators seems particularly unrealistic in the case of higher cognitive functions, which involve the integrated activity of a number of neural areas (Luria 1970). Since the areas involved can be widely distributed anatomically and vary in orientation, it is not usually possible to derive a unique source corresponding to the complex electrical and magnetic field distributions recorded at the scalp. Multi-source solutions may be possible in some instances by using anatomic constraints derived from knowledge obtained from studies of focal brain lesions and radiological metabolic techniques.

Another problem is the distortion of electrical fields as they pass through the tissues between cortex and scalp, resulting in spatial smearing of low frequency potentials and attenuation of higher frequency activity at the scalp. The degree of distortion varies among scalp locations and persons. This distortion can be corrected by 2-dimensional spatial deconvolution (Nicholas and De Loche 1976; Hjorth 1982) and practical techniques for implementing this are being developed (Doyle and Gevins submitted).

The magnetic fields of the brain are relatively undistorted by the tissues between cortex and scalp, and plausible 3-dimensional equivalent dipole localizations of certain highly localized sensory and motor sources have been achieved even with the relatively crude devices currently available (reviews in Erne et al. 1981; Williamson and Kaufman 1981a,b; Kaufman and Williamson 1982; Okada 1983; Weinberg et al. 1985). Magnetic fields measured at the scalp are generated primarily by tangentially oriented sources, rather than the mixture of radial and tangential sources of scalp-recorded electrical fields. Thus the magnetoencephalogram provides complementary information to the electroencephalogram, and a great advance in source localization can be expected when technological developments permit the simultaneous recording of many magnetic and electric channels.

#### 11.6.4.2. *Sources of cognitive signals*

Exogenous ERP components which accompany sensory stimuli and motor actions have patterns of scalp localization corresponding to sources in primary and secondary sensory cortex and motor regions (Goff et al. 1978; Wood et al. 1980, 1982; Allison 1984; also see neuromagnetic references in previous section). The N100 peak is maximal at occipital sites for visual stimuli and midline central sites for auditory stimuli (presumably projected from tangential auditory cortex generators in the temporal lobe). Somatosensory and motor ERPs also have topographies in agreement with neuroanatomic and neurophysiologic localizations. However, no clear-cut cortical or subcortical sources have been determined for endogenous components such as the N200, P300 and slow wave. In the case of P300, intracranial recordings from neurosurgery patients suggest that it arises from multiple subcortical sources (discussed in Wood et al. 1980, 1982; Squires et al. 1983). In one study (Halgren et al. 1980), a strong P300-like wave was observed to reverse polarity between different locations in the hippocampus, suggesting an active generator there, but its peak occurred after the P300 recorded simultaneously from the scalp, which weakens this inference. Polarity reversals of P300-like waves have also been recorded near the thalamus (Yingling and Hosobuchi 1984), and between scalp and nasopharyngeal electrodes located beneath the brain (Perrault and Picton 1984). However, the absence of frontal and parietal P300s in patients with anterior and posterior cortical lesions argues in favor of cortical involvement (Knight et al. 1980). Magnetoencephalographic studies suggest sources in the hippocampus (Okada et al. 1982), but the evidence is somewhat inconsistent, and it is possible that this technique favors sharply localized hippocampal activity over diffuse, distributed cortical activity.

#### 11.6.5. NEUROCOGNITIVE MODELS

Most neurocognitive studies are based on very simple models of neurocognitive processing. For example, in EEG studies it is assumed that neurocognitive processes are relatively stable states which can be characterized by patterns of spectral intensities (the energy in various frequency bands over epochs from several seconds to minutes long). This is unrealistic in view of the split-second timing of the stages of cognitive processing indicated by behavioral and ERP studies.

A more dynamic view of neurocognitive processing is assumed in ERP and ERMF studies. In clinical use of the very early 'far-field' evoked potentials to test the integrity of sensory pathways, there does appear to be a direct correspondence between successive peaks and ascending anatomical structures, but the situation with higher perceptual and cognitive functions is more complex. In cognitive ERP studies, it is usually assumed that once a task has been learned, the brain processes stimuli and generates responses in a deterministic manner. The successive peaks and waves of the averaged ERP, or the principal components corresponding to them, are assumed to reflect the stages of task processing, and between-condition changes in amplitude or timing of a peak are taken as indices of the experimental

manipulation of a particular cognitive function and specific neural sources. The contribution of trial-to-trial variability to such amplitude and latency changes is not usually considered. Although cognitive ERP studies continue to produce interesting results, they are limited by the unrealistic simplicity of their implicit models of neurocognitive processing and the resultant assumption that these complex processes can be indexed by a few amplitude and latency measurements. Similar effects in an ERP component can often be produced by different experimental manipulations, and the behavior of a component in one paradigm frequently conflicts with its behavior in another when interpreted within the context of a simplistic model.

In developing better models for future research, it may be important to consider that the brain systems which generate event-related signals may not be different from those which produce ongoing EEG activity. It is possible that the task stimulus induces a reorganization of ongoing activity in a neural system as a subset of its population becomes engaged in event-related processing (Sayers et al. 1974; Başar 1980). This reorganization may be evident as pre- to poststimulus changes in amplitude, frequency, timing and inter-electrode coordination of low frequency macropotentials. An appropriate model might combine the 'stimulus-evoked activity' and 'pre- to poststimulus reorganization of activity' approaches, and would have the advantage of taking into account the prestimulus activity related to expectancy, preparation and attentional set. Further, because of the brain's complex hierarchical/parallel organization and flexibility, the same overt behavior in a cognitive task might be associated with different configurations of regional activity, especially through the learning, skilled performance and 'automatized' phases of an experiment (John et al. 1977a; Thatcher and John 1977). Improved analytic models should allow for such possible variation in functional organization.

Recent studies in animals are paving the way for improved models of neural processing in humans. Freeman and colleagues have demonstrated that spatial patterns of macropotentials in the olfactory system of rabbits contain information not present in the firing of single neurons, that these patterns are 'neural templates' evoked during conditioned expectation and perception of specific odors, and that there are correlations between the macropotential patterns of olfactory bulb and cortex (Freeman 1975, 1979a,b,c, 1981, 1983; Bressler 1984, 1986; see Chapter 18 in Vol. 1). It is a large leap from rabbit paleocortex to human neocortex, but similar principles of mass neural organization may also apply at the more macroscopic level.

Understanding of human neurocognitive processes will advance in pace with improvements in recording and analytic technology. The next generation of research will probably view neurocognitive processing as a rapidly shifting, distributed network of integrated activity in many cortical and subcortical areas. The first step toward development of such a model will be the measurement of some sign of functional coordination between neural areas during cognitive tasks. In the coming decade we might expect to achieve a high degree of spatial resolution through recordings of more than 200 electric and magnetic scalp sensors combined

with advanced analytic techniques such as spatial deconvolution. In some cases, this may include 3-dimensional localization of multiple, simultaneously active sources.

### Acknowledgements

Manuscript preparation and the authors' research were sponsored by the Office of Naval Research, the Air Force Office of Scientific Research, the National Science Foundation, and the National Institutes of Neurological and Communicative Disorders and Strokes.

Special thanks to Suzanne Hollands and Adi Gevins for editorial assistance, and to Drs. Roy Halliday, Marta Kutas, Walter Ritter and Walter Roth for their valuable and much appreciated critical reviews.

This paper is dedicated to the memory of the late Dr. Samuel Sutton.

### References

- Adams, N. and Collins, G.I. (1978) Late components of the visual evoked potential to search in short-term memory. *Electroenceph. clin. Neurophysiol.*, 44, 147-156.
- Allison, T. (1984) Recording and interpreting event-related potentials. In: E. Donchin (Ed.), *Cognitive Psychophysiology: Event-Related Potentials and the Study of Cognition*, Vol. 1. Erlbaum, Hillsdale, NJ pp. 1-36.
- Ary, J.P., Klein, S.A. and Fender, D.H. (1981) Location of sources of evoked scalp potentials: corrections for skull and scalp thicknesses. *IEEE Trans. bio-med. Engng.* BME-28, 447-452.
- Ary, J.P., Darcey, T.M. and Fender, D.H. (1982) Locating electrical sources in the human brain (abstr.). *IEEE Trans. bio-med. Engng.* BME-28, 587.
- Aunon, J.I. (1978) Computer techniques for the processing of evoked potentials. *Comput. Prog. Biomed.*, 8, 243-255.
- Aunon, J.I., McGiilem, C.D. and Childers, D.G. (1981) Signal processing in evoked potential research: averaging and modeling. *Crit. Rev. Bioengng.* 5, 323-367.
- Başar, E. (1980) *EEG Brain Dynamics: Relation between EEG and Brain Evoked Potentials*. Elsevier, Amsterdam.
- Beaumont, J. (1983) The EEG and task performance: a tutorial review. In: A. Gaillard and W. Ritter (Eds.), *Tutorials in ERP Research: Endogenous Components*. Elsevier, Amsterdam, pp. 385-406.
- Berger, H. (1929) Über das Elektrenkephalogramm des Menschen. *Arch. Psychiat. Nerven.*, 87, 527-570.
- Bonham, B., Morgan, N. and Gevins, A.S. Comparison of frequency-dependent and frequency-independent methods for EOG artifact removal. Unpublished manuscript.
- Bressler, S. (1984) Spatial organization of EEGs from olfactory bulb and cortex. *Electroenceph. clin. Neurophysiol.*, 57, 270-276.
- Bressler, S. (1986) Functional relation of olfactory bulb and cortex. I. Spatial variation of bulbo-cortical interdependence. In preparation.
- Broadbent, D. (1970) Stimulus set and response set: two kinds of selective attention. In: D. Mostofsky (Ed.), *Attention: Contemporary Theory and Analysis*. Appleton-Century-Crofts, New York, pp. 51-90.
- Brown, W., Marsh, J. and Smith, J. (1976) Evoked potential wave form differences produced by the perception of different meanings of an ambiguous phrase. *Electroenceph. clin. Neurophysiol.*, 41, 113-123.

- Brown, W., Marsh, J. and Smith, J. (1979) Principal components analysis of ERP differences related to the meaning of an ambiguous word. *Electroenceph. clin. Neurophysiol.*, 4, 709-714.
- Brunia, C. and Vingerhoets, A. (1980) CNV and EMG preceding a planar flexion of the foot. *Biol. Psychol.*, 11, 181-191.
- Buchsbaum, M. and Fedio, P. (1970) Hemispheric differences in evoked potentials to verbal and non-verbal stimuli in left and right visual fields. *Physiol. Behav.*, 5, 207-210.
- Butler, S. and Glass, A. (1986) EEG alpha asymmetries. In: D. Papakostopoulos, I. Mortin and S.R. Butler (Eds.), *Clinical and Experimental Neuropsychophysiology*. Croom-Helm, Beckenham, in press.
- Cacioppo, J., Petty, R., Morris, K. and Losch, M. (1983) Perioral electromyographic responses uniquely distinguish the parameters of a simple letter matching task. Paper presented at the Annual Meeting of the Society for Psychophysiological Research, September.
- Callaway, E. (1973) Habituation of averaged evoked potentials in man. In: H. Peeke and M. Herz (Eds.), *Habituation*, Vol. 2. Academic Press, New York, pp. 153-174.
- Callaway, E. and Harns, P. (1974) Coupling between cortical potentials from different areas. *Science*, 183, 873-875.
- Callaway, E., Tueting, P. and Koslow, S. (Eds.) (1978) *Event-Related Brain Potentials in Man*. Academic Press, New York.
- Callaway, E., Halliday, R. and Herning, R.I. (1983) A comparison of methods for measuring event-related potentials. *Electroenceph. clin. Neurophysiol.*, 55, 227-232.
- Campbell, K.B., Courchesne, E., Picton, T.W. and Squires, K.C. (1979) Evoked potential correlates of human information processing. *Biol. Psychol.*, 8, 45-68.
- Chapman, R.M. (1977) Conative meaning and averaged evoked potentials. In: H. Begleiter (Ed.), *Evoked Brain Potentials and Behavior*. Plenum Press, New York, pp. 171-196.
- Chapman, R.M., McCreary, J., Chapman, J. and Bragdon, H. (1978) Brain responses to semantic meaning. *Brain Lang.*, 5, 195-205.
- Chapman, R.M., McCreary, J., Chapman, J. and Martin, J. (1980) Behavioral and neural analyses of connotative meaning: word classes and rating scales. *Brain Lang.*, 11, 319-339.
- Chase, W. (1984) The timing of mental acts. In: E. Donchin (Ed.), *Cognitive Psychophysiology: Event-Related Potentials and the Study of Cognition*. Erlbaum, Hillsdale, NJ, pp. 221-247.
- Chase, W., McCarthy, G., Squires, K. and Schvaneveldt, R. (1984) Mental chronometry. In: E. Donchin (Ed.), *Cognitive Psychophysiology: Event-Related Potentials and the Study of Cognition*. Erlbaum, Hillsdale, NJ, pp. 249-301.
- Cohen, D. and Cuffin, N. (1983) Demonstration of useful differences between magnetoencephalogram and electroencephalogram. *Electroenceph. clin. Neurophysiol.*, 56, 38-51.
- Courchesne, E. (1978) Changes in P3 waves with event repetition: long-term effects on scalp distribution and amplitude. *Electroenceph. clin. Neurophysiol.*, 45, 754-766.
- Courchesne, E., Hillyard, S. and Galambos, R. (1975) Stimulus novelty, task relevance and the visual evoked potential in man. *Electroenceph. clin. Neurophysiol.*, 39, 131-143.
- Cover, T.M. (1974) The two best measurements are not the best two. *IEEE Trans. Syst. Man Cybernet.*, SMC-4, 116-117.
- Cover, T.M. and Van Campenhout, J. (1976) On the possible orderings in the measurement selection problem. In: *Proc. 3rd Int. Joint Conf. Pattern Recognition*. IEEE, New York, pp. 245-248.
- Crow, H., Cooper, R. and Phillips, D. (1963) Progressive leucotomy. In: J. Masserman (Ed.), *Current Psychiatric Therapies*, Vol. 3. Grune and Stratton, New York, pp. 100-113.
- Daniel, R. (1966) Electroencephalographic pattern quantification and arousal continuum. *Psychophysiology*, 2, 146-160.
- Darcey, T.M. (1979) *Methods for Localization of Electrical Sources in the Human Brain and Applications to the Visual System*. Ph.D. Thesis, California Institute of Technology, Pasadena, CA.
- Darcey, T.M., Ary, J.P. and Fender, D.H. (1980) Methods for the localization of electrical sources in the human brain. *Prog. Brain Res.*, 54, 128-134.
- Deecke, L. and Kornhuber, H. (1977) Cerebral potentials and the initiation of voluntary movement. In: J. Desmedt (Ed.), *Progress in Clinical Neurophysiology*. Vol. 1. Attention, Concentration and



- Event-Related Potentials*. Karger, Basel, pp. 132-150.
- De Weerd, J.P.C.M. (1981) *Estimation of Evoked Potentials: a Study of a posteriori 'Wiener' Filtering and its Time-Varying Generalization*. Ph.D. Thesis, Katholieke Universiteit te Nijmegen. Krips Repro, Meppel.
- Donald, M. (1983) Neural selectivity in auditory attention. In: A. Gaillard and W. Ritter (Eds.), *Advances in Psychology. Vol. 10. Tutorials in Event-Related Potential Research: Endogenous Components*. Elsevier, Amsterdam, pp. 37-77.
- Donchin, E. (1966) A multivariate approach to the analysis of averaged evoked potentials. *IEEE Trans. bio-med. Engng.* BME-13, 131-139.
- Donchin, E. (1979) Event-related brain potentials: a tool in the study of human information processing. In: H. Begleiter (Ed.), *Evoked Potentials and Behavior*. Plenum, New York, pp. 13-75.
- Donchin, E. (1981) Surprise! ... Surprise? *Psychophysiology*, 18, 493-513.
- Donchin, E. (Ed.) (1984) *Cognitive Psychophysiology: Event-Related Potentials and the Study of Cognition*, Vol. 1. Erlbaum, Hillsdale, NJ.
- Donchin, E. and Heffley, E.F. (1978) Multivariate analysis of event-related potential data: a tutorial review. In: D. Otto (Ed.), *Multidisciplinary Perspectives in ERP Research. EPA-600/9-77-043*. U.S. Government Printing Office, Washington, DC, pp. 555-572.
- Donchin, E., Kutas, M. and Johnson, R. (1974) The CNV does not behave like a 'motor potential.' *Electroenceph. clin. Neurophysiol.*, 37, 484.
- Donchin, E., Tueting, P., Ritter, W., Kutas, M. and Heffley, E. (1975) On the independence of the CNV and P300 components of the human averaged evoked potential. *Electroenceph. clin. Neurophysiol.*, 38, 449-461.
- Donchin, E., Kutas, M. and McCarthy, G. (1977) Electrocortical indices of hemispheric utilization. In: S. Harnard et al. (Eds.), *Lateralization in the Nervous System*. Academic Press, New York, pp. 339-384.
- Donchin, E., Ritter, W. and Cheyne, W. (1978) Cognitive psychophysiology: endogenous components of the ERP. In: E. Callaway, P. Tueting and S. Koslow (Eds.), *Event-Related Brain Potentials in Man*. Academic Press, New York, pp. 349-412.
- Doyle, J.C. and Gevins, A.S. (1986) Spatial filters for event-related brain potentials. Submitted.
- Duffy, F.H., Bartels, P.H. and Burchfiel, J.L. (1981) Significance probability mapping: an aid in the topographic analysis of brain electrical activity. *Electroenceph. clin. Neurophysiol.*, 51, 455-462.
- Duncan-Johnson, C. and Donchin, E. (1982) The P300 component of the event-related brain potential as an index of information processing. *Biol. Psychol.*, 14, 1-52.
- Erkisen, C. and Schultz, D. (1979) Information processing in visual search: a continuous flow conception and experimental results. *Percept. Psychophys.*, 25, 249-263.
- Erne, S., Hahlebohm, H. and Lubbig, H. (1981) *Biomagnetism*. W. de Gruyter, Berlin.
- Fitzgerald, P.G. and Picton, T.W. (1981) Temporal and sequential probability in evoked potential studies. *Canad. J. Psychiat.*, 35, 188-200.
- Ford, J., Roth, W., Mohs, R., Hopkins, W. and Koppell, B. (1979) Event-related potentials recorded from young and old adults during a memory retrieval task. *Electroenceph. clin. Neurophysiol.*, 47, 450-459.
- Freeman, W.J. (1975) *Mass Action in the Nervous System*. Academic Press, New York.
- Freeman, W.J. (1979a) Nonlinear dynamics of paleocortex manifested in the olfactory EEG. *Biol. Cybernet.*, 35, 21-37.
- Freeman, W.J. (1979b) Nonlinear gain mediating cortical stimulus-response relations. *Biol. Cybernet.*, 33, 237-247.
- Freeman, W.J. (1979c) EEG analysis gives model of neuronal template-matching mechanism for sensory search with olfactory bulb. *Biol. Cybernet.*, 35, 221-234.
- Freeman, W.J. (1981) A physiological hypothesis of perception. *Perspect. Biol. Med.*, 24, 561-592.
- Freeman, W.J. (1983) The physiological basis of mental images. *Biol. Psychiat.*, 18, 1107-1125.
- Friedman, D., Simson, R., Ritter, W. and Rapin, I. (1975) Cortical evoked potentials elicited by real speech words and sounds. *Electroenceph. clin. Neurophysiol.*, 38, 13-19.
- Friedman, D., Vaughan, H. and Erlenmeyer-Kimling, L. (1978) Stimulus and response related compo-

- nents of the late positive complex in a visual discrimination task. *Electroenceph. clin. Neurophysiol.*, 45, 319-330.
- Friedman, D., Vaughan, Jr. H.G. and Erlenmeyer-Kimling, L. (1981) Multiple late positive potentials in two visual discrimination tasks. *Psychol. Physiol.*, 18, 635-649.
- Furnival, G.M. and Wilson, R.W. (1974) Regression by leaps and bounds. *Technometrics*, 16, 499-511.
- Fuster, J. (1980) *The Prefrontal Cortex*. Raven Press, New York.
- Gaillard, A. (1978) *Slow Brain Potentials Preceding Task Performance*. Academic Press, Amsterdam.
- Gasser, T., Möcks, J. and Verleger, R. (1983) SELAVCO: a method to deal with trial-to-trial variability of evoked potentials. *Electroenceph. clin. Neurophysiol.*, 55, 717-723.
- Gersch, W. and Goddard, G. (1970) Locating the site of epileptic focus by spectral analysis methods. *Science*, 169, 701-702.
- Gersch, W., Gevins, A.S. and Kitagawa, G. (1983) A multivariate time varying autoregressive modeling of nonstationary covariance time series. *Proc. IEEE CDC Control and Decision Conf.*, Texas, pp. 579-584.
- Gevins, A.S. (1980) Pattern recognition of human brain electrical potentials. *IEEE Trans. Pattern Anal. Mach. Intell.*, PAMI-2, 383-404.
- Gevins, A.S. (1983) Brain potential evidence for lateralization of higher cognitive functions. In: J.B. Hellige (Ed.), *Cerebral Hemisphere Asymmetry: Method, Theory and Application*. Praeger, New York, pp. 335-382.
- Gevins, A.S. (1984) Analysis of the electromagnetic signals of the human brain: milestones, obstacles and goals. *IEEE Trans. bio-med. Engng*, BME-31, 833-850.
- Gevins, A.S. (1986) Quantitative human neurophysiology of cognitive functions. In: H.J. Hannay (Ed.), *Experimental Techniques in Human Neuropsychology*. Oxford Univ. Press, New York, pp. 419-456.
- Gevins, A.S. and Schaffer, R.E. (1980) Critical review of research on EEG correlates of higher cortical functions. *CRC Rev. Bioengng*, 4, 113-164.
- Gevins, A.S., Zeitlin, G.M., Ancoli, S. and Yeager, C.L. (1977) Computer rejection of EEG artifact. II. Contamination by drowsiness. *Electroenceph. clin. Neurophysiol.*, 43, 31-42.
- Gevins, A.S., Zeitlin, G.M., Yingling, C., Doyle, J., Dedon, M., Schaffer, R., Roumasset, J. and Yeager, C. (1979a) EEG patterns during 'cognitive' tasks: I. Methodology and analysis of complex behaviors. *Electroenceph. clin. Neurophysiol.*, 47, 693-703.
- Gevins, A.S., Zeitlin, G., Doyle, J., Schaffer, R. and Callaway, E. (1979b) EEG patterns during 'cognitive' tasks. II. Analysis of controlled tasks. *Electroenceph. clin. Neurophysiol.*, 47, 704-710.
- Gevins, A.S., Zeitlin, G., Doyle, J., Yingling, C., Schaffer, R., Callaway, E. and Yeager, C. (1979c) Electroencephalogram correlates of higher cortical functions. *Science*, 203, 665-668.
- Gevins, A.S., Doyle, J.S., Schaffer, R.E., Callaway, E. and Yeager, C. (1980) Lateralized cognitive processes and the EEG. *Science*, 207, 1005-1108.
- Gevins, A.S., Doyle, J., Cuttillo, B., Schaffer, R., Tannehill, R., Ghannam, J., Gilcrease, V. and Yeager, C. (1981) Electrical potentials in human brain during cognition: new method reveals dynamic patterns of correlation of human brain electrical potentials during cognition. *Science*, 213, 918-922.
- Gevins, A.S., Schaffer, R.E., Doyle, J.C., Cuttillo, B.A., Tannehill, R.L. and Bressler, S.L. (1983) Shadows of thoughts: rapidly changing, asymmetric brain-potential patterns of a brief visuomotor task. *Science*, 220, 97-99.
- Gevins, A.S., Bressler, S.L., Cuttillo, B.A., Doyle, J.C., Morgan, N.H. and Zeitlin, G.M. (1984) *Neurocognitive Pattern Analysis of an Auditory and Visual Numeric Motor Control Task. Part I: Development of Methods*. A.F.O.S.R. Final Report, Contract No. F49620-82-K-0006.
- Gevins, A.S., Doyle, J.C., Cuttillo, B.A., Schaffer, R.E., Tannehill, R.S. and Bressler, S.L. (1985) Neurocognitive pattern analysis of a visuospatial task: low-frequency evoked correlations. *Psychophysiology*, 22, 32-43.
- Gevins, A.S., Cuttillo, B.A., Morgan, N., Bressler, S.L., White, R.M., Illes, J., Greer, D.S., Doyle, J.C. and Zeitlin, G.M. (1986) Spatiotemporal neuroelectric patterns predict human performance accuracy. Submitted.

- Goff, W., Allison, T. and Vaughan, H. (1978) The functional neuroanatomy of event-related potentials. In: E. Callaway, P. Tueting and E. Koslow (Eds.), *Event-Related Brain Potentials in Man*. Academic Press, New York, pp. 1-80.
- Goldman-Rakic, P. (1984) The frontal lobes — uncharted provinces of the brain. *Trends Neurosci.*, 7, 425-429.
- Gratton, G., Coles, M.G.H. and Donchin, E. (1983) A new method for off-line removal of ocular artifact. *Electroenceph. clin. Neurophysiol.*, 55, 468-484.
- Halgren, E., Squires, N.R., Wilson, C.L., Rohrbaugh, J.W., Babb, T.L. and Crandall, P.H. (1980) Endogenous potentials generated in the human hippocampal formation and amygdala by unexpected events. *Science*, 210, 803-805.
- Halliday, R., Callaway, E., Naylor, H. and Prael, R. (1984) Is mental scanning an afterthought? In: *ICON III: Proc. 3rd Int. Conf. on Cognitive Neuroscience*, Bristol, U.K., September.
- Hansen, J.C. and Hillyard, S.A. (1980) Endogenous brain potentials associated with selective auditory attention. *Electroenceph. clin. Neurophysiol.*, 49, 277-290.
- Hansen, J. and Hillyard, S. (1983) Selective attention to multidimensional auditory stimuli. *J. exp. Psychol.: Hum. Percept. Perform.*, 9, 1-19.
- Harman, H. (1976) *Modern Factor Analysis*, 3rd edn. University of Chicago Press, Chicago, IL.
- Harter, M. and Guido, W. (1980) Attention to pattern orientation: negative cortical potentials, reaction time, and the selection process. *Electroenceph. clin. Neurophysiol.*, 49, 461-475.
- Harter, M., Aine, C. and Schroeder, C. (1982) Hemispheric differences in the neural processing of stimulus location and type: effects of selective attention on visual evoked-potentials. *Neuropsychologia*, 20, 421-438.
- Hillyard, S. (1973) The CNV and human behavior: a review. *Electroenceph. clin. Neurophysiol.*, 33, 161-171.
- Hillyard, S. (1984) Event-related potentials and selective attention. In: E. Donchin (Ed.), *Cognitive Psychophysiology: Event-Related Potentials and the Study of Cognition*, Vol. 1. Erlbaum, Hillsdale, NJ, pp. 51-72.
- Hillyard, S., Hink, R., Schwent, V. and Picton, T. (1973) Electrical signs of selective attention in the human brain. *Science*, 182, 177-180.
- Hink, R., Van Voorhis, S., Hillyard, S. and Smith, T. (1977) The division of attention and the human auditory evoked potential. *Neuropsychologia*, 15, 597-605.
- Hjorth, B. (1975) On-line transformation of EEG scalp potentials into orthogonal source derivations. *Electroenceph. clin. Neurophysiol.*, 39, 111-118.
- Hjorth, B. (1982) An adaptive EEG derivation technique. *Electroenceph. clin. Neurophysiol.*, 54, 654-661.
- Horst, R., Johnson, R. and Donchin, E. (1980) Event-related brain potentials and subjective probability in a learning task. *Memory Cognit.*, 8, 476-488.
- Inoue, T., Kazuhiro, S. and Yagasaki, A. (1983) The direction of spread of alpha activity over the scalp. *Electroenceph. clin. Neurophysiol.*, 55, 290-300.
- Isreal, J., Chesney, G., Wickens, C. and Donchin, E. (1980) P300 and tracking difficulty: evidence for multiple resources in dual-task performance. *Psychophysiology*, 17, 259-273.
- John, E.R., Karmel, B.Z., Corning, W.C., Eason, P., Brown, D., Ahn, H., John, M., Harmony, T., Pincus, L., Toro, A., Gershon, I., Bartlett, F., Thatcher, R., Kaye, H., Valdes, P. and Schwartz, E. (1977a) Neurometrics: numerical taxonomy identifies different profiles of brain functions within groups of behaviorally similar people. *Science*, 196, 1393-1410.
- John, E.R., Karmel, B.Z., Pincus, L.S., Ahn, H. and John, M. (1977b) Neurometrics applied to the quantitative electrophysiological measurement of organic brain dysfunction in children. In: C. Shagass, S. Gershon and A.J. Friedhoff (Eds.), *Psychopathology and Brain Dysfunction*. Raven Press, New York, pp. 291-338.
- John, E.R., Pincus, L., Ahn, H., Easton, P., Friedman, J. and Kaye, H. (1983) Neurometric evaluation of cognitive dysfunctions and neurological disorders in children. *Prog. Neurobiol.*, 21, 229-290.
- Just, M. and Carpenter, P. (1976) Eye fixations and cognitive processes. *Cogn. Psychol.*, 8, 441-480.

- Kahneman, D. (1973) *Attention and Effort*. Prentice-Hall, Englewood Cliffs, NJ.
- Kaufman, L. and Williamson, S. (1982) Magnetic location of cortical activity. *Ann. N.Y. Acad. Sci.*, 388, 197-213.
- Kavanagh, R.N. (1972) *Localization of Sources of Human Evoked Responses*. Ph.D. Thesis, California Institute of Technology, Pasadena, CA.
- Kavanagh, R.N., Darcey, T.M., Lehmann, D. and Fender, D. (1978) Evaluation of methods for three-dimensional localization of electrical sources in the human brain. *IEEE Trans. bio-med. Engng*, BME-25, 421-429.
- Khachaturian, Z. and Gluck, H. (1969) The effects of arousal on the amplitude of evoked potentials. *Brain Res.*, 14, 589-606.
- Khachaturian, Z., Chisholm, R. and Kerr, J. (1973) The effects of arousal on evoked potentials to relevant and irrelevant stimuli. *Psychophysiology*, 10, 194.
- Klinke, R., Fruhstorfer, H. and Finkenzeller, P. (1968) Evoked responses as a function of external and stored information. *Electroenceph. clin. Neurophysiol.*, 25, 119-122.
- Knight, R., Hillyard, S., Woods, D. and Neville, H. (1980) The effects of frontal and temporal-parietal lesions on the auditory evoked potential in man. *Electroenceph. clin. Neurophysiol.*, 50, 112-126.
- Kornhuber, H. and Deecke, L. (1965) Hirnpotentialänderungen bei Willkürbewegungen und passiven Bewegungen des Menschen: Bereitschaftspotential und reafferente Potentiale. *Pflügers Arch. ges. Physiol.*, 284, 1-17.
- Kramer, A., Fisk, A. and Schneider, W. (1983) P300, consistency and visual search. Paper presented at 1983 meeting of Society for Psychophysiological Research. In: E. Donchin, C. Wickens and M. Coles (Eds.), *Annual Progress Report*. Air Force Office of Scientific Research. (Abstract in *Psychophysiology*, 20, 453-454.)
- Kutas, M. and Hillyard, S. (1980a) Reading senseless sentences: brain potentials reflect semantic incongruity. *Science*, 207, 203-205.
- Kutas, M. and Hillyard, S. (1980b) Event-related brain potentials to semantically inappropriate and surprisingly large words. *Biol. Psychol.*, 11, 99-116.
- Kutas, M. and Hillyard, S. (1980c) Reading between the lines: event-related brain potentials during natural sentence processing. *Brain Lang.*, 11, 354-373.
- Kutas, M. and Hillyard, S. (1982) The lateral distribution of event-related potentials during sentence processing. *Neuropsychologia*, 20, 579-590.
- Kutas, M., McCarthy, G. and Donchin, E. (1977) Augmenting mental chronometry: P300 as a measure of stimulus evaluation time. *Science*, 197, 792-795.
- Kutas, M., Lindamood, T. and Hillyard, S. (1984) Word probability and event-related brain potentials during sentence processing. In: S. Kornblum and J. Requin (Eds.), *Preparatory States and Processes*. Erlbaum, Hillsdale, NJ, pp. 217-238.
- Lassen, N., Ingvar, D. and Skinhøj, E. (1978) Brain function and blood flow. *Scient. Amer.*, 239, 62-71.
- Lehmann, D. (1971) Multichannel topography of human alpha EEG fields. *Electroenceph. clin. Neurophysiol.*, 31, 439-449.
- Lehmann, D. (1981) Spatial analysis of evoked and spontaneous EEG potential fields. In: N. Yamaguchi and K. Fujisawa (Eds.), *Recent Advances in EEG and EMG Data Processing*. Elsevier, Amsterdam, pp. 117-132.
- Lehmann, D. (1984) EEG assessment of brain activity: spatial aspects, segmentation and imaging. *Int. J. Psychophysiol.*, 1, 267-276.
- Lehmann, D. and Skrandies, W. (1980) Reference-free identification of components of checkerboard-evoked multichannel potential fields. *Electroenceph. clin. Neurophysiol.*, 48, 609-621.
- Lehmann, D. and Skrandies, W. (1984) Spatial analysis of evoked potentials in man — a review. *Prog. Neurobiol.*, 23, 227-250.
- Lehmann, D., Kavanagh, R.N. and Fender, D.H. (1969) Field studies of averaged visually evoked EEG potentials in a patient with a split chiasm. *Electroenceph. clin. Neurophysiol.*, 29, 193-199.
- Livanov, M.N. (1977) *Spatial Organization of Cerebral Processes*. Wiley, New York.
- Loomis, A. et al. (1938) Distribution of disturbance patterns in the human electroencephalogram with

- special reference to sleep. *J. Neurophysiol.*, 1, 413.
- Loveless, N.E. (1979) Event-related slow potentials of the brain as expressions of orienting function. In: H. Kimmel, E. Van Olst and J. Orlebeke (Eds.), *The Orienting Reflex in Humans*. Erlbaum, Hillsdale, NJ, pp. 77-100.
- Low, M., Borda, R., Frost, J. and Kellaway, P. (1966) Surface-negative, slow-potential shift associated with conditioning in man. *Neurology (Minneapolis)*, 16, 771-782.
- Luna, A.R. (1970) The functional organization of the brain. *Scient. Amer.*, 222, 66-72.
- Luna, A.R. (1977) *Higher Cortical Functions in Man*. Basic Books, New York.
- Mane, A., Sirevaag, E., Coles, M. and Donchin, E. (1983) ERPs and performance under stress conditions. In: E. Donchin, C. Wickens and M. Coles (Eds.), *Annual Progress Report*. Air Force Office of Scientific Research, Life Sciences Directorate. (Also abstract in *Psychophysiology*, 20, 458.)
- Mars, N.J.I. and Lopes da Silva, F.H. (1983) Propagation of seizure activity in kindled dogs. *Electroenceph. clin. Neurophysiol.*, 56, 194-209.
- Marsin, G. (1975) Age differences in evoked potential correlates of a memory scanning process. *Exp. Aging Res.*, 1, 3-16.
- McAdam, D. (1973) Physiological mechanisms, a review. In: W. McCallum and J. Knott (Eds.), *Event-Related Slow Potentials of the Brain*. *Electroenceph. clin. Neurophysiol.*, Suppl. 3. Elsevier Amsterdam, pp. 79-86.
- McCallum, W.C. and Walter, W.G. (1968) The effects of attention and distraction on the contingent negative variation in normal and neurotic subjects. *Electroenceph. clin. Neurophysiol.*, 25, 319-329.
- McCarthy, G. and Donchin, E. (1981) A metric for thought: a comparison of P300 latency and reaction time. *Science*, 211, 77-79.
- McCarthy, G. and Donchin, E. (1983) Chronometric analysis of human information processing. In: A. Gaillard and W. Ritter (Eds.), *Tutorials in Event-Related Potential Research: Endogenous Components*. *Advances in Psychology*, Vol. 10. Elsevier, Amsterdam, pp. 251-268.
- McClelland, J.L. (1979) On the time relations of mental processes: an examination of systems of processes in cascade. *Psychol. Rev.*, 86, 287-330.
- McGill, C., Aunon, J. and Childers, D. (1981) Signal processing in evoked potential research: applications of filtering and pattern recognition. *Crit. Rev. Bioengng.*, 6, 225-265.
- Megele, A. and Teyler, T. (1979) Habituation and the human evoked potential. *J. comp. physiol. Psychol.*, 93, 1154-1170.
- Miller, J. (1982) Discrete versus continuous-stage models of human information processing. *J. exp. Psychol.: Hum. Percept. Perform.*, 8, 273-296.
- Molfese, D.L. (1979) Cortical involvement in the semantic processing of co-articulated speech cues. *Brain Lang.*, 7, 86-100.
- Molfese, D.L. (1980) The phoneme and the engram: electrophysiological evidence for the acoustic invariant in stop consonants. *Brain Lang.*, 9, 372-376.
- Molfese, D. (1983) Event-related potentials and language processes. In: A. Gaillard and W. Ritter (Eds.), *Tutorials in Event-Related Potential Research: Endogenous Components*. *Advances in Psychology*, Vol. 10. Elsevier, Amsterdam, pp. 345-368.
- Moray, N. (1969) *Selective Processes in Vision and Hearing*. Hutchinson Educational, London.
- Murray, N. and Cobb, W. (1980) Source derivation in routine EEG practice. *Electroenceph. clin. Neurophysiol.*, 50, 194.
- Näätänen, R. (1982) The N2 component of the evoked potential: a scalp reflection of neuronal mismatch of orienting theory? In: J. Strelau, F. Farley and A. Gale (Eds.), *Biological Foundations of Personality and Behavior*. Hemisphere Press, Washington, DC.
- Näätänen, R. and Gaillard, A. (1983) The orienting reflex and the N2 deflection of the ERP. In: A. Gaillard and W. Ritter (Eds.), *Tutorials in Event-Related Potential Research: Endogenous Components*. *Advances in Psychology*, Vol. 10. Elsevier, Amsterdam, pp. 119-142.
- Näätänen, R. and Michie, P.T. (1979a) Early selective attention effects on the evoked potential. A critical review and reinterpretation. *Biol. Psychol.*, 3, 81-136.

- Näätänen, R. and Michie, P. (1979b) Different variants of endogenous negative brain potentials in performance situations: review and classification. In: D. Lehmann and E. Callaway (Eds.), *Human Evoked Potentials, Applications and Problems. NATO Conf. Ser., Ser. III: Human Factors, Vol. 9*. Plenum, New York, pp. 251-268.
- Näätänen, R., Gaillard, A. and Montysalo, S. (1978) The N1 effect of selective attention reinterpreted. *Acta psychol. (Amst.)*, 42, 313-329.
- Näätänen, R., Gaillard, A. and Varey, C. (1981) Attention effects on auditory EPs as a function of inter-stimulus interval. *Biol. Psychol.*, 13, 173-187.
- Nicholas, C. and De Loche, G. (1976) Convolution computer processing of the brain electrical image transmission. *Int. J. Biomed. Comput.*, 7, 143-159.
- Norman, D. and Bobrow, D. (1976) On data-limited and resource-limited processes. *Cogn. Psychol.*, 7, 44-64.
- Núñez, P.L. (1981) *Electric Fields in the Brain: the Neurophysics of EEG*. Oxford University Press, New York.
- Okada, Y.C. (1983) Inferences concerning anatomy and physiology of the human brain based on its magnetic field. *Nuovo Cimento*, 2, 379-409.
- Okada, Y.C., Kaufman, L. and Williamson, S.J. (1982) Hippocampal formation as a source of endogenous slow potentials. *Electroenceph. clin. Neurophysiol.*, 55, 417-426.
- Perrault, N. and Picton, T. (1984) Event-related potentials recorded from the scalp and nasopharynx. II. N2, P3 and slow wave. *Electroenceph. clin. Neurophysiol.*, 59, 261-278.
- Picton, T.W. and Stuss, D.T. (1980) The component structure of the human event-related potentials. In: H. Kornhuber and L. Deecke (Eds.), *Motor and Sensory Processes of the Brain: Electrical Potentials, Behavior and Clinical Use. Progress in Brain Research, Vol. 54*. Elsevier, Amsterdam, pp. 17-49.
- Posner, M. (1978) *Chronometric Explorations of Mind*. Erlbaum, Hillsdale, NJ.
- Posner, M., Harter, R., Hillyard, S. and Treisman, A. (1984) Selective attention. In: E. Donchin (Ed.), *Cognitive Psychophysiology: Event-Related Potentials and the Study of Cognition*. Erlbaum, Hillsdale, NJ, pp. 73-105.
- Pritchard, W. (1981) Psychophysiology of the P300. *Psychol. Bull.*, 90, 506-540.
- Rebert, C. (1978) Electrogenesis of slow potential changes in the central nervous system: a summary of issues. In: D. Otto (Ed.), *Multidisciplinary Perspectives in Event-Related Brain Potential Research. EPA-600/9-77-043*. U.S. Government Printing Office, Washington, DC, pp. 3-11.
- Rechtschaffen, A. and Kales, A. (1973) *A Manual of Standardized Terminology, Techniques and Scoring System for Sleep Stages of Human Subjects*. Brain Inform. Service, University of California, Los Angeles, CA.
- Renault, B. (1983) The visual evoked potentials: clues for information processing. In: A. Gaillard and W. Ritter (Eds.), *Tutorials in Event-Related Potential Research: Endogenous Components. Advances in Psychology, Vol. 10*. Elsevier, Amsterdam, pp. 159-176.
- Renault, B. and Lesevre, N. (1979) A trial-by-trial study of the visual omission response in reaction time situations. In: D. Lehmann and E. Callaway (Eds.), *Human Evoked Potentials*. Plenum Press, New York, pp. 317-329.
- Renault, B., Ragot, R., Lesevre, N. and Remond, A. (1982) Onset and offset of brain events as indices of mental chronometry. *Science*, 215, 1413-1415.
- Ritter, W., Simson, R. and Vaughan, Jr., H.G. (1972) Association cortex potentials and reaction time in auditory discrimination. *Electroenceph. clin. Neurophysiol.*, 33, 547-555.
- Ritter, W., Simson, R., Vaughan, H. and Friedman, D. (1979) A brain event related to the making of a sensory discrimination. *Science*, 203, 1358-1361.
- Ritter, W., Rotkin, L. and Vaughan, H. (1980) The modality specificity of the slow negative wave. *Psychophysiology*, 17, 222-227.
- Ritter, W., Simson, R., Vaughan, H. and Macht, M. (1982) Manipulation of event-related potential manifestations of information processing stages. *Science*, 218, 909-911.
- Ritter, W., Vaughan, H. and Simson, R. (1983a) On relating event-related potential components and

- stages of information processing. In: A. Gaillard and W. Ritter (Eds.), *Tutorials in Event-Related Potential Research: Endogenous Components. Advances in Psychology, Vol. 10*. Elsevier, Amsterdam, pp. 143-158.
- Ritter, W., Simson, R. and Vaughan, H. (1983b) Event-related potential correlates of two stages of information processing in physical and semantic discrimination tasks. *Psychophysiology*, 20, 168-179.
- Ritter, W., Kutas, S., Kutas, M. and Shiffrin, R. (1984) Preparatory processes. In: E. Donchin (Ed.), *Cognitive Psychophysiology: Event-Related Potentials and the Study of Cognition*. Erlbaum, Hillsdale, NJ, pp. 179-219.
- Rockstroh, B., Elbert, T., Birbaumer, N. and Lutzenberger, W. (1982) *Slow Brain Potentials and Behavior*. Urban and Schwarzenberg, Baltimore, MD.
- Rohrbach, J. and Gaillard, A. (1983) Sensory and motor aspects of the contingent negative variation. In: A. Gaillard and W. Ritter (Eds.), *Tutorials in Event-Related Potential Research: Endogenous Components. Advances in Psychology, Vol. 10*. Elsevier, Amsterdam, pp. 269-310.
- Rohrbach, J., Sydulko, K. and Lindsley, D. (1976) Brain wave components of the contingent negative variation in humans. *Science*, 191, 1055-1057.
- Rohrbach, J., Sydulko, K., Sanquist, T. and Lindsley, D. (1980) Synthesis of the contingent variation brain potential from noncontingent stimulus and motor elements. *Science*, 208, 1165-1168.
- Rosier, F. (1983) Endogenous ERPs and cognition: probes, prospects and pitfalls in matching pieces of the mind-body puzzle. In: A.W.K. Gaillard and W. Ritter (Eds.), *Advances in Psychology, Vol. 10. Tutorials in Event-Related Potential Research: Endogenous components*. Elsevier, Amsterdam, pp. 9-36.
- Rosier, F. and Manzey, D. (1981) Principal components and Varimax-rotated components in event-related potential research: some remarks on their interpretation. *Biol. Psychol.*, 13, 3-26.
- Roth, W. (1973) Auditory evoked responses to unpredictable stimuli. *Psychol. Physiol.*, 10, 125-137.
- Roth, W.T. (1978) How many late positive waves are there? In: D. Otto (Ed.), *Multidisciplinary Perspectives in Event-Related Brain Potential Research, EPA-600/9-77-043*. U.S. Government Printing Office, Washington, DC, pp. 170-172.
- Ruchkin, D. and Sutton, S. (1978) Equivocation and P300 amplitude. In: D. Otto (Ed.), *Multidisciplinary Perspectives in Event-Related Brain Potential Research, EPA-600/9-77-043*. U.S. Government Printing Office, Washington, DC, pp. 175-177.
- Ruchkin, D. and Sutton, S. (1983) Positive slow wave and P300: association and disassociation. In: A. Gaillard and W. Ritter (Eds.), *Tutorials in Event-Related Potential Research: Endogenous Components. Advances in Psychology, Vol. 10*. Elsevier, Amsterdam, pp. 233-250.
- Ruchkin, D.S., Sutton, S. and Tueting, P. (1975) Emitted and evoked P300 potentials and variation in stimulus probability. *Psychophysiology*, 12, 591-595.
- Ruchkin, D., Sutton, S., Kietzman, M. and Silver, K. (1980a) Slow wave and P300 in signal detection. *Electroenceph. clin. Neurophysiol.*, 50, 35-47.
- Ruchkin, D., Sutton, S. and Steg, M. (1980b) Emitted P300 and slow wave event-related potentials in guessing and detection tasks. *Electroenceph. clin. Neurophysiol.*, 49, 1-14.
- Rugg, M. (1983) The relationship between evoked-potentials and lateral asymmetries of processing. In: A. Gaillard and W. Ritter (Eds.), *Tutorials in Event-Related Potential Research: Endogenous Components. Advances in Psychology, Vol. 10*. Elsevier, Amsterdam, pp. 369-383.
- Saito, Y. and Harashina, H. (1981) Tracking of informations within multichannel EEG record — causal analysis in EEG. In: N. Yamaguchi and K. Fujisawa (Eds.), *Recent Advances in EEG and EMG Data Processing*. Elsevier, Amsterdam, pp. 133-177.
- Saltzberg, B. (1985) Special electrophysiological tests: brain spiking, EEG spectral coherence. In: R.C.W. Hail and T.P. Beresford (Eds.), *Handbook of Psychiatric Diagnostic Procedures, Vol. 2*. Spectrum, New York, pp. 137-152.
- Sampson, P. (1967) *BMD07M-Stepwise Linear Discriminant Analysis*. BMD Biomedical Computer Programs. Univ. California Press, Berkeley, CA, pp. 214a-214t.
- Sayers, B., Beagley, H. and Henshall, W. (1974) The mechanisms of evoked EEG responses. *Nature*

- (*Lond.*), 247, 481-483.
- Schneider, W. and Shiffrin, R.M. (1977) Controlled and automatic human information processing. I. Detection, search and attention. *Psychol. Rev.*, 84, 1-66.
- Simon, O., Schultz, H. and Rassman, W. (1977) The definition of waking stages on the basis on continuous polygraphic recording in normal subjects. *Electroenceph. clin. Neurophysiol.*, 42, 48-56.
- Simson, R., Vaughan, H.G. and Ritter, W. (1976) The scalp topography of potentials associated with missing visual or auditory stimuli. *Electroenceph. clin. Neurophysiol.*, 40, 33-42.
- Simson, R., Vaughan, H.G. and Ritter, W. (1977a) The scalp topography of potentials in auditory and visual discrimination tasks. *Electroenceph. clin. Neurophysiol.*, 42, 528-535.
- Simson, R., Vaughan, H.G. and Ritter, W. (1977b) The scalp topography of potentials in auditory and visual go/no-go tasks. *Electroenceph. clin. Neurophysiol.*, 43, 864-875.
- Snyder, E. and Hillyard, S.A. (1976) Long-latency evoked potentials to irrelevant, deviant stimuli. *Behav. Biol.*, 16, 319-331.
- Snyder, E., Hillyard, S. and Galambos, R. (1980) Similarities and differences among the P3 waves to detected signals in three modalities. *Psychol. Physiol.*, 17, 112-122.
- Spehr, W. (1976) Source derivation after Hjorth — an improved EEG derivation technique. *Electro-medica*, 4, 148-155.
- Squires, K., Hillyard, S. and Lindsay, P. (1973) Cortical potentials evoked by feedback confirming and disconfirming an auditory decision. *Percept. Psychophys.*, 13, 25-31.
- Squires, K., Wickens, C., Squires, N. and Donchin, E. (1976) The effect of stimulus sequence on the waveform of the cortical event-related potential. *Science*, 193, 1142-1146.
- Squires, N., Squires, K. and Hillyard, S. (1975) Two varieties of long latency positive waves evoked by unpredictable auditory stimuli in man. *Electroenceph. clin. Neurophysiol.*, 38, 387-401.
- Squires, N., Donchin, E., Squires, K. and Grossberg, S. (1977) Bisensory stimulation: inferring decision-related processes from the P300 components. *J. exp. Psychol.: Hum. Percept. Perform.*, 3, 299-315.
- Squires, N., Halgren, E., Wilson, C. and Crandall, P. (1983) Human endogenous limbic potentials: cross-modality and depth/surface comparisons in epileptic subjects. In: A. Gaillard and W. Ritter (Eds.), *Tutorials in Event-Related Potential Research: Endogenous Components. Advances in Psychology*, Vol. 10. Elsevier, Amsterdam, pp. 217-232.
- Stern, J., Wairath, L. and Goldstein, R. (1984) The endogenous eyeblink. *Psychophysiology*, 21, 22-33.
- Sternberg, S. (1969) The discovery of processing stages: extensions of Donders' method. In: W. Koster (Ed.), *Attention and Performance II*. (Also in *Acta Psychol. (Amst.)*, 30, 276-315.)
- Stuss, D.T., Toga, A., Hutchinson, J. and Picton, T.W. (1980) Feedback evoked potentials during an auditory concept formation task. In: H. Kornhuber and L. Deecke (Eds.), *Monvannon, Motor and Sensory Processes of the Brain: Electrical Potentials, Behavioral and Clinical Use. Progress in Brain Research*, Vol. 54. Elsevier, Amsterdam, pp. 403-409.
- Stuss, D., Sarazin, E., Leech, E. and Picton, T. (1983) Event-related potentials during naming and mental rotation. *Electroenceph. clin. Neurophysiol.*, 56, 133-146.
- Sutton, S., Braren, M., Zublin, J. and John, E. (1965) Evoked potential correlates of stimulus uncertainty. *Science*, 150, 1187-1188.
- Sutton, S., Tuetting, P., Zubin, J. and John, E.R. (1967) Information delivery and the sensory evoked potential. *Science*, 155, 1436-1439.
- Tecce, J. (1972) Contingent negative variation (CNV) and psychological processes in man. *Psychol. Bull.*, 77, 73-108.
- Tecce, J. (1978) A CNV rebound function: preliminary report. In: D. Otto (Ed.), *Multidisciplinary Perspectives in Event-Related Brain Potential Research. EPA-600/9-77-043*. U.S. Government Printing Office, Washington, DC, pp. 22-225.
- Thatcher, R. and John, E. (1977) *Functional Neuroscience. Vol. 1. Foundations of Cognitive Processes*. Erlbaum, Hillsdale, NJ.
- Thickbroom, G., Mastaglia, F., Carroll, W. and Davies, H. (1984) Source derivation: application to



- topographic mapping of visual evoked potentials. *Electroenceph. clin. Neurophysiol.*, 59, 279-285.
- Tueting, P. (1978) Event related potentials, cognitive events and information processing: a summary of issues and discussion. In: D. Otto (Ed.), *Multidisciplinary Perspectives in Event-Related Brain Potential Research*, EPA-600/9-77-043. U.S. Government Printing Office, Washington, DC, pp. 159-169.
- Tueting, P., Sutton, S. and Zublin, J. (1970) Quantitative evoked potential correlates of the probability of events. *Psychol. Physiol.*, 7, 385-394.
- Van Rotterdam, A. (1970) Limitations and difficulties in signal processing by means of principal-components analysis. *IEEE Trans. bio-med. Engng.*, BME-17, 268-269.
- Verbaten, M. (1983) The influence of information on habituation of cortical, autonomic and behavioral components of the orienting response. In: A. Gaillard and W. Ritter (Eds.), *Tutorials in Event-Related Potential Research: Endogenous Components*, *Advances in Psychology*, Vol. 10. Elsevier, Amsterdam, pp. 201-216.
- Verleger, R., Gasser, T. and Mocks, J. (1982) Correction of EEG artifacts in event-related potentials of the EEG: aspects of reliability and validity. *Psychophysiology*, 19, 472-480.
- Wailin, G. and Stålberg, E. (1980) Source derivation in clinical routine EEG. *Electroenceph. clin. Neurophysiol.*, 50, 282-292.
- Walter, D.O. (1963) Spectral analysis for electroencephalograms: mathematical determination of neurophysiological relationships from records of limited duration. *Exp. Neurol.*, 8, 155-181.
- Walter, D.O., Rhodes, J.M. and Adey, W.R. (1967) Discriminating among states of consciousness by EEG measurements: a study of four subjects. *Electroenceph. clin. Neurophysiol.*, 22, 22-29.
- Walter, W.G. (1964) The contingent negative variation: an electrocortical sign of significant association in the human brain. *Science*, 146, 434.
- Walter, W.G., Cooper, R., Aldridge, V., McCallum, W. and Winter, A. (1964) Contingent negative variation: an electrical sign of sensorimotor association and expectancy in the human brain. *Nature (Lond.)*, 203, 380-384.
- Weinberg, H., Stroink, G. and Katila, T. (1985) *Biomagnetism, Applications and Theory*. Pergamon, New York.
- Wickens, C., Kramer, A., Vanasse, L. and Donchin, E. (1983) Performance of concurrent tasks: physiological analysis of reciprocity of information-processing resources. *Science*, 221, 1080-1082.
- Williamson, S.J. and Kaufman, L. (1981a) Biomagnetism. *J. Magnet. magnet. Mater.*, 22, 129-202.
- Williamson, S.J. and Kaufman, L. (1981b) Magnetic fields of the cerebral cortex. In: S.N. Erne, H.D. Hählbohm and H. Lübbig (Eds.), *Biomagnetism*. De Gruyter, New York, pp. 353-402.
- Wood, C. (1975) Auditory and phonetic levels of processing in speech perception: neurophysiological and information-processing analyses. *J. exp. Psychol.: Hum. Percept. Perform.*, 104, 3-20.
- Wood, C.C., Allison, T., Goff, W.R., Williamson, P.D. and Spencer, D.B. (1980) On the neural origin of P300 in man. In: H. Kornhuber and L. Deecke (Eds.), *Movement, Motor and Sensory Processes of the Brain: Electrical Potentials, Behavior and Clinical Use*. *Progress in Brain Research*, Vol. 54. Elsevier, Amsterdam, pp. 51-56.
- Wood, C., McCarthy, G., Squires, N., Vaughan, H., Woods, D. and McCallum, W. (1982) Anatomical and physiological substrates of event-related potentials. *Ann. N.Y. Acad. Sci.*, 388, 681-721.
- Wood, C. and McCarthy, G. (1984) Principal components analysis of event-related potentials: simulation studies demonstrate misallocation of variance across components. *Electroenceph. clin. Neurophysiol.*, 59, 249-260.
- Woods, D. and Courchesne, E. (1983) Event-related potentials during split-second auditory and visual decision making in man. In: F. Denoth (Ed.), *EPIC VII: Preliminary Poster Reports*, pp. 72-73.
- Woody, C.D. (1967) Characterization of an adaptive filter for the analyses of variable latency neuroelectric signals. *Med. Biol. Engng.*, 5, 539-553.
- Yingling, C. and Hosobuchi, Y. (1984) A subcortical correlate of P300 in man. *Electroenceph. clin. Neurophysiol.*, 59, 72-76.
- Yu, K. and McGillem, C. (1983) Optimum filters for estimating evoked potential waveforms. *IEEE Trans. bio-med. Engng.*, BME-30, 730-737.

### Appendix

The probe ERP method is an attempt to obtain information about regional brain activity associated with cognitive processes from ERP waveforms elicited by irrelevant 'probe' stimuli presented at various times during a task. This is an adaptation of the probe reaction-time method used in psychological studies to assess the commitment of limited-capacity processing to a primary task. The basic assumption of the probe ERP method, the 'ceiling' or 'limited capacity' hypothesis, proposes that the neural response to a probe stimulus is reduced by the commitment of a local neural population to primary task processes (reviewed in Papanicolaou and Johnstone 1984). For example, the right-sided lateralization of P100 and N100 peaks for visual probes during an auditory linguistic task (relative to a non-verbal task) was due to lower amplitudes over left hemisphere ('language') sites (Papanicolaou 1980). Reduced probe ERP amplitudes over left hemisphere sites have also been measured during mental arithmetic (Rasmussen et al. 1977) and visuospatial tasks (Papanicolaou et al. 1983).

The significance of the brain's response to non-contingent probes and the effects of probes on task-related processes have not been determined. If the probe ERP is affected by task processes (via the 'ceiling effect'), then probe stimuli may in turn affect those task processes. Questions about the effect of probes on cortical activation and the habituation of responses to frequently presented probes are raised by observations of regional changes in ERP amplitudes and EEG spectral coherence associated with levels of autonomic arousal and stages of conditioning (Gershuni et al. 1960; Khachaturian and Gluck 1969; Khachaturian et al. 1973; Hudspeth and Jones 1975). Habituation of probe ERP amplitudes was evident in a study comparing auditory linguistic and non-linguistic tasks (Shucard et al. 1977). Probes consisting of pairs of tone pips 2 sec apart elicited task-related asymmetries due to larger ERP amplitudes for the second tone over the hemisphere presumed to be involved in each task. This was attributed to a difference in the 'habituation recovery cycle' between engaged and non-engaged hemispheres, implying that the *engaged* hemisphere was 'too busy' to habituate. It is not clear how this result relates to the 'ceiling hypothesis' which proposes that probe amplitudes will be reduced over 'engaged' areas.

Another consideration is the effect of the physical properties of probe stimuli. Lateral ERP asymmetries have been observed even for simple unstructured stimuli (Friedman et al. 1978), and opposite asymmetries to auditory and visual probes in the same task have been reported (Johnstone 1982). Also, the ERP elicited by task-irrelevant probes consists mainly of exogenous peaks, which are thought to be generated by primary sensory processes, and the nature of the interaction of such sensory processing with higher cognitive processes, which may involve different neural populations, is not known.

It has been proposed that the probe ERP method has the attractive advantages of 'ecological validity' and freedom from the need to control stimulus- and response-related factors (Papanicolaou and Johnstone 1984). This would mean that the

probe method might be applied in more naturalistic 'real-life' situations, without the artificial constraints imposed by well-controlled ERP experiments. However, upon reflection, it is clear that the probe method does not avoid the need to control stimulus- and response-related factors and artifacts, since these factors have strong effects on brain potentials which can easily be confused with the effects of cognitive factors *per se*. If probe ERPs are sensitive to local neural activity, they will certainly be affected by neural responses to such stimulus and response factors and will also be affected by eye and muscle artifacts, since random timing of probes cannot eliminate the effects of such activity which would be present in naturalistic situations.

Randomly timed probes do not provide precise information about the split-second stages of cognitive processing. The 'background information probe' method (Thatcher and Maisel 1979) is a more controlled approach which uses probe stimuli consisting of random-dot patterns flashed at *precise times* during a task. In a study of delayed matching of word pairs, the ERP waveforms to probes presented at different times were distinguishable by factor analysis. However, the word stimuli themselves provided more information about the localization of linguistic processes, since the most pronounced asymmetries occurred over the posterior 'language' (Wernicke's) area in response to the second word. It is possible that with appropriate refinements, the probe ERP method could provide useful information, but many issues must be resolved before it can be used with confidence.

#### References for appendix

- Gershuni, G., Kozhevnikov, V., Maruseva, A., Avakyan, R., Radionova, E., Altman, J. and Soroko, V. (1960) Modifications in electrical responses of the auditory system in different states of higher nervous activity. *Electroenceph. clin. Neurophysiol.*, 13, 115-124.
- Hudspeth, W. and Jones, G. (1975) Stability of neural interference patterns. In: P. Greguss (Ed.), *Holography in Medicine*. IPC Science and Technology Press, London.
- Johnstone, J. (1982) *Probe Event-Related Potentials during Language Processing in Children: Comparison of Resource Allocation and Stimulus-Set Models of Attention*. Ph.D. Thesis, University of California, San Francisco, CA.
- Papanicolaou, A., Schmidt, A., Moore, B. and Eisenberg, H. (1983) Cerebral activation profiles in arithmetic and visuospatial processing tasks. *Int. J. Neurosci.*, 20, 283-288.
- Papanicolaou, A. (1980) Cerebral excitation profiles in language processing: the photic probe paradigm. *Brain Lang.*, 9, 269-280.
- Papanicolaou, A. and Johnstone, J. (1984) Probe evoked potentials: theory, method and applications. Unpublished.
- Rasmussen, C., Allen, R. and Tarte, R. (1977) Hemispheric asymmetries in cortical evoked potentials as a function of arithmetic computations. *Bull. psychon. Soc.*, 10, 419-421.
- Shucard, D.W., Shucard, J.L. and Thomas, D.G. (1977) Auditory evoked potentials as probes of hemispheric differences in cognitive processing. *Science*, 197, 1295-1297.
- Thatcher, R. and Maisel, B. (1979) Functional landscapes of the brain: an electrotopographic perspective. In: H. Begleiter (Ed.), *Evoked Brain Potentials and Behavior*. Plenum, New York, pp. 143-169.